NON-PARAMETRIC ESTIMATION OF SPATIAL DISTRIBUTIONS

A DISSERTATION

SUBMITTED TO THE DEPARTMENT OF APPLIED EARTH SCIENCES

AND THE COMMITTEE ON GRADUATE STUDIES

OF STANFORD UNIVERSITY

IN PARTIAL FULFILLMENT OF THE REQUIREMENTS

FOR THE DEGREE OF

DOCTOR OF PHILOSOPHY

By

Jeffery Alan Sullivan

December 1984

ACKNOWLEDGEMENTS

I wish to express my gratitude to Professor Andre Journel for his guidance and many helpful suggestions throughout the course of this study.

I would also like to thank the management of Freeport Gold Company for allowing me access to data from the Bell Mine. I'd especially like to thank Don Birak for his interest in the project and his insights into the geology of the Bell Mine.

Finally, I'd like to thank Harry Parker of Fluor Mining and Metals for his help in obtaining and analyzing the data.

CONTENTS

LIST OF TABLES

LIST OF ILLUSTRATIONS

Chapter I

INTRODUCTION

The field of resource estimation known as geostatistics has made great inroads into many diverse areas of the earth sciences such as mining engineering, petroleum engineering and hydrology since its advent in the early 1960's. A primary factor in the acceptance of geostatistics by such a wide group of practitioners with such varied interests is the simplicity and robustness of the basic estimator of geostatistics, ordinary kriging. The ordinary kriging estimator does, however, have important limitations which reduce its effectiveness in certain instances. One instance in which the ordinary kriging estimator may not be effective is predicting the tonnage and quantity of metal[1] recovered (for a given cutoff) at the time of mining utilizing only sparse exploration data. This estimation problem, termed recoverable reserve estimation, is especially difficult for deposits which present a highly skewed grade distribution and/or contain mineralization which is interspersed with waste material. To handle this difficult problem various recoverable reserve estimators have been introduced. These estimators have not, however, enjoyed the the widespread acceptability and use afforded the ordinary kriging estimator, because they are difficult to comprehend and apply. If recoverable reserve estimators are to attain the level of acceptability of ordinary kriging, methods of

---

[1]Tons of copper or ounces of gold recovered.

estimating recoverable reserves must be developed which are simple, robust, and easy to apply. The development and application of two such estimators, indicator kriging and probability kriging, are presented here.

1.1 THE PROBLEM

The problem of estimating recoverable reserves for deposits with strongly positively-skewed distributions and mineralization which is interspersed with waste material has become important recently due to the strong interest of the mining community in sedimentary uranium and Carlin type gold deposits. Both of these classes of deposits contain mineralization which is so highly variable that it is impossible to distinguish ore from waste until shortly before mining when blasthole assays and detailed geologic mapping become available. Unfortunately, the estimates of recoverable reserves which are required to perform feasibility studies, mine planning, and scheduling must be available months to years prior to the time of mining. Thus the recoverable reserves must be determined from the available sparse exploration data, which are usually located on a grid which is too large to allow the accurate blocking of ore and waste.

Since accurate estimation of recoverable reserves is a crucial step in the evaluation of an orebody, the use of advanced geostatistical techniques is justified. The premise behind any advanced geostatistical recoverable reserves estimator is that the exact location of a selective mining unit[1] (smu) within a panel (comprising a day's to a week's

---

[1]A selective mining unit is defined as the smallest volume of material which can be selected as ore or waste.

production) is unimportant at the planning stage. It is sufficient to know that a certain number of ore grade smus carrying a certain amount of recoverable metal are located somewhere within the panel. This basic premise is reasonable since the planning stage is typically six months to several years prior to the time of mining; so that, knowledge of the estimated grade of each smu would only be marginally more valuable than the tonnage and grade of material within a small region of the deposit. Accepting the basic premise, recoverable reserves can be obtained by estimating the distribution of smus within a panel or equivalently the local spatial distribution (see figure 1) and applying the economic cutoff to this distribution. Given this distribution of smus within a panel, the estimated tonnage recovered for the panel is the percentage of the estimated distribution above cutoff multiplied by the total panel tonnage and the estimated mean recovered grade is the mean grade of the portion of the estimated distribution above cutoff. The quantity of metal recovered is the product of recovered tonnage and mean recovered grade.

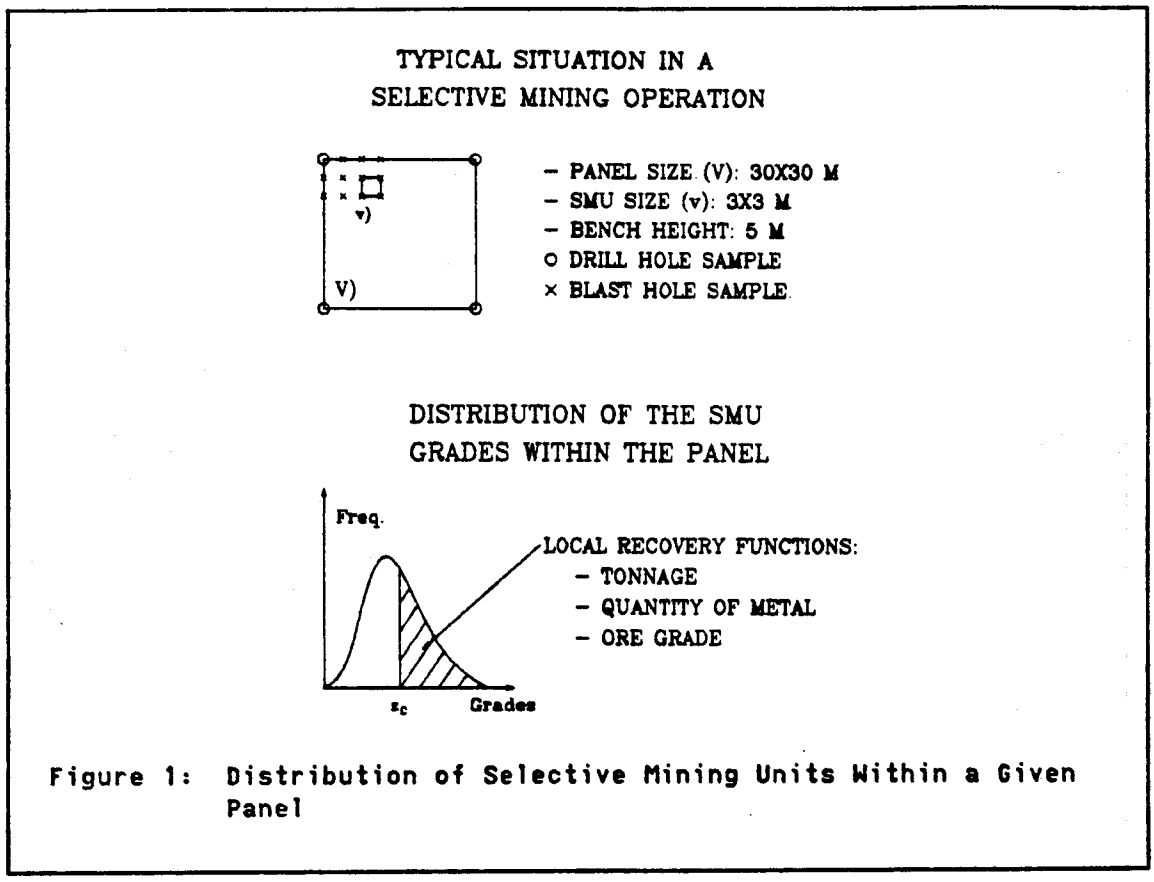

Figure 1: Distribution of Selective Mining Units Within a Given Panel

1.2 PREVIOUS WORK

Various estimators of recoverable reserves have been introduced over the past 10 to 15 years. These estimators can be broadly grouped into parametric and non-parametric estimators.

The common thread connecting the parametric estimators is that all of the estimators within this group make some assumption concerning the distribution of grades. If the grade values are assumed to follow a multivariate normal distribution after a univariate normal scores transform, the distribution of grade values within a particular panel, conditioned by the surrounding data, can be obtained straightforwardly (cf. Anderson, 1972). Parametric estimators of recoverable reserves based on

based on normal score transforms were first introduced by Matheron (1974, 1976a,b). An estimator based on the assumption of multivariate normality after transform, multigaussian kriging (MG), allows derivation of the distributions conditioned to the data. An estimator based on a hypothesis of bivariate normality after transform, disjunctive kriging (DK), allows approximation of these conditional distributions. The MG method has been developed by Verly (1983,1984) while the DK method has been expanded on by Marechal (1976), Jackson and Marechal (1979) and Young (1982). The performances of the DK and MG estimators on a simulated deposit were compared by Verly (1983).

Parametric methods based on the assumption of multilognormality without any univariate transformation have also been introduced. Simple lognormal kriging, which requires knowledge of the stationary mean of the grades was introduced by Parker (1975) and Parker and Switzer (1975). Ordinary lognormal kriging which does not require knowledge of the mean grade was developed by Rendu (1979). Further expansion of this method is found in Parker et al. (1979) and Journel (1980).

All of the previous parametric techniques share a distinct disadvantage in that the parametric hypothesis which forms the basis of the techniques may not hold for any given deposit. Additionally there are no available statistical tests which can be utilized to investigate the validity of multivariate distribution hypotheses. Thus it is possible that these techniques may be applied on deposits which do not conform to the initial hypotheses and, therefore, yield poor results. A further drawback of the parametric methods is that many practitioners find them difficult to comprehend and apply due to their mathematical complexity.

Non-parametric methods, in contrast to parametric methods, require no assumption concerning the distribution of grades. The basis of these techniques is the indicator transform which, essentially, transforms the grade at each sampled location into a distribution function. These transformed data are then used to estimate the local spatial distribution of grades within a panel. In addition to not requiring any distributional hypotheses, the non-parametric solutions are simple to obtain as the estimates are obtained by solving linear kriging systems which are nearly identical to the ordinary kriging system solved to estimate mean grade.

Indicator transforms were first used to estimate distributions of correlated data by Switzer (1977). The goal in his study was to estimate the model cumulative distribution function F(z). This was accomplished by defining indicators from the normal score transforms of the data and utilizing a linear kriging procedure to obtain an estimate of F(z).

Journel (1982,1983) defined indicators on the initial untransformed data. The spatial correlation of these indicators was determined and used to obtain optimal estimates of the local spatial distribution of grades. Further development of this estimator is presented by Lemmer (1984a,b) and Sullivan (1984).

A comparison of parametric and non-parametric techniques is given by Verly and Sullivan (1984).

1.3 ORGANIZATION

The development of non-parametric estimators of spatial distributions for the case of estimating the local distribution of point support[1] units within a specific region is discussed in chapter 2. In chapters 3 and 4 these non-parametric techniques are tested on simulated (chapter 3) and actual (chapter 4) deposits. Chapter 5 discusses the difficult problem of estimating the spatial distribution of non-point support units; that is, the local distribution of block grades and presents a case study illustrating the application of block support distribution estimators on an actual deposit. Finally an appendix is included containing all the computer software necessary to perform non-parametric spatial distribution estimation.

---

[1]The term support is synonymous with the volume on which the grade is defined. For instance grades obtained from drill hole assays are core support assays. Typically core support assays are referred to as point support assays because the volume of a core is insignificant in comparison to the volume of a mining unit or block.

deposit. The set of these random variables is termed a random function. As a set of random variables, the random function expresses both the point and regional behavior of the variable of interest. At a given point in space, the random function $Z(x_1)$ is a random variable, but over a region, the random function contains the complete spatial correlation structure of any set of random variables. Thus the random function describes both the random and structured aspects of the variable of interest.

In any stochastic estimation, some knowledge of the spatial law of the random function must be obtained before an optimal estimator can be defined. The random variables usually considered in the earth sciences, however, have only one realization at each sampled location which yields only one realization of the random function limited to the particular data locations. As it is impossible to infer any property of a random function from a single realization, a stationarity assumption must be included in the model to allow inference of properties of the random function. For reasons which will be discussed later (sec. 2.4), the type of stationarity invoked for non-parametric estimation of spatial distributions is stationarity of the bivariate distributions of Z(x) and Z(x+h) for various distance vectors h:

$$F_{x\ x+h}(z,z') = F_h(z,z')$$

The implication of bivariate stationarity is that the bivariate distribution of two random variables $Z(x_1)$ and $Z(x_2)$ depends on the vector h separating these two random variables not on the particular locations x_1 and x_2.

Chapter II

DEVELOPMENT OF NON-PARAMETRIC ESTIMATORS OF SPATIAL DISTRIBUTIONS

The theory and development of non-parametric estimators of spatial distributions is very similar to the theory and development of non-parametric estimators of local mean grade. The only major differences between these two types of estimators are in the variable estimated and the type of data used. Hence, in this chapter, the data used and the variable estimated are clearly defined at the outset. Having defined the variable of interest and the data which can be used to estimate it, linear kriging type estimators which minimize the variance of errors will be developed to obtain least squares type estimates of the spatial distribution. In the process of developing these estimators the various nuances and strengths of the estimators will be discussed.

Before proceeding with the development of these estimators, however, the underlying stochastic model which provides a basis for the estimators is discussed.

2.1 THE RANDOM FUNCTION CONCEPT

It is convenient to conceptualize the observed variable of interest (for instance, metal grade) at a particular point in space, $z(x_1)$, as a realization of a random variable $Z(x_1)$. As at location x_1, a random variable $Z(x)$ can be defined at each and every location, x, within the

Bivariate stationarity implies stationarity of the univariate distribution; that is, the random variables representing the variable of interest at each particular location, $Z(x_1)$, $Z(x_2)$, ... $Z(x_n)$, are identically distributed usually non-independent random variables.

Given stationarity of the bivariate distribution, non-parametric estimators of spatial distributions can be developed. Before the development of these estimators can proceed, however, the quantity of interest, the spatial distribution, must be defined and cast in the random function framework.

2.2 THE SPATIAL DISTRIBUTION

A spatial distribution is the distribution of grade values defined on a support size or volume within a region or subset of the deposit. In the discussion which follows, only the spatial distribution of point support grades will be considered. Spatial distributions of non-point support grades and their estimation will be discussed in chapter 5.

The local spatial distribution of point support grades within a region A can be defined mathematically as

$$\phi(A,zc) = \frac{1}{\text{meas}(A)} \cdot \int_{x \in A} i(x,zc)dx \qquad (2.2)$$

where: $\phi(A,zc)$ is the spatial distribution of point values within the region A for cutoff zc (i.e. the proportion of point grades within region A less than zc). Region A can have any size or shape[1].

$i(x,zc)$ is an indicator defined as

---

[1]The measure of region A will be denoted as (A) rather than meas(A) in the following equations for notational convenience.

$$i(x,zc) = \begin{cases} 1 \text{ if } z(x) \leq zc \\ 0 \text{ if } z(x) > zc \end{cases} \tag{2.3}$$

$z(x)$ is the observed value at location x

zc is a cutoff or threshold value.

This definition of the spatial distribution is deterministic as it is based solely on realizations of the random variables $Z(x)$ and not the random variable itself. The spatial distribution $\phi(A,zc)$ can be seen in stochastic terms if $\phi(A,zc)$ is considered as a realization of a random variable $\Phi(A,zc)$, where $\Phi(A,zc)$ is the following integral transform of the random variable $Z(x)$.

$$\Phi(A,zc) = \frac{1}{(A)} \cdot \int_{x \in A} I(x,zc)dx \tag{2.4}$$

where $I(x,zc)$ is the indicator random function defined as:

$$I(x,zc) = \begin{cases} 1 \text{ if } Z(x) \leq zc \\ 0 \text{ is } Z(x) > zc \end{cases} \tag{2.5}$$

The expected value of this random variable is easily determined:

$$E[\Phi(A,zc)] = \frac{1}{(A)} \cdot E\left[\int_{x \in A} I(x,zc)dx\right] = \frac{1}{(A)} \cdot \int_{x \in A} E[I(x,zc)]dx \tag{2.6}$$

$$E[\Phi(A,zc)] = \frac{1}{(A)} \cdot \int_{x \in A} [1 \cdot Pr(Z(x) \leq zc) + 0 \cdot (Pr(Z(x) > zc)]dx \tag{2.7}$$

$= Pr(Z(x) \leq zc)$: from stationarity of $Z(x)$

$= F(zc)$

The spatial distribution defined as $\phi(A,zc)$ can thus be seen as a realization of a random function, $\Phi(A,zc)$, whose expected value is equal to the value of the stationary univariate cumulative distribution function F(zc).

2.3 ESTIMATION OF SPATIAL DISTRIBUTIONS

As in the estimation of block grade, where the quantity of interest is the particular realization $z_v(x)$ and not the probability density function (pdf) or any parameter of the pdf of the random function $Z_v(x)$, the quantity of interest in the estimation of a spatial distribution is the particular realization $\phi(A,zc)$ and not the pdf or any parameter of the pdf of the corresponding random function $\Phi(A,zc)$ including its expected value. In non-statistical terms, the quantity of interest is the spatial distribution within a particular region A which would be observed if the region were completely sampled[1]. In reality, no region larger than the sample support is completely sampled, so the local spatial distribution must be estimated utilizing only the sparse information gathered from sampling the deposit. To this point, the exact information which will be used to estimate $\phi(A,zc)$ has not been described. This is the subject of the next section.

---

[1]In this context, completely sampled is taken as sampling at all possible locations within the region A.

2.3.1 Indicator Data

The problem of estimating a spatial distribution is very much like estimating the mean grade of a region. When estimating mean grade, point support data are used to estimate the unknown block support grade. In the case of spatial distribution estimation, the quantity of interest $\phi(A,zc)$ has been defined, however the point support[1] data $\phi(x,zc)$ which will be used to estimate $\phi(A,zc)$ must be determined

$$\phi(x,zc) = \frac{1}{(x)} \cdot \int_{x \epsilon x} i(x,zc)dx$$
$$= i(x,zc). \qquad (2.8)$$

Thus the point support datum is identical to the indicator defined in relation 2.2 as a simple transform of the realization z(x). Since this indicator is defined as a transform of the realization or datum z(x), i(x,zc) is termed an indicator datum.

The spatial distribution at a sampled point, i(x,zc), takes a simple form which is shown in figure 2. This spatial distribution has only two possible values, 0 and 1. The cutoff value at which i(x,zc) jumps from 0 to 1 is the observed realization z(x). Thus all spatial distributions at sampled points, i(x,zc), will have the same basic shape (0 for zc values less than z(x) and 1 otherwise), however the value at which the jump from zero to one occurs will vary from location to location.

---

[1]Actually the data are found on quasi-point or core support. However as the volume of a core is negligible in comparison to the volume of a block, the terms core support and point support are used interchangeably.

Additionally, the indicator data can be interpreted as a conditional probability. That is,

$$i(x_\alpha, zc) = Pr(Z(x_\alpha) \leq zc \mid z(x_\alpha))$$

Thus, given a realization at location x_α there is either a 100% or 0% chance that the random variable at location x_α will take on a value less than or equal to the cutoff zc.

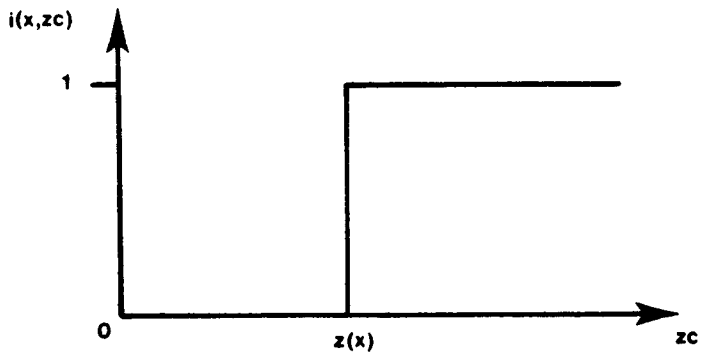

Figure 2: The Spatial Distribution At A Sampled Point

The indicator data, defined here, provide the source of information which can be used to estimate a spatial distribution in the same way that point grade data are used to estimate block grades. The similarity between these two estimation procedures is demonstrated in the following relations.

$$Z_v(y) = \frac{1}{(V)} \cdot \int_{x \epsilon V} z(x)dx$$

$$\phi(V,zc) = \frac{1}{(V)} \cdot \int_{x \epsilon V} i(x,zc)dx \qquad (2.9)$$

Thus any estimator used to determine block grades from point grade data can also be used to determine the spatial distribution from point indicator data. That is, either stochastic or deterministic, linear or non-linear, estimators of $\phi(A,zc)$ could be considered. The chosen estimator, however must be optimal in some sense and it should not be too difficult or expensive to apply.

2.3.2 Properties of the Estimator

There are a large number of estimators utilizing indicator data which could be used to estimate the spatial distribution. The estimators which will be utilized, however, are unbiased, have minimum mean squared error or, equivalently, minimum estimation variance, and are linear combinations of the data. Estimators with these properties will be utilized because the derivation of this type of estimator is not difficult, the criterion of minimum mean squared error is a widely used and accepted criterion of optimality, and such an estimator would be similar in form to the kriging estimators of mean grade. The requirement that the estimator be a linear combination of the data is invoked (although there are superior non-linear estimators) because non-linear estimators are usually difficult to comprehend and apply. In addition, non-linear estimators are almost always distribution

dependent. The above properties, which will be imposed on the estimator, place some definite restrictions on the form the estimator can take. These restrictions are discussed in the following two sections.

2.3.2.1 Unbiasedness

Every conceivable estimator, no matter how complex, will have some error of estimation in nearly all applications unless the unknown region is completely sampled. This error can be treated as a random variable and the histogram of these errors can, in theory, be examined (fig 3). When this histogram of errors has a mean of zero, the estimator is termed an unbiased estimator. In the case of a spatial distribution estimator, unbiasedness entails

$$E[\Phi^*(A,zc) - \Phi(A,zc)] = 0, \quad \text{i.e.}$$

$$E[\Phi^*(A,zc)] = E[\Phi(A,zc)] = F(zc). \tag{2.10}$$

Given a linear estimator of the following form

$$\phi^*(A,zc) = \sum_{\alpha} \lambda_\alpha(zc) \bullet i(x_\alpha,zc) \tag{2.11}$$

where: $i(x_\alpha,zc)$ is an indicator datum obtained by applying the indicator transform to the data values $z(x_\alpha)$.

$\lambda_\alpha(zc)$ is the weight given to the indicator data at each location x_α. Notice that the weight is a function of the cutoff zc.

The conditions for which this linear estimator will be unbiased are easily derived.

$$\begin{aligned} E[\Phi^*(A,zc)] &= E[\sum_{\alpha}\lambda_\alpha(zc)\bullet I(x,zc)] \\ &= \sum_{\alpha}\lambda_\alpha(zc)\bullet E[I(x,zc)] \\ &= \sum_{\alpha}\lambda_\alpha(zc)\bullet F(zc) \end{aligned} \tag{2.12}$$

If the weights $\lambda_\alpha(zc)$ are constrained so that $\Sigma\lambda_\alpha(zc)=1$, the estimator will be unbiased. Due to this constraint on the weights this estimator will be termed the constrained estimator.

An alternative form of this estimator which does not require any constraint on the sum of the weights is

$$\phi^*(A,zc) = \sum_{\alpha}\lambda_\alpha(zc)\bullet i(x_\alpha,zc) + [1-\sum_{\alpha}\lambda_\alpha(zc)]\bullet F^*(zc) \tag{2.13}$$

The expected value of this unconstrained estimator is

$$\begin{aligned} E[\Phi^*(A,zc)] &= E[\sum_{\alpha}\lambda_\alpha(zc)\bullet I(x_\alpha,zc)] + [1-\sum_{\alpha}\lambda_\alpha(zc)]\bullet F^*(zc) \\ &= \sum_{\alpha}\lambda_\alpha(zc)\bullet F(zc) + [1-\sum_{\alpha}\lambda_\alpha(zc)]\bullet F^*(zc) \end{aligned} \tag{2.14}$$

If $F^*(zc)$ is known to equal $F(zc)$

$$E[\Phi^*(A,zc)] = F(zc). \tag{2.15}$$

So providing $F(zc)$ is known, this estimator of $\phi(A,zc)$ will also be unbiased.

2.3.2.2 Minimum Estimation Variance

There are many possible unbiased estimators as the condition which ensures unbiasedness is not very strict. Among the class of unbiased

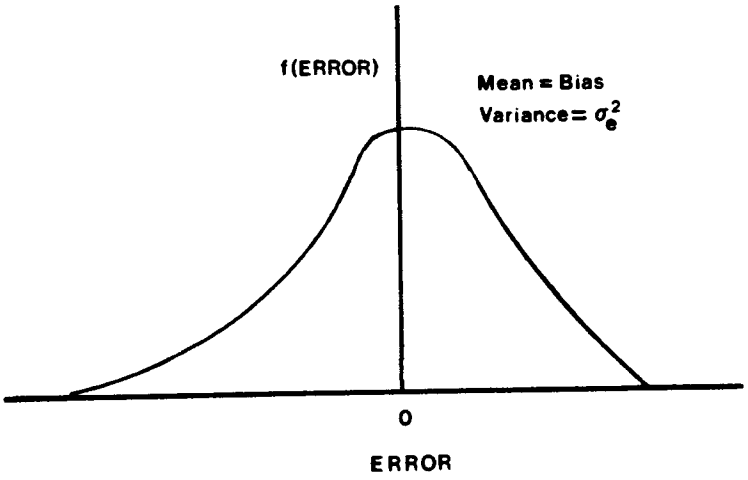

Figure 3: Histogram Of Errors

estimators are deterministic estimators such as polygons of influence and inverse distance squared weighting. These estimators, although unbiased and extremely simple to apply, are not optimal in any sense, hence they will be outperformed by other optimal estimators. In order for an estimator to be optimal it must minimize some measure of spread of the previously described distribution of errors (fig 2). The chosen measure is the mean squared error or variance of the distribution of errors. The variance of this distribution is referred to as the estimation variance of the estimator.

The estimation variance of a spatial distribution estimator is defined as:

$$\sigma_e^2(A,zc) = E[(\Phi(A,zc)-\Phi^*(A,zc))^2]$$
$$= E[\Phi^2(A,zc)]-2\cdot E[\Phi(A,zc)\cdot\sum_\alpha \lambda_\alpha(zc)\cdot I(x_\alpha,zc)] \qquad (2.16)$$
$$+ E[\sum_\alpha \lambda_\alpha(zc)\cdot I(x_\alpha,zc)\cdot\sum_\beta \lambda_\beta(zc)\cdot I(x_\beta,zc)]$$

The weights $\lambda_\alpha(zc)$ will be chosen to minimize this expression. This minimization will be performed by setting the various partial derivatives of $\sigma_e^2(A,zc)$ with respect to the weights λ_α to zero. Notice that the expression for $\sigma_e^2(A,zc)$ contains various $E[I(x_\alpha,zc)\cdot I(x_\beta,zc)]$ and $E[\Phi(A,zc)\cdot I(x_\alpha,zc)]$ terms which have not been discussed, so before proceeding with the determination of the weights $\lambda_\alpha(zc)$ which minimize σ_e^2, the nature of these terms and their inference must be investigated.

2.4 STRUCTURAL FUNCTIONS

In the expression of the estimation variance σ_e^2, various product terms of the form $E[I(x_\alpha,zc)\cdot I(x_\beta,zc)]$ are found. Inference of these terms is crucial; however, as there is only one realization of $I(x_\alpha,zc)$ at each sampled location x_α, there is only one realization of the product $I(x_\alpha,zc)\cdot I(x_\beta,zc)$ for each particular pair of locations x_α and x_β. Certainly it is not possible to infer the expected value of this product from one realization, hence a stationarity hypothesis must be invoked. If it is assumed that $E[I(x_\alpha,zc)\cdot I(x_\beta,zc)]$ depends only on the vector separating locations x_α and x_β inference becomes possible as there are many locations (within given tolerances) separated by a given vector. Under this hypothesis

$$E[I(x_\alpha,zc)\cdot I(x_\beta,zc)] = E[I(x,zc)\cdot I(x+h,zc)]$$

where h is a vector separating x_α and x_β.

The stationarity of this product entails the stationarity of a bivariate probability as,

$$E[I(x+h,zc)\bullet I(x,zc)] = 1\bullet Pr(Z(x)\leq zc \text{ and } Z(x+h)\leq zc) + 0$$

$$= Pr(Z(x)\leq zc \text{ and } Z(x+h)\leq zc)$$

Thus the stationarity of this product entails stationarity of the bivariate distribution of Z(x) and Z(x+h).

It is recognized that $E[I(x+h,zc)\bullet I(x,zc)]$ is the non-centered covariance of I(x+h,zc) and I(x,zc). The centered covariance is defined as

$$C_i(h,zc) = E[I(x+h,zc)\bullet I(x,zc)] - E[I(x+h,zc]\bullet E[I(x,zc)]$$

$$= E[I(x+h,zc)\bullet I(x,zc)] - F(zc)^2$$

since Z(x) is stationary

Given this definition of the covariance $C_i(h,zc)$ it is possible to define the remaining undefined terms in the expression for the estimation variance (eqn 2.16); namely, $E[\Phi(A,zc)\bullet I(x,zc)]$ and $E[\Phi(A,zc)\bullet\Phi(A,zc)]$.

$$\text{Recall} \qquad \Phi(A,zc) = \frac{1}{(A)}\bullet\int_A I(x,zc)\,dx \tag{2.17}$$

$$\text{so} \quad E[\Phi(A,zc)\bullet I(x_\alpha,zc)] = E[\frac{1}{(A)}\bullet\int_A I(x,zc)dx\bullet I(x_\alpha,zc)]\,dx \tag{2.18}$$

$$= \frac{1}{(A)}\bullet\int_A C_i(x-x_\alpha,zc)\,dx + F(zc)^2 \tag{2.19}$$

from the definition of $C_i(h,zc)$

to simplify notation, set

$$\bar{C}_i(x_\alpha,A,zc) = \frac{1}{(A)}\bullet\int_A C(x-x_\alpha,zc)\,dx \qquad (2.20)$$

hence,

$$\bar{C}(x_\alpha,A,zc) = E[\bar{\Phi}(A,zc)\bullet I(x_\alpha,zc)] - F(zc)^2$$

similarly

$$\bar{C}(A,A,zc) = E[\bar{\Phi}(A,zc)\bullet\bar{\Phi}(A,zc)] - F(zc)^2$$

Given that all terms in the expression of the estimation variance (eqn 2.16) can be expressed in terms of the covariance $C_i(h,zc)$, this covariance must be inferred from the data to evaluate the estimation variance.

The indicator covariance can be inferred unbiasedly utilizing the following discrete sum.

$$C_i(h,zc) = \frac{1}{n_h}\bullet\left[\sum_{i=1}^{n_h} i(x_i+h,zc)\bullet i(x_i,zc)\right] - F^{*2}(zc) \qquad (2.21)$$

n_h = the number of pairs of data separated by distance vector h.

$F^*(zc)$ is the best available estimate of $F(zc)$

The chief difficulty with inferring $C_i(h,zc)$ in this manner is obtaining a reliable estimate of $F(zc)$. Estimation of the indicator semi-variogram eliminates this difficulty as it carries the same information as $C_i(h,zc)$ but does not require prior knowledge of $F(zc)$. The indicator semi-variogram is defined as:

$$\gamma_i(h,zc) = C_i(0,zc) - C_i(h,zc)$$
$$\text{with: } C_i(0,zc) = \text{Var}(I(x,zc)) = F(zc)\cdot(1-F(zc)) \qquad (2.22)$$

$$\begin{aligned}\gamma_i(h,zc) &= F(zc) - E[I(x+h,zc)\cdot I(x,zc)] \\ &= .5\cdot(2F(zc) - 2E[I(x+h,zc)\cdot I(x,zc)]) \\ &= .5\cdot E[(I(x+h,zc)-I(x,zc))^2]\end{aligned} \qquad (2.23)$$

Like the indicator covariance, the indicator variogram can also be interpreted as a bivariate probability[1].

$$\begin{aligned}\gamma_i(h,zc) = {} & .5\cdot[1\cdot Pr(Z(x)>zc \text{ and } Z(x+h)\leq zc)+1\cdot Pr(Z(x)\leq zc \text{ and } Z(x+h)>zc)] \\ & + .5\cdot[0\cdot Pr(Z(x)>zc \text{ and } Z(x+h)>zc)+0\cdot Pr(Z(x)\leq zc \text{ and } Z(x+h)\leq zc)]\end{aligned}$$

$$\begin{aligned}\gamma_i(h,zc) = {} & .5\cdot Pr(Z(x)>zc \text{ and } Z(x+h)\leq zc) \\ & + .5\cdot Pr(Z(x+h)\leq zc \text{ and } Z(x)>zc)\end{aligned} \qquad (2.24)$$

The indicator variogram and therefore the indicator covariance (eqn 2.21) can be inferred by

$$\gamma_i(h,zc) = \frac{1}{2n_h}\cdot\sum_{i=1}^{n_h}(i(x_i+h,zc) - i(x_i,zc))^2 \qquad (2.25)$$

2.5 THE INDICATOR KRIGING ESTIMATOR

Given a definition of and a way to infer the indicator covariance, the set of weights which minimize the estimation variance σ_e^2 (eqn. 2.16) can be determined. Recall that both constrained and unconstrained solutions are possible (sec 2.3.2.1). The determination of the optimal solution for the constrained case will be shown in detail. The solution

---

[1]See section 2.6.1 for further discussion of the relation between $\gamma_i(h,zc)$ and the bivariate distribution.

for the unconstrained case is analogous.

2.5.1 Minimization of $\sigma_e^2(A,zc)$ in the Constrained Case

If the estimator described in relation 2.11 is considered, a constraint forcing the sum of the weights to equal one is included in the system to ensure unbiasedness. As previously stated, the optimal weights will be determined by setting the various partial derivatives of $\sigma_e^2(A,zc)$ to zero. The constraint on the weights is included in this optimization through the method of Lagrange multipliers.

$$L(\lambda_\alpha(zc),\mu(zc)) = \sigma_e^2(A,zc) + 2\cdot\mu(zc)\cdot[\sum_\alpha \lambda_\alpha(zc)-1] \tag{2.26}$$

$$= E[\Phi(A,zc)-\Phi^*(A,zc)]^2 + 2\cdot\mu(zc)\cdot[\sum_\alpha \lambda_\alpha(zc)-1] \tag{2.27}$$

$$= E[\Phi(A,zc) - \sum_\alpha \lambda_\alpha(zc)\cdot I(x_\alpha,zc)]^2 + 2\cdot\mu(zc)\cdot[\sum_\alpha \lambda_\alpha(zc)-1] \tag{2.28}$$

$$= E[\Phi^2(A,zc)] - 2\cdot E[\Phi(A,zc)\cdot\sum_\alpha \lambda_\alpha(zc)\cdot I(x_\alpha,zc)] + E[(\sum_\alpha \lambda_\alpha(zc)\cdot I(x_\alpha,zc))\cdot(\sum_\beta \lambda_\beta(zc)\cdot I(x_\beta,zc))] + 2\cdot\mu(zc)\cdot[\sum_\alpha \lambda_\alpha(zc)-1] \tag{2.29}$$

Setting the partial derivatives of $L(\lambda_\alpha(zc),\mu(zc))$ to zero yields[1]:

---

[1]This system of equations is nearly identical to the system of equations utilized to determine the ordinary kriging estimate of mean grade.

$$\sum_{\alpha=1}^{n} C_i(x_\alpha - x_\beta, zc) \cdot \lambda_\alpha(zc) + \mu(zc) = \bar{C}_i(x_\beta, A, zc) \quad \text{for } \beta=1,n$$

$$\sum_{\alpha=1}^{n} \lambda_\alpha(zc) = 1 \tag{2.30}$$

where n is the number of data used to estimate $\phi(A,zc)$.

This system of n+1 linear equations and n+1 unknowns can be solved through gaussian elimination to determine the optimal weights $\lambda_\alpha(zc)$. The form of the estimator of $\phi(A,zc)$ is

$$\phi^*(A,zc) = \sum_{\alpha=1}^{n} \lambda_\alpha \cdot i(x_\alpha, zc) \tag{2.31}$$

and the minimized form of the estimation variance is

$$\sigma_{ikc}^2(A,zc) = \bar{C}_i(A,A,zc) - \sum_{\alpha=1}^{n} \lambda_\alpha(zc) \cdot \bar{C}_i(x_\alpha, A, zc) - \mu(zc). \tag{2.32}$$

The system of equations which must be solved to determine the optimal weights for the unconstrained form of the estimator are similar. The only difference is that the constraint on the sum of the weights and the Lagrange parameter, μ, are absent. The system of equations which must be solved to determine the optimal weights for this estimator has n equations and n unknowns.

$$\sum_{\alpha=1}^{n} C_i(x_\alpha - x_\beta, zc) \cdot \lambda_\alpha(zc) = \bar{C}_i(x_\beta, A, zc) \quad \text{for } \beta=1,n \tag{2.33}$$

where n is the number of data used

The form of the estimator is

$$\phi^*(A,zc) = \sum_{\alpha} \lambda_\alpha(zc) \cdot i(x_\alpha,zc) + [1-\sum_{\alpha=1}^{n} \lambda_\alpha(zc)] \cdot F^*(zc) \qquad (2.34)$$

and the estimation variance for this estimator is

$$\sigma_{iku}^2 = \bar{C}_i(A,A,zc) - \sum_{\alpha=1}^{n} \lambda_\alpha(zc) \cdot \bar{C}_i(x_\alpha,A,zc). \qquad (2.35)$$

Since the value of F(zc) is assumed to be known when using the unconstrained estimator, the constrained estimator has a higher estimation variance than the unconstrained estimator.

$$\sigma_{iku}^2(A,zc) \leq \sigma_{ikc}^2(A,zc) \qquad (2.36)$$

Both forms of this estimator are referred to as indicator kriging (IK) estimators since they are kriging type estimators utilizing the indicator data. In its unconstrained form this estimator, is termed the simple indicator kriging estimator while in its constrained form it is termed the ordinary indicator kriging estimator. These estimators are analogous to the simple and ordinary kriging estimators of mean grade.

2.6 IMPROVING THE INDICATOR KRIGING ESTIMATOR

In any estimation procedure, the quality of the estimator (measured here by the estimation variance) will be improved whenever additional information concerning the unknown is provided. In the case of estimating spatial distributions, both the unknown, $\phi(A,zc)$, and the indicator data are simple nonlinear transforms of the grade. As the grade z(x) is strongly related to the unknown $\phi(A,zc)$, if in addition to

the indicator data, information concerning the actual data grades is included in the estimate of $\phi(A,zc)$, the quality of the estimate will improve. One estimator which utilizes both grade and indicator data is the probability kriging (PK) estimator.

This proposed estimator would utilize both the indicator data and the grade at each sampled location to estimate $\phi(A,zc)$. This is similar, in concept, to a cokriging estimator in which, for instance, the unknown lead grade at a given location is estimated using not only the available lead assays but also the available zinc assays. A difficulty with an estimator which utilizes both indicator and grade data to estimate $\phi(A,zc)$ is that the two sets of data, $i(x,zc)$ and $z(x)$, are measured on different scales. The indicator data is a probability, hence it is bounded by zero and one. The grade datum is measured in percent so it is also a bounded variable, however it is bounded by 100% and 0%. The difficulty caused by this difference in scale is that there is a non-zero probability that a grade datum which is much larger than one will be used to estimate any particular spatial distribution. This high grade datum can make the estimator unstable since if an incorrect weight (caused by incorrect modelling of the variogram) is assigned to this datum the estimate of $\phi(A,zc)$ is likely to be larger than 1 or smaller than zero. A more stable estimator would be obtained if a transform of the grade which is bounded by zero and one is considered rather than the grade itself. One such transform replaces the grade at each location by its cumulative distribution function. This yields a variable which follows a uniform distribution with bounds of zero and one. The transform is expressed as

$$u(x) = F^*(z(x)).$$

where $F^*(z)$ is the best available estimate of the global cumulative distribution function.

$U(x)$ is uniformly distributed with bounds 0 and 1
so $E(U(x)) = .5$
and $Var(U(x)) = 1/12$

This transform is very robust with regards to outliers, since it transforms the highest observed grade value, whether it is 1%, 10%, or 100%, to 1.0. Thus when utilizing this transform, there is no need to trim troublesome outlier values. Hence all of the available data can be utilized if this transform is made.

The uniform transformation is also strongly related to the rank order of the data values, as one estimate of $F^*(z(x))$ is

$$F^*(z(x)) = \{\sum_{j=1}^{N} i(x_j, z(x))\}/N = R.O.(z(x))/N \qquad (2.37)$$

where N is the total number of data
$R.O.(z(x))$ is the rank order of $z(x)$, thus it is an integer between 1 and N inclusive.

From this interpretation it can be seen that an estimator utilizing the $u(x)$ data will make use of the spatial correlations of the rank order of the $z(x)$ data. As statistical measures determined on rank order data are very robust, the inference of spatial correlations for rank order data is more robust than the inference of spatial correlations for untransformed grade data. Thus, utilizing the uniform data will yield a more robust estimator of spatial distributions.

A final interpretation which the uniform transform allows is related to the fact that the uniform data are themselves probabilities. An estimator which utilizes both indicator and uniform data (both of which have probabilistic interpretations) is consistent with the unknown

$\phi(A,zc)$ as all three of these quantities are probabilities. Hence, an estimator which utilizes both the uniform and indicator data can be referred to as the probability kriging estimator.

2.6.1 Development of the Probability Kriging Estimator

A linear estimator which includes both indicator and uniform transform data is

$$\phi_{pk2}^*(A,zc) = \sum_{\alpha=1}^{n}\lambda_\alpha(zc)\cdot i(x_\alpha,zc) + \sum_{\alpha=1}^{n}\nu_\alpha(zc)\cdot u(x_\alpha). \qquad (2.38)$$

For this estimator to be unbiased, two constraints must be placed on the weights $\lambda_\alpha(zc)$ and $\nu_\alpha(zc)$, hence it is termed $\phi_{pk2}^*(A,zc)$. The form of the constraints can be found by examining the following relation.

$$\begin{aligned} E[\Phi_{pk2}^*(A,zc)] &= \sum_{\alpha=1}^{n}\lambda_\alpha(zc)\cdot E[I(x,zc)] + \sum_{\alpha=1}^{n}\nu_\alpha(zc)\cdot E[U(x)] \\ &= \sum_{\alpha=1}^{n}\lambda_\alpha(zc)\cdot F(zc) + \nu_\alpha(zc)\cdot(.5) \end{aligned} \qquad (2.39)$$

The condition which must hold if $\phi_{pk2}^*(A,zc)$ is to be an unbiased estimator is $E[\Phi^*(A,zc)]=E[\Phi(A,zc)]=F(zc)$. This is guaranteed if the following conditions are placed on the weights:

$$\begin{aligned} &\sum_{\alpha=1}^{n}\lambda_\alpha(zc) = 1 \\ &\sum_{\alpha=1}^{n}\nu_\alpha(zc) = 0. \end{aligned} \qquad (2.40)$$

As in the case of the indicator kriging estimator, this estimator can also be written in less constrained forms, provided that the cdf F(zc) is known.

Consider a random variable V(x,zc), defined as

$$V(x,zc) = U(x) - .5 + F(zc)$$

$$E[V(x,zc)] = E[U(x)] - .5 + F(zc)$$

$$= F(zc)$$

An estimator of the form

$$\phi_{pk1}^*(A,zc) = \sum_{\alpha=1}^{n} \lambda_\alpha \cdot i(x_\alpha,zc) + \sum_{\alpha=1}^{n} \nu_\alpha(zc) \cdot v(x,zc) \qquad (2.41)$$

will be unbiased if a constraint of the form

$$\sum_{\alpha=1}^{n} \lambda_\alpha(zc) + \sum_{\alpha=1}^{n} \nu_\alpha(zc) = 1 \qquad (2.42)$$

is imposed.

If, alternatively, an estimator of the following form is considered

$$\phi_{pk0}^*(A,zc) = \sum_{\alpha=1}^{n} \lambda_\alpha(zc) \cdot i(x_\alpha,zc) + \sum_{\alpha=1}^{n} \nu_\alpha(zc) \cdot v(x,zc) + \left[1 - \sum_{\alpha=1}^{n} \lambda_\alpha(zc) - \sum_{\alpha=1}^{n} \nu_\alpha(zc)\right] \cdot F^*(zc) \qquad (2.43)$$

no nonbias constraints are required.

As in deriving the indicator kriging estimator, weights will be found which minimize the estimation variance subject to the imposed constraints.

$$\sigma_{pk}^2 = E[(\Phi_{pk}^*(A,zc) - \Phi(A,zc))^2] \qquad (2.44)$$

Evaluating this quantity will require knowledge of expectations which have not yet been defined. These expectations are related to the following cross and uniform covariances.

$$C_{iu}(h,zc) = E[I(x,zc)\cdot U(x+h)] - F(zc)\cdot(.5)$$

$$C_u(h) = E[U(x)\cdot U(x+h)] - .25$$

Because of the uncertainty in estimating F(zc), the variogram counterparts of $C_{ui}(h,zc)$ and $C_u(h)$, $\gamma_{ui}(h,zc)$ and $\gamma_u(h)$, will be inferred rather than the covariances. The variograms are defined as follows

$$2\cdot\gamma_{ui}(h,zc) = 2\cdot C_{ui}(0,zc) - C_{ui}(h,zc) - C_{iu}(h,zc) \qquad (2.45)$$

where $C_{ui}(0,zc) = E[U(x)\cdot I(x,zc)] - .5\cdot F(zc)$

$$U(x)\cdot I(x,zc) = \begin{cases} U(x) & \text{if } Z(x)\leq zc \\ 0 & \text{if } Z(x)>zc \end{cases} \qquad (2.46)$$

Thus $C_{ui}(0,zc) = E[U(x)\,|\,z(x)\leq zc] - .5\cdot F(zc)$

$$\begin{aligned} 2\cdot\gamma_{ui}(h,zc) &= 2\cdot E[U(x)\cdot I(x,zc)] - E[U(x)\cdot I(x+h,zc)] \\ &\quad - E[I(x,zc)\cdot U(x+h)] \\ &= E[(U(x)\cdot I(x,zc)+U(x+h)\cdot I(x+h,zc)-U(x)\cdot I(x+h),zc) \\ &\quad - I(x,zc)\cdot U(x+h)] \\ &= E[(U(x)-U(x+h))\cdot(I(x,zc)-I(x+h,zc)] \end{aligned} \qquad (2.47)$$

$$\gamma_{ui}(h,zc) = -.5\cdot E[\,|U(x)-U(x+h)|\,|z(x)\leq zc \text{ and } z(x+h)>zc] \qquad (2.48)$$

Also notice that the cross variogram is a conditional expectation which can be interpreted in terms of the bivariate distribution of U(x) and U(x+h). Consider a bivariate distribution of U(x) and U(x+h) (see figure 4 for such a distribution). The hatched area of figure 4 corresponds to the regions where U(x)>uc (uc is the uniform transform of zc) and U(x+h)≤uc, or U(x)≤uc and U(x+h)>uc. The variogram $\gamma_{ui}(h,zc)$, therefore measures the expected difference of |U(x)-U(x+h)| over the hatched area (eqn. 2.48). As U(x)-U(x+h) is the vertical or horizontal distance of a pair (u(x),u(x+h)) from the line of symmetry U(x)=U(x+h), the cross variogram is a measure of dispersion of the hatched areas from the line U(x)=U(x+h). The cross variogram in conjunction with the indicator variogram, which gives only the area of the hatched regions (eqn 2.24), yields more information concerning the bivariate distribution of the grades than the indicator variogram alone and certainly more information than given by the variogram of grade.

The cross variogram, $\gamma_{ui}(h,zc)$ is inferred by

$$\hat{\gamma}_{ui}(h,zc) = \frac{1}{2n_h}\cdot\sum_{i=1}^{n_h}(U(x_i+h)-U(x_i))\cdot(I(x_i+h,zc)-I(x_i,zc)) \qquad (2.49)$$

Similarly, the variogram of the uniform data is defined as

$$\begin{aligned}\gamma_u(h) &= C_u(0) - C_u(h)\\ &= .5\cdot E[(U(x+h)-U(x))^2]\end{aligned} \qquad (2.50)$$

The uniform variogram is inferred by

$$\hat{\gamma}_u(h) = \frac{1}{n_h}\cdot\sum_{i=1}^{n_h}(u(x_i+h)-u(x_i))^2 \qquad (2.51)$$

Given a way to infer and model the various expectations which appear in the expression of $\sigma_{pk}^2(A,zc)$, the optimum weights, λ_α and ν_α, can be determined.

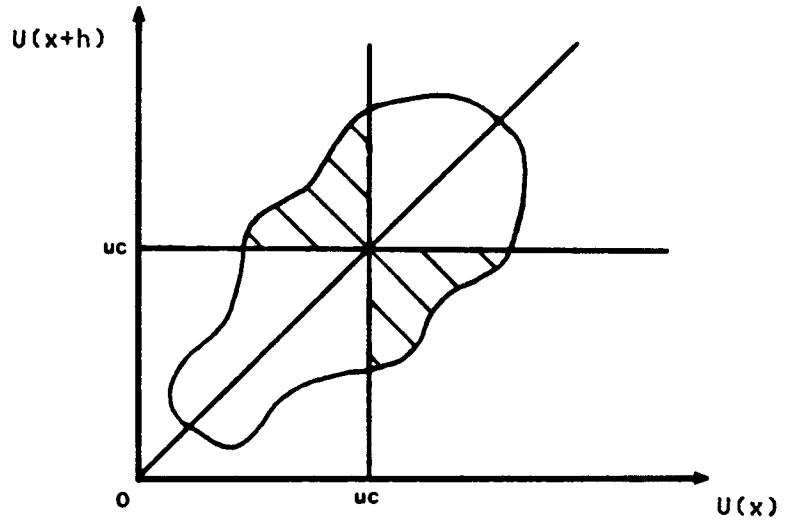

Figure 4: Bivariate Distribution of U(x) and U(x+h)

2.6.2 Minimization of $\sigma_{pk}^2(A,zc)$

Recall that

$$\sigma_{pk}^2(A,zc) = E[(\hat{\Phi}(A,zc) - \hat{\Phi}_{pk}^*(A,zc))^2] \qquad (2.52)$$

where in its most highly constrained form, the estimator of $\hat{\Phi}(A,zc)$ which utilizes both indicator and uniform data is

$$\hat{\Phi}_{pk2}^*(A,zc) = \sum_{\alpha=1}^{n}\lambda_\alpha(zc)\cdot I(x_\alpha,zc) + \sum_{\alpha=1}^{n}\nu_\alpha(zc)\cdot U(x_\alpha). \qquad (2.53)$$

Using the Lagrange multiplier technique, the problem becomes the minimization of

$$L(\lambda_\alpha(zc),\mu_1(zc),\mu_2(zc)) = E[(\Phi(A,zc)-\sum_{\alpha=1}^{n}\lambda_\alpha(zc)\cdot I(x_\alpha,zc)-\sum_{\alpha=1}^{n}\nu_\alpha(zc)\cdot U(x_\alpha))^2] + 2\cdot\mu_1(zc)\cdot[\sum_{\alpha=1}^{n}\lambda_\alpha(zc)-1]+ 2\cdot\mu_2(zc)\cdot[\sum_{\alpha=1}^{n}\nu_\alpha(zc)] \quad (2.54)$$

Taking partial derivatives with respect to $\lambda_\alpha(zc)$ and $\nu_\alpha(zc)$ and setting these partial derivatives to zero yields the following system of linear equations.

$$\sum_{\alpha=1}^{n}\lambda_\alpha(zc)\cdot C_i(x_\alpha-x_\beta,zc)+\sum_{\alpha=1}^{n}\nu_\alpha(zc)\cdot C_{ui}(x_\alpha-x_\beta,zc)+\mu_1(zc)=\bar{C}_i(x_\beta,A,zc) \quad \beta=1,n \quad (2.55)$$

$$\sum_{\alpha=1}^{n}\lambda_\alpha(zc)\cdot C_{ui}(x_\alpha-x_\beta,zc)+\sum_{\alpha=1}^{n}\nu_\alpha(zc)\cdot C_u(x_\alpha-x_\beta,zc)+\mu_2(zc)=\bar{C}_{iu}(x_\beta,A,zc) \quad \beta=1,n \quad (2.56)$$

$$\sum_{\alpha=1}^{n}\lambda_\alpha(zc) = 1 \qquad \sum_{\alpha=1}^{n}\nu_\alpha(zc) = 0 \quad (2.57)$$

The minimized variance is then[1]

$$\sigma_{pk2}^2(A,zc) = \bar{C}_i(A,A,zc)-\mu_1(zc)-\sum_{\alpha=1}^{n}\lambda_\alpha(zc)\cdot\bar{C}_i(A,x_\alpha,zc) - \sum_{\alpha=1}^{n}\nu_\alpha(zc)\cdot\bar{C}_{ui}(A,x_\alpha,zc) \quad (2.58)$$

If an estimator with only one constraint on the sum of the weights is considered, (eqn 2.41), the system of equations is changed by replacing the two constraints on the sum of the weights (eqn 2.40) by a single constraint (eqn 2.42) and eliminating the Lagrange parameter μ_2 from all equations. The estimation variance for this less constrained estimator is

$$\sigma_{pk1}^2(A,zc) = \bar{C}_i(A,A,zc) - \mu_1(zc) - \sum_{\alpha=1}^{n}\lambda_\alpha(zc)\bullet\bar{C}_i(A,x_\alpha,zc) - \sum_{\alpha=1}^{n}\nu_\alpha(zc)\bullet\bar{C}_{ui}(A,x_\alpha,zc) \qquad (2.59)$$

If an estimator without constraints on the weights is considered, (eqn 2.43), the system of equations is obtained from equations 2.55 through 2.57 by eliminating the two constraints on the weights and all Lagrange parameters. The estimation variance for this unconstrained estimator is

$$\sigma_{pk0}^2(A,zc) = \bar{C}_i(A,A,zc) - \sum_{\alpha=1}^{n}\lambda_\alpha(zc)\bullet\bar{C}_i(A,x_\alpha,zc) - \sum_{\alpha=1}^{n}\nu_\alpha(zc)\bullet\bar{C}_{ui}(A,x_\alpha,zc) \qquad (2.60)$$

For a set of estimators it is known that the estimator with the least number of constraints has the largest number of possible solutions hence the lowest estimation variance. Therefore the estimation variance hierarchy among the set of probability kriging estimators is

---

[1]Since the sum of the weights given to the uniform data equals zero, $\mu_2(zc)$ does not appear in this expression.

$$\sigma_{pk0}^2 \leq \sigma_{pk1}^2 \leq \sigma_{pk2}^2$$

Recall that a similar hierarchy was derived for the two IK estimators (eqn. 2.36); namely

$$\sigma_{iku}^2 \leq \sigma_{ikc}^2.$$

Since a PK estimator utilizes more information than an IK estimator, any PK type estimator will have a lower estimation variance than any IK type estimator. Therefore the complete estimation variance hierarchy is;

$$\sigma_{pk0}^2 \leq \sigma_{pk1}^2 \leq \sigma_{pk2}^2 \leq \sigma_{iku}^2 \leq \sigma_{ikc}^2 \qquad (2.61)$$

2.7 ORDER RELATION PROBLEMS

To this point, discussion has centered on estimating $\phi(A,zc)$ at a single fixed cutoff zc. In many applications, however, knowledge of the entire spatial distribution function $\phi(A,zc)$ is required; that is, $\phi^*(A,zc)$ must be determined at several different cutoffs of interest. Since $\phi^*(A,zc)$ is obtained independently for each cutoff zc it is possible that $\phi^*(A,z_1) > \phi^*(A,z_2)$ for $z_1 < z_2$ or that $\phi^*(A,zc)$ be less than zero or greater than 1. Since the unknown quantity of interest is a distribution function, any of the above outcomes is unacceptable. Any estimated distribution which exhibits any of these unacceptable properties is said to have order relation problems.

Order relation problems stem from the fact that the optimal solution at each cutoff zc is obtained without utilizing information concerning

the spatial continuity of the indicator data at other cutoffs. This deficiency can be overcome by solving the kriging systems for all cutoffs within one large system. That is, rather than determining weights which minimize the kriging variance at each cutoff independently, weights are determined which minimize some function of the estimation variances at all cutoffs subject to constraints which force the order relations to hold. One method for determining such a solution involves determining the weights $\lambda_\alpha(zc)$ which;

$$\min \sum_{i=1}^{nc} \sigma_e^2(A,zc_i) \cdot W_i \tag{2.62}$$

subject to

$$\begin{aligned} &\phi^*(A,zc_1) \geq 0 \\ &\phi^*(A,zc_i) \leq \phi^*(A,zc_{i+1}) \quad \text{for } zc_i \leq zc_{i+1} \\ &\phi^*(A,zc_{nc}) \leq 1.0 \end{aligned} \tag{2.63}$$

where: nc is the total number of cutoffs considered
$\sigma_e^2(A,zc_i)$ is the estimation variance at at cutoff i.
W_i is an optional weighting function used to give more weight to important cutoffs.

This problem involves minimizing a quadratic subject to a set of linear constraints containing inequalities. Problems of this type are known as quadratic programs. A quadratic program is solved by first introducing slack variables equal to the number of unknowns (Hillier and Lieberman, 1980, pg 751). Then, the optimal values of the unknown weights are obtained through a modified linear programming algorithm. The implication of this solution process is that a modified linear program containing (2)(nc)(n) unknowns must be solved (where n is the number of data and nc is the number of cutoffs). The solution given by this

quadratic program, although optimal, is several times more costly than the solution obtained by solving for the weights at each cutoff independently.

A less expensive solution to the order relation problem involves solving the kriging systems for each cutoff independently using PK or IK at each of the nc cutoffs of interest. Then, if order relation problems occur, fit a valid distribution function to the observed estimates. The fitted valid distribution function will be chosen on the basis of a minimum squared deviation criterion.

$$\min \sum_{i=1}^{nc} [\phi^{**}(A,zc_i) - \phi^{*}(A,zc_i)]^2 \cdot W_i \qquad (2.64)$$

subject to

$$\begin{aligned} &\phi^{**}(A,zc_1) \geq 0 \\ &\phi^{**}(A,zc_{i+1}) \geq \phi^{**}(A,zc_i) \quad \text{for all cutoffs } zc_{i+1} > zc_i \\ &\phi^{**}(A,zc_{nc}) \leq 1.0 \end{aligned} \qquad (2.65)$$

where $\phi^{*}(A,zc)$ are the optimal estimates given by kriging
$\phi^{**}(A,zc)$ are new estimates which yield a valid distribution function

The valid distribution function obtained using this method will be equal to the solution obtained by kriging at any cutoffs where order relation problems do not occur. This algorithm, thus has the reassuring property that changes in the optimal solution given by kriging are made only when required.

The valid distribution function which is sought can be obtained through quadratic programming, however in contrast to the quadratic program described in relation 2.62, this quadratic program contains only (nc)*2 unknowns, so the solution can be obtained inexpensively. Although cost is an important consideration in determining a method to

obtain the required solution, a cost effective solution is not always the best solution. In this case, however, the proposed cost effective solution (eqn 2.64) has, in several case studies (see sec 3.3.3.3), given exactly the same or nearly the same results as the more complicated, expensive, but strictly correct method described in relation 2.62. This does not imply, however, that these two algorithms are identical as they certainly are not. The practical results merely indicate that for the majority of order relation problems encountered in practice, this simple solution is an adequate approximation of the strict solution.

2.7.1 Graphical Solution For Order Relation Problems

The method of fitting a valid distribution function to spatial distribution function estimates with order relation problems is much simpler than obtaining an estimate which is guaranteed to have no order relation problems. However, this method involves solving a quadratic program (eqn 2.64). As quadratic programming algorithms are not found on every computer system, applying this technique may be impossible because the necessary programs are unavailable. Fortunately the solution to this quadratic program can be obtained graphically so that quadratic programming algorithms are unnecessary.

Consider a case in which estimates are obtained at two cutoffs zc_1 and zc_2 where $zc_2 > zc_1$. For simplicity of notation call these estimates a_1 and a_2 rather than $\phi^*(A,zc_1)$ and $\phi^*(A,zc_2)$. Assume that these two estimates a_1 and a_2 are such that $a_1 > a_2$ so that an order relation problem exists. New estimates will be sought at zc_1 and zc_2 which obey

the order relations and minimize the squared deviation from the original solutions a_1 and a_2. That is solutions which minimize

$$D^2 = (\phi^{**}(A,zc_1) - a_1)^2 + (\phi^{**}(A,zc_2) - a_2)^2 \qquad (2.66)$$

subject to $\phi^{**}(A,zc_1) \leq \phi^{**}(A,zc_2)$

will be sought.

This problem can easily be represented graphically, as the objective, D^2, is a circle of radius D centered on the point (a_1,a_2) and the constraint $\phi^{**}(A,zc_1) \leq \phi^{**}(A,zc_2)$ is a half plane.

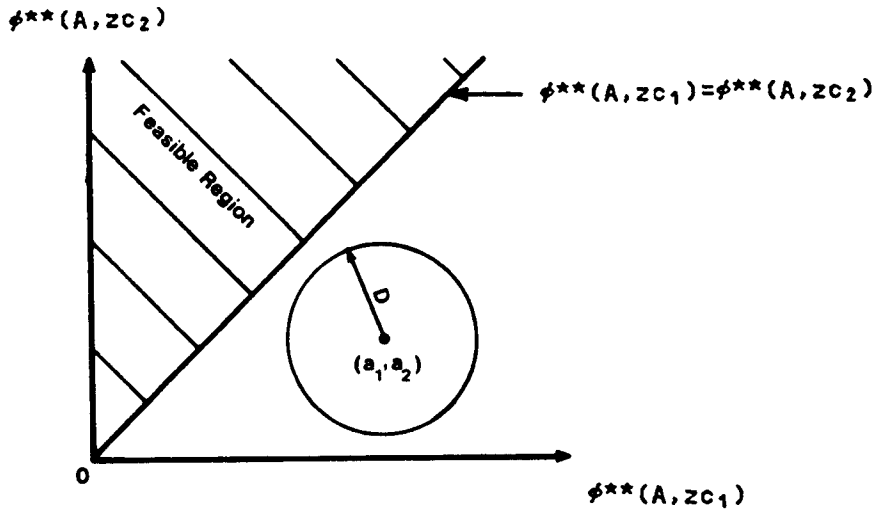

Figure 5: Graphical Representation of the Quadratic Program

The optimal solution is the feasible solution which minimizes the radius of the circle defined by the objective function. The feasible solution which yields the smallest radius D is the solution at which the

circle is tangent to the line $\phi^{**}(A,zc_1)=\phi^{**}(A,zc_2)$, therefore the optimal solution is $\phi^{**}(A,zc_1)=\phi^{**}(A,zc_2)$.

If an order relation problem involving more than two cutoffs occurs, the same logic can be used to obtain the solution. The objective function can be seen as a sphere or hypersphere while the constraint appears as a hyperplane. Again the solution occurs at the point on the hyperplane which is tangent to the hypersphere. That is, given an order relation problem involving n+1 cutoffs, the solution is;

$$\phi^{**}(A,zc_i)=\phi^{**}(A,zc_{i+1})=\ldots=\phi^{**}(A,zc_{i+n}). \qquad (2.67)$$

An example of possible order relation problems and their solution are given in figure 6.

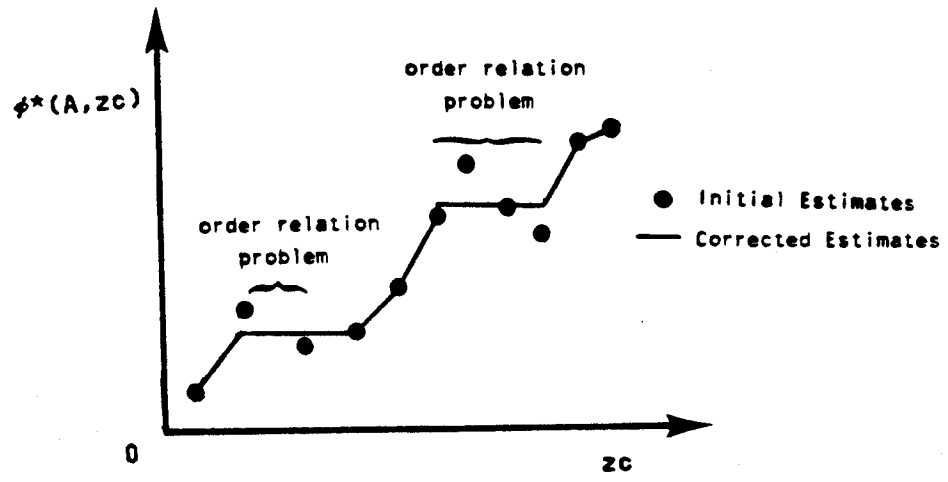

Figure 6: Order Relation Problems and Their Resolution
Notice that the solution $\phi^{**}(A,zc)$ is constant throughout the indicated regions of order relation problems.

As demonstrated by relation 2.67 and figure 6, the proposed solution to the order relation problems yields a constant value for all cutoffs within the region of the order relation problem. The value of this constant must now be determined.

Assume that the order relations are violated over a region comprising n cutoffs. The valid distribution function which minimizes the deviations from the initial kriging solutions is some constant value "a" throughout the region of the problem. It remains to determine the value of this constant value a. Reformulating equation 2.64, the problem is

$$\text{Min } V = (\phi^*(A,zc_i)-a)^2+(\phi^*(A,zc_{i+1}-a)^2+\ldots+(\phi^*(A,zc_{i+n-1}-a)^2 \tag{2.68}$$

The solution to this optimization problem is obtained by setting the derivative of V with respect to a to zero.

$$\frac{dV}{da} = 0 = -2\cdot\phi^*(A,zc_i)-\ldots-2\cdot\phi^*(A,zc_{i+n-1}) + 2\cdot n\cdot a \tag{2.69}$$

$$a = \left(\sum_{j=1}^{n} \phi^*(A,zc_{j+i})\right)/n \tag{2.70}$$

Thus to fit a valid distribution function which minimizes the sum of the squared deviations from an estimated distribution function with order relation problems, simply average the initial estimates within the region of the order relation problems.

2.8 QUANTITY OF METAL ESTIMATION

In mining applications, knowledge of the percentage of material within a given region above or below a cutoff grade is not sufficient. Of equal or greater importance is knowledge of the quantity of metal (i.e. tons of copper or ounces of gold) recovered. The actual quantity of metal above a given cutoff (for point support smus) within a region A can be expressed as

$$Q(A,zc) = \frac{T_a}{(A)} \cdot \int_{x \in A} (1-i(x,zc)) \cdot z(x)\, dx \qquad (2.71)$$

where T_a is the total tonnage of region A.
T_a is assumed equal to 1 in the following discussion to simplify notation.

Following the pattern used in developing an estimator for $\phi(A,zc)$, $Q(A,zc)$ could be randomized, structural functions determined and the quantity of metal within region A could be obtained kriging data defined as $[1-i(x_\alpha,zc)] \cdot z(x_\alpha)$. There are, however, three major obstacles to proceeding in this fashion.

1. The covariance for the random variable $(1-I(x,zc)) \cdot Z(x)$ would be extremely difficult to infer, especially in erratic deposits as the covariance or variogram for this variable would be strongly influenced by large z(x) values.

2. Obtaining accurate estimates of $(1-i(x_\alpha,zc)) \cdot z(x_\alpha)$ is difficult at high cutoffs, as the majority of data are zero while the remainder of the data are very large.

3. The possibility of order relation problems is increased as the quantity of metal and tonnage recovered are interrelated. Order relation problems must be rectified by solving a large quadratic program with a suitable objective function and constraints which ensure that the order relations hold for both $Q^*(A,zc)$ and $\phi^*(A,zc)$.

Due to the above difficulties, the quantity of metal is obtained by a simple non-probabilistic method which has performed well in case studies.

The point support quantity of metal recovered within a given region A is

$$Q(A,zc) = \frac{1}{(A)} \cdot \int_{x \in A} (1-i(x,zc)) \cdot z(x)\, dx \tag{2.72}$$

Examine the quantity $(1-i(x,zc)) \cdot z(x)$,

$$(1-i(x,zc)) \cdot z(x) = \begin{cases} z(x) & \text{if } z(x) > zc \\ 0 & \text{if } z(x) \leq zc \end{cases} \tag{2.73}$$

In Stieltjes integral notation[1],

$$(1-i(x,zc)) \cdot z(x) = \int_{zc}^{\infty} u\, d\phi(x,u) \tag{2.74}$$

where $\phi(x,u)$ is the cdf at point x

Thus,

$$Q(A,zc) = \frac{1}{(A)} \cdot \int_{A} \int_{zc}^{\infty} u\, d\phi(x,u)\, dx \tag{2.75}$$

$$= \frac{1}{(A)} \cdot \int_{zc}^{\infty} \int_{A} u\, d\phi(x,u)\, dx \tag{2.76}$$

---

[1]The Stieltjes integral (Stieltjes, 1918) is an alternative expression for the usual Riemann integral as $\int uf(u)du = \int u dF(u)$ providing f(u) is continuously differentiable.

$$= \frac{1}{(A)} \cdot \int_{zc}^{\infty} u d\phi(A,u) \qquad (2.77)$$

Evaluation of the above Stieltjes integral requires values of $\phi(A,zc)$ at an infinite number of cutoffs and also assumes that the true value of $\phi(A,zc)$ is completely known. Since, in reality, estimates of $\phi(A,zc)$ are available at a limited number of cutoffs, the above integral is replaced by the following discrete approximation.

$$Q^*(A,zc_i) = \sum_{j=i}^{nc-1} c_j \cdot (\phi^*(A,zc_{j+1}) - \phi^*(A,zc_j)) \qquad (2.78)$$

where c_j is some measure of central tendency for the grades found between cutoffs j and j+1.

As the estimates $\phi^*(A,zc)$ can be computed at any cutoff of interest, the only unknowns in the above expression for recovered quantity of metal are the c_j values. Ideally these measures of central tendency for the material between cutoffs zc_j and zc_{j+1} would be conditioned to the particular local environment of the panel being estimated. If the measure of central tendency, c_j, used is the mean grade of material between cutoffs zc_j and zc_{j+1}, local conditioning of the c_j values could conceivably be performed by considering a random variable $C_j(x)$ ($C_j(x)=Z(x)$ for $zc_{j-1} \leq Z(x) \leq zc_j$ and 0 otherwise) and attempting to estimate its realization at each panel of interest. This procedure for estimating local c_j values is not utilized; however, due to the difficulty of inferring the spatial correlation of the variable C_j and the paucity of non-zero realizations of $C_j(x)$ available within any local environment.

Since the c_j values cannot, reliably, be estimated locally, a global value is used. A readily available value for c_j, which was used in all the following case studies, is the average (accounting for clusters) of all exploration data with values between cutoffs zc_{j+1} and zc_j. This simple global approximation of the c_j values has proven to give reliable results in case studies.

Chapter III

ESTIMATION OF SPATIAL DISTRIBUTIONS FOR A SIMULATED DEPOSIT

This chapter contains the first of two case studies involving the application of the non-parametric estimators of point support, spatial distributions developed in the previous chapter. These case studies will emphasize the practical rather than the theoretical aspects of the techniques; thus, at each step in the application of the techniques the procedures which must be followed, the computer programs required, as well as the potential trouble spots will be discussed. After this step by step discussion, the estimates obtained by each estimator will be compared both with estimates obtained by other estimators to determine, if possible, the best non-parametric estimator and with the true local spatial distributions to obtain some idea of the quality[1] of results which can be expected when applying these techniques.

The case study which will be discussed here involves utilizing both the IK and PK estimators to estimate local, point support, spatial distributions for a simulated deposit. A simulated deposit was chosen because this was the first application of the PK estimator and when testing a new estimation technique, a simulation proves invaluable. Not only can the results given by the new technique be compared with the results of other more established techniques, but they can also be

---

[1]The term quality is used here as a qualitative measure of the effectiveness of an estimator in reproducing the true local spatial distribution.

compared with the actual or true value of the variable being estimated. Comparing the estimates with true values gives an indication of the quality of the new estimator and allows one to make a sound judgement, based on concrete evidence rather than on emotion or gut feeling, concerning the performance of the estimator.

As stated, this case study represents the first application of the PK technique, hence the performance of the technique will be examined over a wide range of cutoff values to determine both the strengths and weaknesses of this new technique. This study is thus seen as an investigation of the properties of the PK estimator rather than a test of the ability of the estimator to estimate recoveries at a fixed economic cutoff. Therefore, in this study, only the spatial distribution will be estimated, at cutoffs spanning the range of simulated values, while the economic variables associated with the spatial distribution (tonnage and quantity of metal recovered) will be discussed in the next case study which involves applying non-parametric spatial distribution estimators to an actual deposit.

Before proceeding with the estimation of spatial distributions for this simulated deposit, its properties will be discussed to gain some insight into its nature.

3.1 PROPERTIES OF THE SIMULATED DEPOSIT

The simulated deposit which will be considered is termed the Stanford 2B deposit. This conditional simulation contains 24,200 simulated values located on a regular 1 foot grid within a 110 x 220 foot north-south elongated rectangle defining the deposit limits. The

mineralization (generally taken as copper however this distinction is not important) in the region surrounding the Stanford 2B deposit is concentrated in east-west elongated pods, one of which occurs in the central portion of Stanford 2B. This pod shows clearly on a contour map of 200 point grade values located on a regular 11 foot grid (fig. 7) as the high grade zone of mineralization in the center of the deposit. The continuity of the grades is stronger in the east-west direction as demonstrated by the relative elongation of the contours in that direction. The extreme northern and southern sections of the deposit are essentially barren and would be of little interest in any actual study where the quantity of interest was local recoveries. However, as this study is designed to examine the effectiveness of spatial distribution estimation techniques over a wide range of conditions, estimation of spatial distributions will also be performed in these low grade regions.

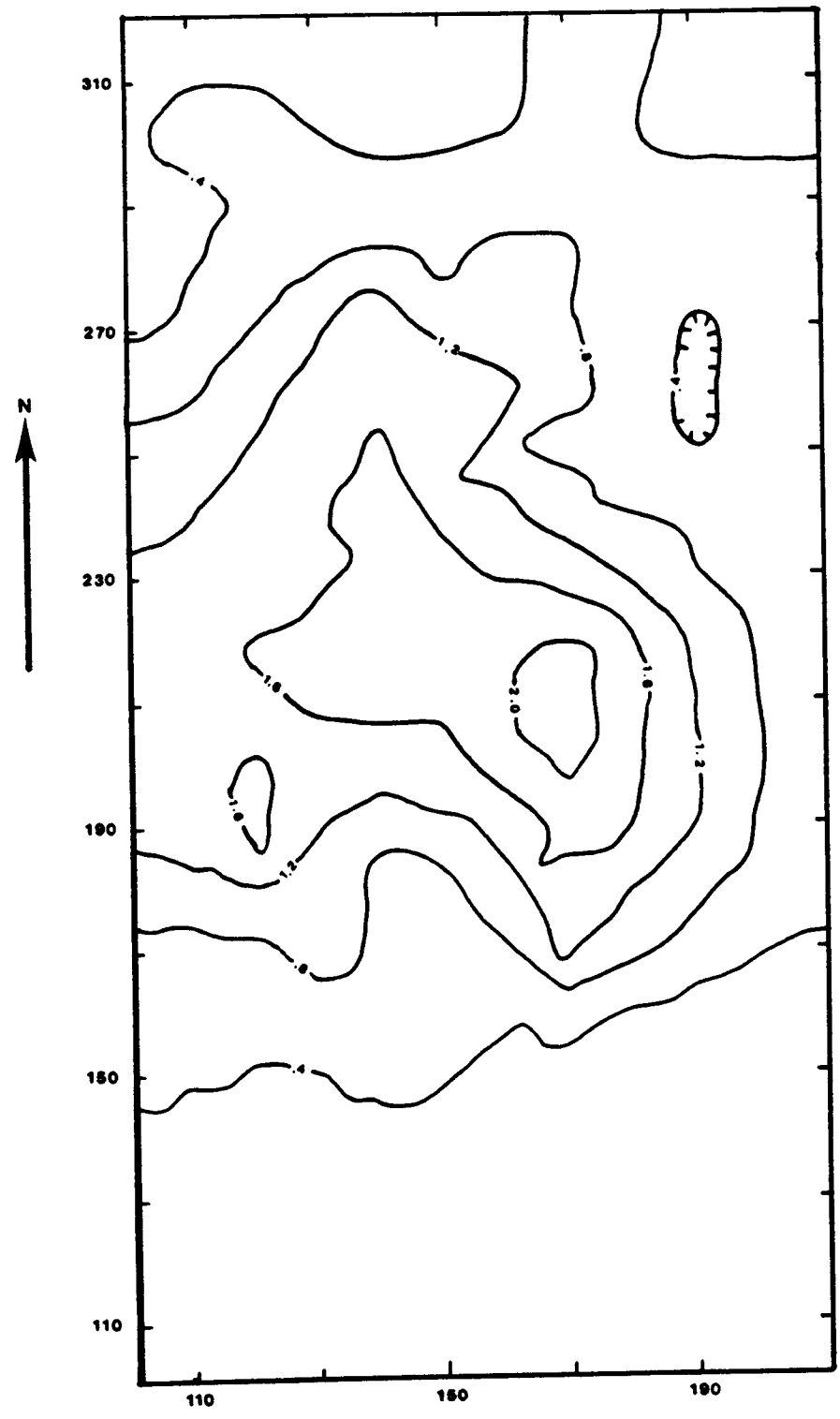

Figure 7: Contour Map of the Stanford 2B Deposit

3.1.1 Basic Statistics

The mean, m, of the 24,200 conditionally simulated values is .75% with a standard deviation, σ, of .672%. The coefficient of variation, σ/m, which gives a unitless measure of the variability of the deposit is .90. This is rather low compared to the coefficients of variation observed in deposits with erratic mineralization such as the Jerritt Canyon deposit which will be discussed in the next case study. The distribution of the simulated values (fig. 8) shows that 22% of the values are equal to zero. These values will be referred to as the spike. The maximum observed value, 3.45%, is a factor of 4.6 times larger than the mean value. This factor is small in comparison with those found in erratic gold or uranium deposits, where values that are 20 times larger than the mean commonly occur. In comparison to erratic deposits then, this deposit does not have many of the outlier values which can cause an estimator to give poor results. This lack of outliers coupled with the relatively low coefficient of variation of the simulated values indicate that this is not an extremely erratic deposit, so a sound estimation technique should perform well.

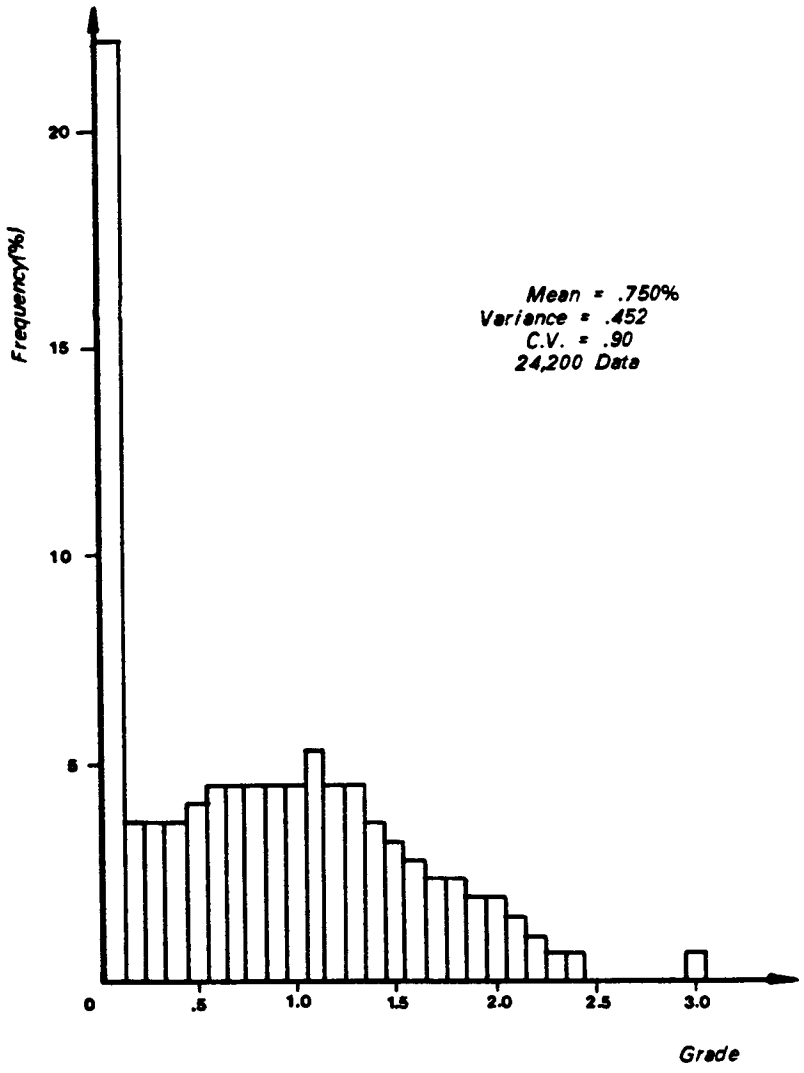

Figure 8: Histogram of the 24,200 Simulated Values

3.1.2 Variogram Analysis

The variogram of the 24,200 simulated values calculated parallel and perpendicular to the assumed direction of maximum continuity (east-west) shows a zonal anisotropy for distances greater than 25 feet (fig. 9).

The east-west variogram can be modelled by a single spherical structure with a range of about 30 ft. and a total sill of .28%^{2}. The north-south variogram rises very quickly to a maximum value of .75%^{2} at 90 feet, then decreases rapidly. For distances near 210 feet, the variogram value is close to zero; thus, this variogram exhibits a hole effect. The large north-south variogram values correspond to distances for which one of the pair of data is located in a low grade zone while the other is located in a high grade zone. At a distance of approximately 210 feet, however, both data are located in low grade material (fig. 7), hence the variogram value is small. This observed hole effect in the north-south direction is therefore predictable by an examination of the contour map of the data.

Both the north-south and east-west variograms indicate that this deposit is not large enough for the variograms to exhibit a true sill. The variogram in the east-west direction definitely does not show its final sill over the distance of observation. The observed sill is merely an intermediate structure. The observed dispersion variance of the data in the deposit, .452%^{2}, is much greater then the observed sill of the east-west variogram. Since $.452=D^2(0/D)<D^2(0/\infty)=\gamma(\infty)=Var(Z(x))$, the east-west variogram will rise at large distances to some value greater than .452%^{2}.

The north-south variogram shows such a prominent hole effect because there is only one high grade pod of mineralization within the deposit. If the deposit continued in the north-south direction, and more high grade pods were found, the observed hole effect would dampen out, as these high grade pods are not regularly spaced.

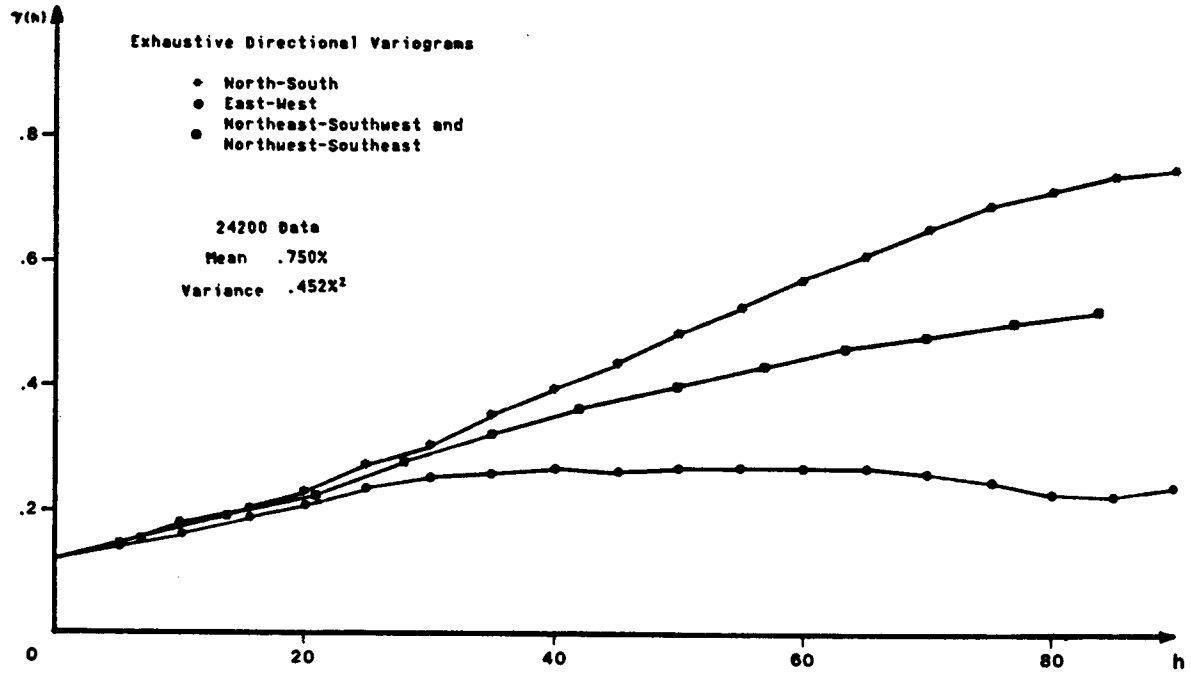

Exhaustive Directional Grade Variograms

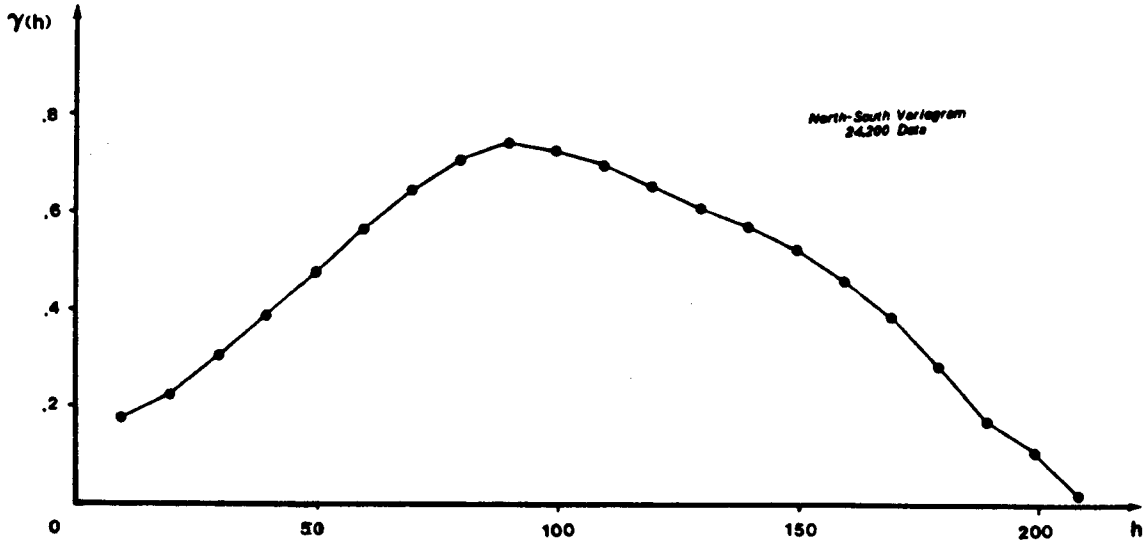

Exhaustive North-South Variogram of Grade at Large Distances

Figure 9: Variograms of the 24,200 Simulated Values

3.1.3 True Spatial Distributions

A major portion of this case study will be devoted to a comparison of the estimated distributions obtained by non-parametric estimators with the true or actual distributions. Hence a discussion of the method of determining the actual distributions is warranted.

To determine actual spatial distributions, the deposit is divided into 200 square non-overlapping 11 ft. x 11 ft. panels (see figure 10). Each panel contains 121 simulated values on a regular 1 foot grid which are used to determine the true or actual distribution of points within the panel. For instance, to determine $\phi(A,zc)$ for a given cutoff zc and panel A simply determine the proportion of the 121 simulated points located within the panel with values less than or equal to zc.

3.2 EXPLORATION DATA BASE

In an estimation procedure, the results obtained are dependent on both the quality and the quantity of the available data. The importance of this statement varies from deposit to deposit and from estimator to estimator. This statement is very important, however, when testing a new estimator since testing a new estimator is a delicate procedure in which the quality of the results obtained by the estimator determine, if the estimator is of acceptable quality, or if enhancements of the estimator must be made, or if the estimator is of such low quality that it should be discarded. It is, therefore, of the utmost importance that the data base does not introduce any errors that might bias any conclusions drawn concerning the performance of the estimator. As this case study represents the first application of the PK technique it was

considered as a test of the performance of the technique, thus to eliminate any false impressions a fairly dense, regular data set will be considered.

The chosen data set which will be utilized by both the IK and PK techniques consists of 200 values located at the centers of each of the 200 previously defined panels (fig. 10), These data are, thus, located on a perfectly regular 11 foot grid. This set of 200 data will be termed the exploration data base as it mimics the set of data which would be obtained by exploratory drilling of this orebody under ideal conditions.

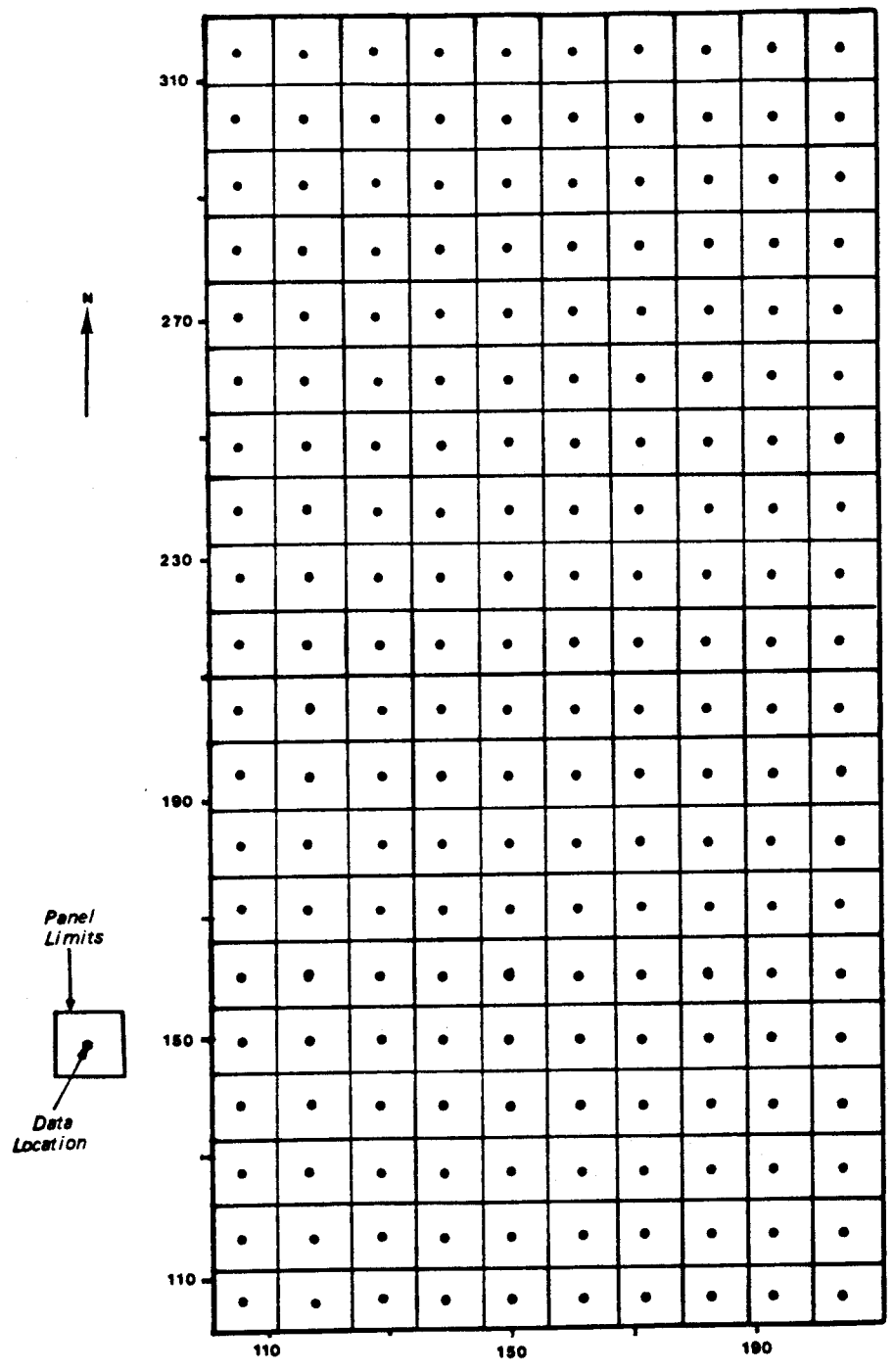

Figure 10: Map of Stanford 2B Deposit Showing Data Locations and Panel Limits

3.3 STEPS IN OBTAINING A NON-PARAMETRIC ESTIMATE OF A SPATIAL DISTRIBUTION

The non-parametric estimation of spatial distributions involves three major steps which are similar to the steps which are followed when estimating mean block grade.

Step 1: Data analysis
Step 2: Variogram computation and modelling
Step 3: Kriging

The importance of each of these steps as well as their relative cost, in terms of human and computer time, are discussed below.

The data analysis step is very important as it gives one a general understanding of the nature of the data. Although important and time consuming this step involves little computer cost. This step normally includes an examination of the geology to determine if statistically different geologic populations can be identified, checking for any proportional effect between the local mean and standard deviation, examining the data base closely to make sure no data entry errors are present, and various other procedures which come under the heading of exploratory data analysis. This step is normally time consuming; however, in this study the scope of the data analysis step is greatly reduced as the data are chosen from a single population conditional simulation which by definition implies that the data are accurate and come from one geologic population. In this case, therefore, the data analysis step will be reduced to computing univariate statistics of the data.

The major step in a non-parametric estimation study, both in terms of time and expense, and in terms of obtaining an accurate estimate, is the variography step. Variogram estimation and modelling is time consuming because there are such a large number of variograms. If an estimate of the complete local distribution is required, estimates of $\phi(A,z_c)$ must be obtained at a sufficiently large number of cutoffs (approximately 10) to adequately discretize the range of cutoff values. As an indicator variogram is required at each cutoff of interest when applying the IK estimator and both indicator and cross variograms plus a variogram of the uniform transform data are required at each cutoff when applying the PK estimator, a large number of variograms are required to estimate the entire spatial distribution. Each of these variograms must be modelled as accurately as possible because, in addition to the available data, the variogram model is the only piece of information utilized by these estimators. Thus, the quality of the estimates will depend to a large degree on the quality of the variogram models.

The primary cost in the variography step of the study is the modelling and not the computation of the variograms. If variograms are required at several cutoffs, these variograms, both direct and cross, can be determined in one run of a multivariate variogram program (see sec 7.1 for such a routine), thus the cost in terms of computer time is not significantly greater than the cost of determining the variogram for one variable. The time required and therefore the cost of modelling the various variograms can be reduced considerably by utilizing an interactive computer terminal to examine and enhance the fit of a model.

Both kriging and obtaining the final estimates are performed entirely by the computer and therefore require no human time. The kriging computation time will be decreased significantly if kriging is performed for all cutoffs at the same time. This eliminates the high cost of searching the data base for each cutoff. Since searching the data base to find the data in the kriging neighborhood is one of, if not the most expensive step in kriging, simultaneously solving the kriging systems at several cutoffs is not significantly more time consuming than solving a kriging system for one variable, especially if the system solving routine is set up to handle more than one variable (see subroutine ksol, see sec 7.2).

3.3.1 Data Analysis - Stanford 2B Deposit

The Stanford 2B deposit has been sampled by 200 simulated drill holes on 11 ft. centers. Sampling the simulation on a regular grid removes the possibility of encountering troublesome clustered data. A subset of data is termed clustered when the interdistance between the data in the subset is less than the average interdistance between data throughout the deposit. Clustered data are a problem because the data within the cluster have a higher degree of redundancy than the remaining data in the deposit; thus, clustered data should receive less importance than non-clustered data when computing statistics of the data. If clustered data had been encountered, the influence of the clusters would have been down weighted to obtain an accurate estimate of the global histogram. One method for removing the influence of clusters is the cell declustering technique (Journel, 1982). Performing unconstrained

indicator kriging or any form of probability kriging without first declustering the data will certainly introduce errors into the estimation as both of these methods require a prior reliable estimate of the global histogram.

Given that the 200 available data are located on a regular grid, no declustering is required. In addition, there is no geology associated with this simulation, so no attempt will be made to separate the simulation into different geological populations as is often done in actual studies. The only data analysis required for this simulation is calculating histograms and examining contour maps.

The histogram of the 200 data (fig 11) shows many of the same features as the histogram of the 24200 simulated values (fig 8). Some of the features of these histograms can be compared through a simple table (see table 1).

TABLE 1

Comparison of Comprehensive and Exploration Data Sets

	Data Set	
	200 Data	24200 Simulated Values
mean	.728	.750
variance	.430	.452
coefficient of variation (σ/m)	.901	.896
% of values = 0	20.0	22.18
maximum value	3.09	3.45

Although the mean and variance of the 200 data are less than the comprehensive values, the comparison between these two sets of values is

generally good and indicates that the 200 data provide a representative sample of the deposit. A better indication of the representativity of the set of 200 data is given by comparing the cumulative distribution function (cdf) of the 200 data with the cdf of the 24,200 data which comprise the simulation.

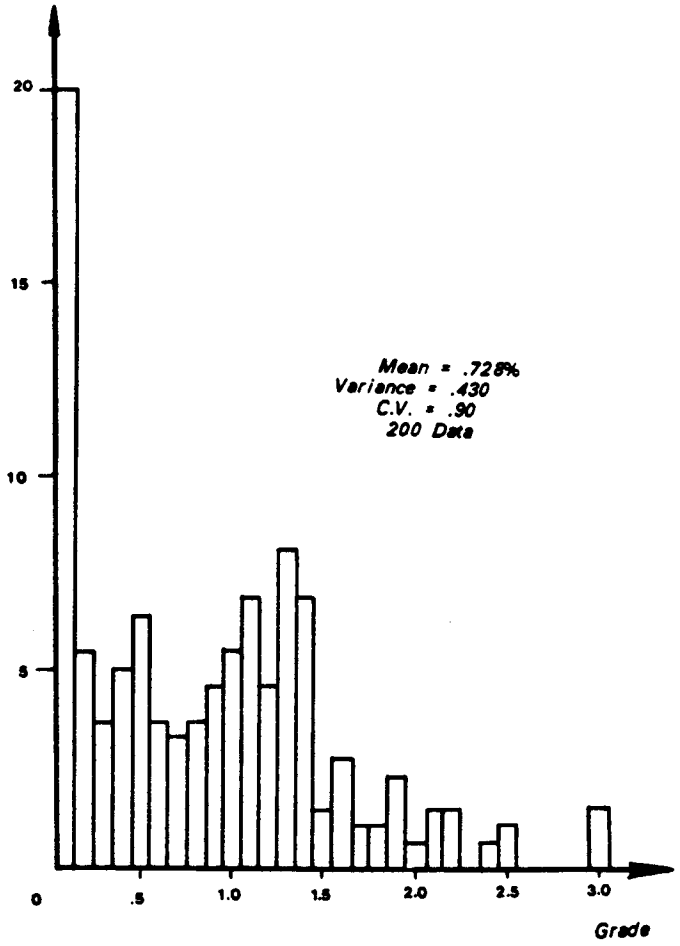

Figure 11: Histogram of the 200 Exploration Data

The cutoffs at which these two cdfs will be compared are identical to those at which the local cdfs will be estimated. These cutoffs were chosen so that they span the entire range of grades. The lowest cutoff, 0%, is determined naturally by the spike of zero grades. Twenty two percent of the 24200 data are zero's so the non-zero cutoffs were determined by dividing the remaining 78% of the values into 10 approximately equal frequency classes. The ten cutoffs and the percentage of the data below these cutoffs are given in table 2.

TABLE 2

Comparison of CDF's at Selected Cutoffs

CUTOFF	% OF DATA ≤ CUTOFF	% OF SIM. VALUES ≤ CUTOFF
0.	20.	22.2
.175	27.	28.6
.325	36.	34.5
.510	44.5	42.5
.740	51.	53.4
.905	60.	61.0
1.03	68.5	67.8
1.14	75.5	72.9
1.28	84.	78.5
1.73	91.7	90.7

The values in table 2 indicate that the cdf of the 200 data provides a good representation of the cdf of the 24,200 simulated values at all cutoffs except 1.28%. At the 1.28% cutoff there is a large difference between the two cdfs. This implies that the 200 data are unrepresentative of the 24,200 simulated values at this cutoff. As the

non-parametric techniques which will be used are strongly based on the available data, the unrepresentativity of the data at this cutoff will most probably translate into a bias in both the PK and IK estimates, for this particular cutoff value.

Before proceeding with the next step, variography, some simple transforms of the data on which the variograms will be calculated must be computed. These transforms are the uniform transform (sec 2.6) and the indicator transform (sec 2.3.1). The indicator transform can be performed on any set of data regardless of the data or cutoff grades considered; thus, in this sense it is a completely general transform. To perform the indicator transform for the Stanford 2B data set simply compare each of the 10 cutoffs (table 2) to each of the 200 data. When the cutoff is larger than the data value, the indicator datum for that cutoff is 1 otherwise it is zero. For this deposit then the single grade datum at each location is transformed into 10 indicator data or equivalently the grade z(x) is replaced by a discretized version of the point spatial distribution $\phi(x,zc)$. In contrast to the indicator transform, the uniform transform is not completely general as it contains a constraint that the transform be one to one. That is, each and every z(x) value must map into one and only one uniform transform value u(x). Often, as is the case for the Stanford 2B deposit, there is duplication of a certain z value. In such instances the transform from the z data to the u data is not one to one as more than one z value maps into one u value.

Duplication of certain z values is easily dealt with when only two or three of the z data share the same value. One randomly adds a very

small but different increment to each of the duplicated values which yields new z values with no duplicated values. This simple procedure is acceptable when the number of duplicated values is small; however, when a significant proportion of the data share a single value a random method of removing these multiple duplications may destroy the spatial correlation of the transformed values. Hence a procedure which removes multiple duplications of a given z value but preserves, to some extent, the spatial correlation of the data must be utilized.

Multiple duplication of a given z value is often referred to as a spike. In this data set 20% of the data are zero, hence the histogram is said to have a spike at zero. The spike at zero will be removed utilizing a deterministic procedure which "despikes" the data (Verly, 1984). The spike removing procedure is based on the notion that if two data values are equal, the value surrounded by larger data values should be considered larger for the purposes of the transform. This procedure, thus, utilizes information concerning the spatial continuity of the data in dissolving the spike.

The spike removing algorithm which was used finds all data within a given radius (16 ft. was used in this case study) of each zero grade datum and takes the average of all data found. For each spike value, therefore this algorithm calculates a local average. The spike data are now ranked by their local average and transformed. A small example of this procedure is given in table 3.

The uniform transform which was performed on the Stanford 2B data set is shown in simplified form in figure 12. Following this transform the data follow a uniform distribution bounded by zero and one, so that $E[U(x)]=.5$ and $Var[U(x)]=.0833$.

TABLE 3

An Example of the "Despike" Procedure

Consider a spike at zero consisting of 5 data

Grade z(x)	Local Average	Rank of Local Average	u(x)
0.	.15	5	5/N
0.	.03	2	2/N
0.	.01	1	1/N
0.	.09	3	3/N
0.	.11	4	4/N

Where N is the total number of data.

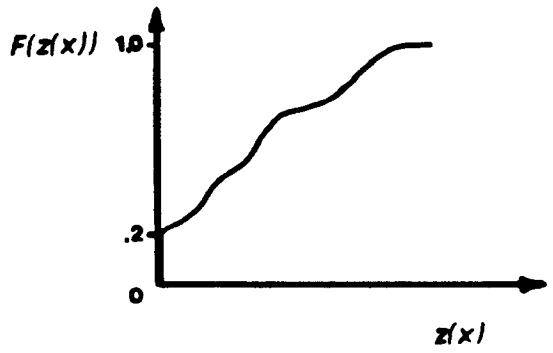

Schematic CDF of the 200 Exploration Data Showing the Spike at Zero

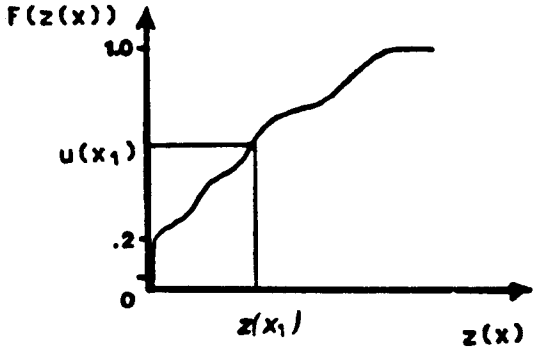

The "Despiked" CDF of the 200 Exploration Data

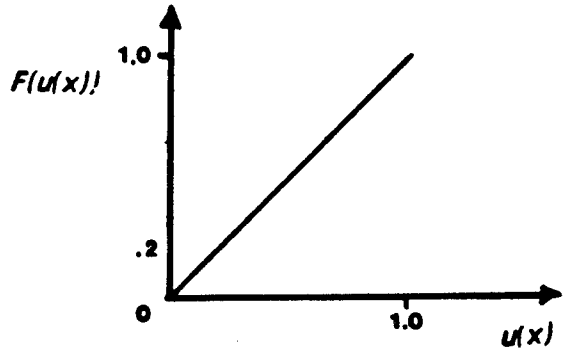

The CDF of the Uniform Transformed Values u(x)

Figure 12: Graphical Representation of the Uniform Transform

3.3.2 Variography

The variography step of an indicator or probability kriging study is of primary importance. As these techniques do not rely on any distributional model, all of the information concerning the bivariate properties of the data must be obtained by modelling the various indicator and cross variograms (see section 2.6.1).

To obtain an indicator kriging estimate of $\phi(A,zc)$ at a given cutoff zc, an indicator variogram model is required. Hence for each cutoff of interest, 10 in this case, an indicator variogram must be computed and modelled. The indicator variograms for the 10 cutoffs of interest all show anisotropies at large distances similar to that shown by the indicator variogram at the median cutoff, .74, (fig 13). Notice that the anisotropy is not accentuated for distances less than 33ft; therefore, if no variogram values are required for distances greater than 30ft, an isotropic variogram model will be sufficient. In order to make variogram modelling as simple as possible, a small kriging neighborhood will be considered so that isotropic variogram models will be sufficient. The 10 omnidirectional experimental variograms and the corresponding isotropic models are given in figures 14 through 17. The models for all 10 cutoffs are summarized in table 4.

The indicator variograms show a large nugget effect at all cutoffs. The relative nugget effect is much larger at cutoffs less than the fiftieth percentile of the 200 data, where at 30 feet the nugget effect explains at least 75% of the variability (see table 4). As the cutoff increases the nugget effect accounts for less of the total variability, hence the material at high cutoffs appears to be more structured and

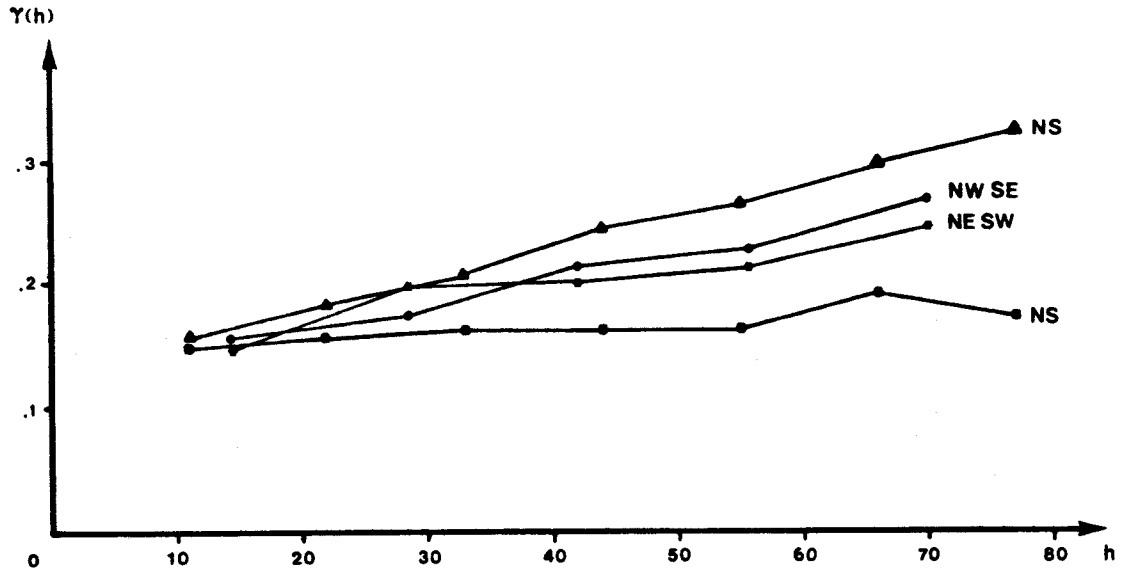

Figure 13: Experimental Directional Indicator Variograms for the .74% Cutoff

TABLE 4

Indicator Variogram Models

Cutoff	Model	nugget/γ_i(30)
0.	$\gamma_i(h) = .100 + .00025 \cdot h$	.93
.175	$\gamma_i(h) = .120 + .000556 \cdot h$	.88
.325	$\gamma_i(h) = .126 + .00098 \cdot h$	.81
.51	$\gamma_i(h) = .130 + .00120 \cdot h$	.78
.74	$\gamma_i(h) = .130 + .00144 \cdot h$	.75
.905	$\gamma_i(h) = .120 + .00190 \cdot h$	.68
1.03	$\gamma_i(h) = .120 + .00160 \cdot h$	.71
1.14	$\gamma_i(h) = .100 + .00167 \cdot h$	.66
1.28	$\gamma_i(h) = .070 + .00156 \cdot h$	.60
1.73	$\gamma_i(h) = .040 + .00188 \cdot h$	.41

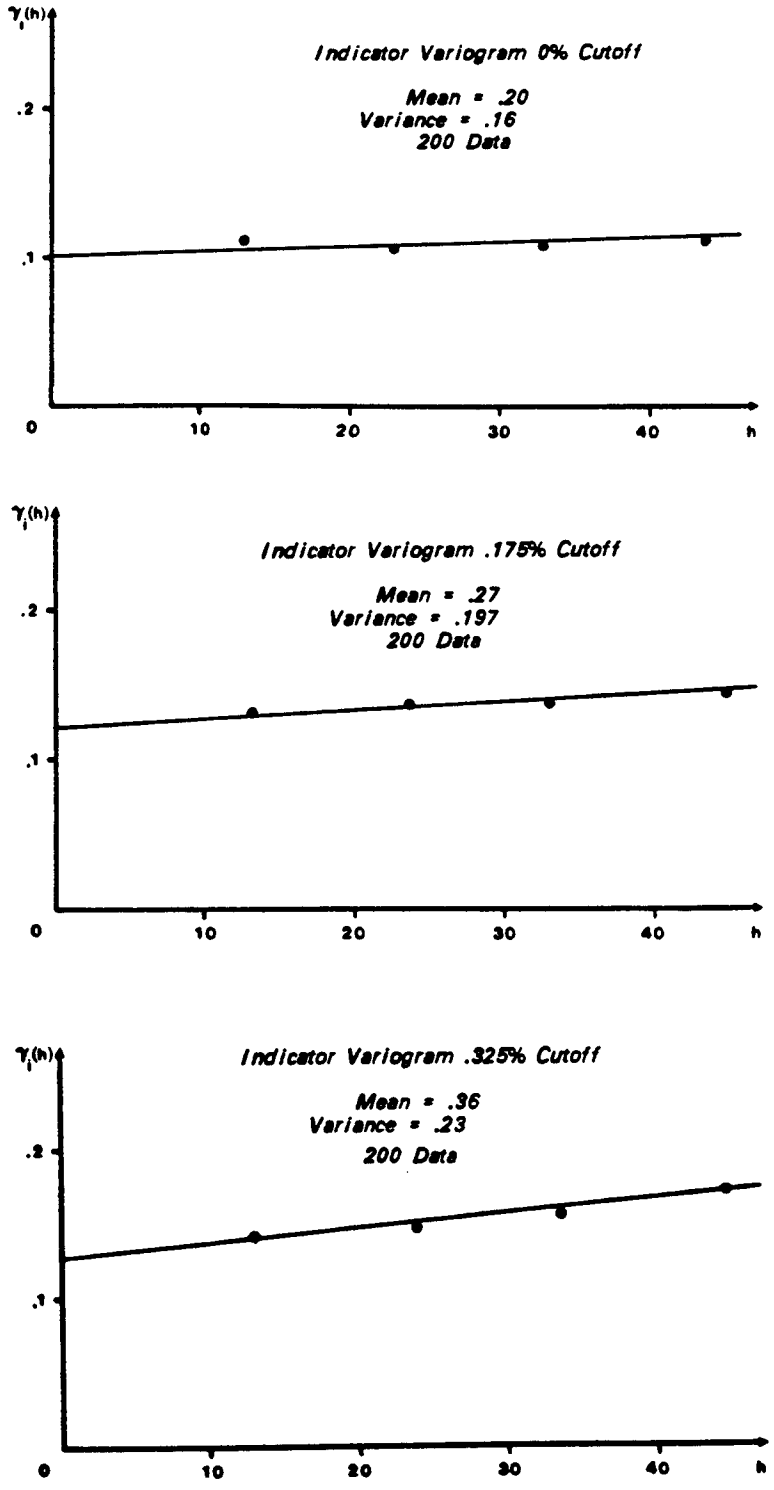

Figure 14: Indicator Variograms for the 0%, .175% and .325% Cutoffs

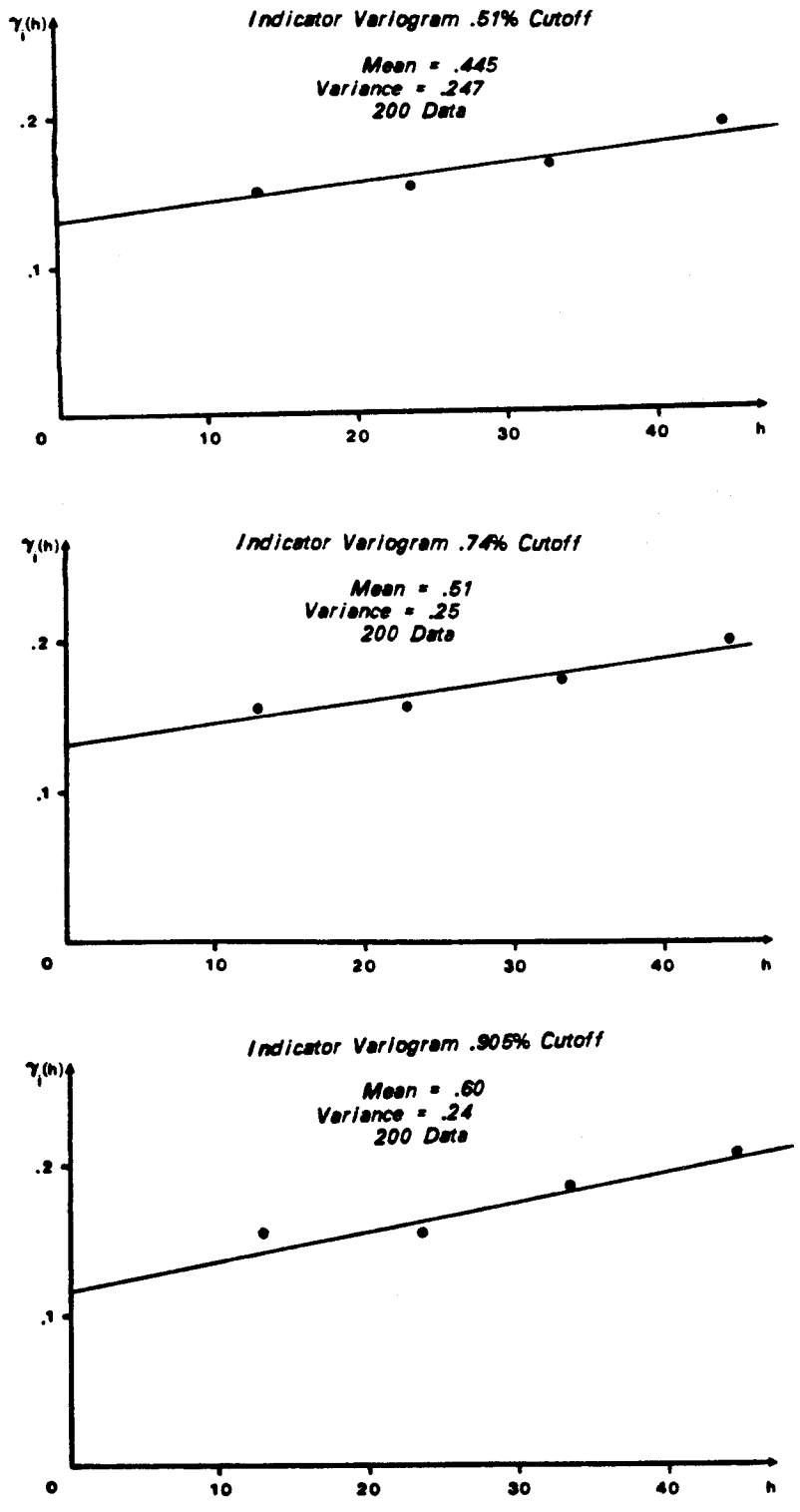

Figure 15: Indicator Variograms for the .51%, .74% and .905% Cutoffs

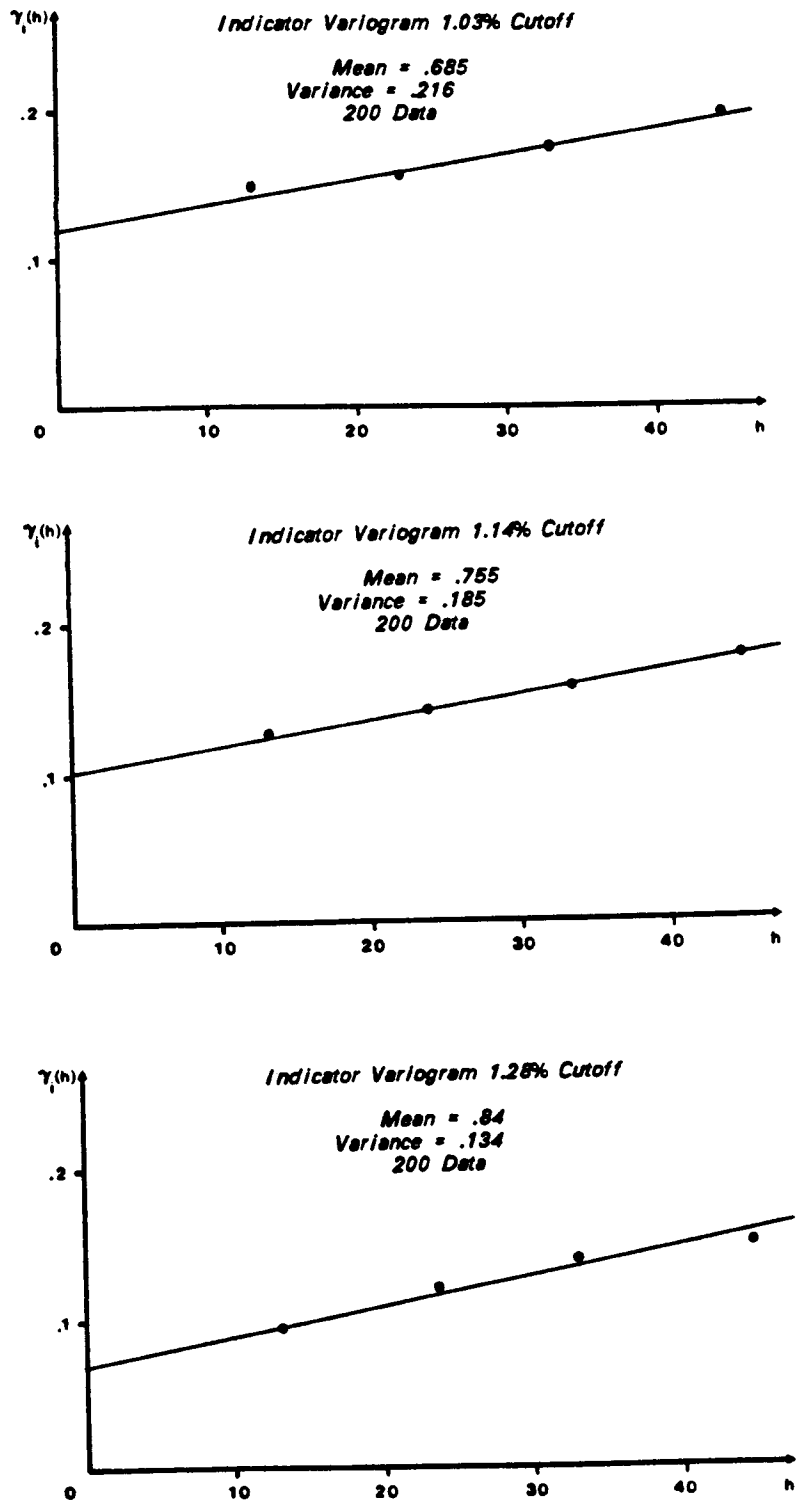

Figure 16: Indicator Variograms for the 1.03%, 1.14% and 1.28% Cutoffs

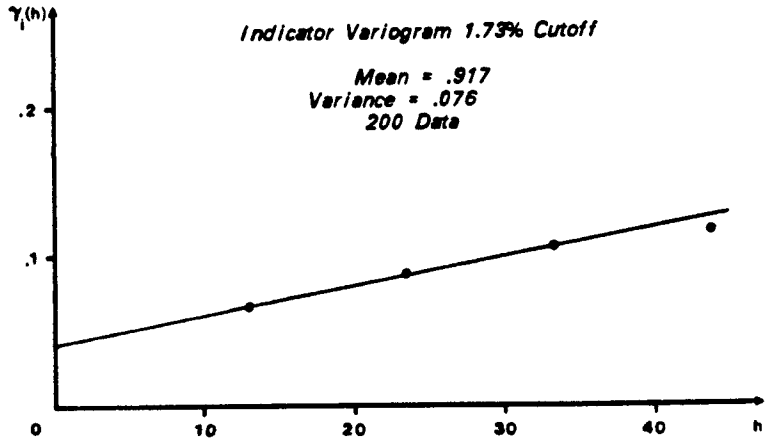

Figure 17: Indicator Variogram for the 1.73% Cutoff

less random than the material at low cutoffs. Simple linear variogram models were used as a linear model fits the experimental points very well and fitting a linear model is extremely simple.

To obtain a probability kriging estimate of $\phi(A,zc)$ at a given cutoff zc three variogram models are required. These three variograms include the previously discussed indicator variogram plus the variogram of the uniform transform and the uniform-indicator cross variogram. Modelling this coregionalization between the uniform and indicator data is slightly more demanding than modelling the simple regionalization of the indicator variable as the conditions necessary to ensure positive definiteness of a coregionalization put some constraints on the form of the model.

The positive definite conditions which ensure that all calculated variances will be positive; namely,

$$\begin{aligned} &\mathrm{Var}(Y) \geq 0 \\ &\text{where } Y = \sum_{i=1}^{n} \lambda_i \cdot I(x_i, zc) \\ &\text{and } \mathrm{Var}(Y) = \sum_{i}\sum_{j} \lambda_i \lambda_j C_i(x_i - x_j) \end{aligned} \tag{3.2}$$

are verified if a positive definite covariance model is chosen (see Journel and Huijbregts[1], 1978, pg. 161-171 for some of these covariance models). Notice that not all conceivable covariance models are positive definite. Similarly not all conceivable sets of covariance models for a coregionalization are positive definite. Thus, even if the indicator, uniform, and cross covariances are modelled by positive definite covariance functions this is no guarantee that the corresponding coregionalization model is positive definite. The condition which guarantees a positive definite coregionalization model is that the matrix of covariances be positive definite for any data configuration.

A positive definite coregionalization model can be obtained by considering a linear model of coregionalization (JH, pg 171). Under this model, both the cross and direct variograms are assumed to contain the same number and type of basic covariances. That is

$$C_{kj}(h) = \sum_{i=1}^{n} b_{kj}^{i} \cdot K_i(h) \tag{3.3}$$

where C_{kj} is the covariance between variables k and j for distance h.

---

[1]For convenience the reference Journel and Huijbregts, 1978 will be referred to as JH.

n is the number of nested positive definite covariances.

b_{kj}^{i} is the coefficient for structure i for the covariance between variables k and j.

$K_i(h)$ is the ith basic covariance.

The coregionalization model is positive definite when the determinant of the entire b_{kj}^{i} matrix as well as the determinants of its diagonal minors are positive for all i=1,n.

The practical implication of this linear model of coregionalization is that any covariance or variogram models which appear in the cross covariance model must also appear in the direct covariance models. Therefore, in this case study, the cross and uniform variogram models must be linear models of the form

$$\gamma(h) = C_0 + C \cdot h$$

to utilize a linear model of coregionalization. Furthermore, to ensure positive definiteness, the following inequalities must hold for the coefficients C_0 and C of the cross and uniform variogram models at each cutoff.

$$C_i \cdot C_u > C_{iu}^2, \; C_i > 0, \; C_u > 0$$

where C_i is C_0 or C for the indicator variogram model

C_u is C_0 or C for the uniform variogram model

C_{ui} is C_0 or C for the cross variogram model

The 10 cross and 1 uniform variograms in this study were modelled so that the above relations hold.

The cross and uniform variograms are modelled as isotropic since no significant anisotropy is observed for distances less than the diameter of the envisioned kriging neighborhood (31 ft.). These variograms and their models are given in figures 18 through 21. Note that the cross variogram is negative at all distances h. This is due to the negative correlation between the indicator and uniform data. The models used for these variograms are summarized in table 5.

TABLE 5

Cross and Uniform Variogram Models

Cross Variogram Models

Cutoff	Model	nugget/$\gamma_{ui}(30)$
0.	$-\gamma_{ui}(h) = .030 + .0004 \cdot h$	.93
.175	$-\gamma_{ui}(h) = .038 + .0005 \cdot h$	.88
.325	$-\gamma_{ui}(h) = .040 + .0008 \cdot h$	.81
.51	$-\gamma_{ui}(h) = .044 + .0009 \cdot h$	.78
.74	$-\gamma_{ui}(h) = .041 + .00105 \cdot h$	.75
.905	$-\gamma_{ui}(h) = .041 + .00105 \cdot h$	.75
1.03	$-\gamma_{ui}(h) = .038 + .00100 \cdot h$	.71
1.14	$-\gamma_{ui}(h) = .031 + .000825 \cdot h$	.66
1.28	$-\gamma_{ui}(h) = .018 + .000864 \cdot h$	.60
1.73	$-\gamma_{ui}(h) = .010 + .000469 \cdot h$	.41

Uniform Variogram Model

$\gamma_u(h) = .027 + .0007 \cdot h$

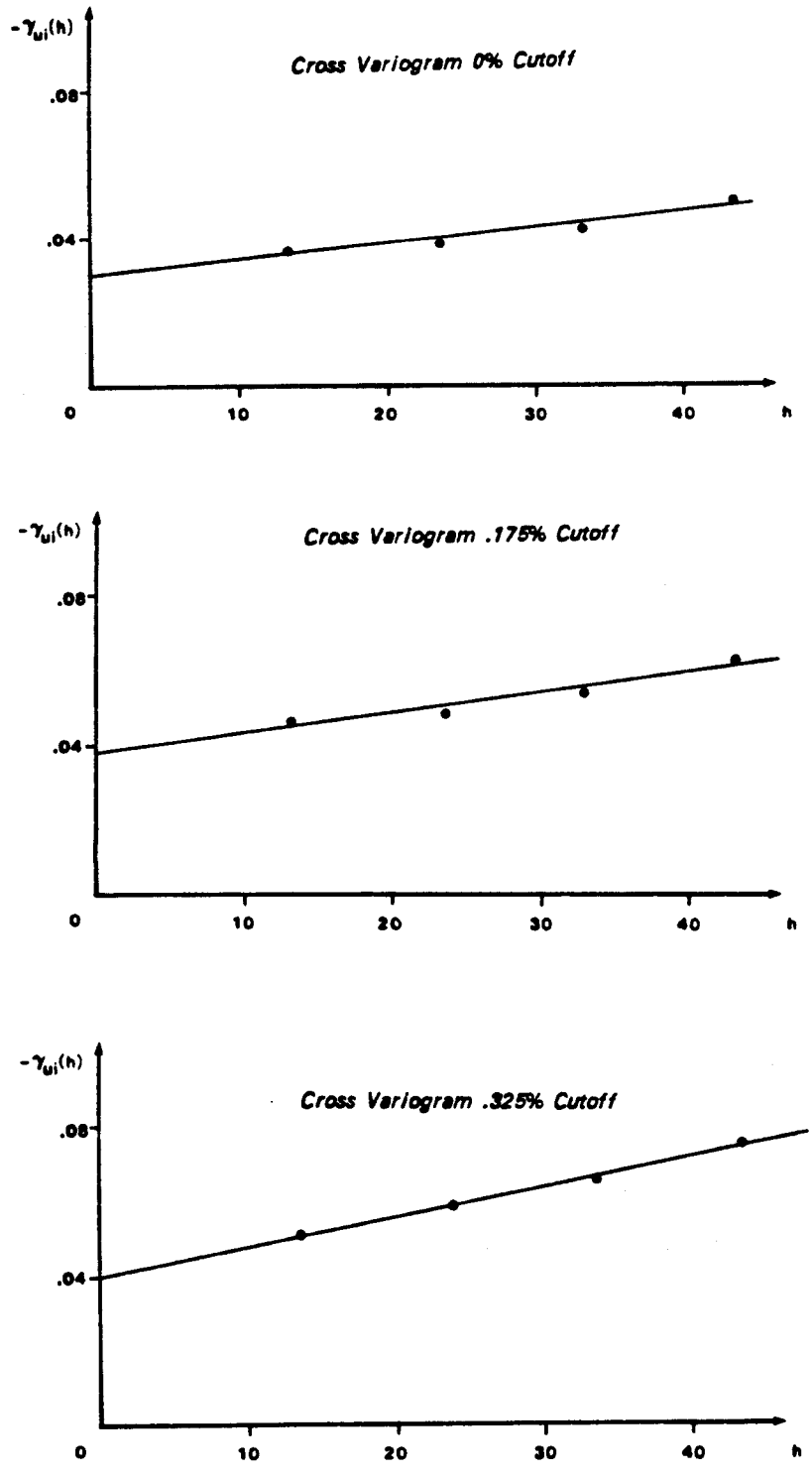

Figure 18: Cross Variograms for the 0%, .175%, and .325% Cutoffs

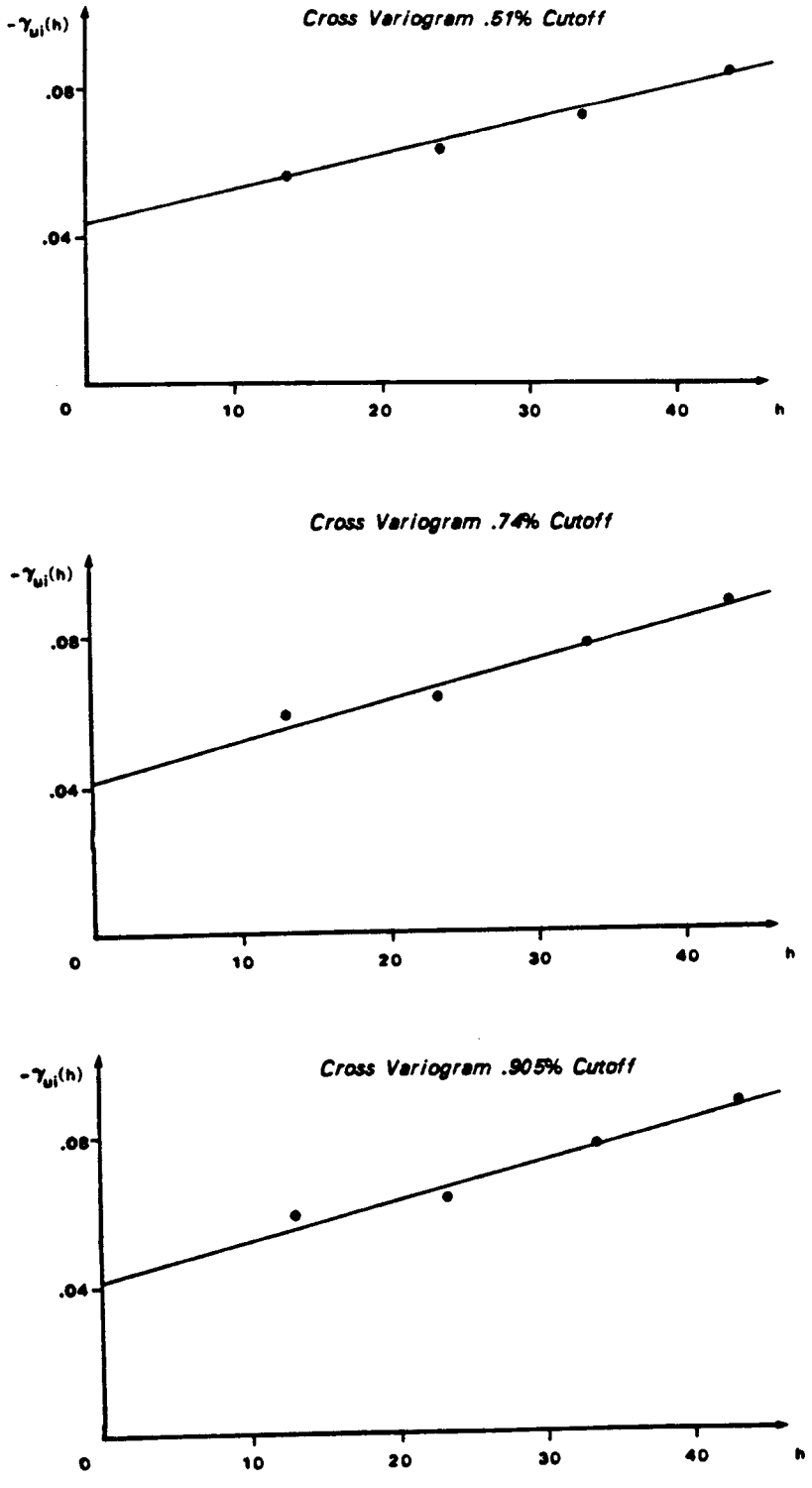

Figure 19: Cross Variograms for the .51%, .74%, and .905% Cutoffs

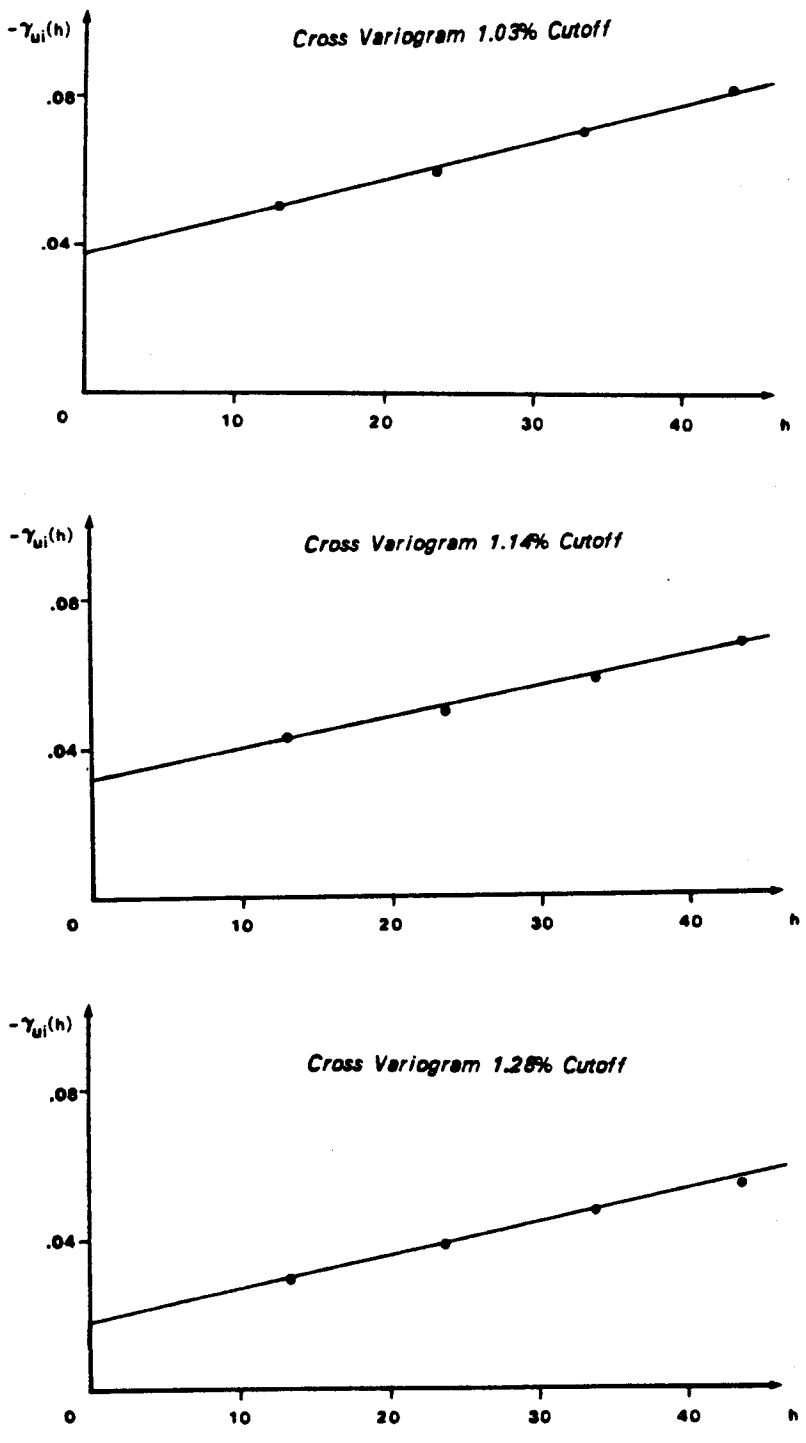

Figure 20: Cross Variograms for the 1.03%, 1.14% and 1.28% Cutoffs

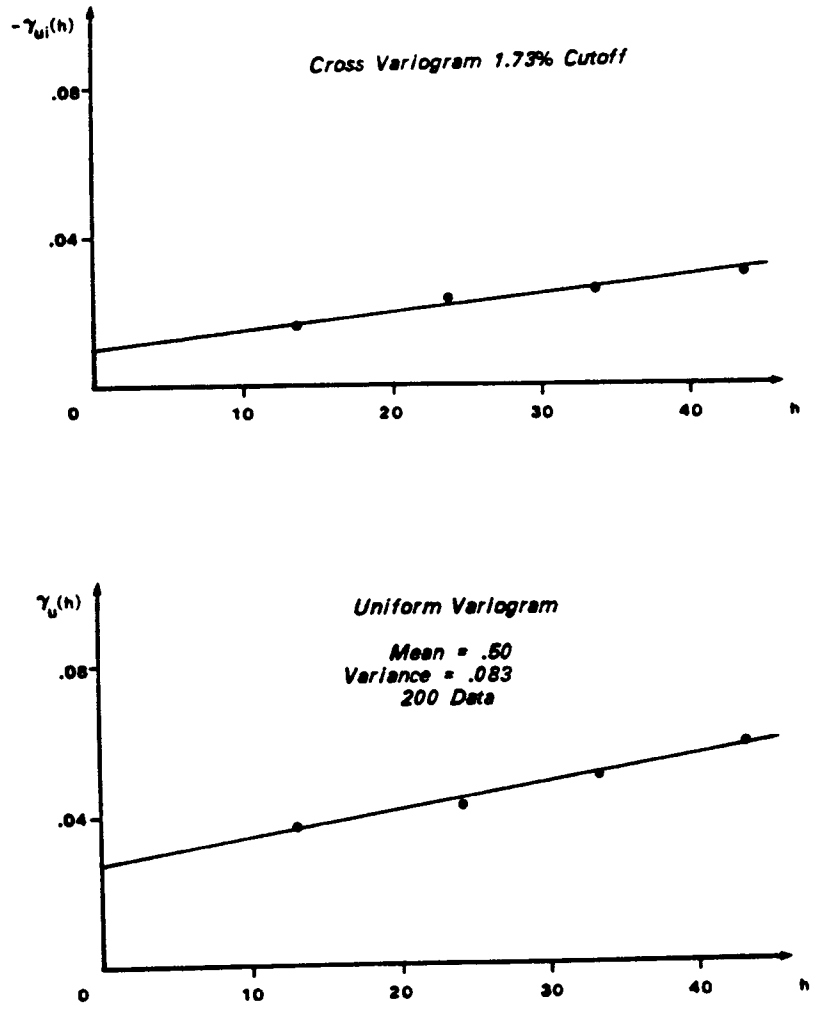

Figure 21: Cross Variogram for the 1.73% Cutoff and the Variogram of the Uniform Transform

3.3.3 Kriging Estimates of $\phi(A,zc)$

The spatial distribution of points within an 11 ft by 11 ft. panel will be estimated using both the indicator and probability kriging estimators. The obtained estimates of $\phi^*(A,zc)$ will be compared to the

actual $\phi(A,zc)$ determined from the 121 grade values within each 11 ft. by 11 ft. panel. The estimators which will be considered are the unconstrained indicator kriging estimator (sec 2.3.2.1) and the probability kriging estimator with two constraints (sec 2.6.1).

3.3.3.1 Properties and Advantages of the Chosen Estimators

The unconstrained indicator kriging estimator is chosen because it has a lower estimation variance than the constrained form of the estimator. The lower estimation variance stems from the fact that the mean grade of the indicator data at the cutoff of interest, F(zc), is assumed known and used in the estimate of $\phi(A,zc)$. Recall the form of the unconstrained estimator.

$$\phi^*(A,zc) = \sum_{\alpha=1}^{n} \lambda_\alpha(zc) \cdot i(x,zc) + \left(1-\sum_{\alpha=1}^{n} \lambda_\alpha(zc)\right) \cdot F^*(zc) \qquad (3.4)$$

where n is the number of data within the kriging neighborhood.

This estimator, by utilizing the cdf of all 200 available data, $F^*(zc)$, implicitly includes all of the data in determining an estimate of $\phi(A,zc)$. That is, since $F^*(zc)$ is the summation of $i(x_\alpha,zc)$ over all 200 sampled locations α, each indicator datum outside the kriging neighborhood is weighted by $(1-\Sigma\lambda_\alpha(zc))/N$ (where N is the total number of data), while the data within the kriging neighborhood are weighted by $\lambda_\alpha(zc)+(1-\Sigma\lambda_\alpha(zc))/N$. The final weight received by each datum can, thus, be seen as the superposition of two weighting schemes. The first gives equal weight to all indicator data inside and outside of the kriging neighborhood. The second gives zero weight to all data outside

the kriging neighborhood and some additional weight, whose magnitude depends on the solution of the kriging system, to each datum inside the kriging neighborhood. The effect on the estimate of $\phi(A,zc)$ is that the basic underlying estimated distribution for each panel is identical to the shape of the global histogram. This underlying estimated distribution does not, however, have the magnitude of the global distribution as the maximum value is $(1-\Sigma\lambda_\alpha(zc))$ rather than 1. Superimposed on this basic shape are the jumps associated with the weights given to the indicator data

The most highly constrained form of the probability kriging estimator was chosen in spite of the fact that it has higher estimation variance than the less constrained forms because the less constrained forms can give undesirable weighting schemes (see sec 4.7) which cause these estimators to be unstable. Thus estimation variance is sacrificed to obtain a stable estimator.

3.3.3.2 Kriging Plan

In modelling the various variograms, it was stated that an isotropic model is sufficient provided the variogram is not evaluated at distances greater than 33 feet. Because of this restriction, the kriging neighborhood will be restricted to a maximum of 9 data. For a panel in the center of the deposit, the kriging neighborhood is:

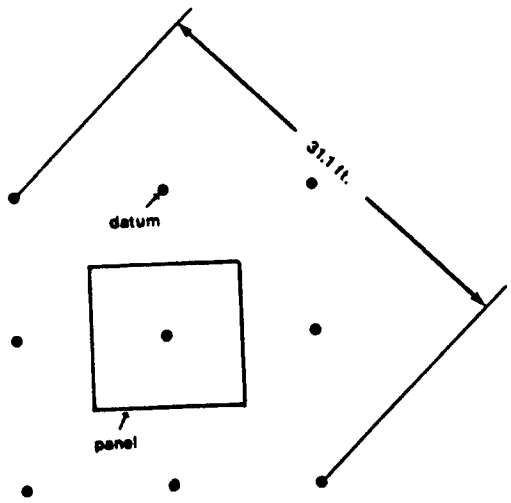

Using this pattern the maximum distance for which the variogram must be estimated is (1.414)•22=31.1 feet. As significant anisotropies were not observed in any of the experimental variograms at this distance, isotropic variogram models are acceptable for this kriging plan.

3.3.3.3 Correction of Order Relation Problems

The possibility of obtaining an estimated distribution which is not a valid distribution function, because it violates the order relations which all distribution functions must obey ($\phi^*(A,zc_1) \geq 0$, $\phi^*(A,zc_{i+1}) \geq \phi^*(A,zc_i)$, $\phi^*(A,zc_{max} \leq 1)$ is present in many instances when the kriging weights applied to the indicator data are not identical for all cutoffs. Identical weights can be obtained by using exactly the same shape variogram model at all cutoffs. This approach, known as median indicator or probability kriging ensures no order relation problems because the indicator data are non-decreasing functions of cutoff (see Journel, 1982).

Unfortunately, for this simulated deposit, the indicator variogram shapes are different for each cutoff (see table 4) so median indicator kriging or probability kriging should not be used. Since the weights received by the indicator data, in this case, are a function of cutoff, order relation problems may occur and must be rectified when they do. Two methods for resolving the order relation problems were discussed previously (sec 2.7). Briefly, the first and more complicated method involved solving for the kriging weights at all cutoffs in one large system through quadratic programming. The second less complicated method involved solving for $\phi^*(A,z_c)$ at each cutoff independently. If order relation problems occurred in these initial solutions, a valid distribution function which minimized the squared deviation from the initial estimates is obtained.

In the course of applying indicator and probability kriging to the simulated deposit, order relation problems did occur. In one panel, which had the largest observed order relation problems both methods for removing order relation problems were tested. The results are given in table 6. Notice that although these were the worst order relation problems observed in any panel, the problems are restricted to the third significant figure. Hence for this deposit any reasonable technique for correcting the order relation problems will give good results.

Interestingly both methods for resolving the order relation problems give identical results in this case. Although there is no guarantee that both methods will give identical results for all panels, the results from this panel indicate that; first the order relation problems encountered are not serious and; second either of these methods can be

TABLE 6

Solution of Order Relation Problems

Cutoff	IK Estimate	Strict QP	Fit Valid CDF
0.	.3905	.3905	.3905
.175	.4733	.4733	.4733
.325	.5799	.5799	.5799
.510	.6680	.6680	.6680
.740	.9275	.9275	.9275
.905	.9947	.9927	.9927
1.03	.9907	.9927	.9927
1.14	.9945	.9940	.9940
1.28	.9967	.9940	.9940
1.73	.9908	.9940	.9940

Where Strict QP refers to the solution obtained by minimizing the sum of the estimation variances.

Fit Valid CDF refers to fitting a valid CDF to the IK or PK solution

used successfully. For these reasons only the method based on correcting the initial kriging estimates will be used in all future studies, as this method is far less expensive than the strict quadratic programming method.

3.4 RESULTS

As stated at the outset, this case study is designed merely to point out the strengths and weaknesses of the probability and indicator kriging techniques. To accomplish this task, both global and local results for both estimators will be given for all ten cutoffs of

interest without regard to what an economic cutoff might be. Futhermore as the quantities of economic interest, the tonnage and quantity of metal recovered, are determined directly from the estimate of the spatial distribution, $\phi^*(A,zc)$, it will be sufficient, for the purposes of this case study, to analyze only the estimates of the spatial distribution.

3.4.1 Global Results

For each of the 200 panels defined within the simulation and each of the 10 cutoffs both PK and IK estimates of the local spatial distribution are available; thus, there are obviously a large number of estimates and corresponding true values. One way to analyze this mass of information is to compress the information into meaningful measures. Two such measures, which are computed without regard to particular panel location, are the global error and smoothing of the two estimators.

3.4.1.1 Global Error

In any estimation procedure it is expected that there will be little or no global error or bias in the estimates and the estimation of local spatial distributions is no different in this respect. It has been demonstrated that $E[\hat{\Phi}(A,zc)]=F(zc)$ (see sec 2.2) so it is expected that the global cdfs obtained by regrouping the local IK or PK estimates of $\phi(A,zc)$ should be close to the actual cdf F(zc) as IK and PK are unbiased estimators. In other words, since

$$E[\hat{\Phi}_{ik}^*(A,zc)]=E[\hat{\Phi}_{pk}^*(A,zc)]=E[\hat{\Phi}(A,zc)]=F(zc) \qquad (3.5)$$

it is expected that the estimates

$$F_{ik}^*(zc) = \left(\sum_{i=1}^{200} \phi_{ik}^*(A_i, zc)\right)/200 \qquad (3.6)$$

and

$$F_{pk}^*(zc) = \left(\sum_{i=1}^{200} \phi_{pk}^*(A_i, zc)\right)/200 \qquad (3.7)$$

should be nearly equal to F(zc). The comparison of $F_{ik}^*(zc)$, $F_{pk}^*(zc)$, F(zc), and F*(zc) determined from the 200 data is given in table 7.

TABLE 7

Comparison of Global CDF Estimates

Cutoff		Estimates		
zc	F(zc)	$F_{ik}^*(zc)$	$F_{pk}^*(zc)$	F*(zc)
0.	.222	.197	.202	.20
.175	.286	.264	.267	.27
.325	.345	.355	.361	.36
.51	.425	.445	.446	.445
.74	.534	.513	.509	.51
.905	.610	.598	.596	.60
1.03	.678	.684	.685	.685
1.14	.729	.754	.754	.755
1.28	.785	.839	.838	.840
1.73	.907	.919	.918	.917

In examining table 7 two features should be noticed. First, at all but the 1.28% cutoff, the global cdf values determined from the IK and PK estimators are within ± .03 of the true global cdf value. This

result indicates that the IK and PK estimates do not on the whole exhibit any serious global bias. The second feature of the table is that the IK and PK global estimates are almost identical to the cdf determined from the 200 regularly spaced data, F*(zc). This extremely close correspondence between the global cdf of the data and the IK and PK global cdf estimates occurs in this case study because the 200 data are located on a perfectly regular grid and the variogram models are isotropic. Such close correspondence will not, in general, be observed for deposits with irregular sampling configurations and/or anisotropic variogram models.

These global results indicate the importance of obtaining a representative data set. Notice in table 7 that at all cutoffs for which the cdf of the 200 data is similar to the true cdf the IK and PK estimates have almost no global error. At the 1.28% cutoff, however, the cdf obtained from the 200 data is unrepresentative of the true cdf. This unrepresentativity translates into a global error or bias in the IK and PK estimators. As the data are sampled on a regular grid, the cdf obtained from the data should be representative at all cutoffs, hence the poor global results at the 1.28% cutoff must be attributed to bad luck in sampling and not to any shortcomings in the estimation techniques.

3.4.1.2 Smoothing

The family of kriging type, minimum estimation variance, estimators (of which the IK and PK estimators are members) are known to be smooth estimators (JH, pg 450); that is, the variance of the IK or PK estimates

will be less than the variance of the corresponding true values at a given cutoff. This smoothing is an acceptable shortcoming of this type of estimator as the primary purpose is to estimate a mean rather than a variance. Ideally, however, an estimator should not be too smooth, as smoothing generally implies that the estimated local cdfs do not capture the spatial variability of the actual values, hence the local estimates may be inaccurate. Therefore, everything else being equal, an estimator with a lesser degree of smoothing is preferred to a highly smoothed estimator.

The smoothing of the IK and PK estimators can be compared by examining a plot of the variances of the IK estimates $\phi_{ik}^*(A,zc)$, the PK estimates $\phi_{pk}^*(A,zc)$, and true values $\phi(A,zc)$ versus cutoff (fig 22), where these three variances are computed utilizing relations similar to the following which is used to calculate the variance of the true spatial distributions.

$$\text{Var}(\phi(A,zc)) = \sum_{i=1}^{200} (\phi(A_i,zc) - F(zc))^2/200 \qquad (3.8)$$

The results indicate that the variance of the PK estimates is closer to the variance of the true values than is the variance of the IK estimates at all cutoffs. Hence the PK estimates are less smoothed and therefore better capture the spatial variability of the true spatial distribution values.

This observation that the PK estimates are less smoothed than the IK estimates can be demonstrated theoretically (see section 3.6). Thus it is no accident that the PK estimates are less smooth than the IK estimates for this deposit.

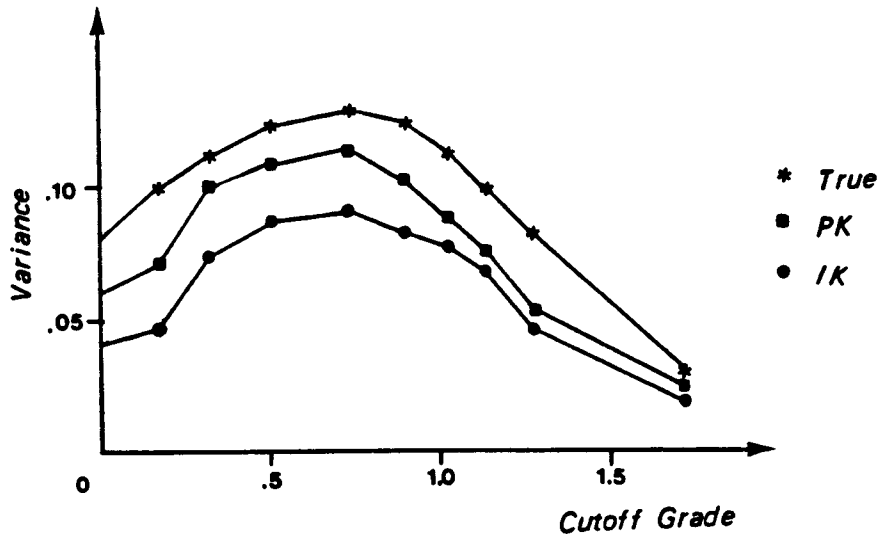

Figure 22: Smoothing of the PK and IK Estimators

3.4.2 Local Results

The IK and PK estimators are billed as local estimators of spatial distributions, therefore it is important to examine the local performance of these estimators. The particular quantity of interest is the error made for each individual panel and cutoff, $\phi^*(A_i,zc)-\phi(A_i,zc)$. At a given cutoff, there are 200 such errors corresponding to the 200 panels comprising the deposit. The sheer number of errors, thus, make any meaningful analysis difficult. As an aid in interpretation the errors made at each particular cutoff will be presented in graphical form; that is, for each cutoff, a scattergram of true versus estimated spatial distribution will be utilized. Each of these scattergrams (fig 23-32) contains 200 points whose coordinates correspond to the estimated and true spatial distribution values for each of the 200 panels. In all

of these scattergrams, a solid 45^0 line bisects the figure. This line corresponds to true equals estimated value so any point which plots on this line corresponds to a zero estimation error for a particular panel. Ideally all of the points in the scattergram would plot on this line as such an estimator would be perfect in that no error is present in any panel. All points corresponding to imperfectly estimated panels will lie either above or below the 45^0 line. Those points lying above the line correspond to panels which were underestimated as the true value is larger than the estimate. Conversely points lying below the line correspond to overestimated panels as the estimated value $\phi^*(A_i,zc)$ exceeds the true value $\phi(A_i,zc)$. The magnitude of the error made in any panel is given by the length of the vertical or horizontal line connecting the point representing the panel and the 45^0 line. Thus, an estimator with less local error than another estimator will produce a scattergram of true versus estimate which is more tightly grouped around the 45^0 line.

Various types of bias also appear in a scattergram. If the center of mass of the scattergram does not fall on the true equals estimated line, there is a global bias in the estimates. This condition is normally recognizable when the bias is large since the majority of the cloud of points and large errors are found on one side of the true equals estimate line. In addition to overall bias, an estimator can also have conditional biases. That is

$$E[\Phi(A,zc)\,|\,\Phi^*(A,zc)=p] \neq p \qquad (3.9)$$

In a scattergram this condition can be recognized by determining the center of mass of points within a band of estimated values. If this center of mass does not fall on the true equals estimate line, a conditional bias is present. Notice that an estimator can be globally unbiased but be conditionally biased as conditional biases of opposing sign can compensate for each other.

For each cutoff, two scattergrams corresponding to the PK and IK estimators will be compared. As this comparison will be between two estimators which are used to estimate exactly the same quantity, the best comparison will be achieved by examining the scattergrams for both estimators simultaneously (fig 23-32).

3.4.2.1 Local Estimates, Low Cutoffs

The estimates given by the PK and IK estimators for the cutoffs 0, .175, .325 (approximately 20th to 36th percentiles) show the same behavior so they are discussed together. The primary feature of these scattergrams is the conditional bias of the indicator kriging estimator (fig 23-25). This conditional bias is such that the large $\phi(A,zc)$ values are underestimated while the small values are overestimated. The implication of this conditional bias is that in high or low grade regions of the deposit the IK estimates of $\phi(A,zc)$ will be biased and therefore poor. In practical applications such as the estimation of local recoveries the consequences of utilizing a conditionally biased estimator would be a dramatic difference in the predicted and recovered tonnages for given local regions of the deposit. The PK estimator also shows some conditional bias at these cutoffs however the magnitude of

the conditional bias is much less than the conditional bias of the IK estimator. For this reason the PK estimator is considered superior to the IK estimator at these low cutoff grades.

3.4.2.2 Local Results, Middle Cutoffs

The four middle cutoffs, .51, .74, .905, and 1.03% (40th to 70th percentiles), yield similar results for both the PK and IK estimators (fig. 26-29). The conditional bias presented by the IK estimator at low cutoffs is not present to a significant degree at these middle cutoffs. For these middle cutoffs the results given by both estimators are remarkably similar without either estimator showing conditional or global biases. Hence for these cutoffs neither estimator is clearly superior.

3.4.2.3 Local Results, High Cutoffs

The local results at the high cutoffs 1.14, 1.28 and 1.73% (72nd to 90th percentiles) show the difficulty of estimating local spatial distributions at high cutoffs (fig 30-32). The local spatial distributions are fairly well estimated at the 1.14% cutoff, however the results show that both estimators are slightly conditionally biased and have a tendency to make large errors.

At the 1.28% cutoff, the tendency toward conditional bias observed at the 1.14% cutoff has increased as both estimators are severely conditionally biased at this cutoff. In analyzing the results at this cutoff it must be remembered that the data are unrepresentative (see table 7) so that both estimators have significant global biases. This

bias is seen in the scattergrams of both estimators as the majority of the points plot below the true equals estimated line (overestimation).

The results at the 1.73% cutoff do not show the bias or conditional bias observed at the 1.28% cutoff, however the scattergrams show that both estimators have significant errors for almost all panels. The results at this cutoff indicate that estimation of spatial distributions at extremely high quantiles should be approached with great care and the results should be examined with an amount of skepticism.

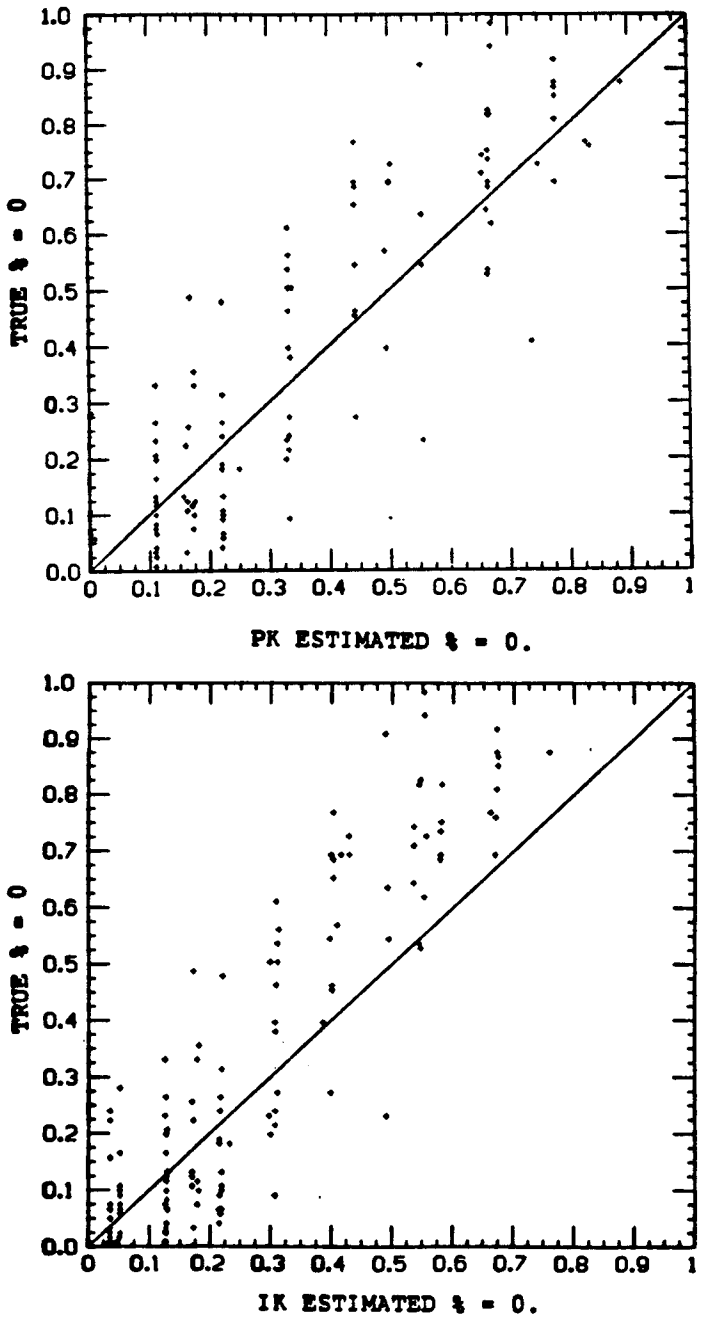

Figure 23: Local IK and PK Results for the 0% Cutoff

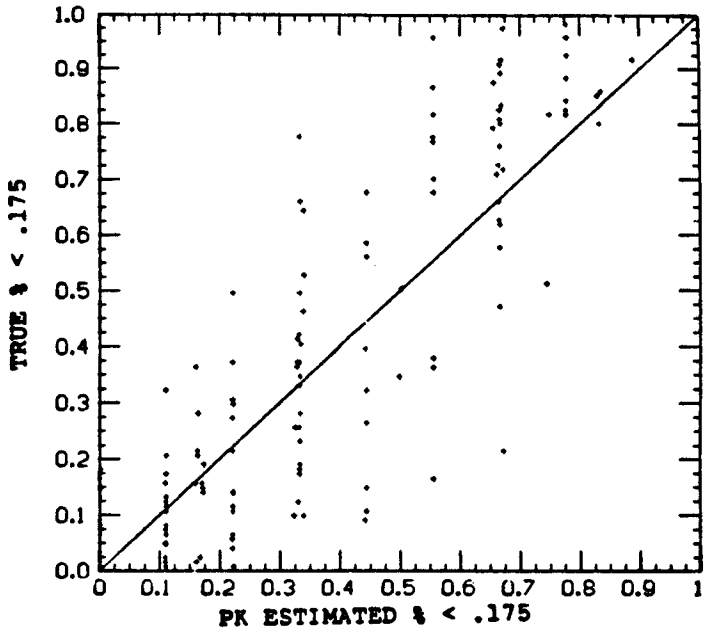

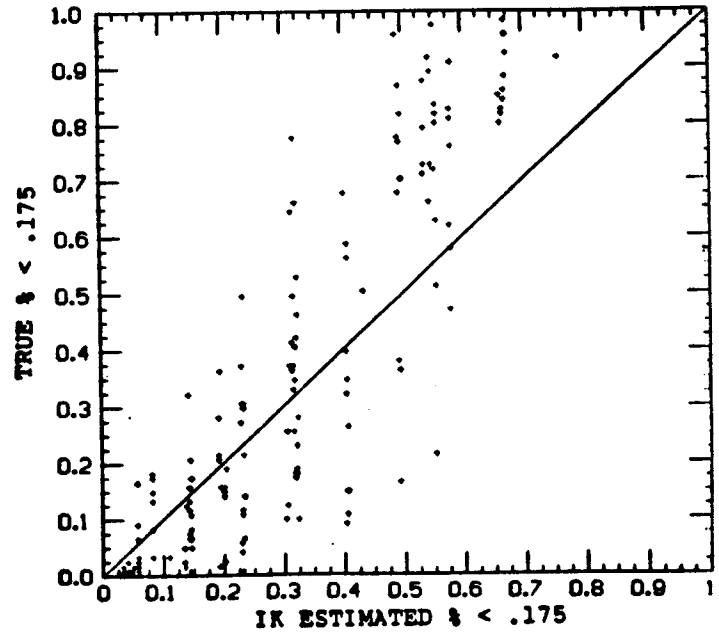

Figure 24: Local IK and PK Results for the .175% Cutoff

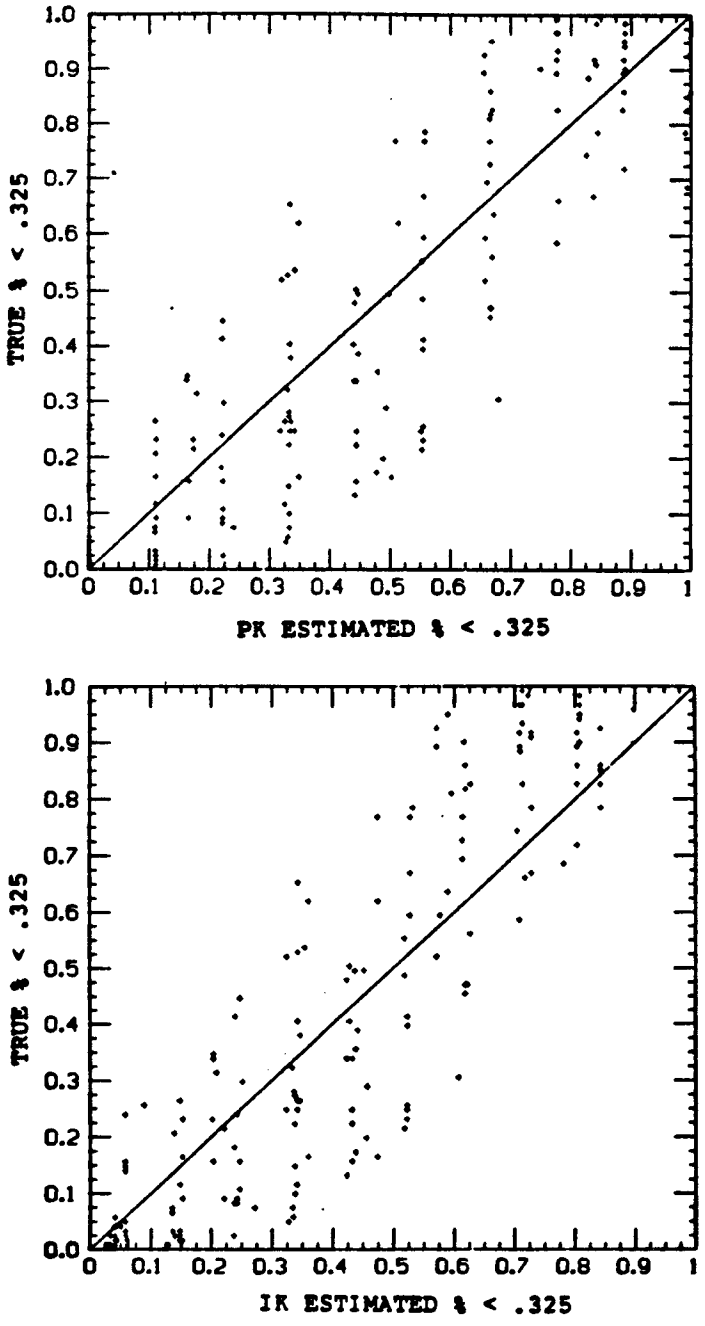

Figure 25: Local IK and PK Results for the .325% Cutoff

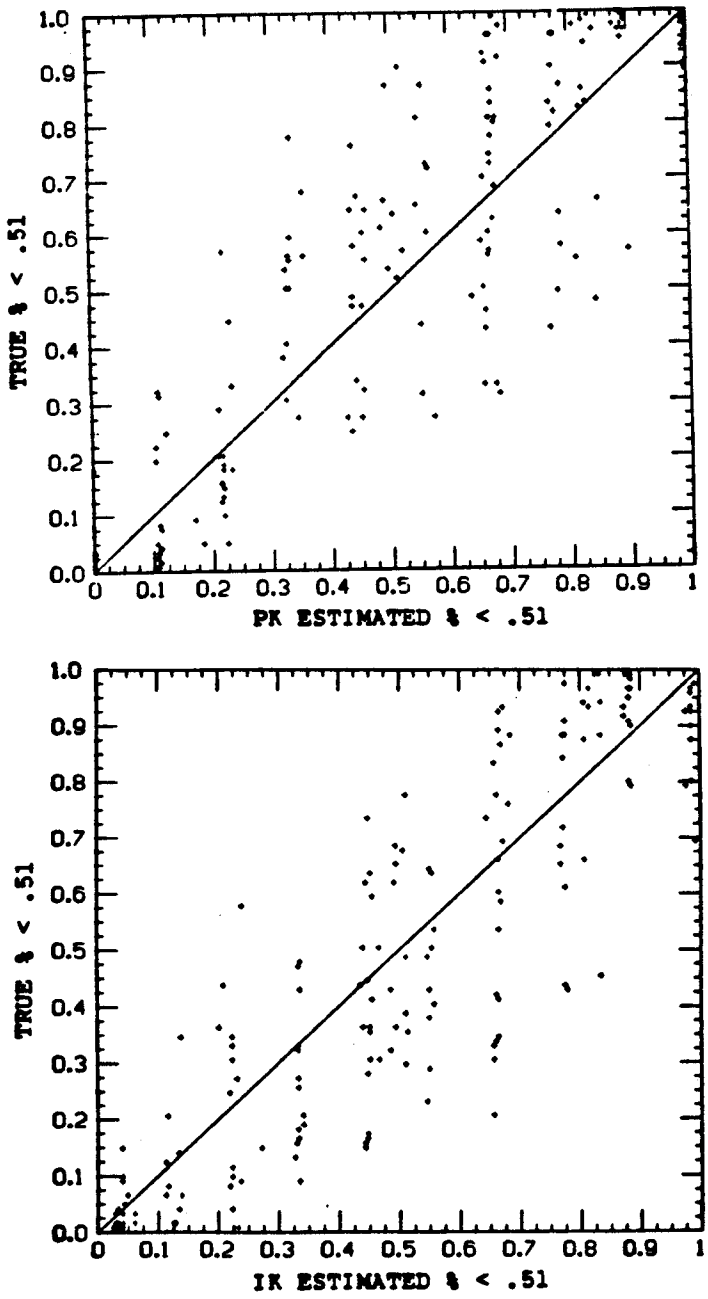

Figure 26: Local IK and PK Results for the 51% Cutoff

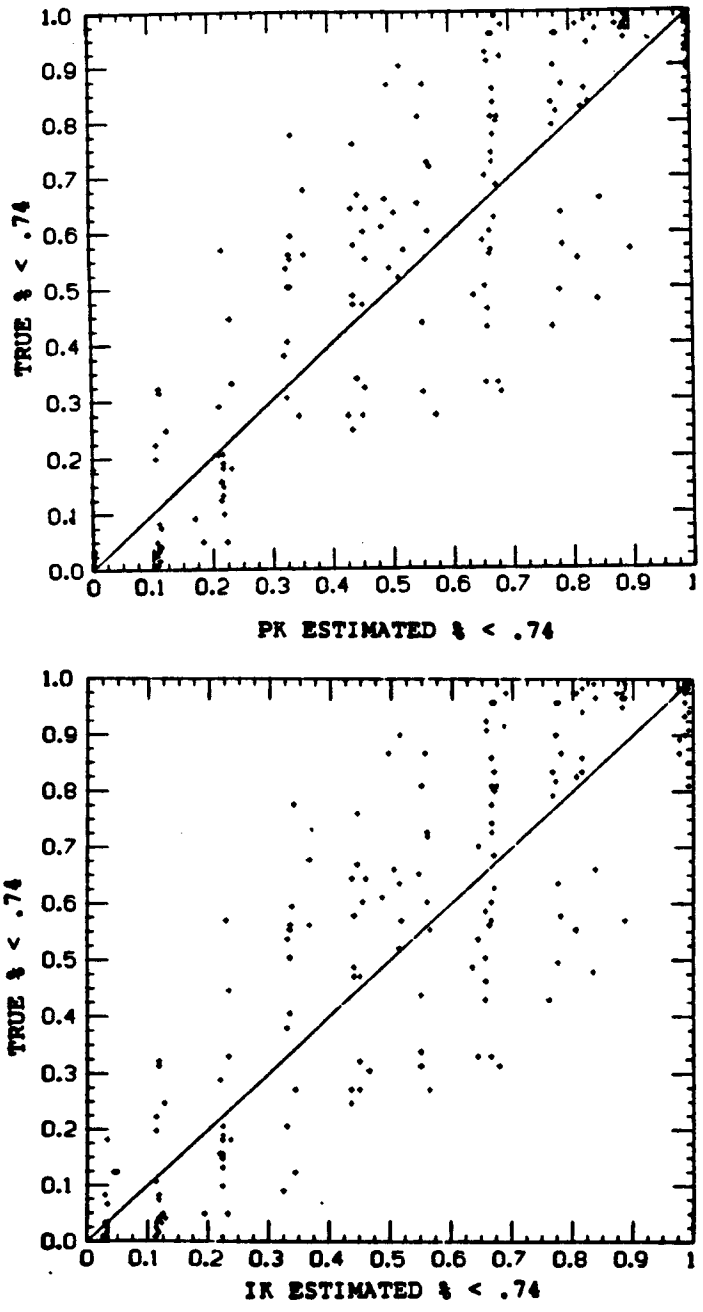

Figure 27: Local IK and PK Results for the 74% Cutoff

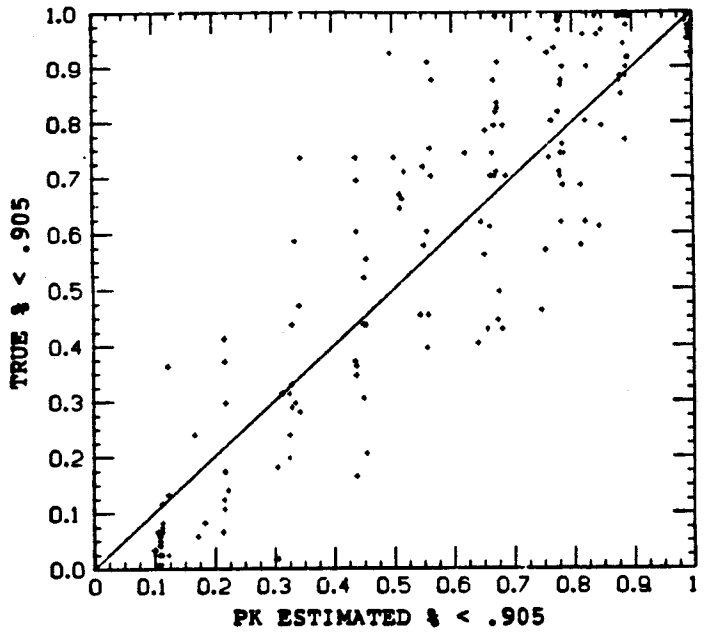

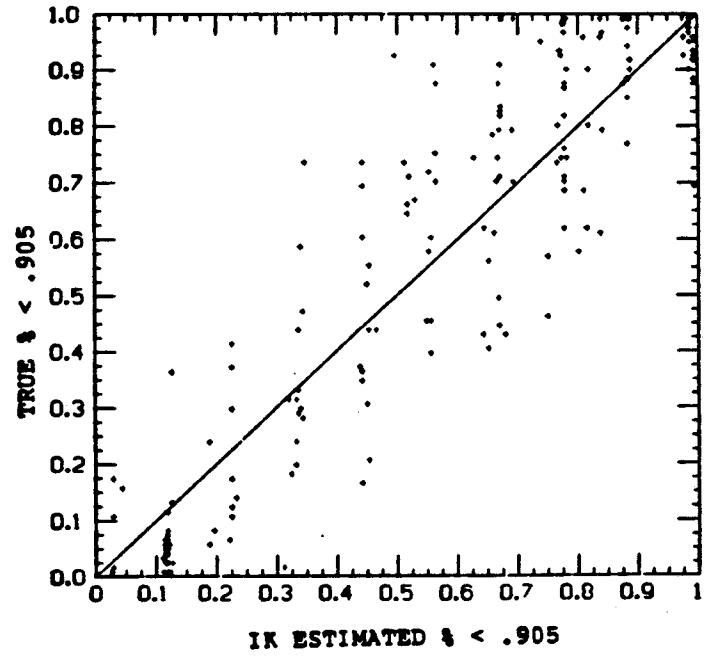

Figure 28: Local IK and PK Results for the .905% Cutoff

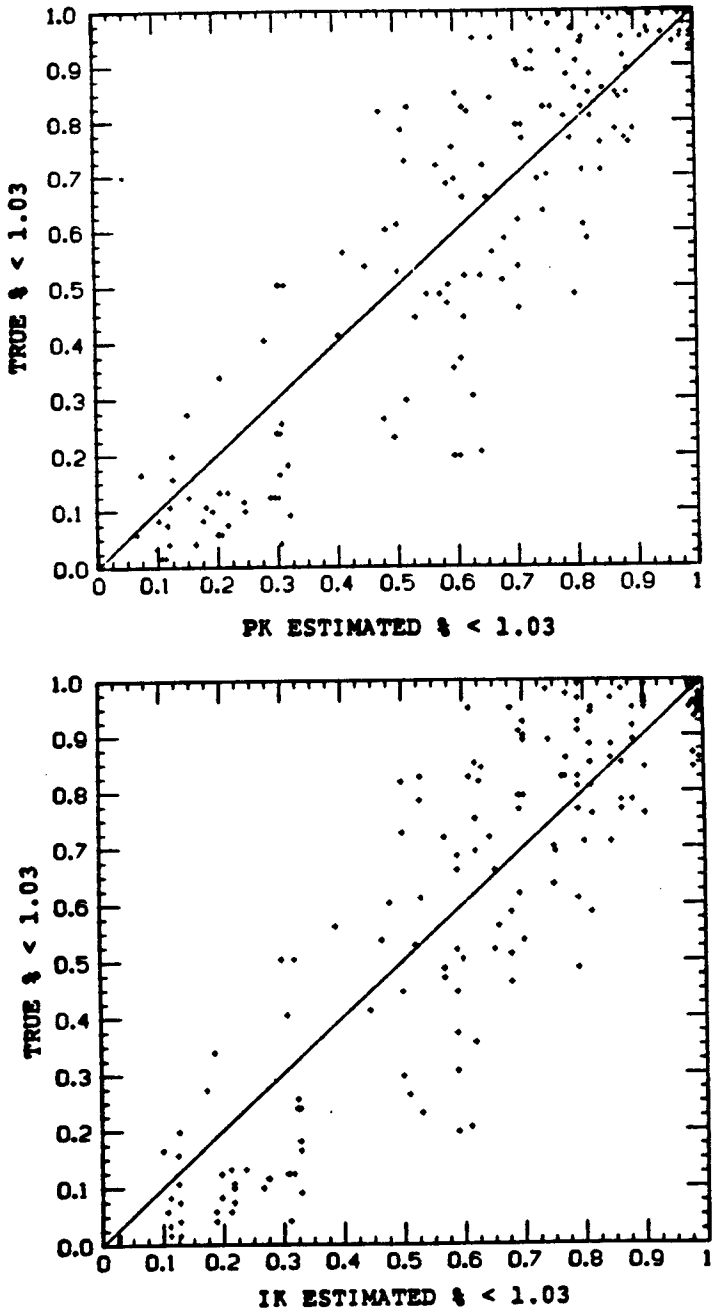

Figure 29: Local IK and PK Results for the 1.03% Cutoff

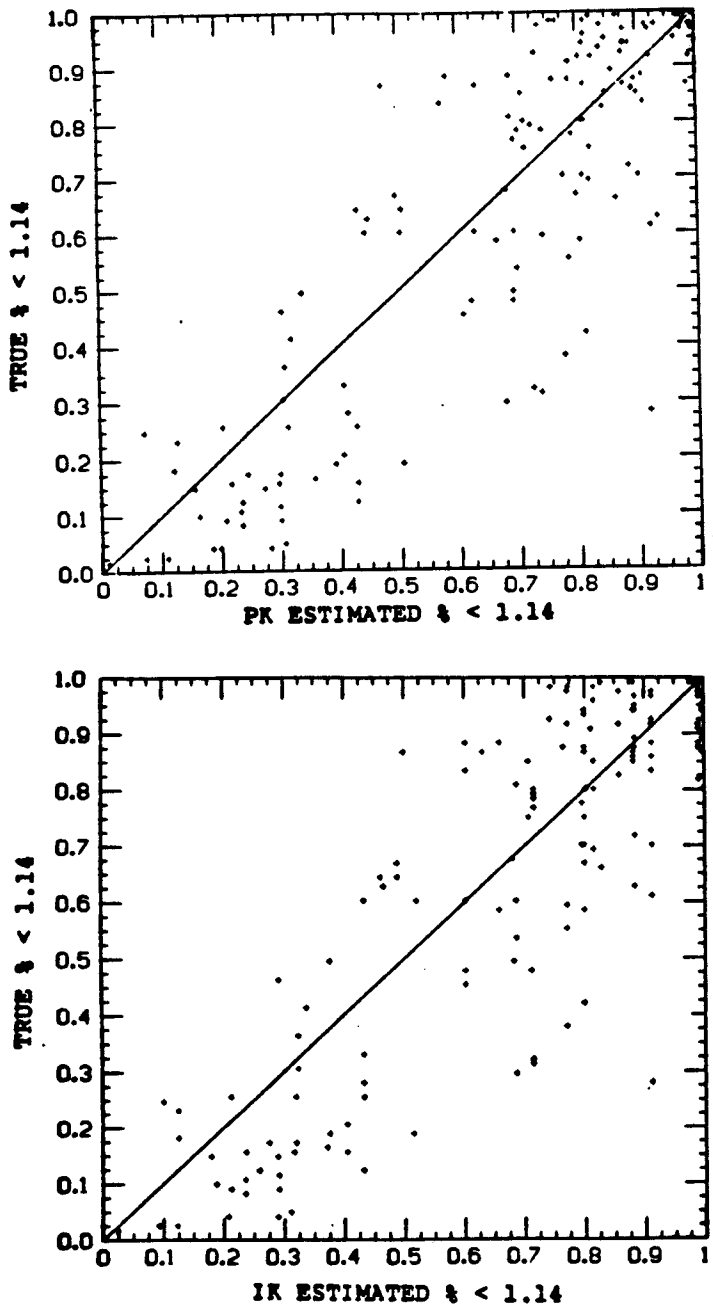

Figure 30: Local IK and PK Results for the 1.14% Cutoff

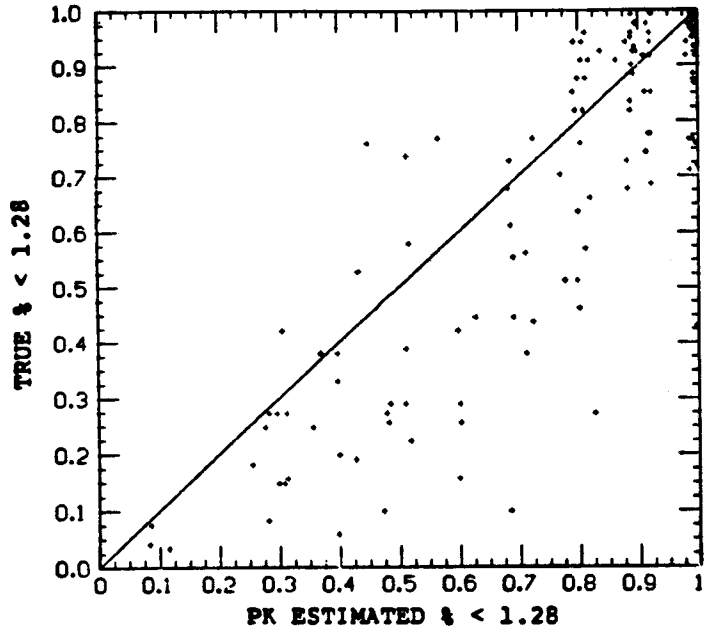

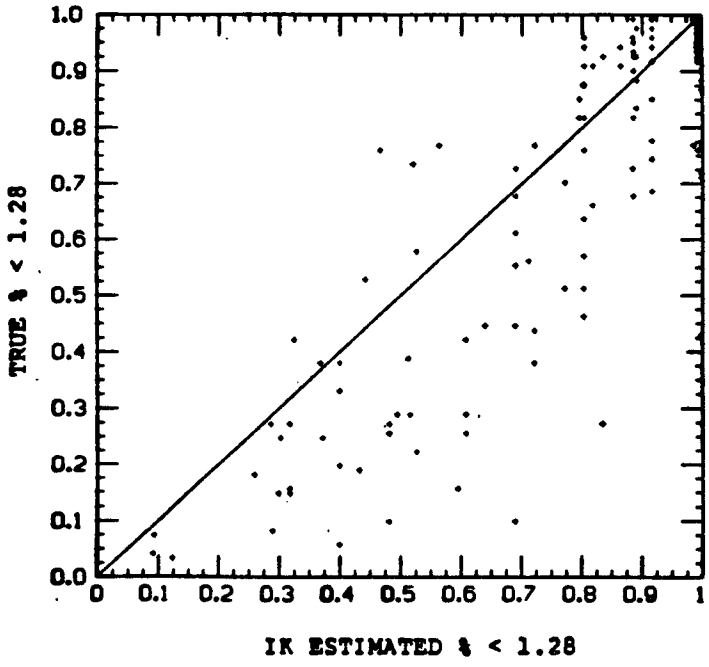

Figure 31: Local IK and PK Results for the 1.28% Cutoff

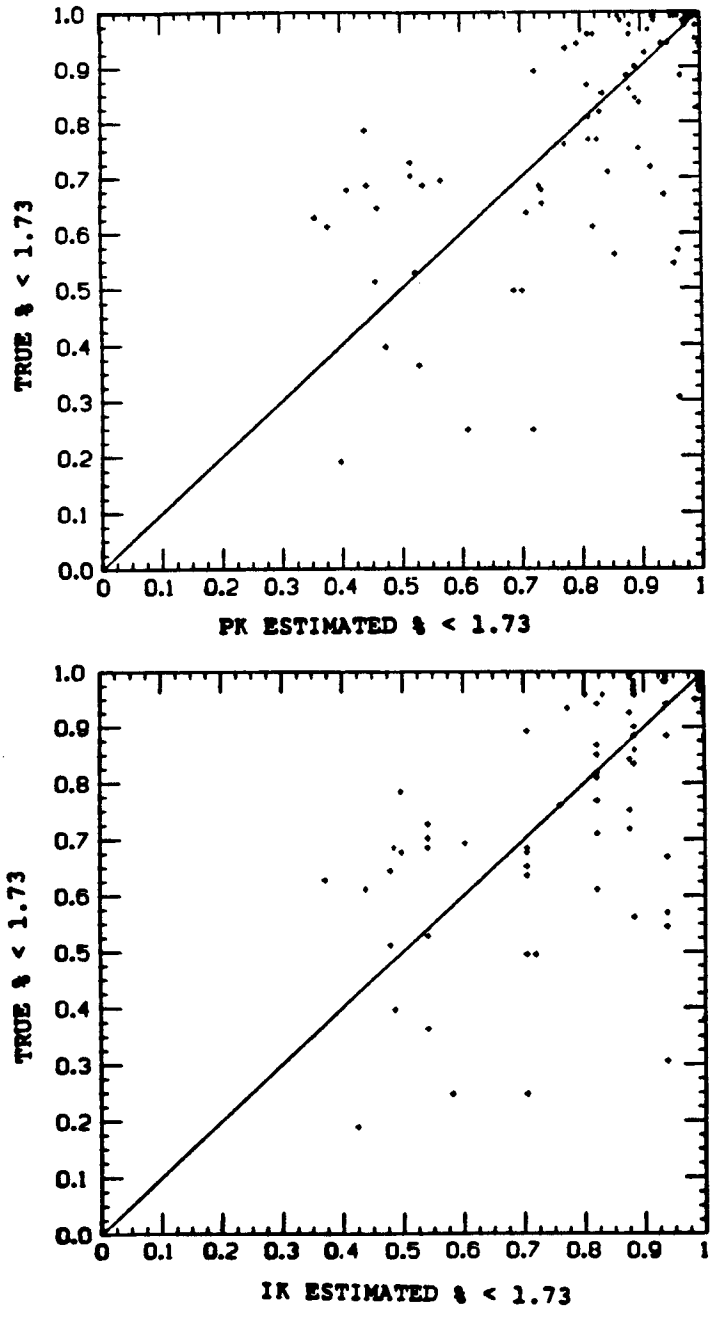

Figure 32: Local IK and PK Results for the 1.73% Cutoff

3.5 SUMMARY OF RESULTS

In this case study both the IK and PK estimators achieved similar results, for the most part, in both global and local estimation. The major differences being that the IK estimator is a smoother estimator than the PK estimator and has a higher propensity to be conditionally biased as evidenced by the local results at low cutoffs. These local and global results have shown that either of these estimators can be used to reliably estimate local spatial distributions, however the PK estimator is the preferred choice.

3.6 APPENDIX - SMOOTHING OF IK AND PK

In the course of applying the IK and PK techniques on the Stanford 2B simulated deposit it has been observed that the IK estimates are smoother than the PK estimates at all cutoffs (sec 3.4.1.2). This observation is a reflection of the fact that the IK estimator is theoretically a smoother estimator than the PK estimator as can be demonstrated as follows (Note: The deposit D is divided in K equal regions A_k).

The true variance of $\phi(A,zc)$ within the deposit D is

$$S^2(zc) = 1/k \sum_k (\phi(A_k,zc) - \bar{\phi}(A,zc))^2$$

$$\bar{\phi}(A,zc) = 1/k \sum_k \phi(A_k,zc) = \phi(D,zc)$$

$$S^2(zc) = 1/k \sum_k \phi^2(A_k,zc) - \phi^2(D,zc)$$

$$E[S^2(zc)] = 1/k \sum_k E[\phi^2(A_k,zc)] - E[\phi^2(D,zc)]$$

$$E[\phi^2(A,zc)] = 1/V^2 \iint E[I(x,zc) \cdot I(x',zc)]\, dx\, dx'$$

$$= \bar{C}(A,A,zc) + F(zc)^2$$

$$E[\phi^2(D,zc)] = \bar{C}_i(D,D,zc) + F(zc)^2$$

$$E[S^2(zc)] = \bar{C}_i(A,A,zc) - \bar{C}_i(D,D,zc)$$

To determine the variance of the IK estimates within the deposit D consider the unconstrained IK estimator

$$\phi^*(A,zc) = \sum_\alpha \lambda_\alpha(zc)\bullet(i(x_\alpha,zc) - F^*(zc)) + F^*(zc)$$

The associated kriging system is

$$\sum_\alpha \lambda_\alpha(zc)C_i(x_\alpha - x_\beta,zc) = \bar{C}_i(A,x_\beta,zc) \quad \text{for } \beta = 1 \text{ to } n$$

The estimation variance of this IK estimator is defined as

$$\sigma_{ik}^2 = \bar{C}_i(A,A,zc) - \sum_\alpha \lambda_\alpha(zc)\bar{C}_i(A,x_\alpha,zc)$$

The variance of the IK estimates is defined as

$$S^{*2}(zc) = 1/k \sum_k (\phi^*(A_k,zc) - \phi^*(D,zc))^2$$

$$= 1/k \sum_k (\phi^*(A_k,zc) - F^*(zc))^2$$

$$E[S^{*2}(zc)] = 1/k \sum_{k\alpha\beta\beta} \lambda_\alpha(zc)\lambda_\beta(zc)\, C_i(x_\alpha - x_\beta,zc)$$

$$= 1/k \sum_{k\alpha} \lambda_\alpha(zc)\bar{C}_i(A_k,x_\alpha zc)$$

$$= 1/k \sum_k (\bar{C}_i(A_k,A_k,zc) - \sigma_{ik}^2(A_k,zc))$$

$$= \bar{C}(A,A,zc) - \bar{\sigma}_{ik}^2(A,zc)$$

$$\text{as } D \to \infty \quad E[S^2(zc)] = \bar{C}(A,A,zc)$$

Hence the smoothing of the IK estimator is simply:

$$E[S^2(zc) - S^{*2}(zc)] = \bar{\sigma}_{ik}(A,zc)$$

By similar logic the smoothing of the PK estimator with zero non-bias constraints is

$$E[S^2(zc) - S^{*2}(zc)] = \overline{\sigma}_{pk}^2(A,zc)$$

Since the estimation variance of the PK estimator is less than the estimation variance of the IK estimator (sec 2.6.2), the PK estimator is less smooth than the IK estimator.

Chapter IV

ESTIMATION OF POINT SPATIAL DISTRIBUTIONS AT THE BELL MINE

In the previous chapter, the performance of the probability and indicator kriging estimators was examined in an application to a simulated deposit. As another example of the performance of the estimators and to introduce concepts such as the practice of quantity of metal estimation which have not yet been discussed, the estimators are applied to an actual gold deposit.

The gold deposit which will be considered is a section of the Enfield Bell mine located within the Jerritt Canyon district, north central Elko County, Nevada approximately 50 miles north of the town of Elko (figure 33). The Bell mine is found in the center of the Jerritt Canyon District within a window of the Roberts Mountains thrust fault. The mine is owned by a 70/30 joint venture between Freeport Gold Company and FMC Gold Incorporated.

The Bell Mine, which began production in 1981, has current reserves of 13.7 million tons at an average grade of .205 troy ounces of gold per ton. These reserves are spread over four orebodies known (in decreasing order of reserves) as the Marlboro Canyon, North Generator Hill, West Generator Hill, and Alchem deposits.

Mining is performed using hydraulic shovels which remove material in 15 foot lifts and load it into 85 ton trucks for haulage to the mill or dump (see figure 34). Blasting, on 12 foot centers, is light due to the

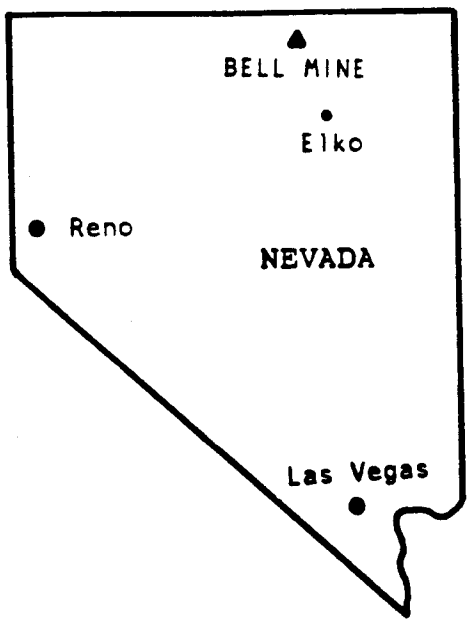

Figure 33: Map of Nevada Showing the Location of the Bell Mine

sheared state of the rock; hence, there is little mixing of ore and waste due to blasting. The selective mining unit, defined by four corner blast holes and the bench height, is effectively a 12x12x15 foot rectangular prism. Mining takes place four days a week on 2 ten hour shifts, and ore is processed by the mill seven days a week at a rate of 3200 tons per day.

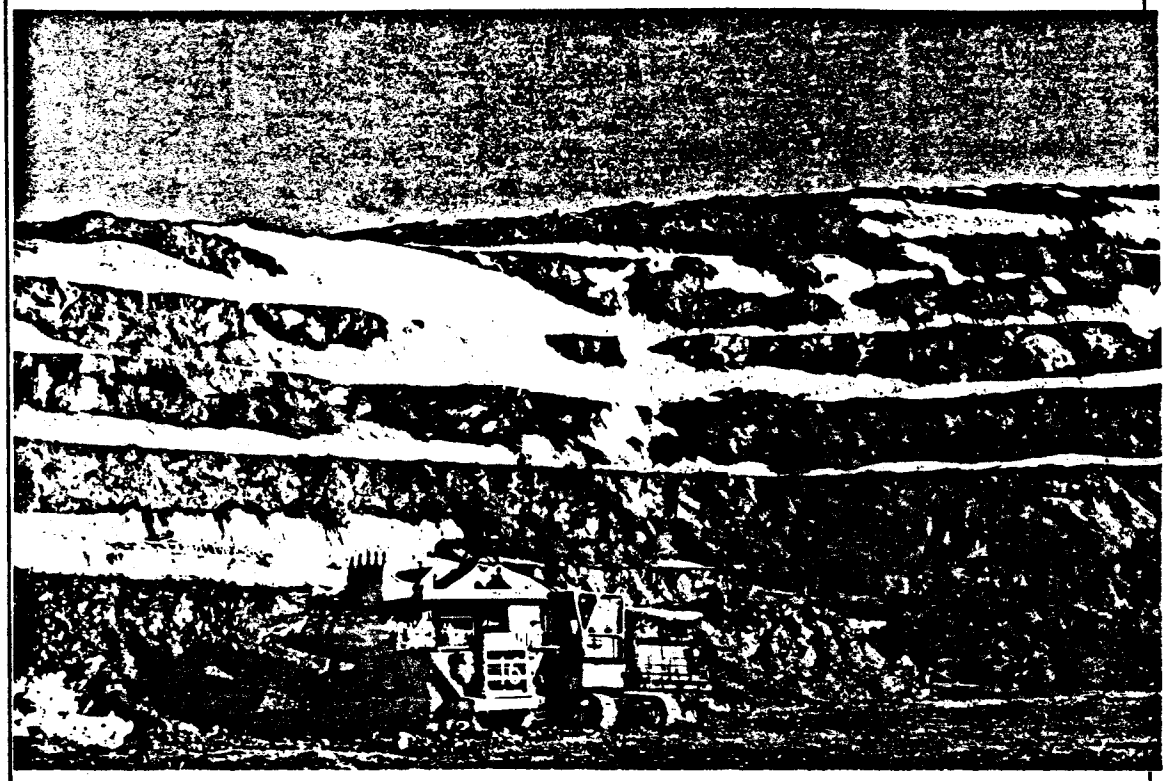

Figure 34: Loading of Waste in the Marlboro Canyon Deposit

4.1 GEOLOGY

The geology of this deposit is similar to a class of deposits known as "Carlin" type deposits named after the Carlin mine which was the first major mine opened in the area. A major feature of these deposits is that gold occurs as very fine grained particles within the host rock. The gold particles are generally less than 2 microns in diameter and cannot be observed without the aid of an electron microscope.

Carlin type deposits are classified by Boyle (1979) as disseminated deposits in chemically favorable beds. Three prerequisites for the genesis of these types of deposits are stressed by Roberts et al. (1971).

1. A source for gold bearing solutions.
2. Fractured or permeable ground to permit access of solutions.
3. Precipitants such as carbonate and/or organic carbon.

There is some debate concerning the exact chemical composition of the host rock which is most favorable to precipitation of the gold from the acidic hydrothermal solutions. Radtke and Scheiner (1970) believe that carbonaceous material is of primary importance. Wells (1971), on the other hand, found no particular association between gold and carbonaceous material. From this debate it appears that the hydrothermal solutions react differently with similar host rocks in different situations. In other words, it is expected that ore and waste will be found within the same lithologic units; that is, ore and waste will be interspersed in Carlin type deposits.

4.1.1 Regional Geology

The geology of the Jerritt Canyon district (Birak and Hawkins, 1984) is dominated by Paleozoic sedimentary and volcanic rocks of the upper and lower plates of the Roberts Mountains thrust fault. The upper plate is composed of Ordovician eugeosynclinal sedimentary and volcanic rocks which are not found in the mine area. The lower plate contains miogeosynclinal sedimentary rocks which were thrust eastward over the upper plate rocks along the Roberts Mountains thrust fault during the late Devonian Antler Orogeny (Merriam and Anderson, 1942). Low angle normal and reverse faults which are contemporaneous with the Roberts Mountains thrust occur frequently throughout the district and provide excellent pathways for hydrothermal fluids.

4.1.1.1 Stratigraphy

The oldest unit of the lower plate rocks is the middle Ordovician Eureka Quartzite which occurs exclusively in the southern portion of the district. This unit is 500 to 650 feet thick and has a gradational upper contact with the important Hanson Creek Formation.

The Hanson Creek Formation is late Ordovician to early Silurian in age. This formation is of major importance since it is the major host to gold mineralization at the Bell Mine. The formation has been divided into 5 units: SOhc I (youngest) to SOhc V (oldest) (Birak 1979). The lower three units are composed of alternating bands of micritic limestone and laminated, dolomitic limestone. The basal unit (SOhc V) is 15 to 100 feet thick and is overlain by the thicker (100 to 135 feet) SOhc IV unit which contains abundant black chert nodules. Neither of these units are major hosts to gold mineralization. The overlying, 300 foot thick SOhc III unit is, however, the major gold host within the formation. Gold is deposited, preferentially, in the more permeable laminated limestone bands. Chert is common in this unit with beds reaching thicknesses of four inches. The overlying SOhc II unit represents a slight change in lithology as the limestones in this and the SOhc I unit contain various textures of limestones and dolomites interbedded with black chert. The SOhc II unit is 100 feet thick while the SOhc I unit is from 10 to 130 feet thick. The contact with the overlying Roberts Mountains Formation is disconformable.

The Roberts Mountains Formation is of Middle Silurian to Early Devonian age and is 1000 feet thick. The lower 100 feet are a major host to gold mineralization. The major rock type is a laminated, fissile, calcareous to dolomitic siltstone.

The upper plate rocks within the Jerritt Canyon district are Ordovician age and are termed, in ascending order of age, the Snow Canyon Formation, the McAfee Quartzite, and the Jacks Peak Formation. As these formations do not occur in the mine area, they will not be discussed further.

4.1.2 Bell Mine Geology

The Bell Mine is found in the northern portion of the Jerritt Canyon window. The horizontal extent of the mine area is 2 miles in the east-west direction and .75 miles in the north-south direction. Within this area there are four known ore deposits. The mineralization is both structurally and lithologically controlled within the upper banded limestones of the SOhc III unit and the lower siltstones of the Roberts Mountains Formation. Lesser amounts of mineralization are found in silicified portions of these units.

Faulting is common throughout the mine area and is related to mineralization. Three major sets of faults are present: the Roberts Mountains thrust fault and sympathetic low angle normal and reverse faults; high angle east-west trending faults; and high angle northwest and northeast trending faults. Within the orebody, the major pathways for gold-bearing hydrothermal fluids are the east-west trending faults. Included among these east-west trending faults are the Bell fault within the North Generator Hill orebody and the Marlboro Canyon fault (see figure 35) within the Marlboro Canyon orebody. Each of these faults is the major mineralizing fault for its respective orebody. All faulting is believed to be pre-ore.

Three major types of alteration occur within the Bell Mine: (1) silicification, (2) oxidation and argillization, and (3) carbonization. Of these three types of alteration, silicification is the most prominent.

Figure 35: Marlboro Canyon Fault Separating Carbonized and Silicified Limestones of the Hanson Creek Formation

Silicification is responsible for the alteration of limestones to jasperoids. This alteration is believed to be pre-ore. Jasperoids are common in the mine area comprising 35 to 40% of the rocks. They are, however, weakly mineralized so that less than 10% of the ore is found in the jasperoids. Silicification occurs in the rocks of both the Hanson

Creek and Roberts Mountains Formations; however, silicification is most intense in the limestones of the Hanson Creek Formation.

Oxidation and argillization are discussed together as they are spatially and temporally associated in that they affect the same rock types. This type of alteration is economically important because the highest gold values occur in oxidized zones and this gold is easily recovered by standard cyanidation techniques. Oxidation occurs preferentially in the permeable SOhc III unit while argillization occurs preferentially along structures and produces local clay rich zones.

Carbonization is structurally controlled. Zones affected by carbonization are easily identified since this type of alteration produces black sooty rock which stands out from the surrounding light brown oxidized rock. Gold grades in carbonized zones are high near the controlling structures, but otherwise they are less than the grades found in oxide material; in addition, carbonized rock is more difficult to treat at the mill than the oxides resulting in a higher cutoff for carbonized rock.

4.2 NATURE OF THE PROBLEM

Although the underlying geology at the Bell Mine is fairly well known and can be accurately mapped after mining, the high density of faults and lesser structures occurring at various orientations, as well as the high degree of alteration make determination of structural and lithological control nearly impossible from exploration data only, even when the data are on 100 foot centers. This complex structural and lithological pattern combined with the property that the ore and waste

are interspersed make it impossible to precisely block out ore and waste zones given only exploration data. Unfortunately, only exploration data are available when recoverable reserve estimates required for mine planning, production scheduling, and economic evaluation must be calculated.

Before geostatistical solutions were developed for this problem, correction factors were used to correct polygonal or other deterministic estimators which commonly overestimate both tonnage and ounces recovered. These correction factors are commonly referred to as dilution or mining loss factors. Determination of these factors requires experience at the deposit in question, hence they cannot reliably be used at the development stage of a new prospect since no mining has taken place. Often these factors determined at one particular deposit are applied to deposits of similar genesis which have not been developed. This practice is risky, arbitrary, and has no theoretical justification; in contrast, geostatistical solutions use only the exploration data available at the deposit of interest to estimate the recoverable reserves.

4.2.1 Approach of the Geostatistical Solutions

The geostatistical approach to the problem of estimating recoverable reserves is discussed in section 1.1, however a brief review is presented here to reinforce the concepts behind this approach.

The geostatistical approach to the problem of accurately estimating recoverable reserves in erratic deposits is based on estimating the distribution of selective mining units (smus)[1] within a region termed a

panel. In other words, rather than estimate the grade of each selective mining unit directly, the local spatial distribution of selective mining units is determined (fig 36). In contrast to the usual geostatistical study where mean block grade is estimated, the variables which must be estimated, in this type of study, are the tonnage and quantity of metal recovered in each panel. The recovery information obtained through this approach is sufficient at the development stage of a study, as it is not necessary, at this early stage, to know the grade of each individual selective mining unit.

When first examining this problem, one may think that it is possible to obtain the recoverable reserves within a panel by kriging the mean grade of each selective mining unit in the panel. This approach will fail, however due to the smoothing of the kriging estimator. Selective mining units near the center of the panel (or any other particular location) will all receive nearly the same grade; thus, these estimates do not accurately represent the actual variability of selective mining units within the panel and will therefore yield a poor local estimate of the recoverable reserves.

---

[1]A selective mining unit is defined as the volume of material which is sent to the dump or mill based on an analysis of its value at the time of mining.

INFORMATION AVAILABLE

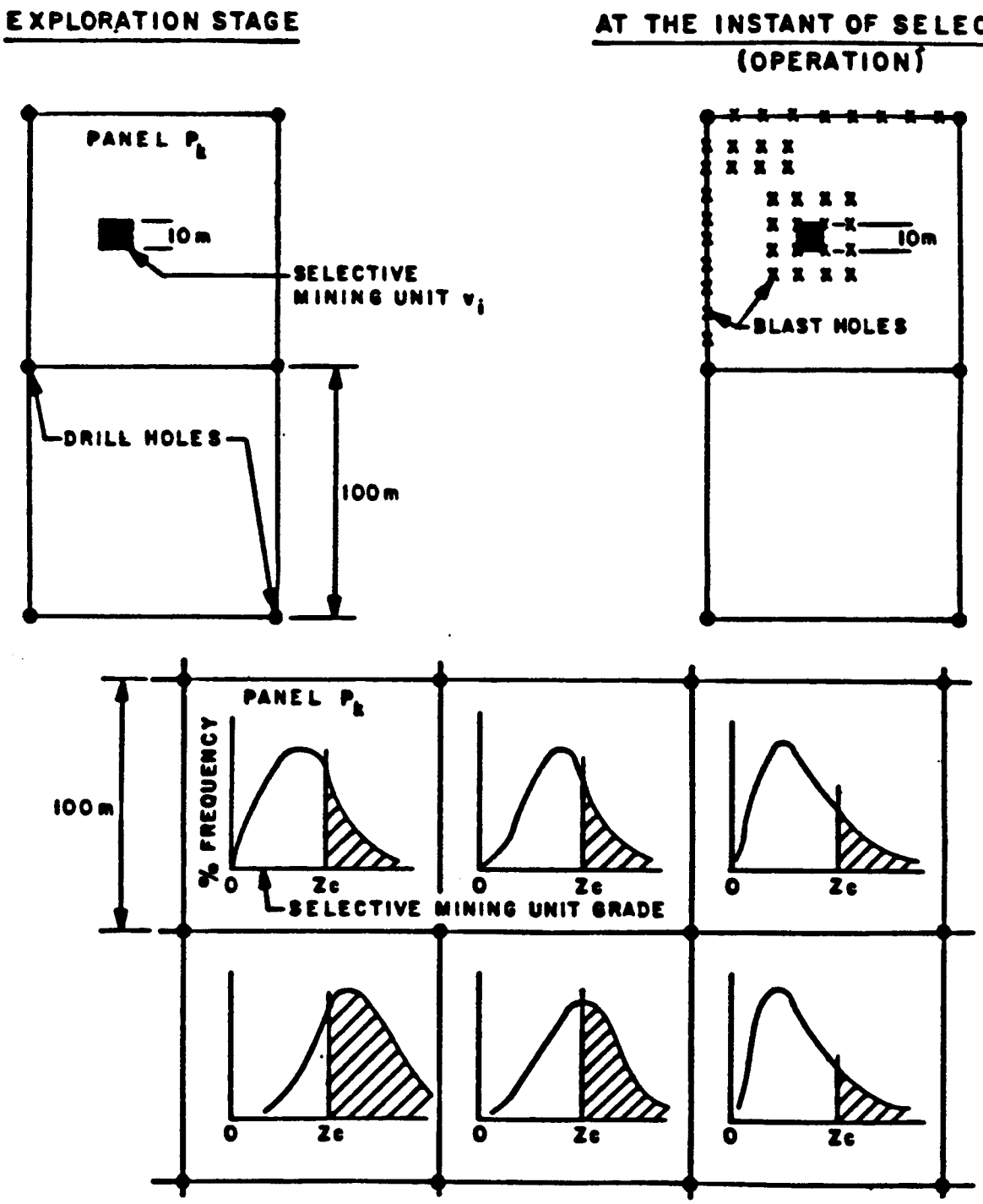

Figure 36: Estimation of Local Spatial Distributions (After Journel (1980))

4.2.2 Approach at the Bell Mine

In this study, the distribution of hypothetical point support[1] selective mining units will be estimated using both indicator and probability kriging. The study will be performed on five benches of the Lower North Generator Hill orebody which have been mined out. Since mining has been completed on these five benches, a substantial amount of blast hole information is available. In fact, over 10,000 blast hole assays were graciously provided by the management of the Bell Mine. Samplings[2] from these 10,000 values are taken, at various spacings, to simulate exploration data. Using these exploration data, the recovered tonnage and quantity of metal is estimated for a number of pre-defined panels. These estimated recoveries are then compared with the actual recoveries determined from all the blastholes located within the panel to check the quality of the estimators used.

4.3 DATA BASE

The data provided are blast hole gold assays from five fifteen foot benches of the Lower North Generator Hill orebody. The lowest bench is the 7600 foot level and the uppermost bench is the 7660 level. All assays are fire assays except for 484 samples from the 7600 bench for which only roasted atomic absorption assays were available. Fire assays for these samples were estimated by a linear regression based on 364 samples for which both fire and atomic absorption assays were available. The correlation coefficient for this regression is .989.

---

[1]In actuality the smu support size is much larger than a point. The important topic of non point support selective mining units is discussed in chapter 5.

[2]These samplings contain from approximately 200 to 600 blastholes.

To define panels for which the local recoveries will be estimated, a square 100 foot grid was laid over each of the five benches. The squares defined by the grid, which contained a complete and uniform coverage of blast holes were termed panels (see figure 37). A total of 119 panels (see figures 38 through 42) were defined in this manner. A total of 7,979 data are located within these panels yielding an average of 67 data per panel. A histogram of these 7,979 data is given in figure 43. This histogram shows that the mean grade of the assays found within panels is .105 oz/ton with a variance of .0381 $(oz/ton)^2$. The coefficient of variation, σ/m, is 1.86 which is fairly high indicating that the mineralization is highly variable. A second measure of the high variability of this deposit is that 1% of the values are a factor of 10 times larger than the mean and the highest values are a factor of 30 times larger than the mean. The shape of this distribution is close to but not lognormal as shown by a lognormal probability plot (fig. 44).

Examining the parameters of the grade distributions on a bench by bench basis shows that there is some vertical variability in the grades. The mean value and coefficient of variation for the data on each of the benches are summarized below.

Bench	Number of Data	Mean(oz/ton)	Coefficient of Variation
7660	1174	.1198	1.80
7645	1694	.1167	1.89
7630	1249	.1400	1.59
7615	1833	.1015	1.74
7600	2029	.0687	2.14

The top two benches have very similar mean grades and coefficients of variations. The middle bench, the 7630 level, shows the highest mean grade. The reason for the higher grade on this bench is related to the

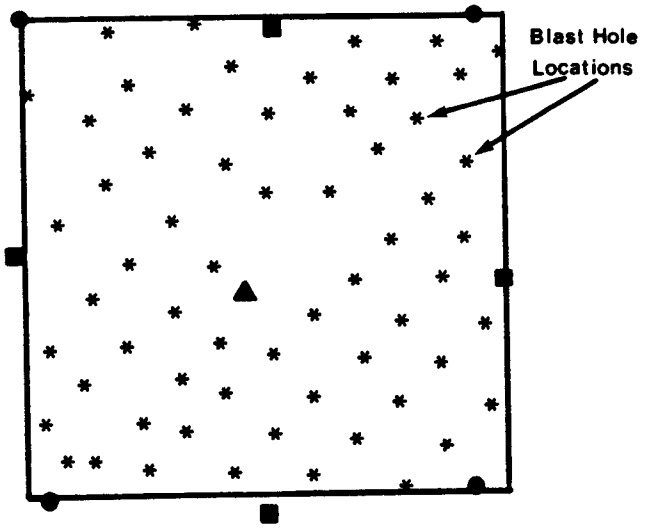

EXPLANATION:

- ● SAMPLE CAMPAIGN 1
- ▲ SAMPLE CAMPAIGN 2
- ■ SAMPLE CAMPAIGN 3

Figure 37: Typical Data Coverage Within a Panel

rock type found on this bench and is discussed in the next section. The 7615 bench is again similar to the upper benches, although the mean grade and coefficient of variation are lower. The 7600 bench has a much lower mean grade than any of the other four benches. This lower mean grade thus introduces a slight vertical drift into the data. This drift is not significant enough, however, to consider a nonstationary grade model.

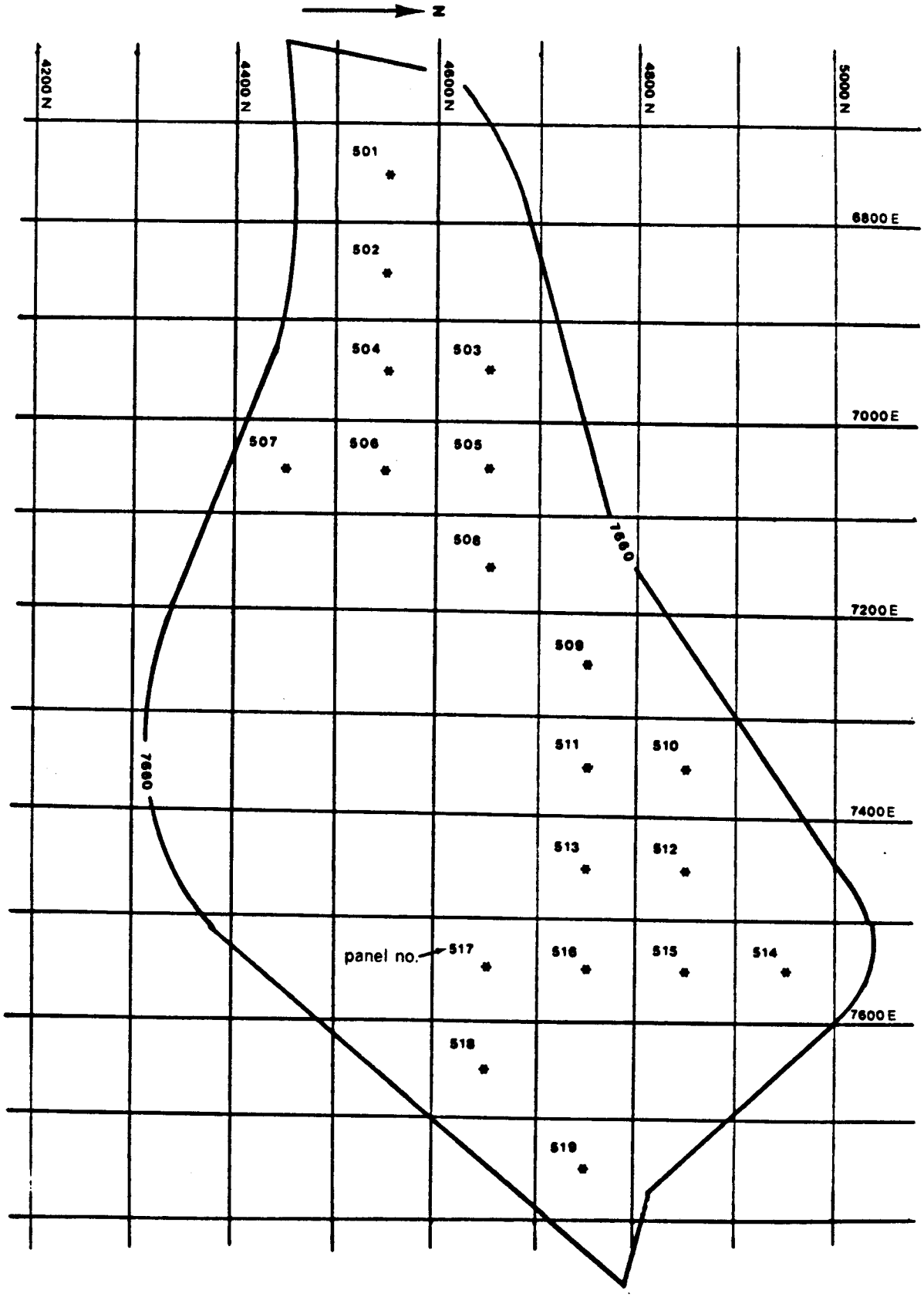

Figure 38: Panel Locations 7660 Bench

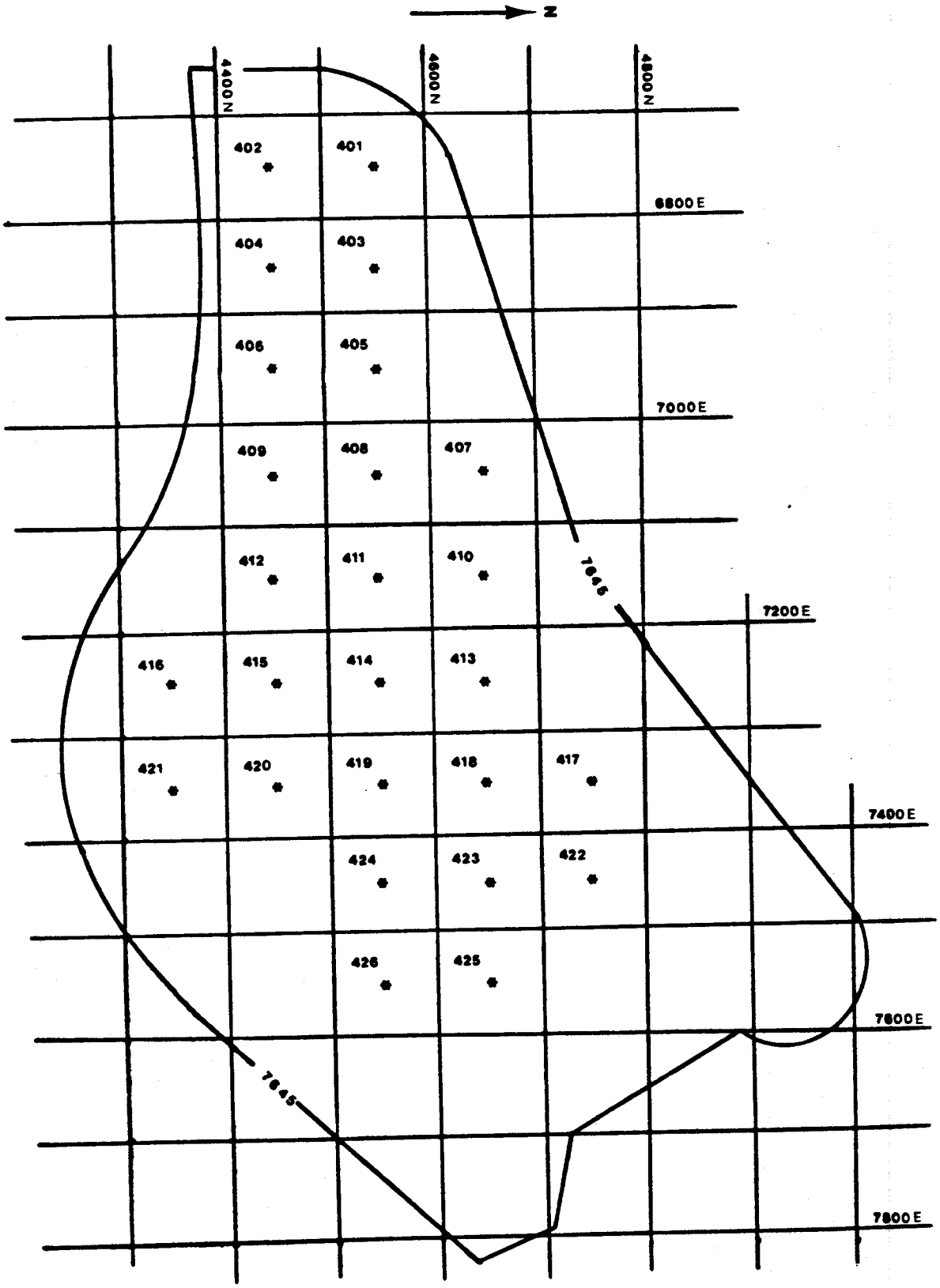

Figure 39: Panel Locations 7645 Bench

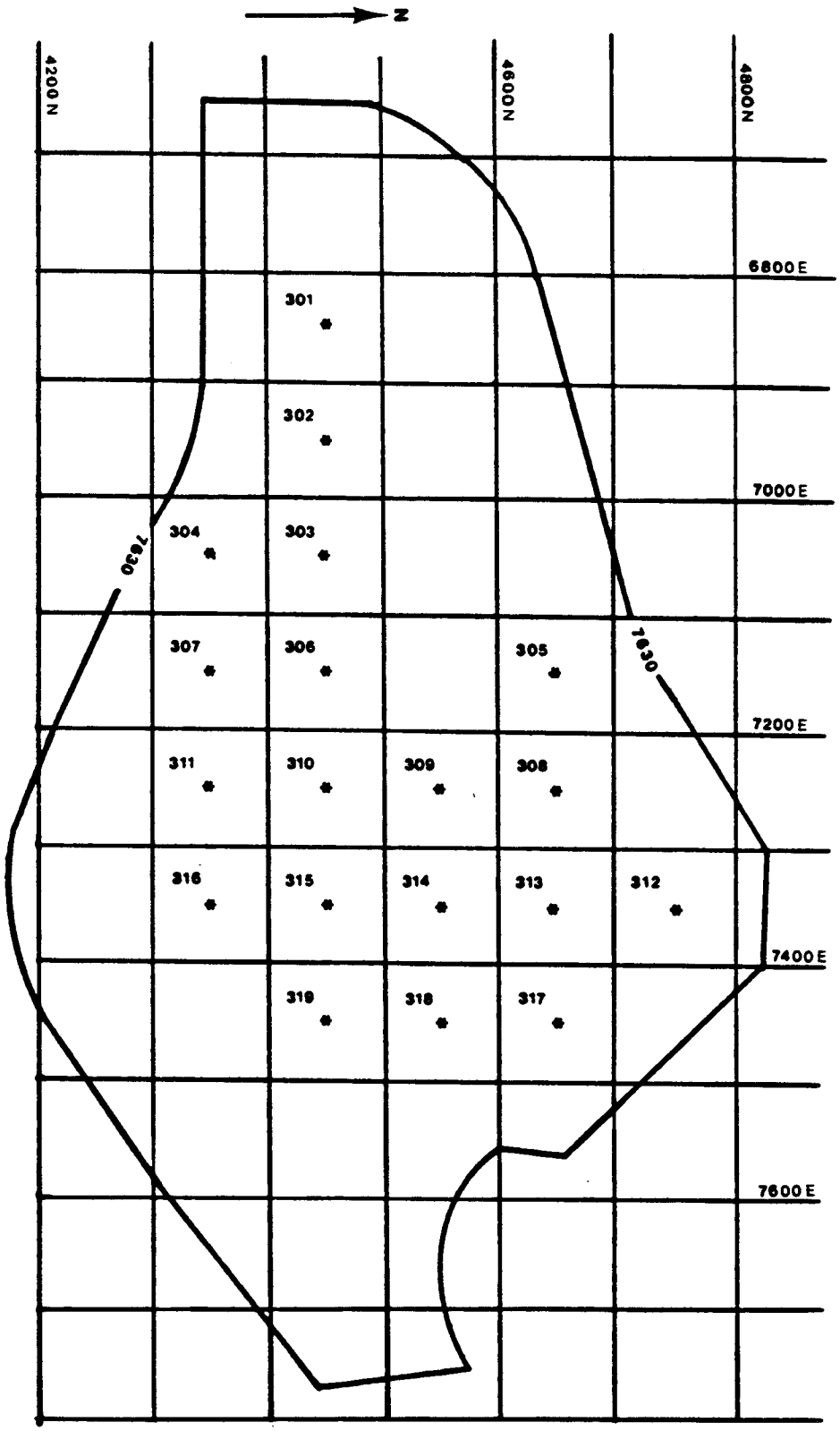

Figure 40: Panel Locations 7630 Bench

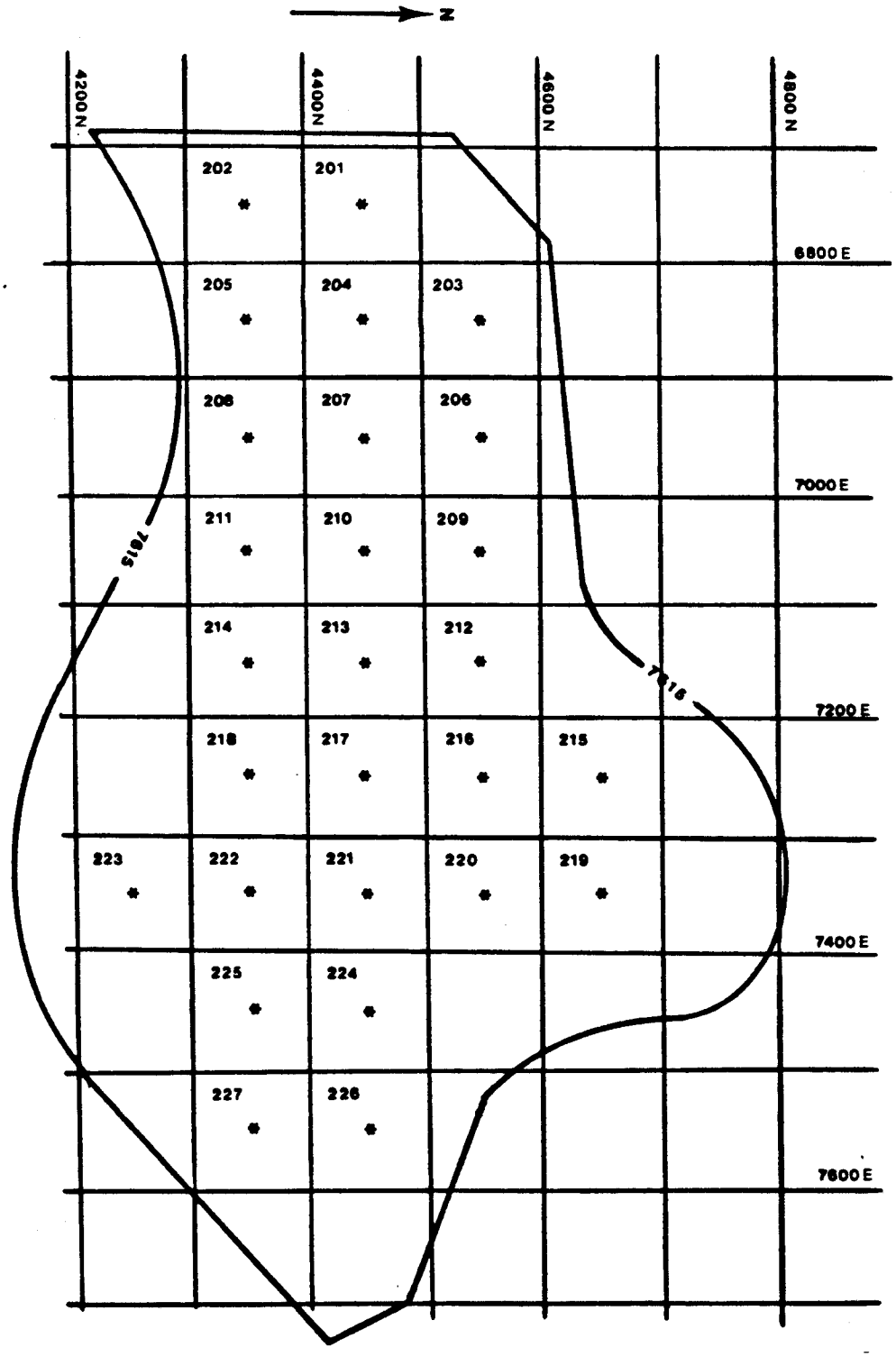

Figure 41: Panel Locations 7615 Bench

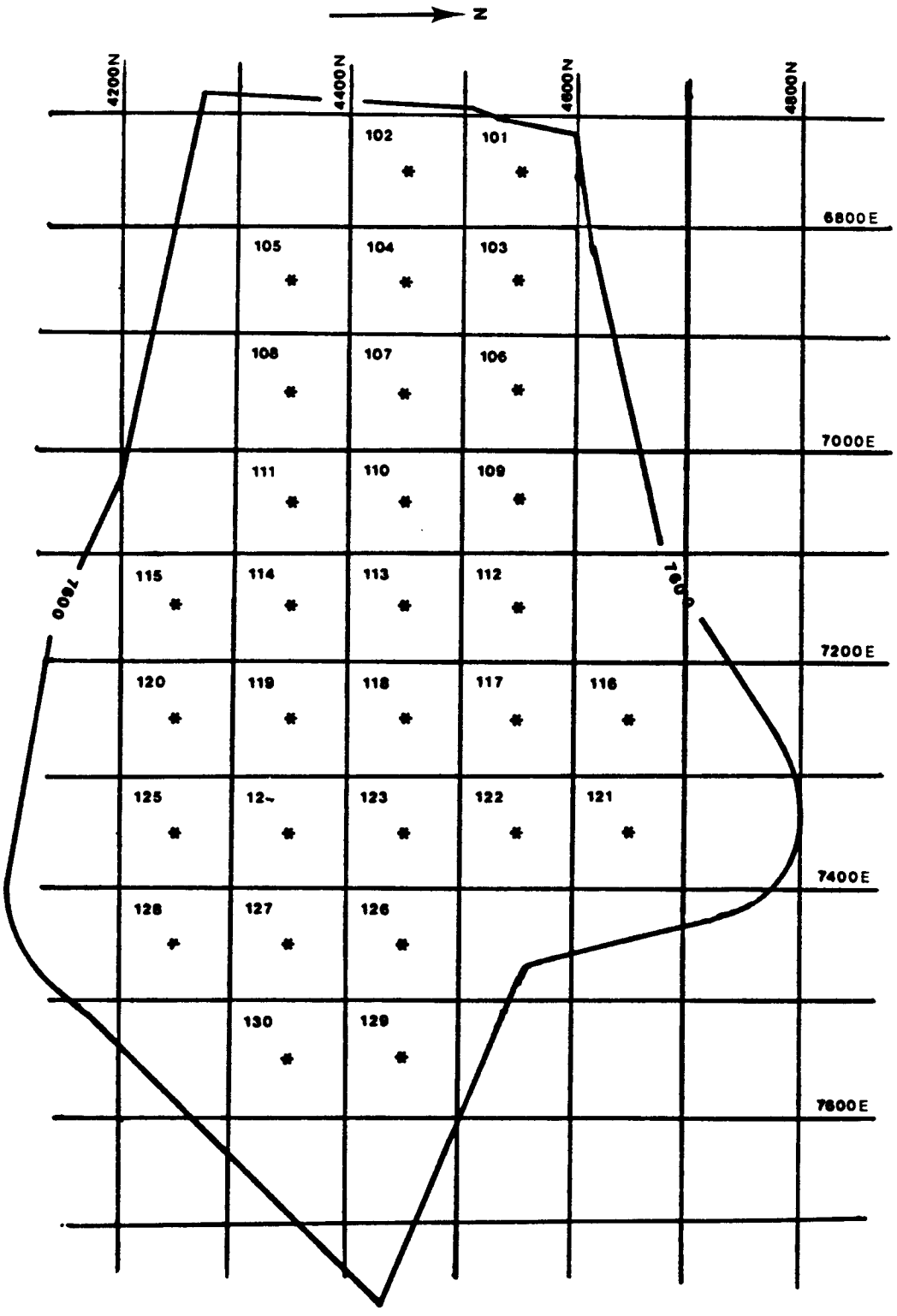

Figure 42: Panel Locations 7600 Bench

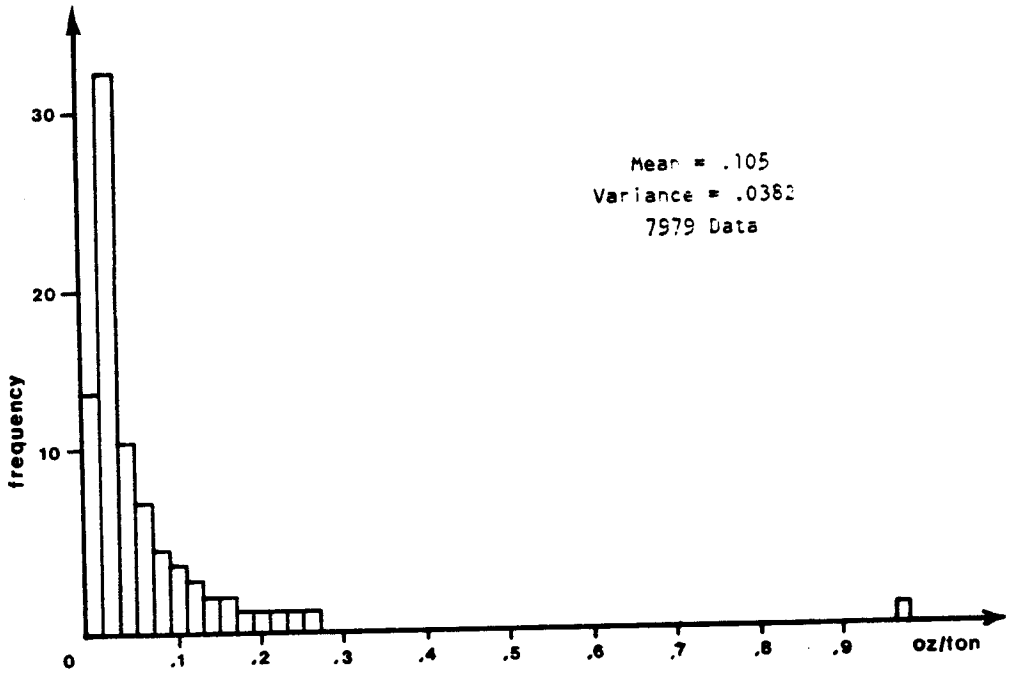

Figure 43: Histogram of the 7979 Blasthole Assays

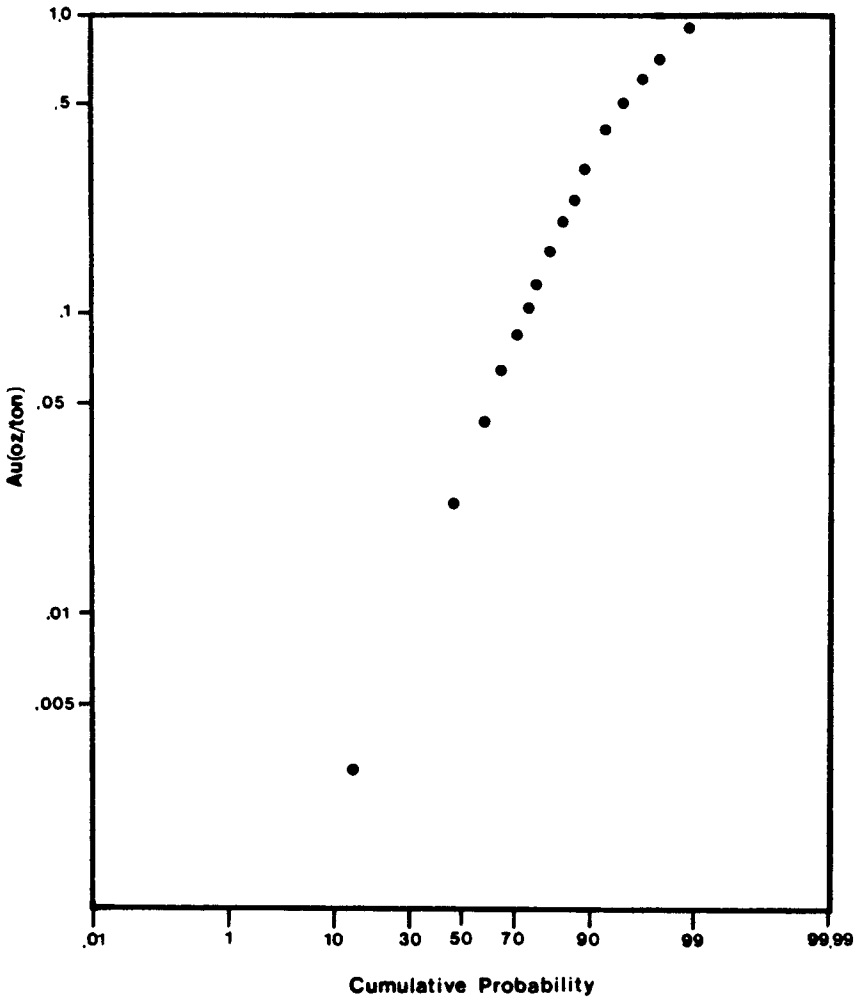

Figure 44: Lognormal Probability Plot of the 7979 Blasthole Assays

4.3.1 Influence of Geology on the Grade Distribution

The five benches of the Lower North Generator Hill orebody which will be studied contain rocks from the Roberts Mountains Formation and members 1, 2, and 3 of the Hanson Creek Formation. This portion of the deposit is transversed by two major east-west trending faults: the Bell fault and the Lower North Generator fault. These two faults are, in turn, cut by several northwest and northeast trending faults (fig 45).

The blastholes located within each of the various rock types have been determined and basic statistics, which are summarized in table 8, were calculated.

This table indicates that the major host to gold mineralization throughout this portion of the deposit is the oxidized and unaltered rocks of the third member of the Hanson Creek Formation. This fact explains the relatively high grade of the data from the 7630 bench since this bench contains a much higher proportion of this rock type than the other benches. The highly silicified portions of the orebody composed primarily of jasperoids carry significantly less gold than the unsilicified portions. A slight contradiction to this observation is that the partly silicified rocks which are found on the 7600 and 7615 benches contain relatively high gold grades. The high grades in these rocks are most likely due to structural rather than lithological control as the zones of partly silicified limestone are found adjacent to the Bell fault which is the main mineralization conduit for this orebody. The Roberts Mountains Formation occurs on both the 7645 and 7660 benches and carries significant amounts of gold.

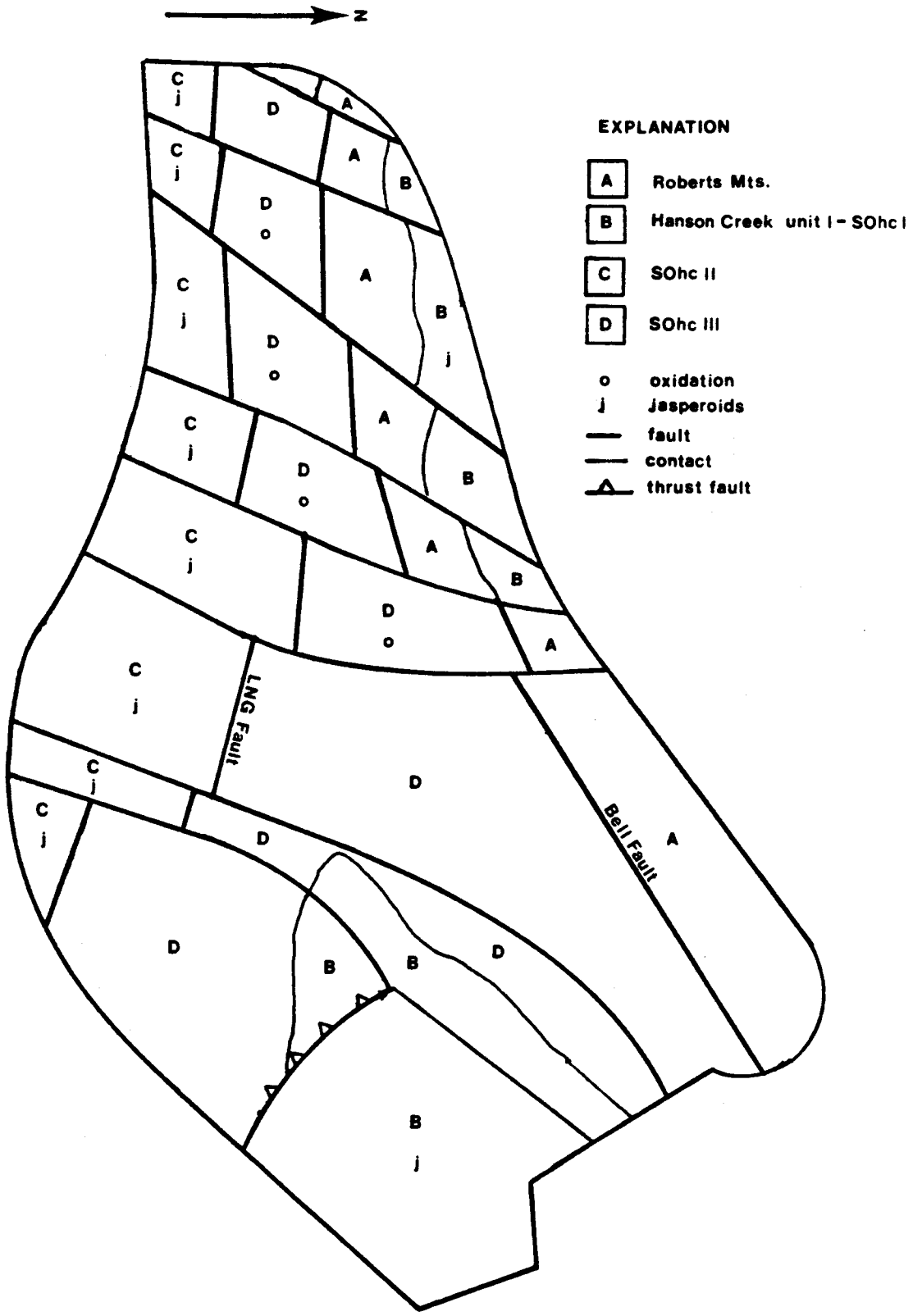

Figure 45: Schematic Geologic Map of the 7630 Bench of the Bell Mine

TABLE 8

Mean Grade of Blastholes in Various Rock Types

ROCK TYPE	BENCH 7600	7615	7630	7645	7660	
SOhc 3 LMS + ox. LMS	.059(1315)	.112(1365)	.152(1023)	.165(860)	.236(311)	.123(4874)
Roberts Mountains	--------	---------	--------	.077(281)	.085(558)	.082(839)
SOhc 1 + 2 Jasperoids	.074(455)	.072(276)	.112(143)	.080(397)	.066(143)	.078(1414)
SOhc 1 Jasperoids	.015(134)	.019(146)	.036(83)	.016(156)	.066(162)	.0305(681)
SOhc 3 partly silicic	.208(125)	.220(46)	-------	--------	--------	.211(171)
	.069(2029)	.102(1833)	.140(1249)	.117(1694)	.120(1174)	.105(7979)

explanation: .1(100)

.1 is the mean grade of the 100 blastholes found within a particular rock type on a particular bench

The conclusion that can be drawn from this analysis of the blast hole assays by rock type is that there certainly are separate statistical populations present in this deposit which are controlled by geology, and should be dealt with separately if sufficient exploration data is available to allow such a separation. Unfortunately the amount of data present at the exploration stage of a study is significantly less than the amount of data used in this analysis; hence, only a limited number of exploration data will fall within each of the various geologic rock types. Thus in an actual application, separation of this deposit into distinct geologic populations would be very uncertain and therefore may not be attempted. It is assumed that the exploration data which are used for this deposit do not allow an accurate separation of the geologic populations; therefore, for the purposes of this study the deposit will be considered as a single homogeneous geologic population.

4.3.2 Proportional Effect

The final procedure in analyzing the 7,979 data which comprise the base knowledge of this deposit will be examining the relation between panel mean and the variance of data within a panel. The mean and standard deviation of data falling within each of the 119 panels was computed and plotted as a point on a scattergram of panel standard deviation versus panel mean (fig 46). The relation between the standard deviation and the mean is nearly linear, hence the variance of the points in a panel is nearly proportional to the panel mean squared. This is the well known proportional effect which is often observed in many types of deposits exhibiting a lognormal-type distribution of data.

In the past three sections it has been shown that the type of stationarity model required to perform PK or IK may not be acceptable for the Bell Mine; since the data show

1. A vertical trend
2. Different mean grades within different geologic populations
3. Proportional effect

In developing the PK and IK estimators a key hypothesis was that the bivariate distribution of grades was stationary over the deposit. Apparently this hypothesis is not acceptable for the Bell Mine and most likely is not acceptable for any other actual deposit. Since in most practical applications it is very difficult to identify and treat various causes of non-stationarity, it is important to examine the sensitivity of the IK and PK estimators to departures from the stationarity assumption. Therefore in this case study no attempt will

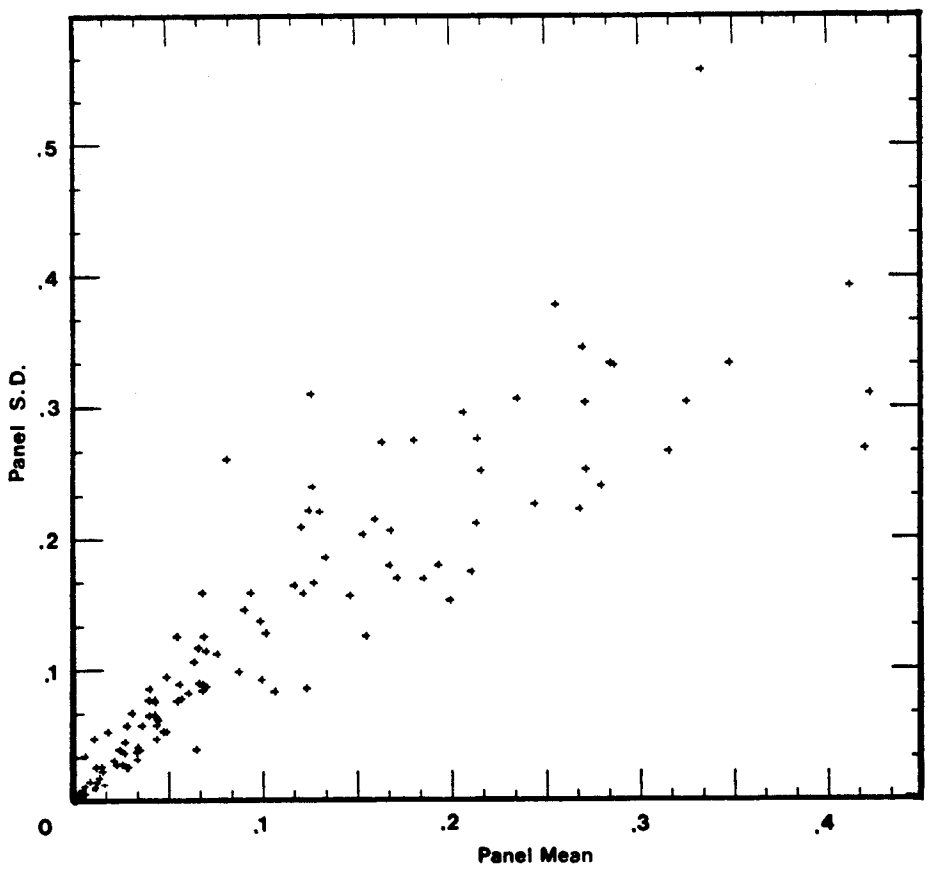

Figure 46: Plot of Panel Standard Deviation Versus Panel Mean

be made to treat any type of non-stationarity and the results obtained, if of acceptable quality, will demonstrate the insensitivity of the PK and IK techniques to departures from the underlying stationarity hypothesis.

4.4 ESTIMATION OF RECOVERABLE RESERVES

To test the efficiency and accuracy of the indicator and probability kriging techniques, samples will be taken from the data base to simulate drilling campaigns. Three drilling campaigns will be considered to test the influence of increasing the number of exploration data on the results. The first campaign is comprised of 193 data on an approximately regular 100 foot grid. The second campaign is comprised of 313 data on an approximately regular 71 foot grid and lastly the third campaign is comprised of 623 data on an approximately regular 50 foot grid. Campaign 1 is comprised of the closest blasthole to each of the four corners of each panel. Campaign 2 includes the information used in campaign 1 plus the blasthole nearest the center of the panel is also taken to produce a 5 spot pattern. Campaign 3 includes the data from campaign 2 and adds the blastholes closest to the centers of the edges of the panel (fig 37). Using these data the recoverable reserves based on point support smus will be estimated and compared to the actual recoveries determined from the values within the panel.

The estimation of recoverable reserves will be performed bench by bench; that is, the estimates obtained for any panel are based solely on data located on the same bench as the panel. The reasons for performing a two dimensional estimation rather than a three dimensional estimation are not related to any theoretical or practical deficiencies of the estimators as these techniques can easily be applied on three dimensional data sets. The study will be performed utilizing two dimensional data sets primarily because the data base is not a true three dimensional data set. The data set used is not a set of

exploration drill holes which penetrate all five benches under consideration, rather the blasthole data which is available are located on each bench independently of the locations of blastholes on other benches. Thus the data do not line up vertically from bench to bench so it is difficult to compute a meaningful vertical variogram.

The steps which will be followed in obtaining the estimate of recoverable reserves are identical to the steps followed in estimating spatial distributions (sec 3.3). One trivial difference is that, in recoverable reserve estimation, one is interested in tonnage above cutoff so $1-\phi(A,zc)$ is the quantity of interest rather than $\phi(A,zc)$. In proceeding through the various steps of the estimation procedure, all drilling campaigns will be treated within each step to easily compare results from the various campaigns.

4.4.1 Data Analysis

One of the primary tools in data analysis is the histogram of the data (fig 47). The histograms from all three campaigns present the same general features. All show a spike due to values less than .003 oz/ton, which is considered to be the detection limit of the fire assay technique, containing between 16 and 18% of the available data. The shape of the distribution in all campaigns is lognormal in appearance and similar to that of all 7,979 values (fig 43). The parameters of these distributions are summarized in table 9.

Notice that all three sampling campaigns are representative of the complete data base of 7,979 values as far as mean and coefficient of variation are concerned. Suprisingly the least representative sampling

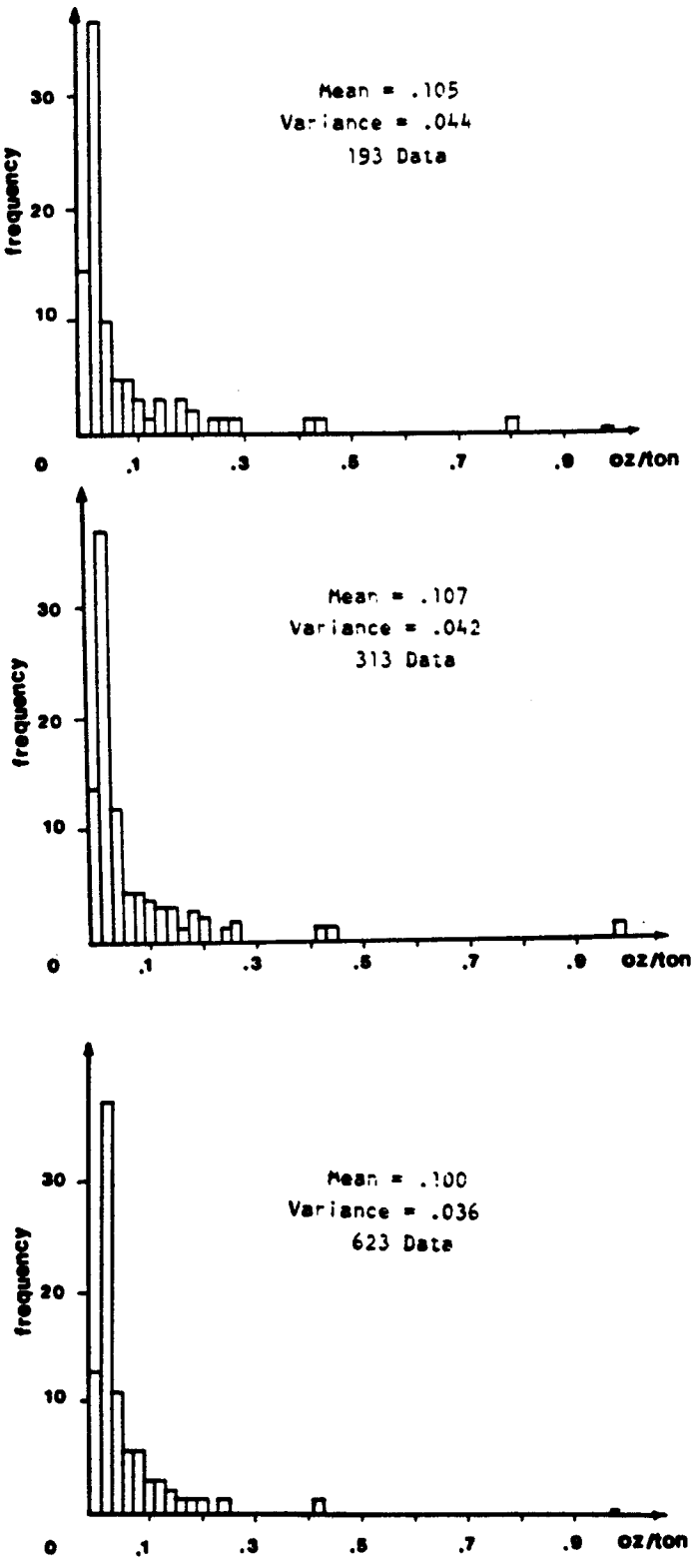

Figure 47: Histograms of the Data From Campaigns 1, 2, and 3

TABLE 9

Parameters of the Exhaustive and Exploration Histograms

	Number of Data	Mean	Variance	Coefficient of Variation
Campaign #1	193	.105	.044	2.00
Campaign #2	313	.107	.042	1.91
Campaign #3	623	.100	.036	1.90
Exhaustive	7979	.105	.038	1.86

campaign is campaign number 3 which, although containing the most data, underestimates the global mean grade of the deposit. This unfortunate result can only be attributed to bad luck in sampling.

Variograms of grade in each of the three sampling campaigns show similar spherical type structures with ranges between 100 and 150 feet. No anisotropies are observed so only the omnidirectional variograms are plotted (fig 48). Without information at short distances, accurate modelling of these variograms is impossible as there is no way, even with the campaign 3 data, to predict the nugget effect. Information at short distance is provided by twinning 20 of the blast hole assays (four on each bench) to provide an estimate of the variogram value at 12 feet. Twin holes were used rather than a single fence of 20 data for two reasons. First, grades obtained from a fence located within a single region of the deposit will be influenced by the strong proportional effect present in the deposit so the information obtained could be misleading. Second, a fence of data is generally useless for estimating indicator variograms as the indicator data in the fence are usually all

above or below any cutoff of interest so that the variogram value is usually zero. Twin holes provide more information concerning the behavior of the indicator variograms at short distances because the twins can be located throughout the deposit, hence the entire distribution of grades tends to be sampled and the influence of the proportional effect is minimized. The twin hole information is used only to estimate the various variograms required. It is not used in either the histograms of the various sampling campaigns nor will it be used in the kriging.

Using the twin hole information, models were fit to the variograms of the grade data from each campaign.

Campaign	Variogram Model
1	$\gamma(h) = .007 + .013\ Sph_{65}(h) + .0224\ Sph_{110}(h)$
2	$\gamma(h) = .006 + .019\ Sph_{65}(h) + .0155\ Sph_{175}(h)$
3	$\gamma(h) = .007 + .012\ Sph_{60}(h) + .019\ Sph_{140}(h)$

These variogram models as well as the variogram of all 7979 data are plotted in figure 48. Notice that the variogram of the 7979 data has a significantly larger nugget effect than the variogram models derived from the data from the three campaigns. In effect the true nugget effect has not been modelled correctly. Therefore variances or gamma bar values calculated using the variogram models determined from the data of the three sampling campaigns will be different from the true values. This error in modelling will be most important when calculating gamma bar values for small block sizes.

The final step in the data analysis step is determining the cutoffs at which estimates will be computed so that the transformed grades i(x,zc) and u(x) can be determined. In actual applications the chosen

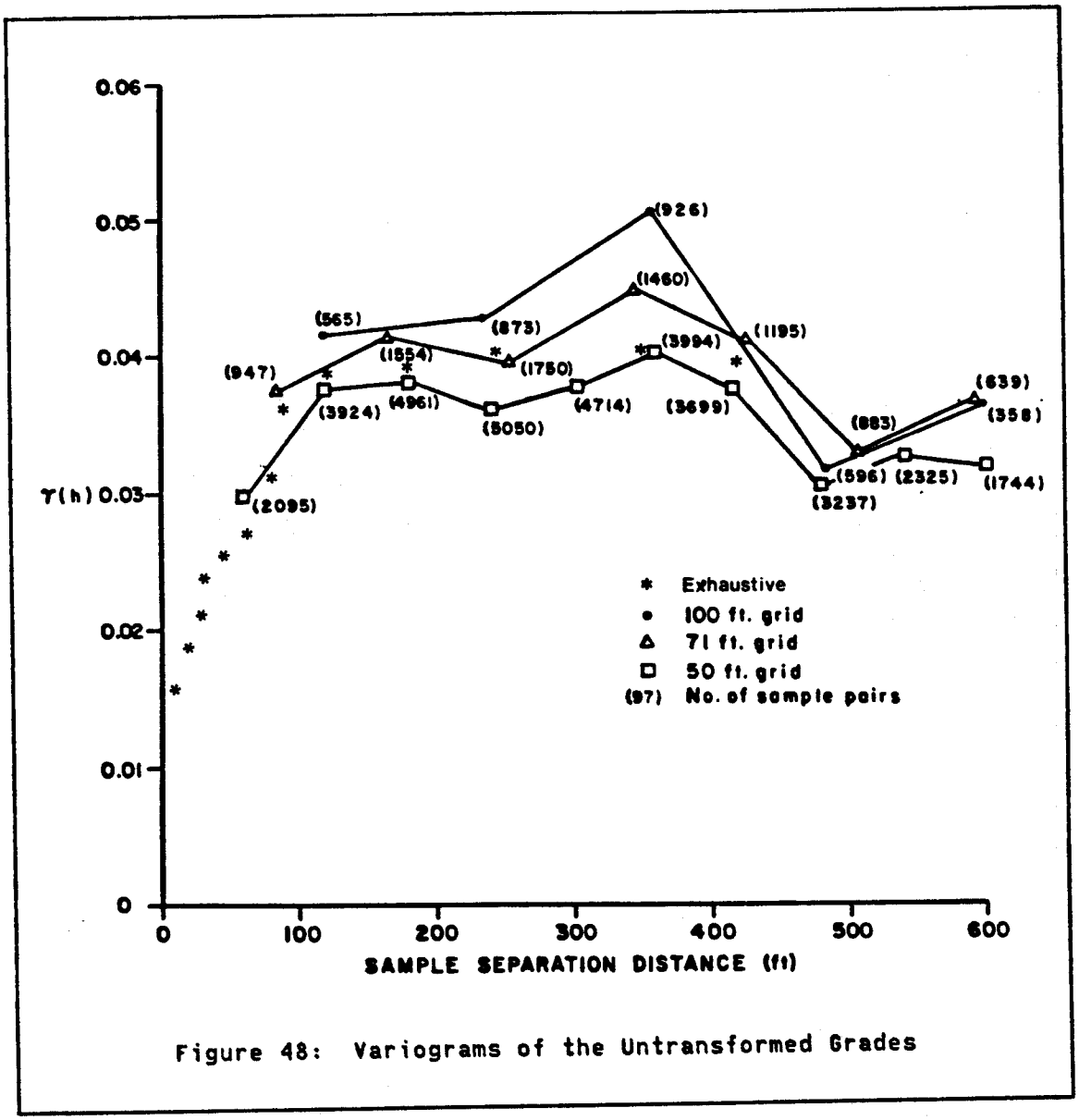

Figure 48: Variograms of the Untransformed Grades

cutoffs will have some physical significance (i.e. an economic cutoff or threshold); however, as the purpose of this study is to demonstrate the effectiveness of the new estimation techniques over a range of possible conditions, the cutoffs which are chosen span the range of all possible cutoffs. The chosen cutoffs are the detection limit of the fire assay technique plus the remaining 8 deciles of the distribution of the 7979

blast hole assays. The chosen cutoffs plus the percentage of data below each cutoff for the three sampling campaigns are shown in table 10 which shows that the percentages of data below each of the 9 cutoffs is similar for all three sampling campaigns and for the exhaustive data base. Thus the data of all three sampling campaigns are representative of the exhaustive data base which is not surprising since all three sampling campaigns are comprised of data on a nearly regular grid.

TABLE 10

Cutoffs Chosen

Cutoff(oz/ton)	Percentage of Distribution Below Cutoff			
	Campaign #1	Campaign #2	Campaign #3	All 7979 Data
.003	15	14.1	13.5	14
.005	19.7	19.5	19.	20.
.010	33.7	32.3	30.5	30.
.017	45.6	42.8	41.8	40.
.027	53.9	52.7	52.7	50.
.046	63.2	63.3	63.3	60.
.079	71.	70.3	72.5	70.
.144	79.3	80.2	82.1	80.
.313	90.7	89.5	90.	90.

To proceed with either the IK or the PK estimators, indicator transforms of the data must be computed for each of the 9 cutoffs. As seen in sections 2.3.1 and 3.3.1 this transform is quick and simple to perform. In addition to the indicator transform of the data, the uniform transform (sec 2.6.1 and 3.3.1) of the data is also required to perform probability kriging. As in the previous case study, there is a

large spike in the data. Hence, before the uniform transformation of the data this spike must be removed through the despiking procedure (see sec 3.3.1). For all three campaigns, a circular despiking neighborhood with a radius of 150 ft. was used.

Once the transforms are completed, the next, very important, step of variography is performed.

4.4.2 Variography

Computing and modelling indicator, cross and uniform transform variograms is a time consuming and tedious step in distribution free estimation of recoverable reserves, as both indicator and cross variogram models are required at each cutoff. Although time consuming and tedious, this is arguably also the most important step in the study, as poor variogram modelling can adversely affect the quality of the results. For this reason, the modelling of these variograms should be performed carefully and patiently; resisting the urge to pass quickly through this step and move on to the kriging step.

4.4.2.1 Indicator Variography

The indicator variograms, for all three campaigns, are modelled by nested spherical structures. Anisotropies were not observed at any cutoff in any of the three sampling campaigns. The omnidirectional models which were fit for the three campaigns are given in table 11.

The criteria used in fitting the models (shown in table 11) to the experimental points varies for the different campaigns. For example, when modelling the indicator variograms for campaign 1 the shape of the

TABLE 11

Indicator Variogram Models

Model[1] $\gamma_i(h) = C_0 + C_1 Sph_{r1}(h) + C_2 Sph_{r2}(h)$

	Campaign #1			Campaign #2					Campaign #3				
Cutoff	C_0	C_1	r_1	C_0	C_1	r_1	C_2	r_2	C_0	C_1	r_1	C_2	r_2
.003	.07	.05	250	.03	.08	200			.07	.04	180		
.005	.05	.11	350	.06	.09	240			.08	.06	220		
.010	.05	.17	300	.06	.07	100	.10	340	.08	.03	40	.10	260
.017	.09	.16	300	.06	.06	40	.13	280	.08	.04	40	.12	280
.027	.10	.15	200	.08	.06	40	.12	280	.10	.03	40	.12	250
.046	.09	.14	180	.09	.04	40	.11	290	.08	.06	40	.10	250
.079	.06	.15	170	.06	.06	40	.10	260	.08	.04	40	.09	200
.144	.04	.13	140	.06	.03	40	.07	170	.04	.02	40	.09	140
.313	.04	.05	130	.05	.05	100			.04	.06	90		

[1]where Sph_{r1} is a spherical model with range r_1.

model at short distances is strongly dependent on the value of $\gamma(12)$ obtained from the twenty twinned blast hole assays. This dependence on $\gamma(12)$ decreases in campaigns 2 and 3, since more data at short distances, $\gamma(71)$ and $\gamma(50)$ respectively, become available. For campaigns 2 and 3 the behavior at short distances can be extrapolated from the experimental variogram values. When this extrapolated value of $\gamma(12)$ is widely different from $\gamma(12)$ calculated from twin hole data a compromise is made with more weight given to the extrapolated value. At some cutoffs, .027 oz/ton in particular (fig 50), the $\gamma(12)$ value obtained from the twinned data is obviously a poor estimate of the actual $\gamma(12)$. In these cases, the short scale behavior of the indicator variogram is obtained by a combination of extrapolation and examining

the short scale behavior at similar cutoffs. The experimental omnidirectional indicator variograms and the fitted models for three representative cutoffs are given in figures 49-51 with an example of the directional variograms given in figure 52. Table 12 summarizes the number of data used in computing each experimental variogram value.

TABLE 12

Pairs of Data Used to Calculate Experimental Indicator Variograms

Campaign #1		Campaign #2		Campaign #3	
Distance	# of Pairs	Distance	# of Pairs	Distance	# of Pairs
100.	307	71.	280	50.	650
199.	586	102.	478	71.	770
299.	613	141.	398	100.	880
406.	380	196.	890	141.	729
505.	310	293.	1243	200.	1403
		393.	1462	300.	1893
				401.	1882

There are several trends which are evident in the models of the indicator variograms. First the nugget effect and the total sill of the models tend to be largest at the median cutoff, .027 oz/ton, and smallest at the extreme cutoffs. This is not surprising since the sill of indicator variogram model is related to the variance of the indicator data. Recall

$$\text{Var}\,(I(x,zc)) = F(zc)\,(1 - F(zc))$$

$$= F(zc)^2 - F(zc)$$

This quantity is maximum when

$$d(F(zc)^2 - F(zc))/dF(zc) = 0$$

or

$$2\ F(zc) = 1$$

$$F(zc) = .5$$

So one expects to find the maximum sill near the median cutoff. Since the magnitude of the absolute nugget effect is usually related to the magnitude of the sill it is understandable why the nugget effect is also maximum near the median cutoff.

Another trend which is noticeable in all three campaigns is that the range of the indicator variograms decrease as cutoff increases. This trend provides information concerning the spatial continuity of the high and low grade material in this deposit. The low grade material, as evidenced by the long range on the indicator variograms at low cutoffs, is distributed over a wide portion of the deposit, while the high grade material, as evidenced by the short range of these variograms, occurs in small pods or lenses.

The conclusions reached concerning the decreasing range of the indicator variograms with increasing cutoff grade are supported by what is known about the mineralization in this deposit. The ore and waste in this deposit are interspersed, hence waste material can occur within any portion of the deposit so an indicator variogram with a long range is expected. High grade material, on the other hand, has definite local structural controls which localize the ore; hence, an indicator variogram with a short range is expected.

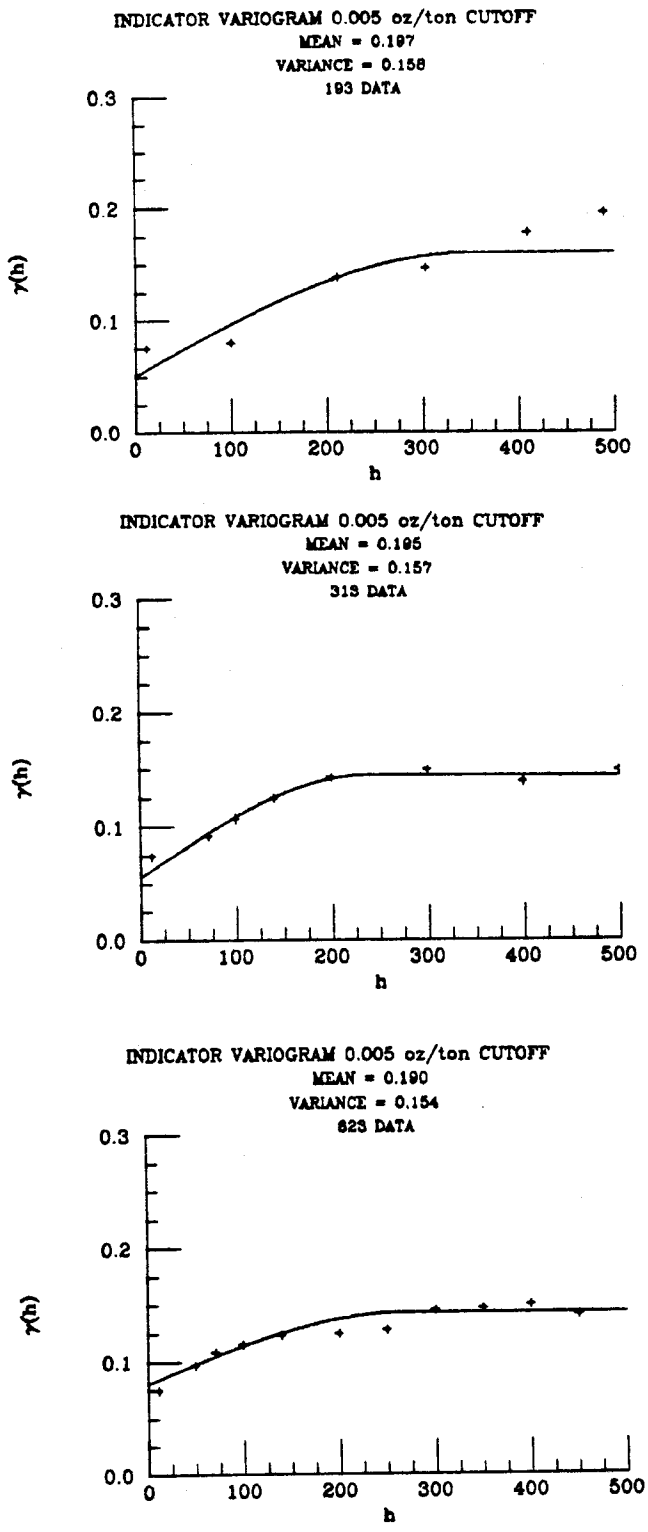

Figure 49: Indicator Variograms for the .005 oz/ton Cutoff

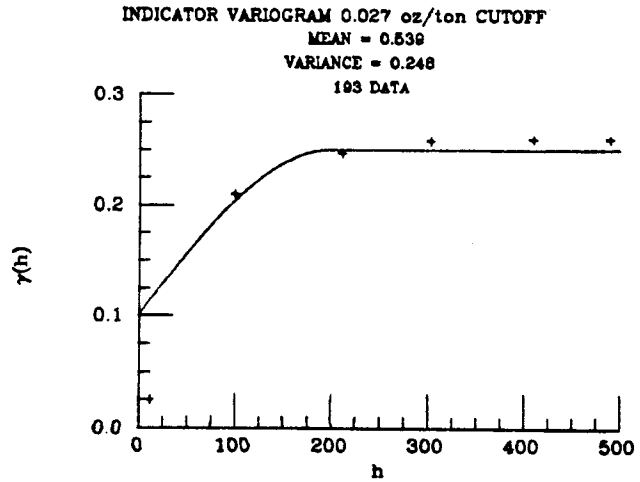

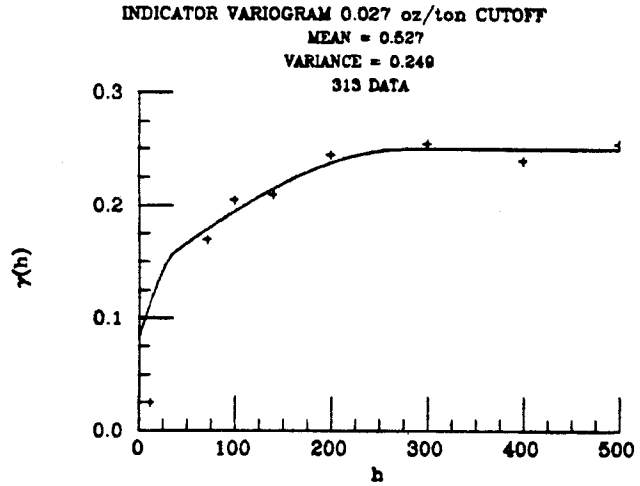

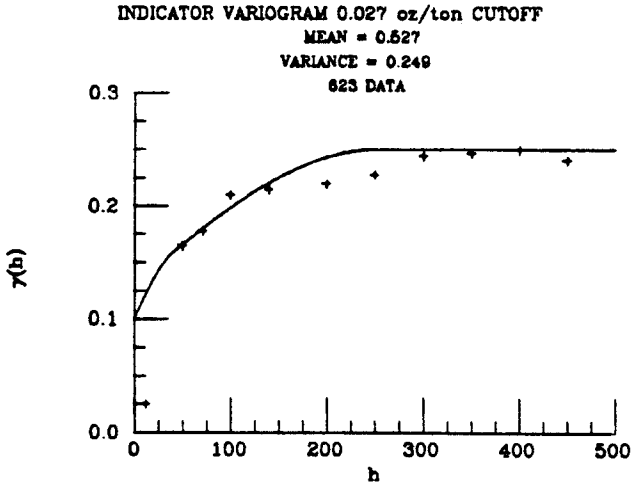

Figure 50: Indicator Variograms for the .027 oz/ton Cutoff

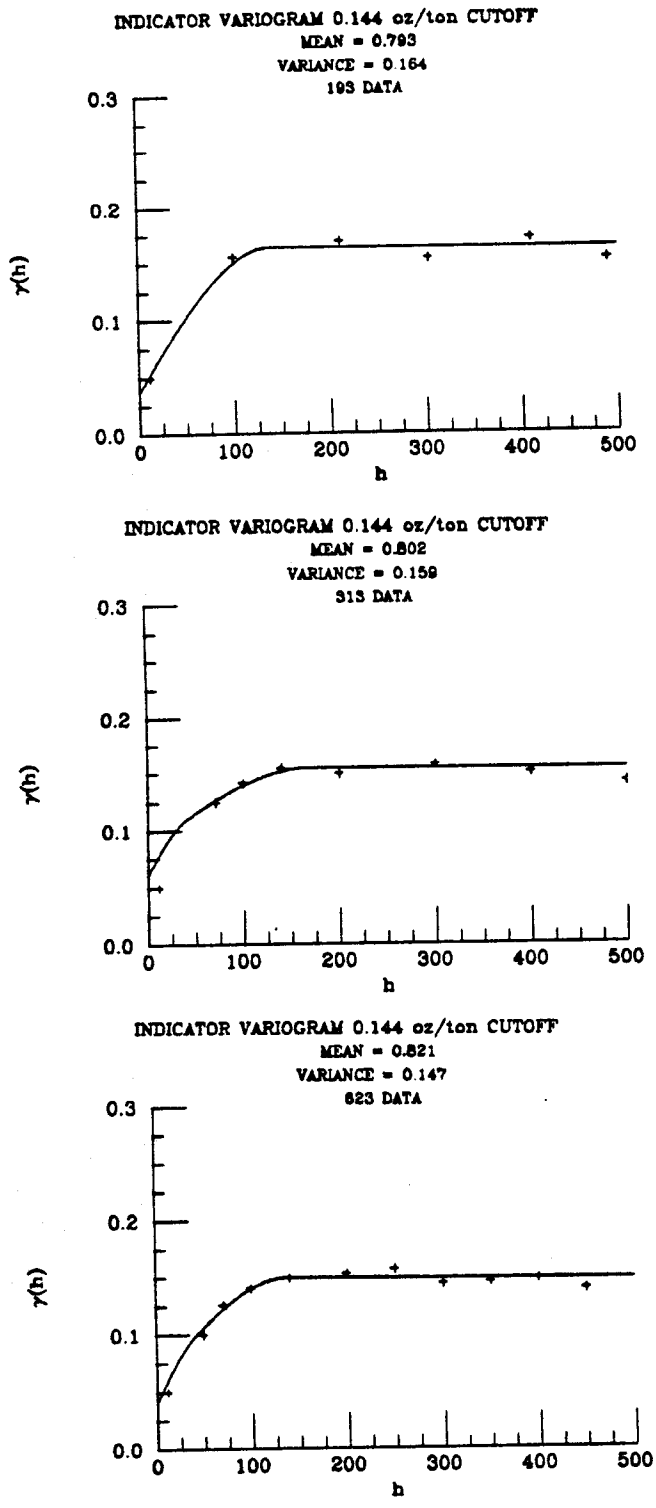

Figure 51: Indicator Variograms for the .144 oz/ton Cutoff

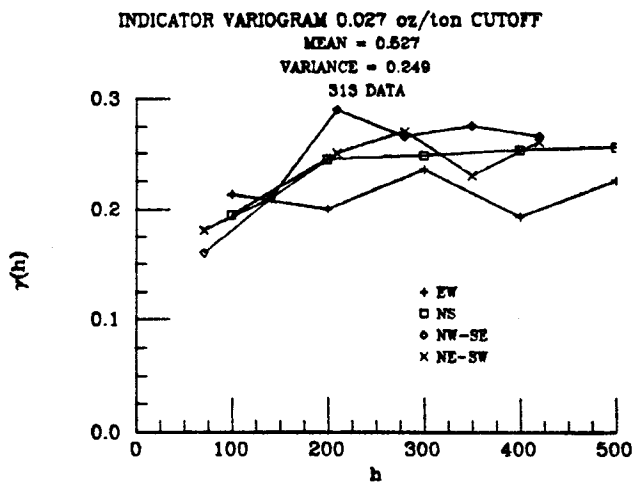

Figure 52: Directional Indicator Variograms for the .027 oz/ton Cutoff

4.4.2.2 Cross Variography

Cross variograms between the indicator data and the uniform transform of grade are required at each cutoff of interest to perform probability kriging. As with the indicator variograms no anisotropies were observed at any cutoff in any of the three sampling campaigns. The omnidirectional models which were fit for the three campaigns are given in table 13. The same criteria used in modelling the indicator variograms were also used to obtain the cross variogram models.

Again the same trends which appear in the indicator variogram models also appear in the cross variogram models. Again the absolute sill of these variograms is maximum near the median cutoff and decreases towards the extreme cutoffs. This trend can be predicted since the sill of the cross variogram is related to $C_{ui}(0,zc)$ which is maximum at the median cutoff.

TABLE 13

Cross Variogram Models

Model[1] $-\gamma_{iu}(h) = C_0 + C_1 Sph_{r1}(h) + C_2 Sph_{r2}(h)$

	Campaign #1			Campaign #2					Campaign #3				
Cutoff	C_0	C_1	r_1	C_0	C_1	r_1	C_2	r_2	C_0	C_1	r_1	C_2	r_2
.003	.02	.05	420	.02	.05	420			.02	.04	210		
.005	.02	.07	430	.02	.07	430			.02	.05	200		
.010	.04	.08	400	.02	.02	40	.08	400	.03	.07	190		
.017	.04	.08	300	.02	.02	40	.08	300	.02	.02	40	.08	250
.027	.05	.08	240	.02	.02	40	.09	270	.02	.03	40	.08	240
.046	.02	.09	190	.02	.02	40	.09	360	.02	.03	40	.07	240
.079	.02	.09	190	.02	.02	40	.08	300	.02	.02	40	.07	250
.144	.01	.08	180	.01	.02	40	.05	360	.01	.02	40	.05	230
.313	.01	.03	150	.01	.01	40	.03	140	.01	.04	150		

[1]where Sph_{r1} is a spherical model with range f_1.

$$C_{ui}(0,zc) = E[U(x)\cdot I(x,zc)] - E[U(x)]\cdot E[I(x,zc)]$$

$$= \int_0^{F(zc)} udu - .5\cdot F(zc) \qquad (4.2)$$

$$= F(zc)^2/2 - F(zc)/2$$

$$d\{F(zc)^2/2 - F(zc)/2\}/dF(zc) = F(zc) - .5 = 0$$

$$F(zc) = .5$$

The critical point again occurs at the median cutoff, so the absolute sill should be maximum at the median cutoff.

The omnidirectional experimental cross variogram values and the fitted models are given in figures 53 through 55. An example of the directional variograms is given for the median cutoff of .027oz/ton (fig 56).

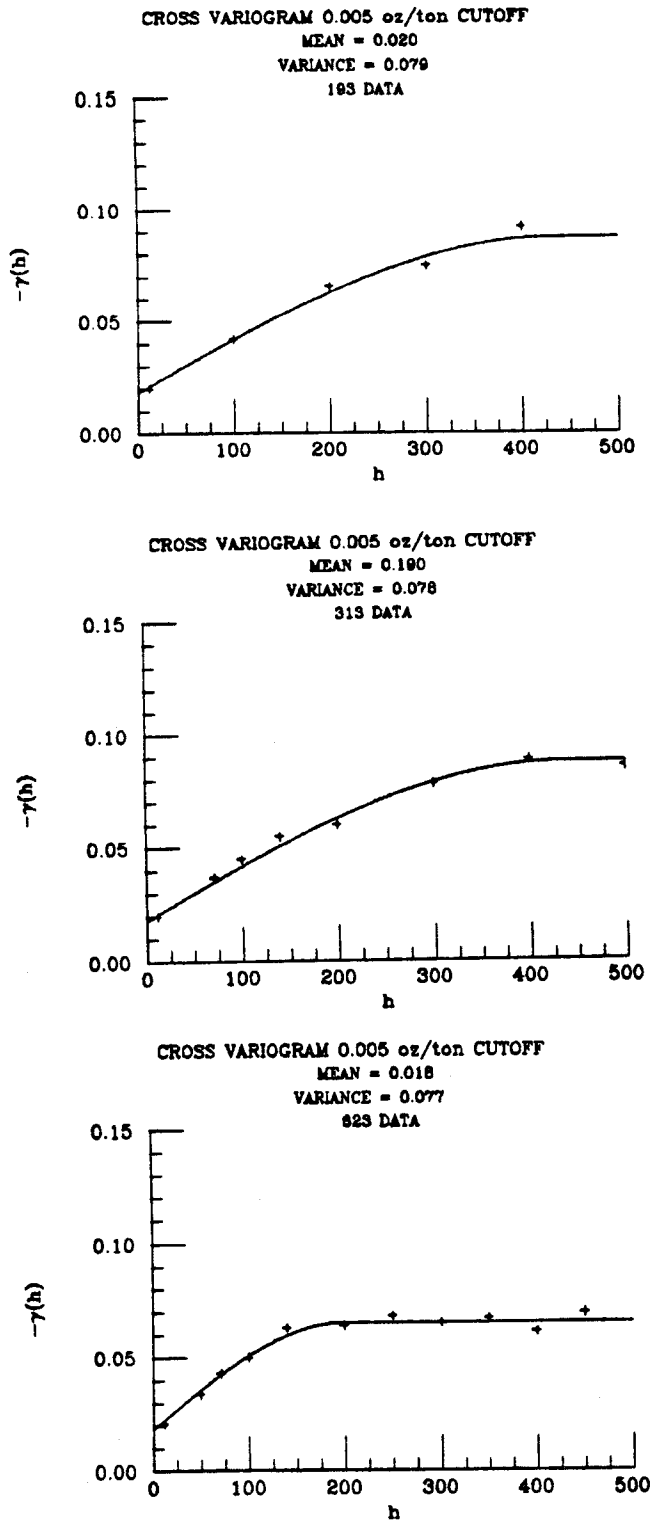

Figure 53: Cross Variograms .005 oz/ton Cutoff

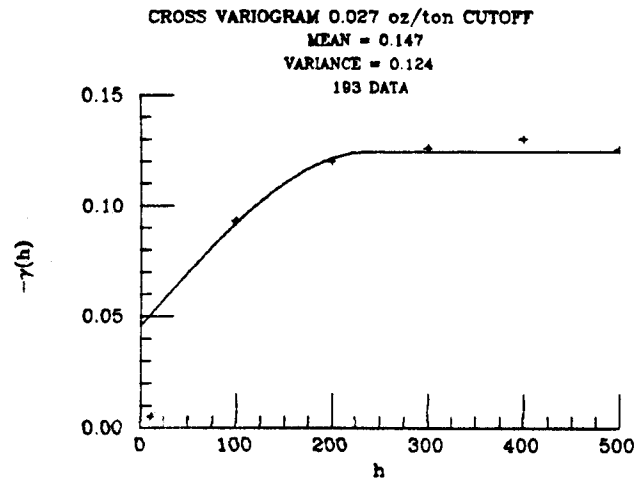

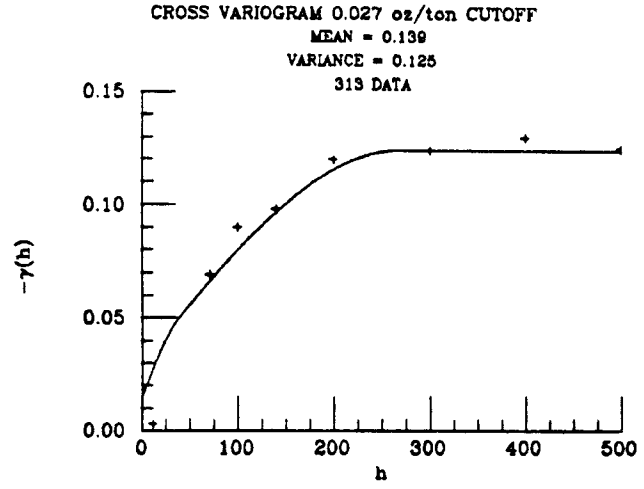

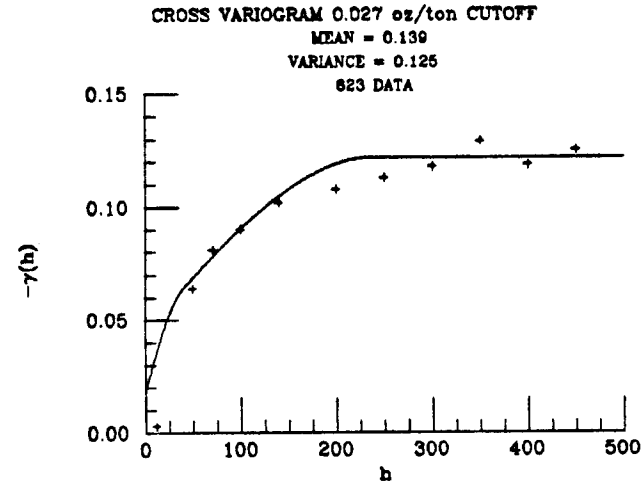

Figure 54: Cross Variograms .027 oz/ton Cutoff

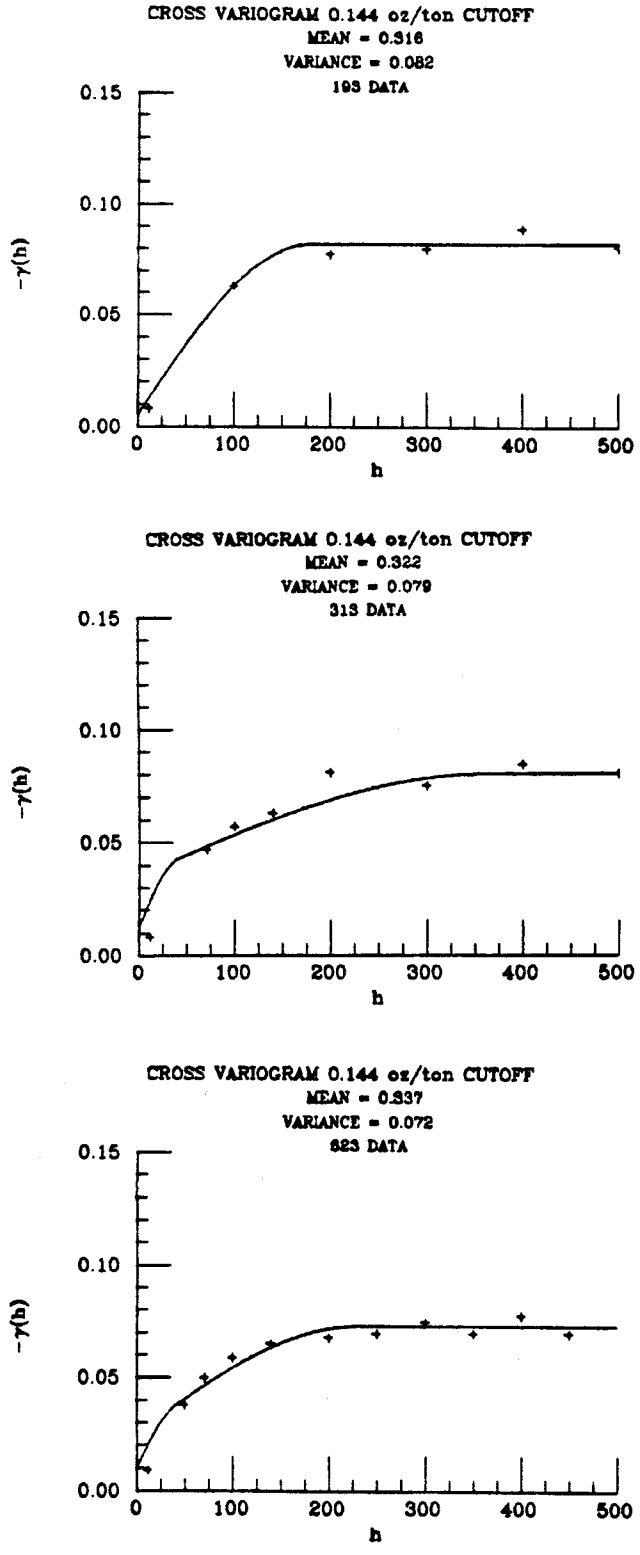

Figure 55: Cross Variograms .144 oz/ton Cutoff

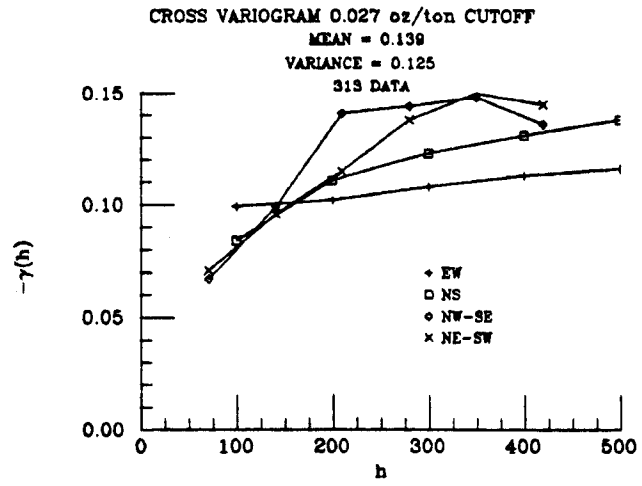

Figure 56: Directional Cross Variograms .027 oz/ton Cutoff

4.4.2.3 Variography of the Uniform Transform Data

A single uniform variogram for each drilling campaign is required to obtain a probability kriging estimate of recoverable reserves. Modelling of the short scale (less than the data spacing) structure of this variogram is not important since only the correlations between the uniform data locations and not the correlation between the data location and the panel are required. In other words, the uniform variogram or covariance appears only on the left hand side of the probability kriging system of equations (eqn 2.55, 2.56). The modelling of this variogram is thus simplified since the only concern is that the model pass near the experimental variogram points.

The uniform variograms for the 3 campaigns (fig 57) show no anisotropies, so isotropic models have been used. The models are

Campaign #1 $\gamma_u(h) = .04 + .049\ Sph_{420}(h)$
Campaign #2 $\gamma_u(h) = .02 + .02\ Sph_{40}(h) + .049\ Sph_{420}(h)$
Campaign #3 $\gamma_u(h) = .027 + .057\ Sph_{255}(h)$

Notice that the range of the variograms computed on the uniform transform of the grade z(x) have far longer ranges than the variograms computed on the untransformed values (see figure 48). This increase in range indicates that the uniform data are more highly correlated than the untransformed data. Thus, an estimator utilizing the uniform transform data should produce a better estimate of $\phi(A,zc)$ than an estimator utilizing the untransformed grades z(x), as estimation variance decreases as correlation increases. The increase in linear correlation after transform is possible because the uniform transform is a non-linear transform.

A second advantage of making a uniform transform of the data is that the experimental variogram values determined from the transformed grades are much less erratic than the experimental variogram values determined from the untransformed grades; thus, fitting the transformed grade u(x) variogram model is easier than fitting the untransformed grade z(x) variogram model. The reduction in the erratic nature of the experimental variogram is a result of the robust nature of the transform.

4.4.2.4 Positive Definiteness

As discussed in section 3.3.2, in order to preclude the possibility of obtaining a negative estimation variance, the matrix of covariances must be positive definite. The matrix of covariances used for the indicator kriging estimator will be positive definite since the

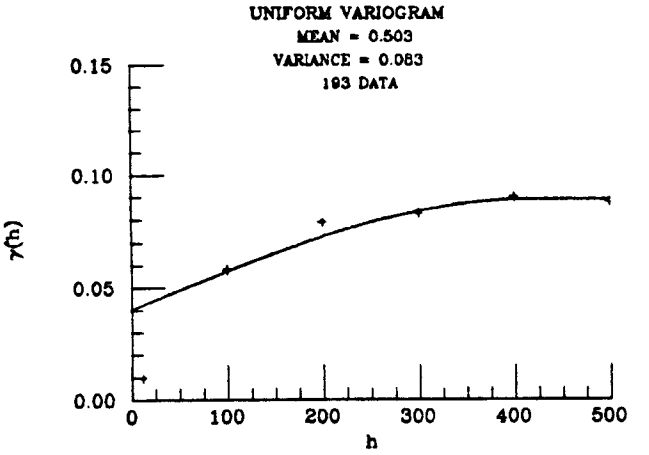

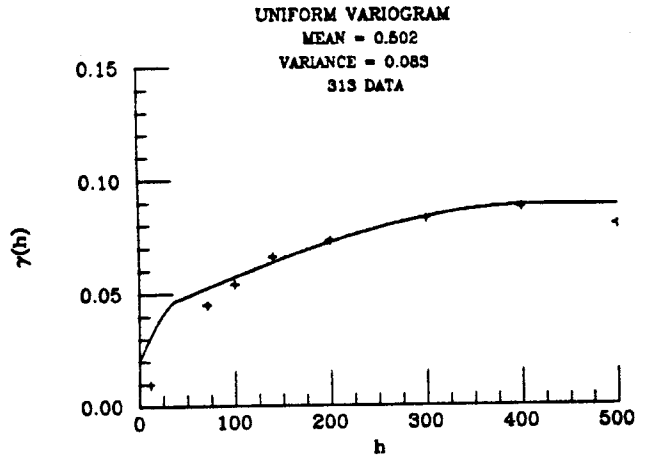

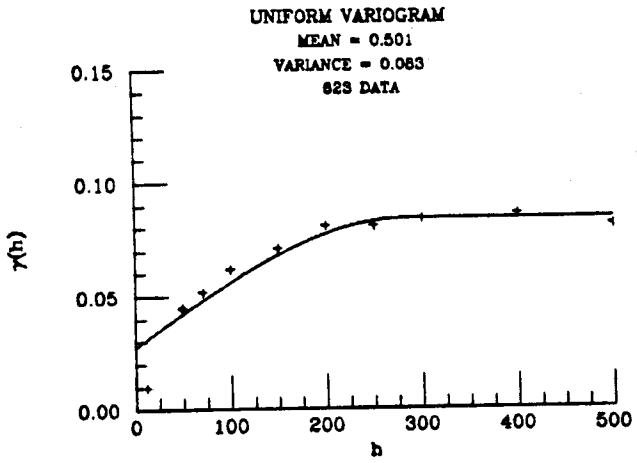

Figure 57: Uniform Variograms

spherical model, which is guaranteed to yield a positive definite matrix, was used at all cutoffs. In the case of probability kriging, however, the variogram models used for this case study do not by themselves guarantee a positive definite matrix of covariances since the linear model of coregionalization (sec 3.3.2) has not been used. A check of the positive definiteness of the PK covariance matrix was performed, however, and the PK covariance matrices are indeed positive definite. The check which was performed involved computing the determinant and all minor determinants of a covariance matrix from each sampling campaign. That is, the necessary and sufficient condition for a real matrix A to be positive definite is

$$x'Ax > 0 \quad \text{for all non-zero vectors } x.$$

An equivalent necessary and sufficient condition is;

All submatrices, of the matrix A, A_k have positive determinants

where:

$$A_1 = a_{11}$$

$$A_2 = \begin{bmatrix} a_{11} & a_{12} \\ a_{21} & a_{22} \end{bmatrix}$$

$$A_3 = \begin{bmatrix} a_{11} & a_{12} & a_{13} \\ a_{21} & a_{22} & a_{23} \\ a_{31} & a_{32} & a_{33} \end{bmatrix}$$

a_{ij} is the element in the ith row and jth column of matrix A.

Thus the determination of whether any covariance matrix under consideration is positive definite can be made by examining the determinants of the submatrices A_k. Only one covariance matrix from each campaign was checked because the data are located on a regular grid; hence, the covariance matrix is identical for all panels. The result of this check was that all of the determinants were positive; therefore, the variogram models which were utilized are acceptable given the particular regular sampling pattern encountered in the case study.

In future case studies it is recommended that the linear model of coregionalization be used to avoid any possibility of non-positive definite matrices. The linear model was not used in this case because it restricts the form of the variogram models to some degree and, since the data are located on a regular grid the check for positive definiteness was not difficult.

4.4.3 Kriging

In contrast to the previous variography step, the kriging step is not human labor intensive. It is, however computer intensive so great care must be taken when performing the kriging to minimize computer costs. The major steps which can be used to minimize the cost of kriging are

1. Use an efficient method for determining the data in the kriging neighborhood of the panel of interest (i.e. use the superblock concept).

2. Limit the number of data in the kriging neighborhood without affecting the resolution of the results.

3. Solve as few kriging systems as possible (i.e. if possible limit the number of cutoffs of interest and use data on a regular grid).

Point 3, although intuitive, can result in significant cost reductions. Recall the form of the indicator and probability kriging estimators.

$$\text{IK} \quad \phi^*(A,zc) = \sum_{\alpha=1}^{n} \lambda_\alpha(zc) \cdot i(x_\alpha,zc) + \left(1-\sum_{\alpha=1}^{n} \lambda_\alpha(zc)\right) \cdot F^*(zc) \qquad (4.3)$$

$$\text{PK} \quad \phi^*(A,zc) = \sum_{\alpha=1}^{n} \lambda_\alpha(zc) \cdot i(x_\alpha,zc) + \sum_{\alpha=1}^{n} \nu_\alpha(zc) \cdot u(x_\alpha) \qquad (4.4)$$

The weights, $\lambda_\alpha(zc)$ and $\nu_\alpha(zc)$, are, in this general expression, a function of cutoff, thus a kriging system must be solved at each cutoff. If the number of kriging systems which must be solved can be reduced, the computer cost will be reduced correspondingly. Since variograms having the same shape will yield the same kriging weights, it is necessary to solve only one kriging system for all of the cutoffs with identically shaped variograms. At the limit, all variograms may have the same shape, in which case, only one kriging system must be solved and the cost of performing PK or IK will be similar to that of kriging mean grade (i.e. ordinary kriging).

In some cases, particularly when using probability kriging, it is difficult to determine if variograms from different cutoffs have shapes which are similar enough to justify using the same weights. It is best, in these cases, to print out the weights given by the estimator at each cutoff. These weights give the user numerical values to compare in deciding whether weights at different cutoffs are close enough to be considered equal. The criterion used in determining if weights at different cutoffs are similar enough to be considered equal must be determined by the user based on cost constraints and the nature of the problem.

4.4.3.1 Kriging Plans

To further reduce the cost of kriging, one should consider the configuration of kriging data (also known as the kriging plan) that contains the smallest number of data which does not adversely affect the quality of the estimates. This is easily done by examining the weights given to data for various search radii. Those data locations receiving minimal weights should be eliminated from the kriging plan thus reducing the cost of kriging. The kriging plans used for the three campaigns are given in figure 58.

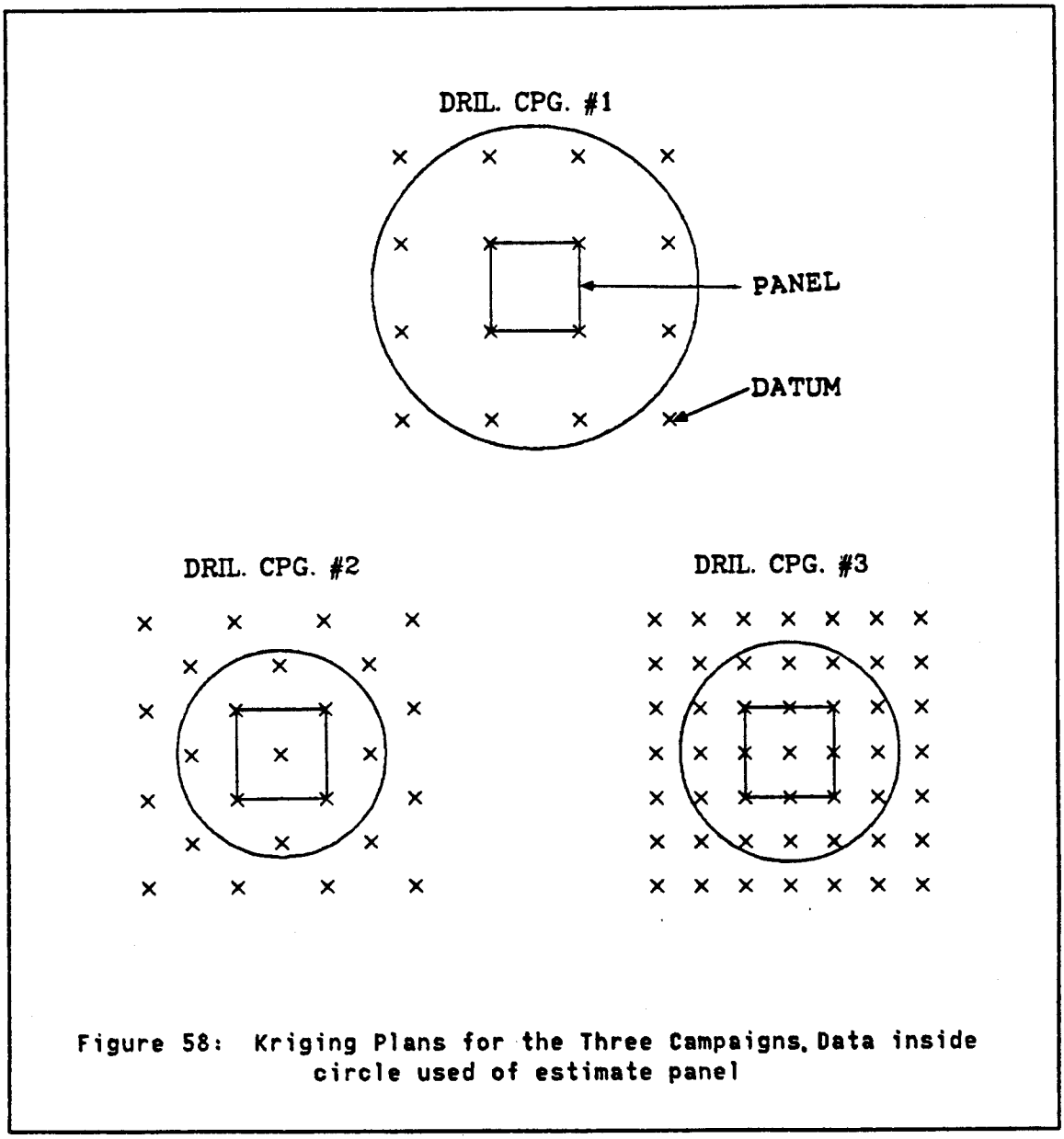

Figure 58: Kriging Plans for the Three Campaigns, Data inside circle used of estimate panel

4.4.4 Quantity of Metal Estimation

The discussion, to this point, has centered on estimating the spatial distribution, $\phi(A,zc)$, or equivalently the tonnage recovered based on a point support selective mining unit $(1-\phi(A,zc))$. Of equal or greater importance than the recovered tonnage is the recovered quantity of

metal, Q(zc). Recall that Q(zc) is not estimated by direct kriging (sec 2.8). Rather the quantity of metal estimate is based on the estimates of tonnage recovered. Recall the definition of recovered quantity of metal (eqn 2.76).

$$Q(zc) = T_a \cdot \int_{zc}^{\infty} z\,d\phi(A,z) \tag{4.5}$$

where T_a is the total tonnage of region A.
In the following T_a is assumed equal to 1.

This expression can also be written as

$$Q(zc) = \int_{0}^{\infty} z\,d\phi(A,z) - \int_{0}^{zc} z\,d\phi(A,z) \tag{4.6}$$

$$\text{with:} \quad \int_{0}^{\infty} z\,d\phi(A,z) = m_a \tag{4.7}$$

$$m_a = \text{the mean grade of region A} \tag{4.8}$$

$$\text{thus:} \quad Q(zc) = m_a - \int_{0}^{zc} z\,d\phi(A,z) \tag{4.9}$$

In practice $\phi(A,zc)$ is available for a discrete number of cutoffs, so these integral expressions must, in practical applications, be replaced by discrete sums.

$$Q^*(zc_k) = \sum_{\alpha=k}^{nc-1} [\phi^*(A,zc_{\alpha+1}) - \phi^*(A,zc_\alpha)] \cdot c_{\alpha+1} \tag{4.10}$$

$$Q^*(zc_k) = m_a^* - \sum_{\alpha=1}^{k-1}[\phi^*(A,zc_{\alpha+1})-\phi^*(A,zc_\alpha)]\cdot c_{\alpha+1}-\phi^*(A,zc_1)\cdot c_1 \qquad (4.11)$$

where: nc = number of cutoffs
zc_k is the cutoff of interest
m^*_a is an estimate of mean panel grade
c_α is a measure of central tendency for the material between cutoffs $zc_{\alpha+1}$ and zc_α

note: $\phi(A,zc_{nc})$ is assumed equal to 1 for all panels.
i.e. zc_{nc} is at least as large as the largest value observed.

The expression in equation 4.10 will be referred to as the direct quantity of metal estimate since the estimate of Q*(zc) is based solely and directly on the tonnage estimates. The expression in equation 4.11, on the other hand, is strongly based on the estimated mean panel grade which introduces an additional order relation which must be obeyed when using this expression:

$$m_a^* = \sum_{\alpha=1}^{nc-1}[\phi^*(A,zc_{\alpha+1})-\phi^*(A,zc_\alpha)]\cdot c_{\alpha+1} + \phi^*(A,zc_1)\cdot c_1 \qquad (4.12)$$

This method of estimating Q(zc) is, therefore, referred to as the indirect method.

4.4.4.1 The Direct Method

The only unknown values in the expression for the direct method are the central values c_α. As stated these values must be some measure of central tendency for the material between cutoffs zc_α and $zc_{\alpha-1}$. Ideally, this c_α value would be conditioned to the local environment entailing that c_α would be different for each panel A. However (sec

2.8) such local conditioning is not feasible due to practical considerations.

Since the c_α value cannot reliably be estimated locally, a global value must be used. A readily available value for c_α is the average of all data with grades between cutoffs $zc_{\alpha+1}$ and zc_α. This choice for the c_α's has the property that

$$m_d^* = \sum_{\alpha=1}^{nc-1} [F^*(zc_{\alpha+1}) - F^*(zc_\alpha)] \cdot c_\alpha + c_1 \cdot F^*(zc_1) \qquad (4.13)$$

where m_d^* is the mean of the exploration data
$F^*(zc_\alpha)$ is the value of the global cdf determined from the exploration data for cutoff zc_α.

If the data are located on a regular grid, the mean of the data is an unbiased estimate of the global mean. Thus when the data are located on a regular grid this choice of c_α will yield an unbiased estimator of global mean grade.

In cases where data are not located on a regular grid, the c_α values must be obtained by a weighted average of the data between cutoffs $zc_{\alpha+1}$ and zc_α. The weights[1] used are those obtained from declustering the data. If the declustering weights yield unbiased estimates of F(zc) and the deposit mean, then the c_α's chosen by this process will also yield an unbiased estimator of global mean grade.

---

[1] One method for obtaining the declustering weights is to lay a rectangular mesh equal in size to the average cluster over the deposit. The number of data in each cell, defined by the mesh, are counted. Each datum is given a weight equal to 1/(ND•N) where ND is the number of data in the cell and N is the number of cells in the deposit. This method is described in more detail by Journel (1983).

4.4.4.2 The Indirect Method

The direct method of estimating recovered quantity of metal is straightforward and simple to apply, however there are two reasons why the indirect method is preferred in some cases.

1. Biases in estimated quantity of metal recovered at high cutoffs are carried over to lower cutoffs when using the direct method.
2. Not all available information is used in the direct method.

Point 1 refers to the fact that the summation used to determine the quantity of metal recovered using the direct method at any cutoff includes the final term $[\phi^*(A,zc_{nc})-\phi^*(A,zc_{nc-1})]\bullet c_{nc}$. This term is typically much larger than the remaining terms in the series[1], so any error made in this term can not be easily compensated for by errors of opposite sign made at lower cutoffs. Therefore any error made at the largest cutoff will usually be transmitted to all lower cutoffs. This problem is especially prominent when the deposit is sparsely sampled as the estimates of $\phi(A,zc_{nc})$ will tend to be poor. This transmission of errors does not occur when using the indirect method, as the summation (eqn 4.11) is performed from lowest to highest cutoff, so errors at high cutoffs affect only the estimates at high cutoffs.

Point 2 refers to the fact that the direct method ignores a valuable piece of information: the quantity of metal recovered at 0 cutoff or equivalently the mean panel grade.

The indirect method of quantity of metal estimation is written as

---

[1]This is especially true at the Bell mine, as the material above the .313 oz/ton cutoff accounts for 10% of the global tonnage but 60% of the global ounces of gold.

$$Q^*(zc_k) = m_a^* - \sum_{\alpha=1}^{k-1}[\phi^*(A,zc_{\alpha+1}) - \phi^*(A,zc_\alpha)]\cdot c_\alpha - \phi^*(A,zc_1)\cdot c_1 \qquad (4.14)$$

To avoid any inconsistencies in the quantity of metal estimates, the following property must hold for each panel.

$$Q^*(zc_0) = m_a^* = \sum_{\alpha=1}^{nc-1}[\phi^*(A,zc_{\alpha+1}) - \phi^*(A,zc_\alpha)]\cdot c_\alpha + c_1\cdot\phi^*(A,zc_1) \qquad (4.15)$$

Thus, another order relation is introduced and the tonnage estimates obtained must verify this order relation. These tonnage estimates are obtained through quadratic programming similar to that used previously (sec 2.7).

$$\min \sum_{i=1}^{nc}(\phi^*(A,zc_i) - \phi^{**}(A,zc_i))^2 \qquad (4.16)$$

$$\text{subject to:} \quad \phi^{**}(A,ac_1) \geq 0$$
$$\phi^{**}(A,zc_{nc}) \leq 1$$
$$\phi^{**}(A,zc_{i+1}) \geq \phi^{**}(A,zc_i)$$

$$m_a^* = \sum_{\alpha=1}^{nc-1}[\phi^{**}(A,zc_{i+1}) - \phi^{**}(A,zc_i)]\cdot c_\alpha \qquad (4.17)$$

These new tonnage estimates, $\phi^{**}(A,zc)$, are thus as close as possible to the optimal estimates, $\phi^*(A,zc)$, but they uphold all order relation constraints. Practice has shown that when the ordinary kriging estimate of mean panel grade, m_a^*, is superior to the nonlinear estimate $Q^*(zc_0)$, the tonnage estimates and quantity of metal estimates provided by the indirect method are superior to those provided by the direct method. On the other hand, the results obtained by the direct method are superior when $Q^*(zc_0)$ is a better estimate of panel grade than the ordinary kriging estimate m_a^*. Unfortunately there is no exact criterion to indicate when each of these methods should be used.

As an aside it should be noted that the indirect method can be used to obtain tonnage and quantity of metal estimates when the data show a trend or drift in a given direction and hence are nonstationary. The estimate m^*_a used in such a case is simply the mean panel grade obtained through universal kriging.

4.5 RESULTS

In the previous sections three methods for obtaining distribution free estimates of conditional distributions were discussed. These methods: indicator kriging, probability kriging and probability kriging utilizing the mean panel grade, were used to estimate tonnage and quantity of metal recovered, assuming a point support selective mining unit, for each of 119 panels, 9 cutoff grades, and 3 drilling campaigns. Given the large number of cutoffs, campaigns and methods, a large amount of results have been generated, so it will be impossible to discuss all of the results in complete detail. Through the use of figures, however, the results, both global and local, can be summarized for presentation. The global results portion of this section will consist of an examination of the global bias, mean squared error, and smoothing of each estimator. Local results consist primarily of scattergrams of true versus estimated recoveries over all 119 panels for each cutoff and estimator. These scattergrams and associated statistics will give an indication of the local accuracy of each estimator.

The local and global results presented here give an indication of the overall capabilities of these estimators for varying amounts of data and give an indication of the quality of results one can expect when

applying these techniques to deposits with similar characteristics. Also as none of these estimators is perfect, this section will point out some of the strong and weak point of each estimator.

4.5.1 Global Results

Global results refer to total recoverable reserves. The most important of these global results is how accurately each technique predicts the global recovery. For completeness, however, other properties such as the mean square error and smoothing of the estimator will also be examined.

These global results are summarized in figures 59 through 70. In each of these figures the following nomenclature is used.

- A solid line represents the true values obtained from the 7979 blasthole assays which comprise the complete data base.
- The square symbol corresponds to the probability kriging (PK) estimator (sec 2.5).
- The diamond symbol corresponds to the indicator kriging (IK) estimator (sec 2.6).
- The x with a hole in the center corresponds to the probability kriging estimator which utilizes a prior ordinary kriging estimate of mean panel grade (PK-OK sec 4.4.4.2).

For each global property (e.g. tonnage recovery, tonnage mean square error...) examined, there are three figures corresponding to the three drilling campaigns. Therefore the improvement due to an increase in information can be readily seen by examining the three figures.

4.5.1.1 Global Tonnage Recovery Factor

The global tonnage recovery factor, T(zc), is defined as the percentage of the 119 panels which would be recovered at a given cutoff if mining

were performed on point support selective mining units. Multiplying this factor by the total tonnage of the 119 panels yields the potentially recoverable tonnage for the cutoff of interest.

The estimated tonnage recovery factor is determined by

$$T^*(zc) = \sum_{i=1}^{119}(1-\phi^*(A_i,zc))/119 \qquad (4.18)$$

While the true tonnage recovery factor is determined by

$$T(zc) = \sum_{i=1}^{119}(1-\phi(A_i,zc))/119 = 1 - F(zc) \qquad (4.19)$$

The plots of tonnage recovery factor versus cutoff (fig 59-60) show that all three estimators are fairly good estimators of recovered tonnage. Certainly at low cutoffs there are no problems with bias in the estimates, however at high cutoffs (.144 oz/ton and above) all three estimators tend to overestimate the recovered tonnage (the symbols plot above the solid line corresponding to true recovery). This overestimation is most severe for the probability kriging estimator utilizing the ordinary kriged mean especially at the highest cutoff, .313 oz/ton. The overestimation of this estimator at this cutoff can be traced back to the definition of the estimator. Recall (sec 4.4.4.2) that the PK-OK estimator has no nonbias constraints except that the mean panel grade is an unbiased estimator of the true panel grade. Recall also that the estimated mean panel grade is identified to the ordinary kriging estimate of the panel grade through a quadratic programming algorithm which changes the estimated tonnages to effect this identity. Due to the set up of the algorithm (eqn 4.24) and the fact that, for

this deposit, the 10% of the total tonnage above .313 oz/ton carries 60% of the total ounces of gold, the solution to the quadratic program causes the largest change in the estimated tonnage above the .313 oz/ton cutoff. Therefore, the estimates of tonnage above the .313 oz/ton cutoff are not reliable and biases are to be expected. On the other hand, since the tonnages above the .313 oz/ton cutoff absorb most of the change, the estimated tonnages at lower cutoffs are not greatly changed and hence remain globally unbiased.

Aside from the PK-OK estimator's poor performance at the highest cutoff, all three estimators are reasonably unbiased at all cutoffs with none of the estimators showing clear superiority.

As the number of data increase from campaign #1 to campaign #3, the accuracy of all three estimators increase. Utilizing the data from campaign #3, in fact, the symbols for all three estimators (fig 60) plot nearly on the line corresponding to the true value.

4.5.1.2 Quantity of Metal Recovery Factor

The quantity of metal recovery factor is a unitless value which when multiplied by the total tonnage of the deposit yields the total number of potentially recoverable ounces of gold within the deposit. Hence quantity of metal recovery factor has units of oz/ton or grade. In particular, the mean grade of the deposit is the quantity of metal recovery factor when no cutoff is applied.

Quantity of metal recovery factor is determined for the three estimators through the following relationship:

$$QF(zc) = \sum_{i=1}^{119} Q_i(zc)/119 \qquad (4.20)$$

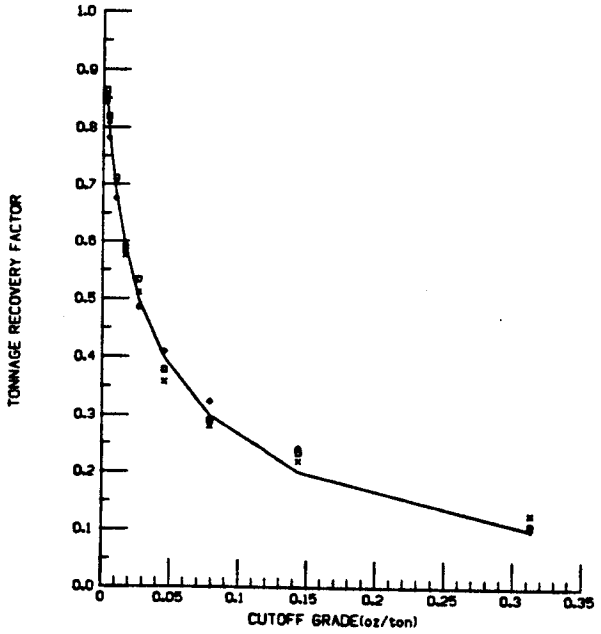

TONNAGE RECOVERY FACTOR VERSUS CUTOFF
CAMPAIGN #1

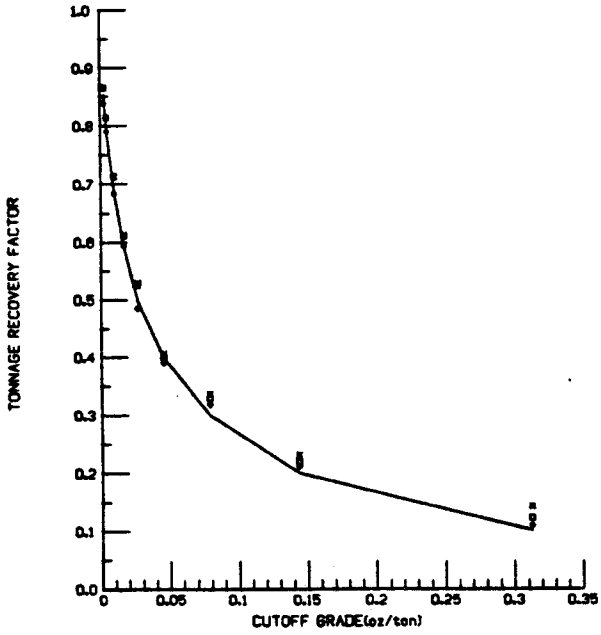

TONNAGE RECOVERY FACTOR VERSUS CUTOFF
CAMPAIGN #2

Figure 59: Global Tonnage Recovery Factor vs. Cutoff, Campaigns #1 and #2

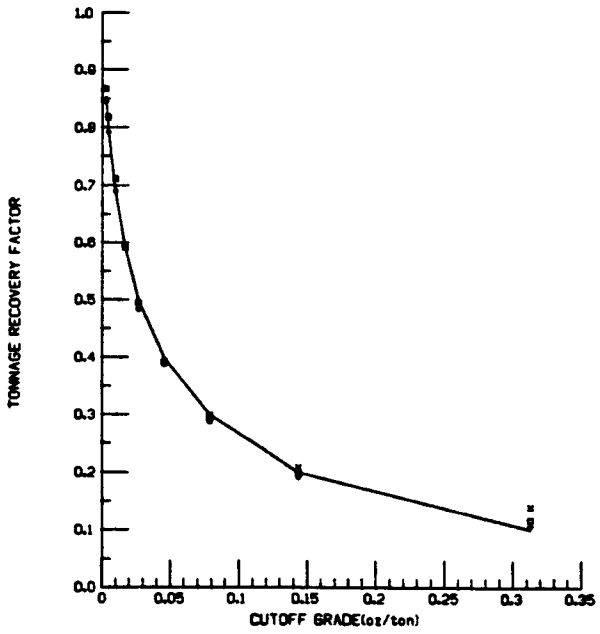

Figure 60: Global Tonnage Recovery Factor vs. Cutoff, Campaigns #3

The true quantity of metal recovery factor is simply the mean grade of those blast hole assays from the 7979 available which are larger than the cutoff of interest zc.

The IK and PK estimators give similar results for all three campaigns and 9 cutoffs (figs 61-62). This is not surprising since PK and IK give similar estimates of global tonnage recovery and global quantity of metal recovery is a simple function of global tonnage recovery (eqn 4.10) which is identical for both estimators. Both the PK and IK estimates are very close to the true values for the great majority of cutoffs in campaigns #1 and #2 (fig 61). In campaign #3 (fig 62),

however, both PK and IK underestimate the true recoveries at all but the highest cutoff. Recall (sec 4.4.1) that the mean grade of the 623 samples comprising the campaign #3 data base is .100 oz/ton while the mean grade of the 7979 blastholes comprising the exhaustive data base is .106 oz/ton. Since the quantity of metal recovery factor at zero cutoff is equal to the mean grade of the data and the c_j values (measures of class centers) are chosen to reflect the mean of the 623 data (sec 4.4.4.1) this result is not surprising. Thus the poor results observed in campaign #3 are not due to any deficiency in the method, rather they are due to bad luck which is not controllable by theory.

The results given by the PK-OK estimator are inferior to those given by the IK and PK estimators in campaigns #1 and #2 and are essentially equal in campaign #3. The results given by the PK-OK estimator in campaign #1 are not as good as those given by the PK or IK estimators, but, ignoring the results at high cutoffs, they are still not too bad. The poor results at high cutoffs are expected, as the PK-OK estimator is not reliable at high cutoffs since no non-bias constraints are utilized. The PK-OK results for campaign #2 (fig 61) are, however, poor at all cutoffs. As mentioned the local quantity of metal recovery factor at zero cutoff is the mean panel grade. As will be shown (sec 4.5.2), the ordinary kriging estimates of mean panel grade, which the PK-OK estimates are based on, are poor for campaign #2 as they are globally biased. Thus it is not surprising that the PK-OK estimates of global quantity of metal recovered are poor for campaign #2.

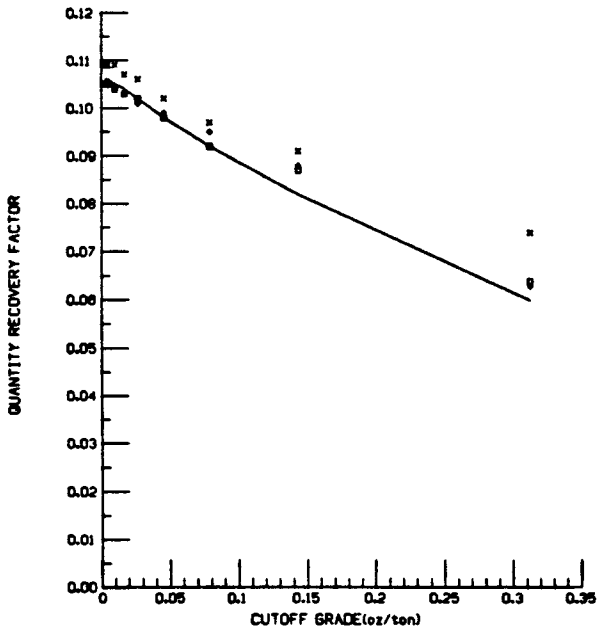

QUANTITY RECOVERY FACTOR VERSUS CUTOFF
CAMPAIGN #1

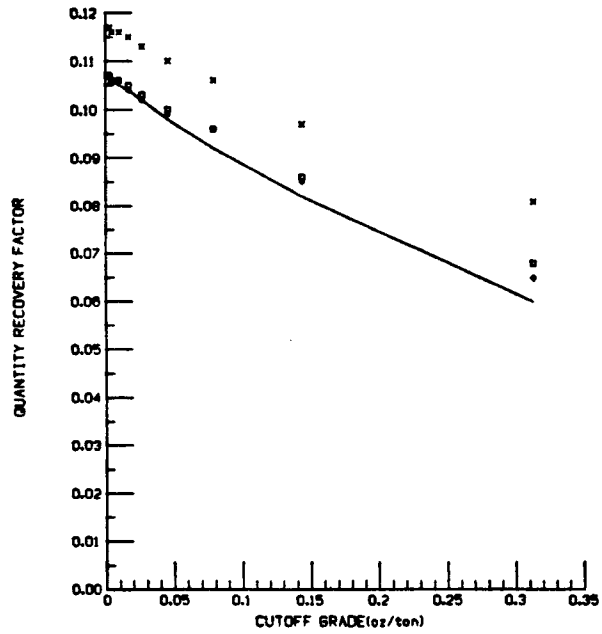

QUANTITY RECOVERY FACTOR VERSUS CUTOFF
CAMPAIGN #2

Figure 61: Global Quantity of Metal Recovery Factor, Campaigns #1 and #2

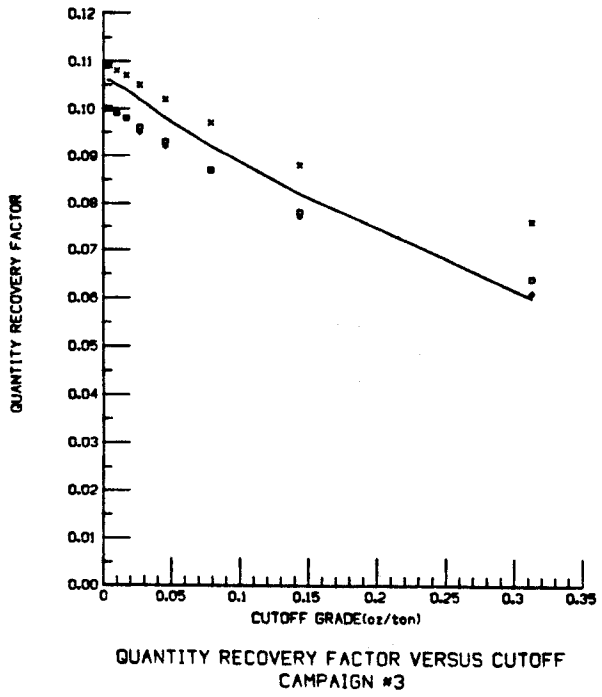

Figure 62: Global Quantity of Metal Recovery Factor, Campaign #3

4.5.1.3 Tonnage Mean Squared Error

The tonnage mean squared error is defined as the sum of the squares of the tonnage factor error made at each panel divided by the number of panels. In other words this value is the average squared error of estimation of the tonnage recovery per panel. This value gives an indication of the local accuracy of each technique as the estimator with the smallest mean squared error is, in average, the most accurate local estimator of tonnage. Plots of tonnage mean squared error versus cutoff are given in figures 63 and 64.

The estimator with the lowest mean square error, at the great majority of cutoffs, for campaign #1, is the probability kriging estimator which utilizes the kriged estimate of mean panel grade. For campaign #2, however this estimator has higher mean squared error than either of the other two estimators while in campaign #3 all three estimators are essentially equivalent. The efficiency of the PK-OK estimator, thus appears to be strongly dependent on the reliability of the ordinary kriging estimate of panel grade as compared to the estimate obtained directly through indicator or probability kriging (i.e. the estimate of quantity of metal recovered at zero cutoff). As will be shown (sec 4.5.2) the ordinary kriging estimator of panel mean grade is superior to the other estimators given the data available in campaign #1 it is inferior however in campaign #2, due to the large bias of the ordinary kriging estimator, and roughly equal given the data of campaign #3. The tonnage estimates obtained from the PK-OK estimator are conditioned to the OK estimated mean grade so it is not surprising that an overall measure of local accuracy such as the mean square error should also reflect the relative accuracy of the mean grade estimate.

In all three campaigns, the mean squared error of the IK estimator is less than that for the PK estimator. Since the mean squared error is essentially a realization of the estimation variance at a given cutoff and theoretically the estimation variance of the PK estimator is less than the estimation variance of the IK estimator, this result is somewhat surprising.

The influence of the increase in data manifests itself strongly in the magnitude of tonnage mean squared error, as it steadily decreases as

the number of data increases. There is a significant decrease in mean squared error when a single datum is added to each panel in going from the campaign #1 to the campaign #2. On this basis the additional hole per panel is justified regardless of cutoff. Going from campaign #2 to campaign #3 however an average of 3 data were added to each panel. At high cutoffs, such as .144 oz/ton, these additional holes caused very little improvement in the statistic. At lower cutoffs, there is improvement, however the cost of the additional data would probably not be justified by the observed improvement.

4.5.1.4 Quantity of Metal Mean Squared Error

The quantity of metal mean squared error is a measure of the local accuracy of an estimator in determining quantity of metal recovered. This measure is defined as

$$MSE_q = \sum_{i=1}^{119} (Q_i(zc) - Q_i^*(zc))^2/119 \qquad (4.21)$$

where: $Q_i(zc)$ is the true quantity of metal recovered for panel i and cutoff zc.

$Q_i^*(zc)$ is the estimated quantity of metal for panel i and cutoff zc.

The results obtained by the PK-OK estimator in campaign #1 at low cutoffs are very good compared to those obtained by the other two estimators (fig 65). Since the estimates of quantity of metal at low cutoffs are essentially equal to the mean panel grade (only minute amounts of gold are found below the lowest cutoffs), the mean squared error measures the local accuracy of the estimated mean panel grade. The ordinary kriging estimate of mean panel grade is obviously much

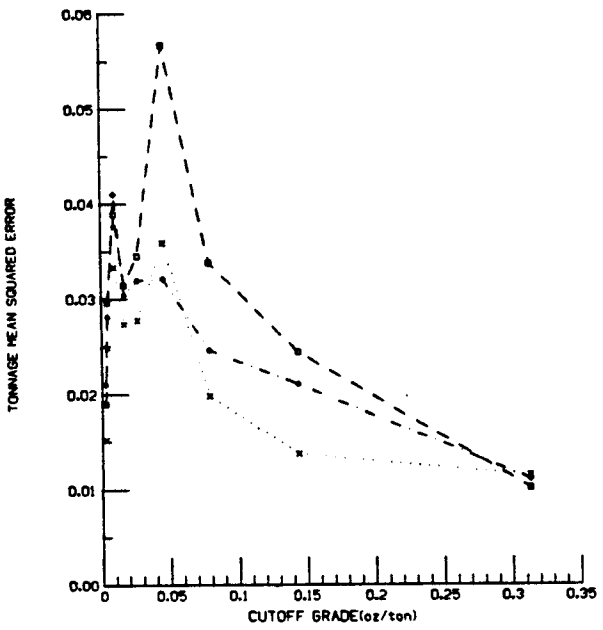

TONNAGE MEAN SQUARED ERROR VERSUS CUTOFF
CAMPAIGN #1

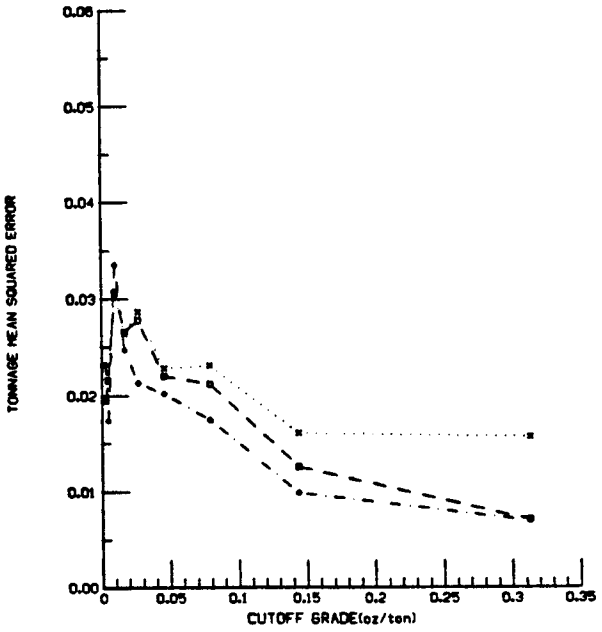

TONNAGE MEAN SQUARED ERROR VERSUS CUTOFF
CAMPAIGN #2

Figure 63: Tonnage Mean Squared Error for Campaigns #1 and #2

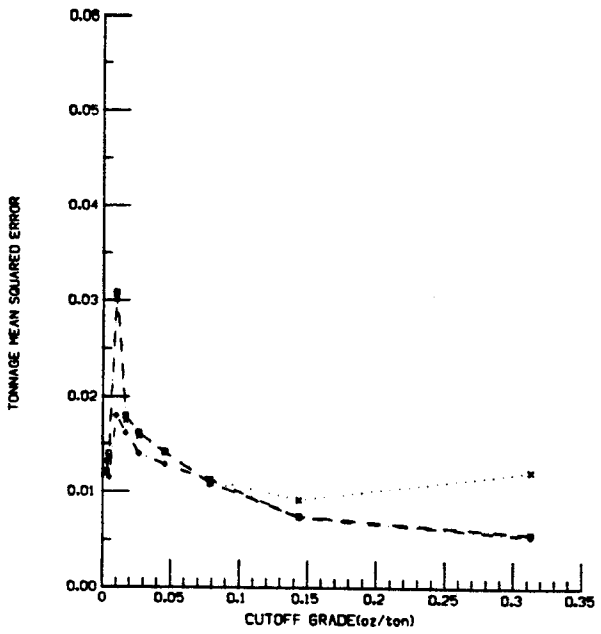

Figure 64: Tonnage Mean Squared Error for Campaign #3

better than the estimate given by IK or PK given the campaign #1 data (see section 4.5.2). Given the campaign #2 data the situation is reversed, as the PK-OK estimator yields a much larger mean squared error value than the standard PK or IK estimators (fig 65). In campaign #3 there is no great difference between the three estimators (fig 66), at low cutoffs, indicating that both the ordinary kriging and the IK and PK estimates of mean panel grade are similar.

For campaigns #2 and #3, the PK estimator has lower mean squared error than the IK estimator. Since the IK and PK estimates of quantity of metal are both strongly based on the tonnage estimates and the IK

estimator consistently had lower tonnage mean squared errors, this result is unexpected. This unexpected result does, however point to the fact that the mean squared error does not completely measure the local accuracy of the tonnage estimates.

The improvement in quantity of metal mean squared error when moving from campaign #1 to campaign #2, through the addition of 1 datum per panel, is substantial. For the IK and PK estimators the improvement amounts to a reduction in the mean squared error of nearly 50% at all cutoffs. The improvement obtained in moving from campaign #2 to campaign #3 is not substantial, indicating that obtaining the additional data is probably not cost effective.

4.5.1.5 Variance of Tonnage Estimates

The variance of the tonnage recovery estimate is defined as

$$\text{Var}^*(zc) = \sum_{i=1}^{119}[\phi^*(A_i,zc) - (\sum_{i=1}^{119}\phi^*(A_i,zc))/119)]^2/119 \qquad (4.22)$$

This value is compared to the true variance of the tonnage recovered

$$\text{Var}(zc) = \sum_{i=1}^{119}[\phi(A_i,zc) - F(zc)]^2/119 \qquad (4.23)$$

The discrepancy between the variance of the true recovered tonnage and the variance of the estimated recovered tonnage gives a measure of the smoothing of the estimator.

A smoothed estimator is not ideal since the smoothing very often is an indication of an estimator which underestimates the recoveries from rich blocks and overestimates the recoveries from poor blocks. That is smoothing is often an indicator of a conditionally biased estimator.

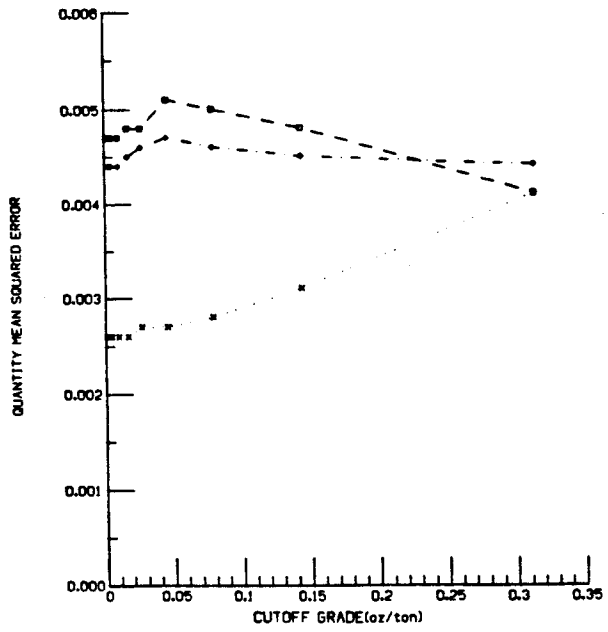

QUANTITY MEAN SQUARED ERROR VERSUS CUTOFF
CAMPAIGN #1

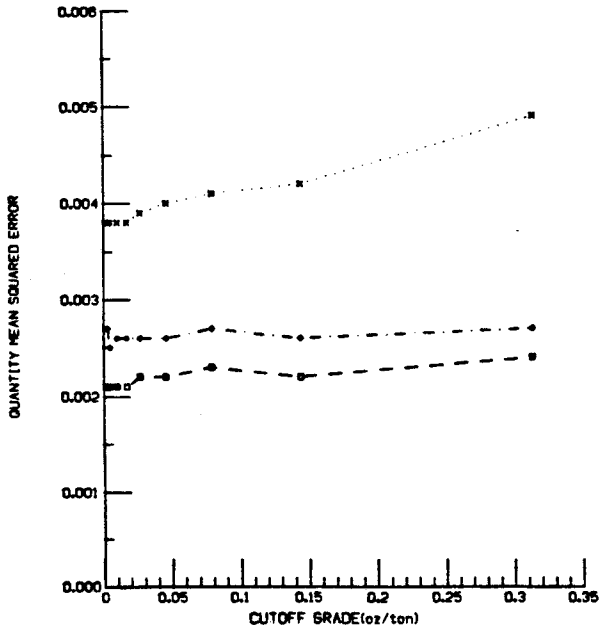

QUANTITY MEAN SQUARED ERROR VERSUS CUTOFF
CAMPAIGN #2

Figure 65: Mean Square Error of Quantity of Metal Estimates for Campaigns #1 and #2

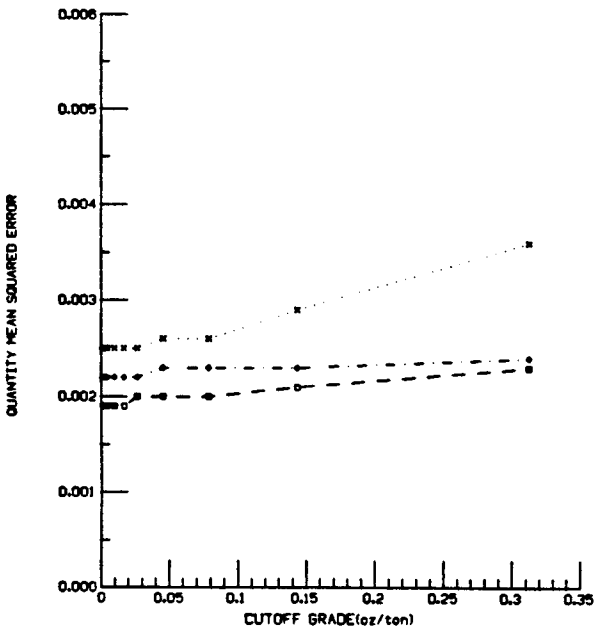

Figure 66: Mean Square Error of Quantity of Metal Estimates for Campaign #3

In all three campaigns (figs 67 and 68), the three estimators show the same pattern. The PK-OK estimator is the least smooth (often it shows inverse smoothing), and the IK estimator is the most smooth. Thus it is expected that the IK estimator will show more conditional bias than than either the PK or PK-OK estimators.

The degree of smoothing is largely independent of the number of data. Granted, there is some decrease in smoothing as the number of data increase, however this decrease is not substantial or particularly important.

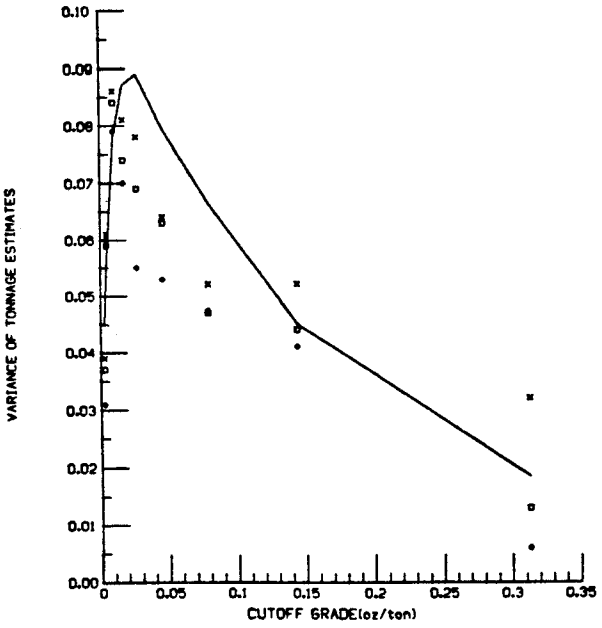

VARIANCE OF TONNAGE ESTIMATES VERSUS CUTOFF
CAMPAIGN #1

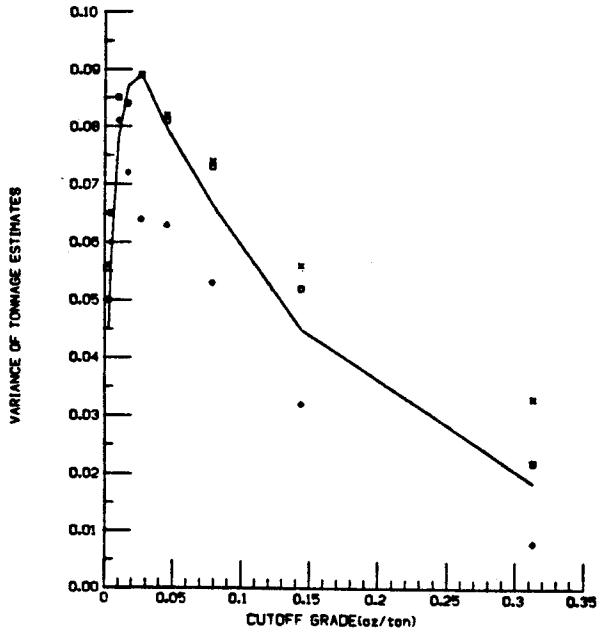

VARIANCE OF TONNAGE ESTIMATES VERSUS CUTOFF
CAMPAIGN #2

Figure 67: Variance of Tonnage Estimates for Campaign #1 and #2

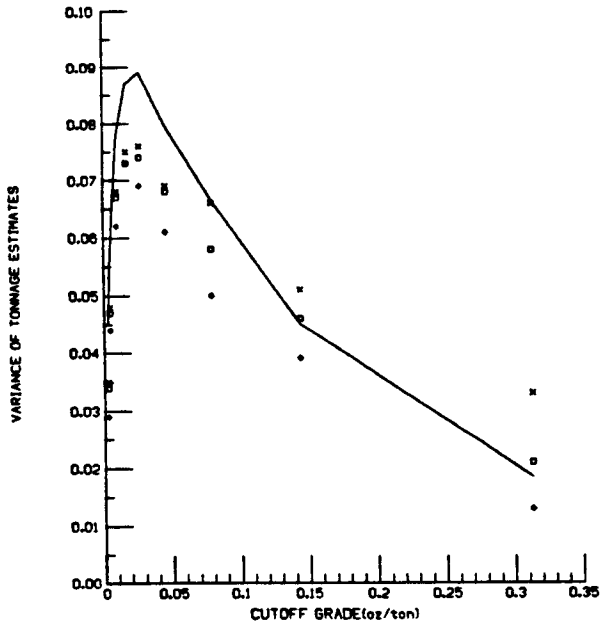

Figure 68: Variance of Tonnage Estimates for Campaign #3

4.5.1.6 Variance of the Quantity of Metal Estimates

The variance of the quantity of metal estimates and the true variance of the quantity of metal recovered are defined analogously to the variance of the tonnage recoveries. Again smoothing tends to indicate a conditionally biased estimator.

The results for this criterion (figs 69 and 70), for all three campaigns indicate that the IK estimator is smoother than either of the other two estimators. The effects of this smoothing will be pointed out in more detail in the local results section.

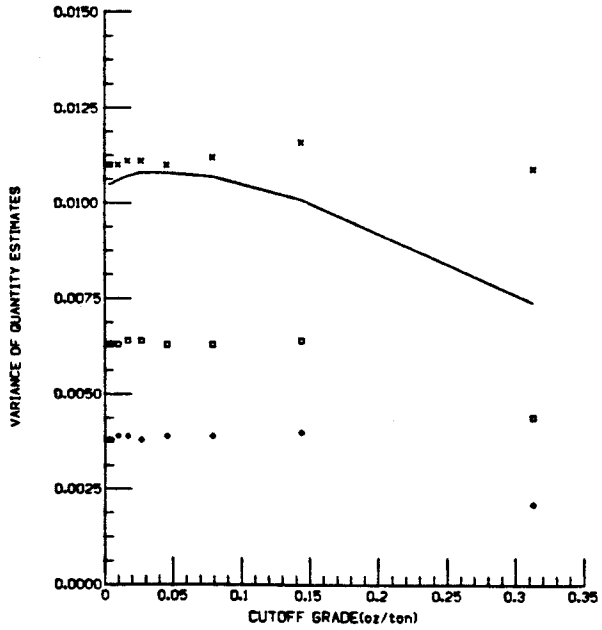

VARIANCE OF QUANTITY ESTIMATES VERSUS CUTOFF
CAMPAIGN #1

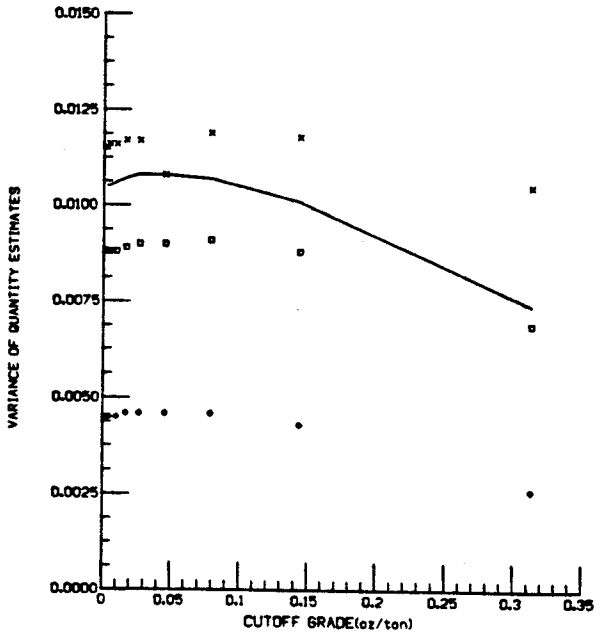

VARIANCE OF QUANTITY ESTIMATES VERSUS CUTOFF
CAMPAIGN #2

Figure 69: Variance of the Quantity of Metal Estimates Campaigns #1 and #2

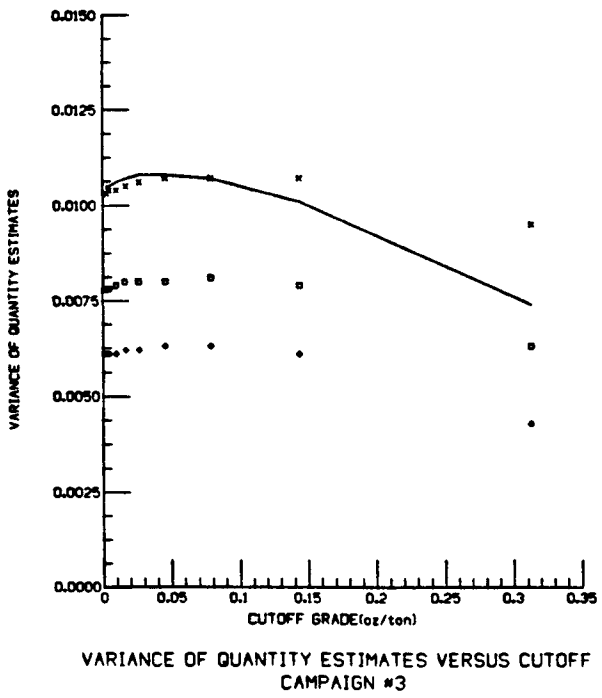

Figure 70: Variance of the Quantity of Metal Estimates Campaign #3

4.5.2 Panel Mean Estimation

In the previous section concerning global results, there were various references to the quality of the panel mean estimates in explaining the quality of the observed results. In this section two estimates of panel mean will be examined for each campaign. The first estimator is the PK estimate of quantity of metal recovered at zero cutoff, $Q^*(0,x)$ (eqn 4.20). The second estimator is the ordinary kriging (OK) estimate of mean panel grade, $m_{ok}^*(x)$. The IK estimator of quantity of metal recovered at zero cutoff could also be used to estimate mean panel

grade, however as this estimator is similar to $Q^*(0,x)$ determined by PK only the PK estimates are discussed.

The estimator $Q^*(0,x)$ is a non-linear estimate of panel mean, therefore the estimation variance associated with $Q^*(0)$ is theoretically less the m_{ok}^*. However, the linear estimator m_{ok}^* has proven to be a robust estimator, therefore it may outperform $Q^*(0,x)$ in certain instances.

Both the $m_{ok}^*(x)$ and $Q^*(0,x)$ estimators were used to estimate the mean grade of each of the 119 panels for each of the 3 drilling campaigns. The results from campaign #1 are summarized by utilizing scattergrams of true versus estimated panel means in figure 71. These results show that the ordinary kriging estimate of panel mean $m_{ok}^*(x)$ is far superior to the PK estimate $Q^*(0,x)$ given the campaign #1 data set. The PK estimate shows a clear conditional bias which causes severe underestimation of high grade panels. In contrast the ordinary kriging estimates are well centered about the 45^0 line representing true equals estimate. Furthermore the ordinary kriging estimates have greater correlation with the true mean grades and have less mean squared error than the PK estimates of mean grade. These results help explain the good global results obtained by the PK-OK estimator for campaign #1.

The quality of the results given by these two estimators for campaign #2 (fig 72) are quite different from those observed in campaign #1. An important observation concerning these results is that the OK estimates are definitely biased as the deposit mean is overestimated by .011 oz/ton or 10%. This result is reflected in the PK-OK estimates of global quantity of metal recovered (fig 61) as these estimates are

consistently larger than the true values. In addition to having less bias than the ordinary kriging estimator the PK estimates $Q^*(0,x)$ show greater correlation with the true values, less scatter, and lower mean squared error. Due to the superiority of the PK estimates $Q^*(0,x)$ for this sampling campaign, it is expected that the PK estimates of local recovered tonnage and quantity of metal recovered will be superior to the PK-OK estimates.

The results for campaign #3 (fig 73) do not show that either estimator is clearly superior. The PK estimates $Q^*(0,x)$ show less scatter than the OK estimates; however, the PK estimates are globally biased. The OK estimates do not have a large global bias, however, the scatter about the true equal estimate line is relatively large. Thus each estimator has certain advantages so it is difficult to choose the best estimator for this drilling campaign.

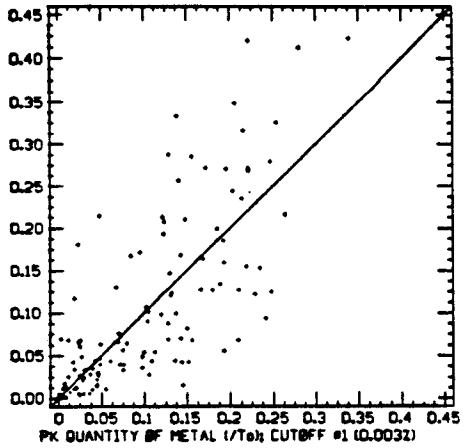

SUMMARY STATISTICS

	MEAN	VARIANCE
EST.	0.105	0.0063
TRUE	0.106	0.0105

RELATIVE BIAS = -0.0132

MEAN SQUARED ERROR = 0.0047

CORRELATION COEF. = 0.745

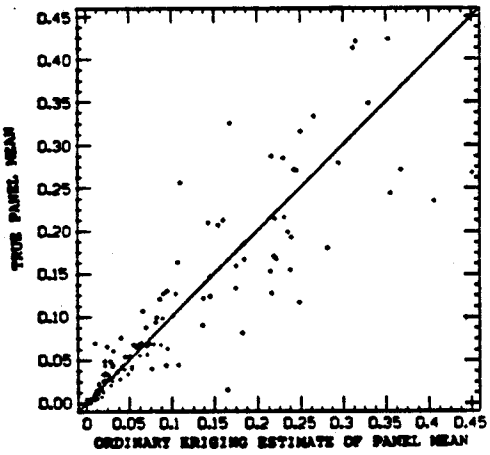

SUMMARY STATISTICS

	MEAN	VARIANCE
EST.	0.109	0.0110
TRUE	0.106	0.0105

RELATIVE BIAS = 0.0294

MEAN SQUARED ERROR = 0.0026

CORRELATION COEF. = 0.879

Figure 71: True versus OK and PK Estimated Panel Mean, Campaign #1

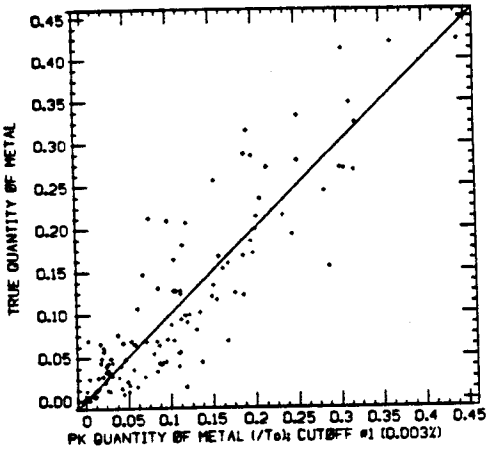

SUMMARY STATISTICS

	MEAN	VARIANCE
EST.	0.107	0.0088
TRUE	0.106	0.0105

RELATIVE BIAS = 0.0035
MEAN SQUARED ERROR = 0.0021
CORRELATION COEF. = 0.895

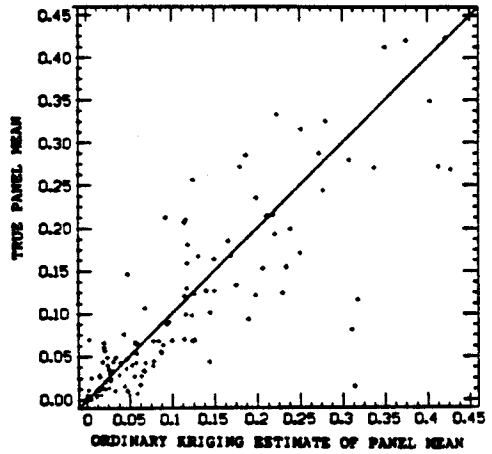

SUMMARY STATISTICS

	MEAN	VARIANCE
EST.	0.117	0.0115
TRUE	0.106	0.0105

RELATIVE BIAS = 0.0965
MEAN SQUARED ERROR = 0.0038
CORRELATION COEF. = 0.834

Figure 72: True versus OK and PK Estimated Panel Mean, Campaign #2

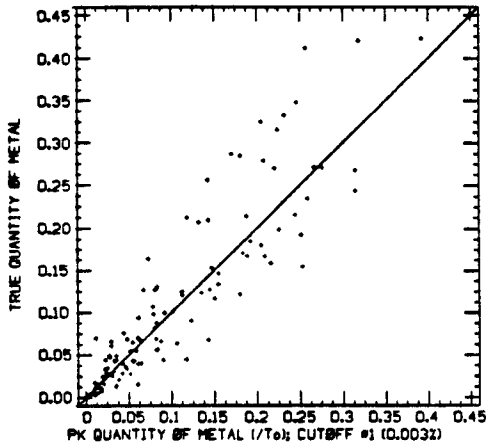

SUMMARY STATISTICS

	MEAN	VARIANCE
EST.	0.100	0.0078
TRUE	0.106	0.0105

RELATIVE BIAS =-0.0600

MEAN SQUARED ERROR = 0.0019

CORRELATION COEF. = 0.907

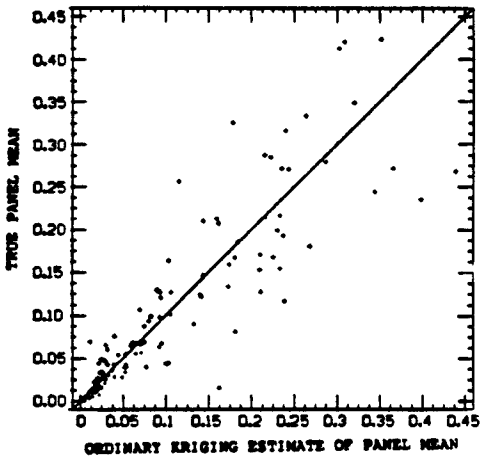

SUMMARY STATISTICS

	MEAN	VARIANCE
EST.	0.109	0.0103
TRUE	0.106	0.0105

RELATIVE BIAS = 0.0256

MEAN SQUARED ERROR = 0.0025

CORRELATION COEF. = 0.883

Figure 73: True versus OK and PK Estimated Panel Mean, Campaign #3

4.5.3 Local Results

The estimators which have been introduced are designed as local estimators of recovery. Although the global features of the estimator, particularly global recovery, are important, the strength of these estimators is that they can be used to obtain accurate local estimates which can be used in mine planning, design, and scheduling. Importantly, these accurate local estimates cannot be obtained by linear estimators which can be used to obtain, sometimes tolerable, estimates of global recovery.

In examining the local results, the feature of prime interest is the error made at each panel. Since there are 119 panels, there are 119 such errors for each cutoff of interest. To summarize these errors, a scattergram of true versus estimated recovery is plotted for each cutoff. Each scattergram contains 119 points corresponding to the 119 panels. The location of each of the 119 points within the scattergram is determined by the true and estimated recoveries for the panel. The central feature within each scattergram is a 45^0 line corresponding to true equals estimated recovery. The horizontal or vertical distance between any point and this line is exactly equal to the error made in estimating the recovery for that particular panel.

The scattergram, therefore, not only displays the error made at each panel, but by examining the gross features of the cloud of points the global features of the estimator can be determined. In any scattergram where the majority of points fall below the 45^0 line, a global bias (overestimation) is present. Additionally, for any range of estimated

grades, if the cloud of points moves away from the 45° line a conditional bias is present. Thus, a conditionally biased estimator is biased within a particular range of recoveries.

In this study there are 3 drilling campaigns, 3 estimators, 9 cutoffs, and 2 variables of interest. Therefore, there are a great number of scattergrams. The total number of scattergrams is so large, 162, that not all of them can be discussed in detail. Hence only the scattergrams for selected cutoffs will be discussed. The remaining scattergrams are included in section 4.8. The cutoffs which have been chosen for detailed analysis are .027 oz/ton (median cutoff) and the 1.44 oz/ton (80th percentile cutoff). These two cutoffs were chosen because they span the range of possible economic cutoffs.

4.5.3.1 Tonnage Recovery Campaign #1 .027 oz/ton Cutoff

The data configuration used in kriging in campaign #1 (sec 4.4) is such that only four data are within the range of the indicator variogram for high cutoffs. Therefore only four indicator data will receive significant weight in the estimation of local recoveries for each panel. The data configuration of this campaign will, thus provide a difficult test of the three techniques.

The tonnage estimates given by the three techniques (figs 74-76) at the median cutoff of .027 oz/ton are a bit disappointing. The results given by the IK estimator show a primary weakness of the estimator. Since only four data in the kriging neighborhood receive significant weight, the data are located on a regular grid, and the indicator variogram model is isotropic, there are only five possible estimates of

tonnage recovery for each panel. Each indicator datum can take on only two values, 0 or 1; therefore, the five possible estimates correspond to:

1. All four of the indicator data in the neighborhood are equal to 0.
2. Three of the indicator data in the neighborhood equal 0.
3. Two of the data equal 0.
4. One of the data equals 0.
5. All four of the data equal 1.

If the constrained form of the indicator kriging estimator were used, the four weights given to the data would be forced to sum to 1. Due to the symmetry of the data locations and the isotropic variogram model, the five estimates would be; 0,.25,.5,.75, and 1.0. Recall, however that the unconstrained form of the estimator is used, so the weights are not forced to sum to one. Therefore although there are still only five possible estimates at each cutoff for the unconstrained estimator, the values of these five estimates vary from cutoff to cutoff depending on the amount of weight given to the overall mean $F^*(z_c)$.

The tonnage recovery scattergram for the IK estimator (fig 74) reflects the fact that only five IK estimates are possible given the configuration of data in campaign #1. The estimates are all found within five narrow vertical bands[1] while the true values are found over a wide range of values. Thus for those true values which do not happen

---

[1]The bands show some thickness because the data are located on an approximately regular grid (sec 4.4) hence all indicator data do not receive exactly the same weight.

to have a value equal to one of the five possible estimates, the IK estimator must make an error. This limitation of the IK estimator is undesirable in local estimation.

One interesting point which should be noted concerns whether one should use the unconstrained or constrained version of the IK estimator. As previously stated, both estimators will yield the vertical bands found in figure 74. The difference lies in the location of the bands. If the constrained form of the estimator were used, the bands would be shifted along the x axis of the scattergram so that they would be centered on 0,.25,.5,.75,1.0. Note however that the shape and number of points in each band would be unaffected. This shifting would cause conditional bias in the estimates especially for the extreme estimates. Given the location of the bands determined by the unconstrained estimator, there is no noticeable conditional bias. That is:

$$\left(\sum_{i=1}^{n} \phi(A,zc) \,\middle|\, \phi^*(A,zc)=p\right)/n = p. \qquad (4.24)$$

where: n is the number of points falling within a band

If however the band presently centered on $\phi^*(A,zc)=.88$ were shifted to $\phi^*(A,zc)=1.0$, a definite conditional bias would be present. Thus the constrained estimator would be a poorer local estimator than the unconstrained estimator which was used. For this reason the unconstrained estimator was chosen over the constrained estimator.

A final note concerning the bands given by the IK estimator concerns the conditional distribution of the estimates. Since there are a number of data within each band a representative estimate of the conditional distribution

$$f(\phi(A,zc)\,|\,\phi^*(A,zc)=p) \qquad (4.25)$$

can be examined. If this distribution were normal, it would be very advantageous, since normality would allow easy access to confidence limits on the estimate $\phi^*(A,zc)$. Such confidence limits would be very helpful when performing mine scheduling and in drawing up short term mine plans. Unfortunately the values within the bands show little indication of following a normal or any other recognizable distribution. There simply are not enough data points congregated around the 45^0 line to indicate the peakedness present in the normal distribution. The conditional distributions observed indicate, rather, a smaller percentage of small errors and a larger percentage of medium to large sized errors than a normal distribution with the same variance.

In spite of the rather poor local characteristics of this estimator the global statistics are fairly good. The estimator is nearly unbiased and there is a reasonable correlation between the true and estimated values as measured by the correlation coefficient of .8. This scattergram, thus, definitely points out the difference between a local and a global estimator. The IK estimator is a good global estimator, by all indications, but a poor local estimator. This difference in the quality of the estimator for different purposes should be kept in mind when choosing an estimator.

The PK estimator was designed to improve on some of the shortcomings of the IK estimator. Particularly, the PK estimator is not restricted to any particular limited set of estimated values because of the inclusion of a source of continuous data. The scattergram corresponding to the PK estimate of recovered tonnage (fig 75) shows remnants of the

bands present in the IK estimator but the estimates are obviously no longer restricted to narrow bands as in the IK case. Since the PK estimates are not restricted to a small number of possible values, this estimator should provide a better local estimator than IK. However a comparison of the scattergrams does not show that PK is significantly better. In fact, the majority of the estimates are better than those of IK, however a few poor estimates (<10% of the total) make the quality of the scattergram appear much worse than it actually is. Additionally, the poor estimates have introduced an overall bias into the estimation. Thus it can be seen that when there are not a great number of data in the kriging neighborhood a great deal of importance is given to the additional information included in the PK estimator. In the majority of cases the additional information is helpful and the estimator is improved. When the additional information is spurious, however the quality of the estimator is damaged and large errors are introduced.

It can be seen that when there are few data in the kriging neighborhood, great care must be taken to ensure that the uniform transform of the data is performed correctly so that no errors are introduced. However even if this transform is perfect, large errors can occur with the PK estimator when the transformed data are simply not representative of the true values found within the panel. This type of occurrence is simply "bad luck" and cannot be compensated for when data are sparse. When these bad luck estimates are eliminated from the scattergram, the PK estimator is a much better local estimator than the IK estimator. However an absolute judgement as to which estimator is better is difficult since the bad luck values have introduced a bias

into the PK estimator. The final decision as to which estimator is better must be left to the person applying the technique. This decision must be based on the particular variable being estimated and the effects of certain types of errors.

The third estimator to be considered at this cutoff is the PK estimator conditioned so that the quantity of metal recovered when no cutoff is applied equals the mean panel grade determined by ordinary kriging. This conditioning is primarily used to improve the local quantity of metal estimates at low cutoffs, however as, indicated by figure 76, this conditioning also improves the tonnage estimates. The PK-OK scattergram is similar in many respects to the PK scattergram. This is not surprising since the PK-OK estimator is strongly based on the PK estimates. The major difference between the two scattergrams is that the PK-OK estimator has less large errors and less global bias. Hence the conditioning to the mean panel grade brought about a significant improvement in the quality of the estimator for this particular cutoff. In particular the additional information provided by the estimated mean panel grade compensated, in part, for the unrepresentative information surrounding some panels and reduced the number of large errors.

The improved quality of the PK-OK estimator is reflected in the statistics associated with the plots. The PK-OK estimator is nearly unbiased and the scattergram has a correlation coefficient of .84. This is significantly higher than the .80 values attained by the IK and PK estimators. It must be concluded that the additional complexity and cost involved with obtaining the PK-OK estimates are justified for this particular cutoff.

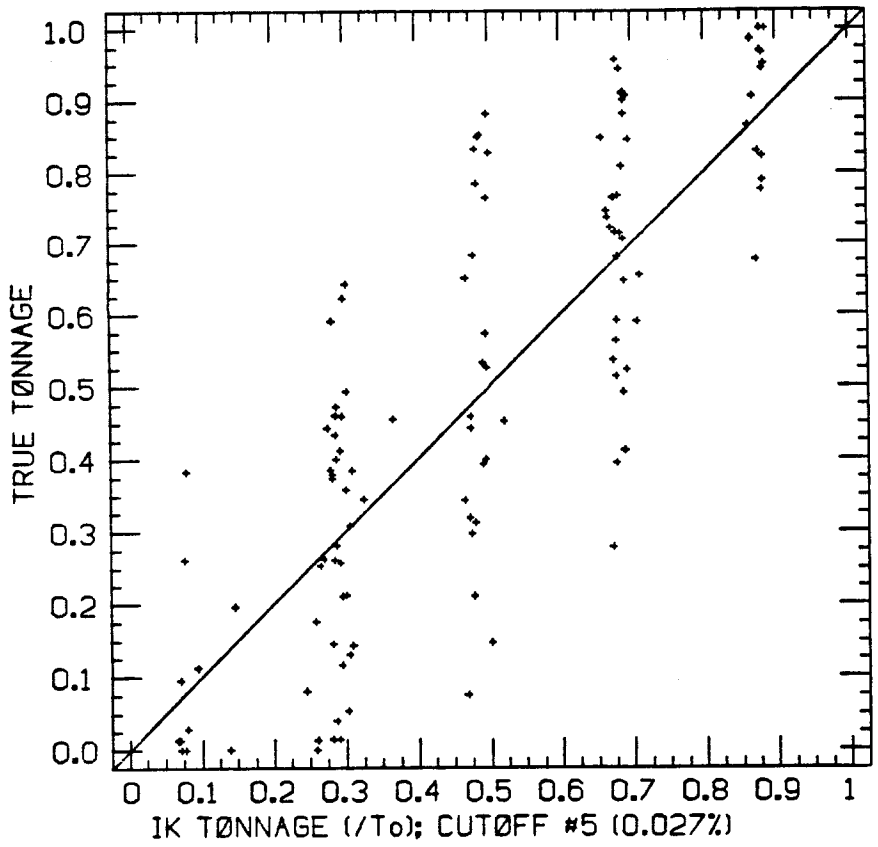

SUMMARY STATISTICS

	MEAN	VARIANCE
EST.	0.486	0.0553
TRUE	0.499	0.0890

RELATIVE BIAS =-0.0262

MEAN SQUARED ERROR = 0.0319

CORRELATION COEF. = 0.802

Figure 74: True vs. IK Estimated Tonnage, .027 oz/ton Cutoff, Campaign #1

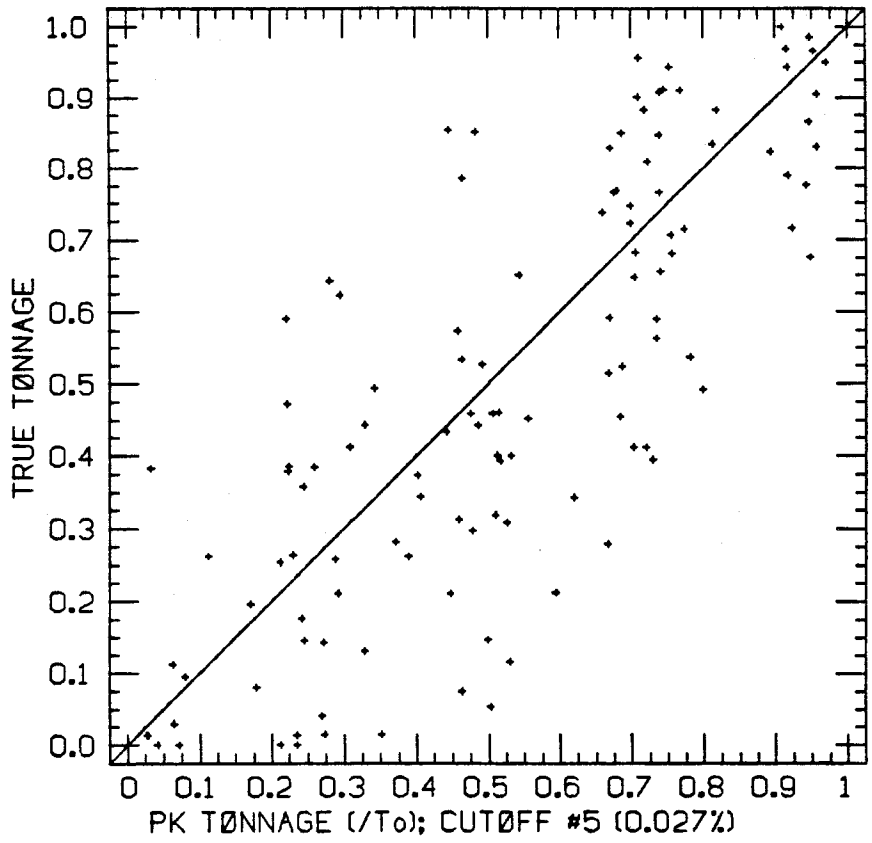

SUMMARY STATISTICS

	MEAN	VARIANCE
EST.	0.533	0.0686
TRUE	0.499	0.0890

RELATIVE BIAS = 0.0684

MEAN SQUARED ERROR = 0.0345

CORRELATION COEF. = 0.796

Figure 75: True vs. PK Estimated Tonnage, .027 oz/ton Cutoff, Campaign #1

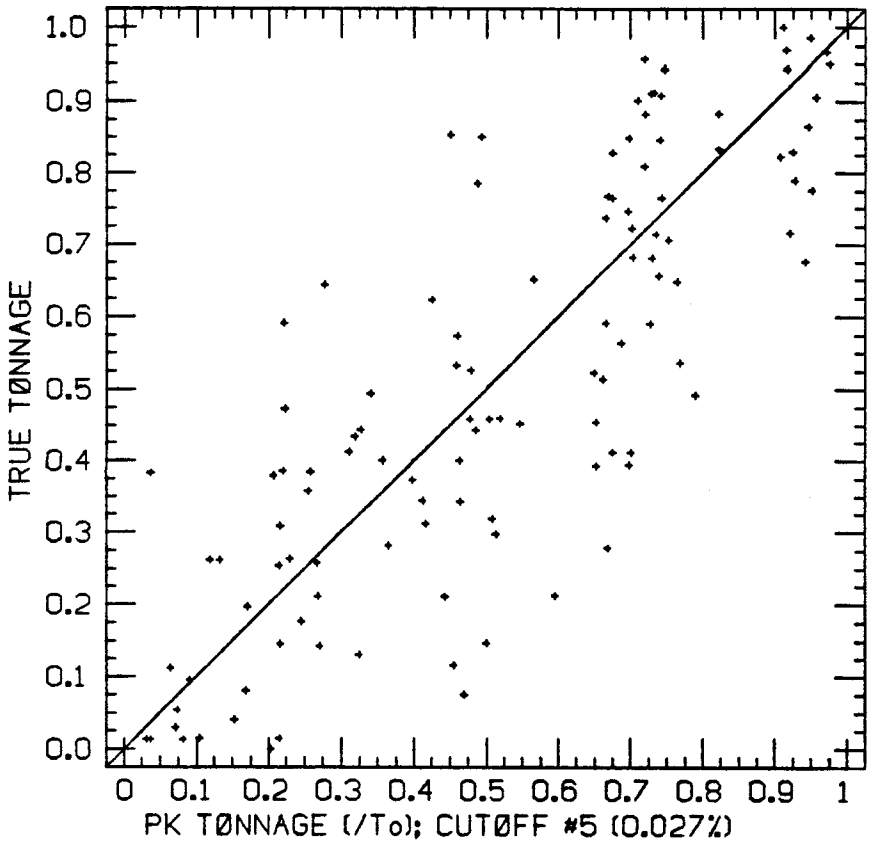

SUMMARY STATISTICS

	MEAN	VARIANCE
EST.	0.512	0.0778
TRUE	0.499	0.0890

RELATIVE BIAS = 0.0270

MEAN SQUARED ERROR = 0.0278

CORRELATION COEF. = 0.836

Figure 76: True vs. PK-OK Estimated Tonnage, .027 oz/ton Cutoff, Campaign #1

4.5.3.2 Tonnage Recovery Campaign #1, .144 oz/ton Cutoff

As opposed to the .27 oz/ton cutoff, which is the median cutoff, the .144 oz/ton cutoff corresponds to the 80th percentile of the 7979 available blasthole assays. Thus, this is a rather extreme quantile and thus provides a different test of the estimators.

The IK estimator (fig 77) does not perform well at this cutoff. In addition to having a large global bias, +20%, the estimates are conditionally biased. That is the mean grade of the values in each of the bands does not fall on the true equals estimate line. Thus the IK estimator at this cutoff is neither a good local estimator nor a good global estimator.

The PK estimator (fig 78) improves slightly on both the local and global results obtained by the IK estimator. As at the .027 oz/ton cutoff the PK estimates are not restricted to fall within any bands. Also, the additional information utilized by the PK estimator has, in this case, worked to slightly reduce the overall bias. This reduction in overall bias produces a PK estimator which, on visual inspection of the PK and IK scattergrams, appears to be a better local estimator of local tonnage.

Far and away the best local and global estimator of recovered tonnage at this cutoff is the PK-OK estimator (fig. 79). The additional information provided by the kriged, panel mean grade has worked to reduce not only the global bias of the PK estimator, but also has reduced the number of large errors present in the scattergram. Removing these large errors results in a scattergram which is much better centered about the true equals estimate line and thus yields a better estimator of local recovered tonnage.

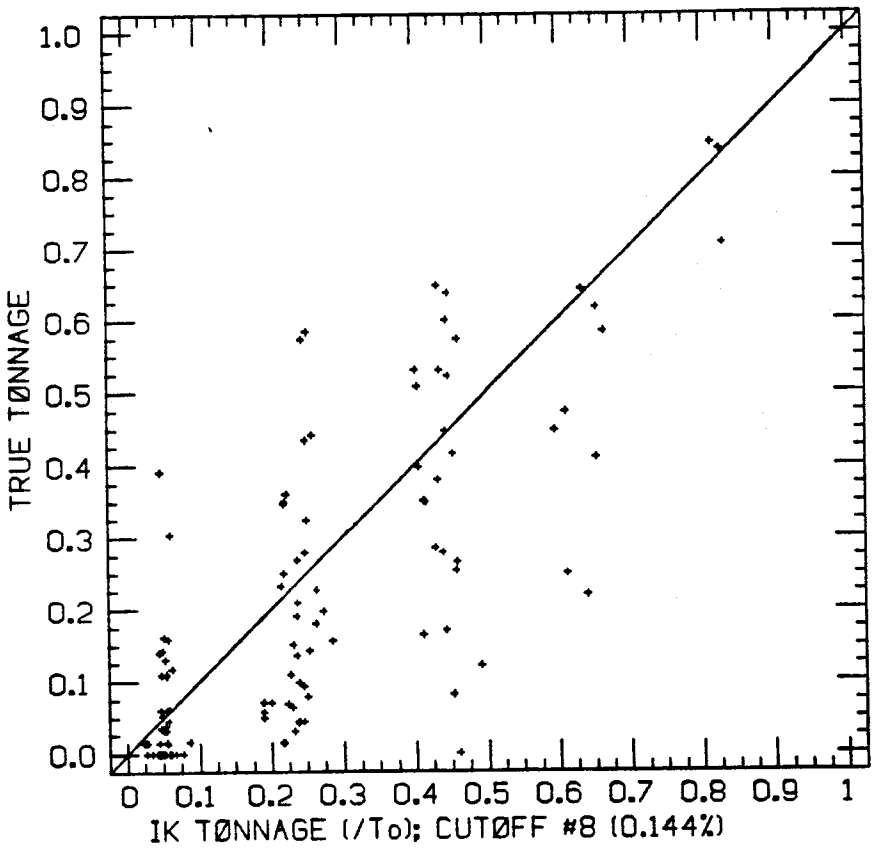

SUMMARY STATISTICS

	MEAN	VARIANCE
EST.	0.242	0.0412
TRUE	0.201	0.0454

RELATIVE BIAS = 0.2010

MEAN SQUARED ERROR = 0.0210

CORRELATION COEF. = 0.777

Figure 77: True vs. IK Estimated Tonnage Recovery for the .144 oz/ton Cutoff, Campaign #1

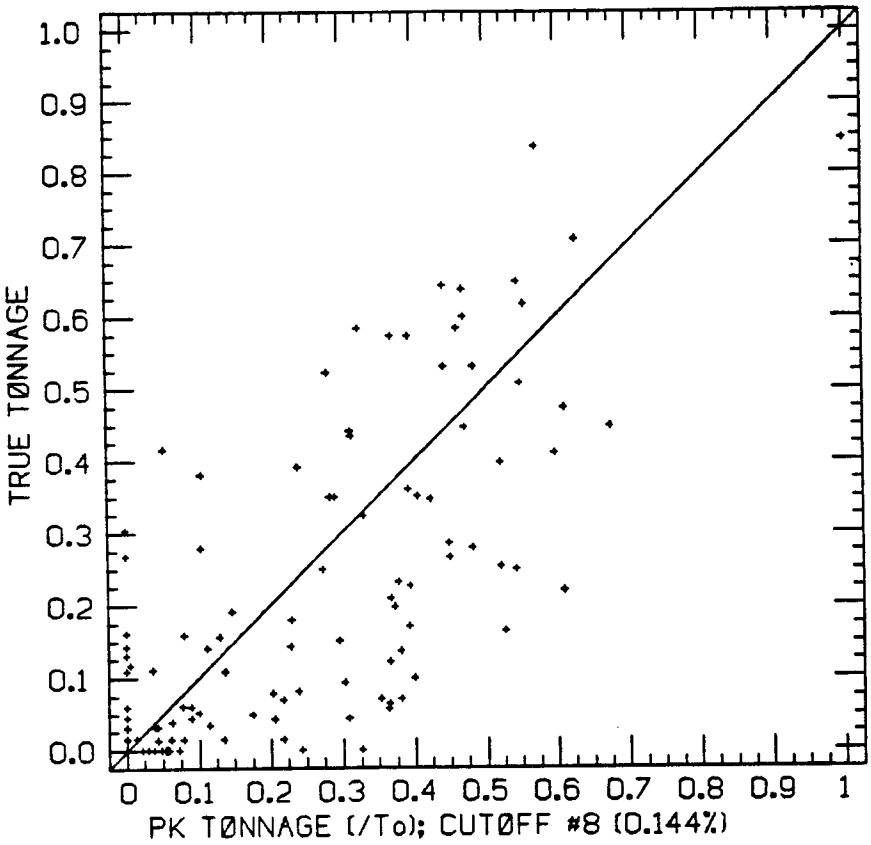

SUMMARY STATISTICS

	MEAN	VARIANCE
EST.	0.234	0.0441
TRUE	0.201	0.0454

RELATIVE BIAS = 0.1611

MEAN SQUARED ERROR = 0.0244

CORRELATION COEF. = 0.739

Figure 78: True vs. PK Estimated Tonnage Recovery for the .144 oz/ton Cutoff, Campaign #1

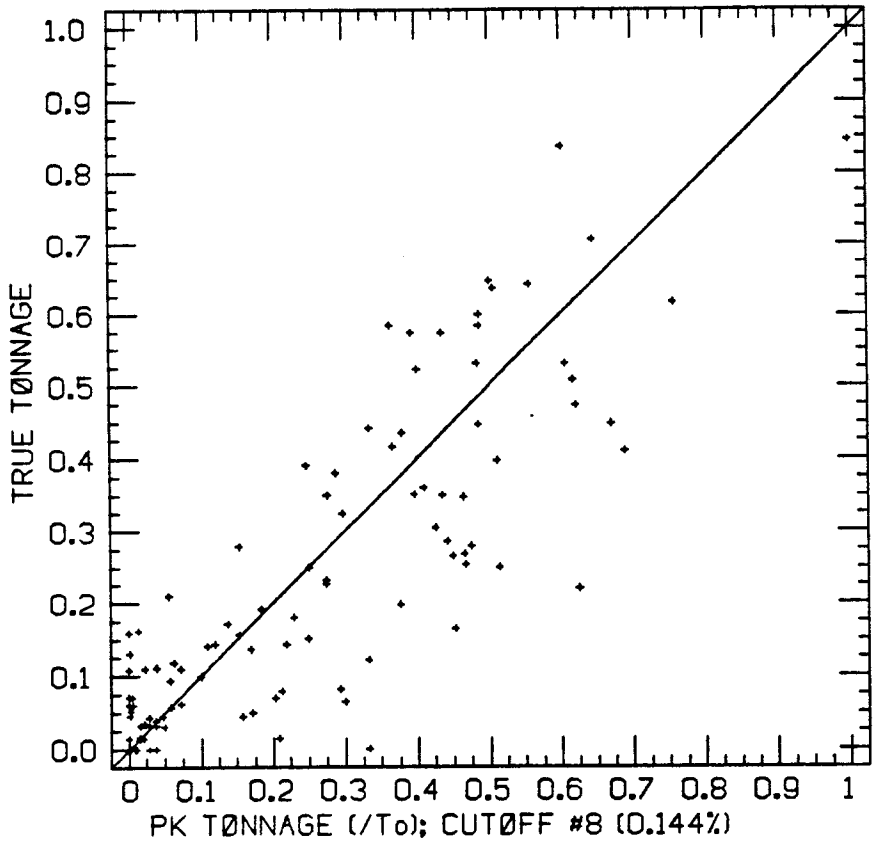

SUMMARY STATISTICS

	MEAN	VARIANCE
EST.	0.220	0.0518
TRUE	0.201	0.0454

RELATIVE BIAS = 0.0911

MEAN SQUARED ERROR = 0.0137

CORRELATION COEF. = 0.864

Figure 79: True vs. PK-OK Estimated Tonnage Recovery for the .144 oz/ton Cutoff, Campaign #1

4.5.3.3 Quantity of Metal Recovered Campaign #1

Quantity of metal recovery estimation for the direct IK and PK estimators is estimated by a simple linear combination of the estimated recovered tonnages (sec 4.4.4.1). Therefore if the estimated tonnages are poor, the estimated quantities of metal can also be expected to be poor. This is in fact what is observed. In contrast to the IK and PK estimators the PK-OK estimator is dependent on both the PK tonnnage estimates and the ordinary kriging estimate of mean panel grade. Recall from the discussion on global recoveries that 80% of the total ounces are recovered at the .144 oz/ton cutoff, therefore all lesser cutoffs will have quantity of metal estimates which are essentially equal to the panel mean estimate (see eqn 4.10). For this reason, when the kriged mean estimate is good so are the quantity of metal estimates at low cutoffs.

The real impact of the conditioning to the OK estimated mean panel grade is demonstrated by the two sets of scattergrams corresponding to the results of the three quantity of metal estimators at the .027 oz/ton and .144 oz/ton cutoffs (figs 80-85). At both of these cutoffs, the IK and PK estimators are strongly conditionally biased and exhibit a propensity to make large errors. The conditional bias of these two estimators is such that when recovering the rich panels more ounces would be recovered than predicted and when recovering the poorer panels less ounces would be recovered than predicted. This type of inaccuracy, which, by the way, does not appear in the global statistics, can cause serious problems for a mine planner attempting to accurately predict short term recoveries.

Thus, the PK-OK estimator which shows no conditional bias is easily the best available estimator of recovered quantity of metal given the sparse campaign #1 data set.

Considering both the tonnage and quantity of metal results of all three estimators, the best estimator of local recoveries is the PK-OK estimator. Thus in cases where the data set is sparse, the PK-OK estimator should be strongly considered.

4.5.3.4 Tonnage Recovery Campaign #2

The most striking feature of the scattergrams of recovered tonnage (figs 86-91) is the improvement over the results obtained in campaign #1. In general the campaign #2 scattergrams show fewer large errors than the corresponding scattergrams for campaign #1. This visual observation is backed up by the statistics associated with the scattergrams. The campaign #2 mean squared error values are less and the correlation coefficients are more than the corresponding values for campaign #1.

For each of the two selected cutoffs, the best results, in terms of visual inspection of the scatter and the plots' associated statistics, are given by the indicator kriging estimator. For both cutoffs considered the IK estimator yields a globally unbiased estimator with small local errors. The only shortcoming of the IK estimates is that they are slightly conditionally biased. This bias is introduced in part by the fact that the unconstrained IK estimator cannot estimate 0% or 100% recovered because the overall mean always receives some weight. Thus in the cases where all indicator data are zero or one (the cases

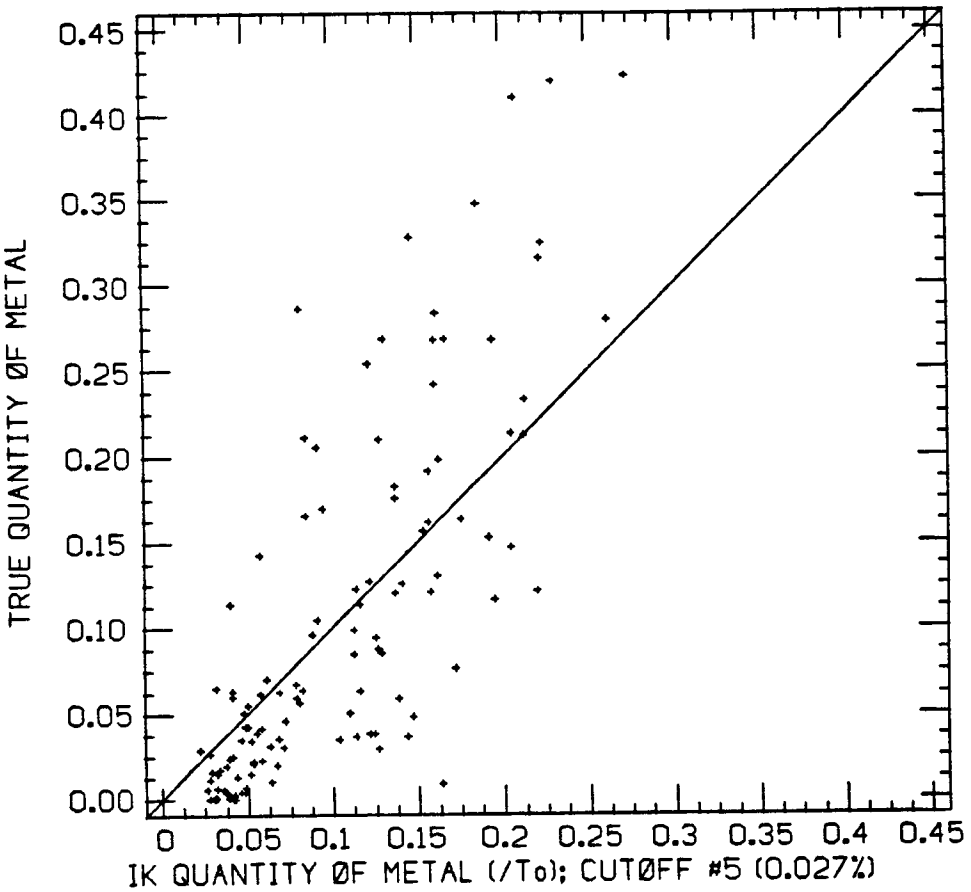

SUMMARY STATISTICS

	MEAN	VARIANCE
EST.	0.101	0.0038
TRUE	0.102	0.0108

RELATIVE BIAS =-0.0086

MEAN SQUARED ERROR = 0.0046

CORRELATION COEF. = 0.781

Figure 80: True vs. IK Estimated Quantity of Metal Recovery .027 oz/ton Cutoff, Campaign #1

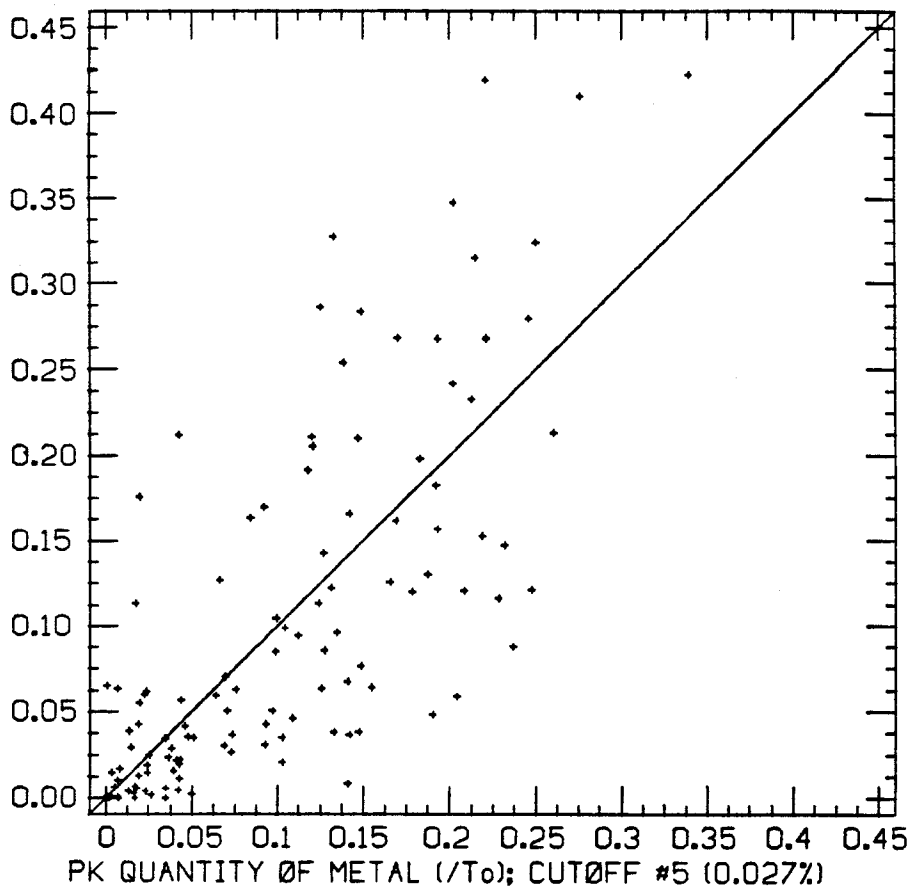

SUMMARY STATISTICS

	MEAN	VARIANCE
EST.	0.102	0.0064
TRUE	0.102	0.0108

RELATIVE BIAS =-0.0001

MEAN SQUARED ERROR = 0.0048

CORRELATION COEF. = 0.743

Figure 81: True vs. PK Estimated Quantity of Metal Recovery .027 oz/ton Cutoff, Campaign #1

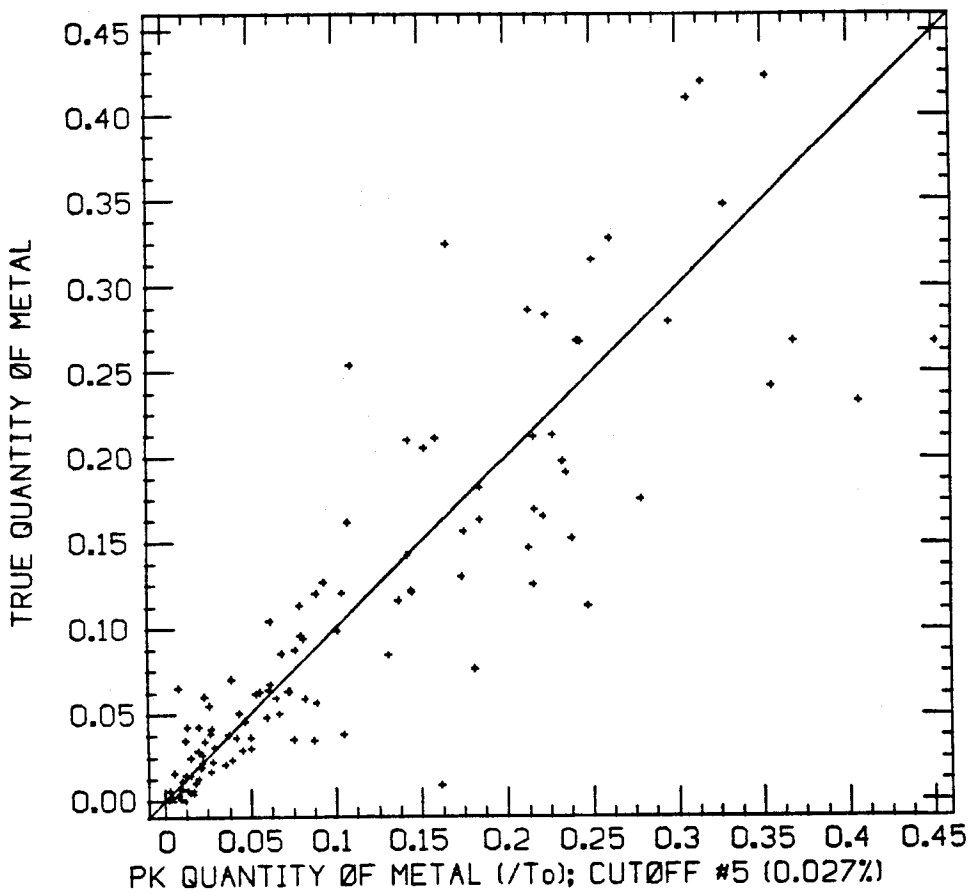

SUMMARY STATISTICS

	MEAN	VARIANCE
EST.	0.106	0.0111
TRUE	0.102	0.0108

RELATIVE BIAS = 0.0426

MEAN SQUARED ERROR = 0.0027

CORRELATION COEF. = 0.879

Figure 82: True vs. PK-OK Estimated Quantity of Metal Recovery .027 oz/ton Cutoff, Campaign #1

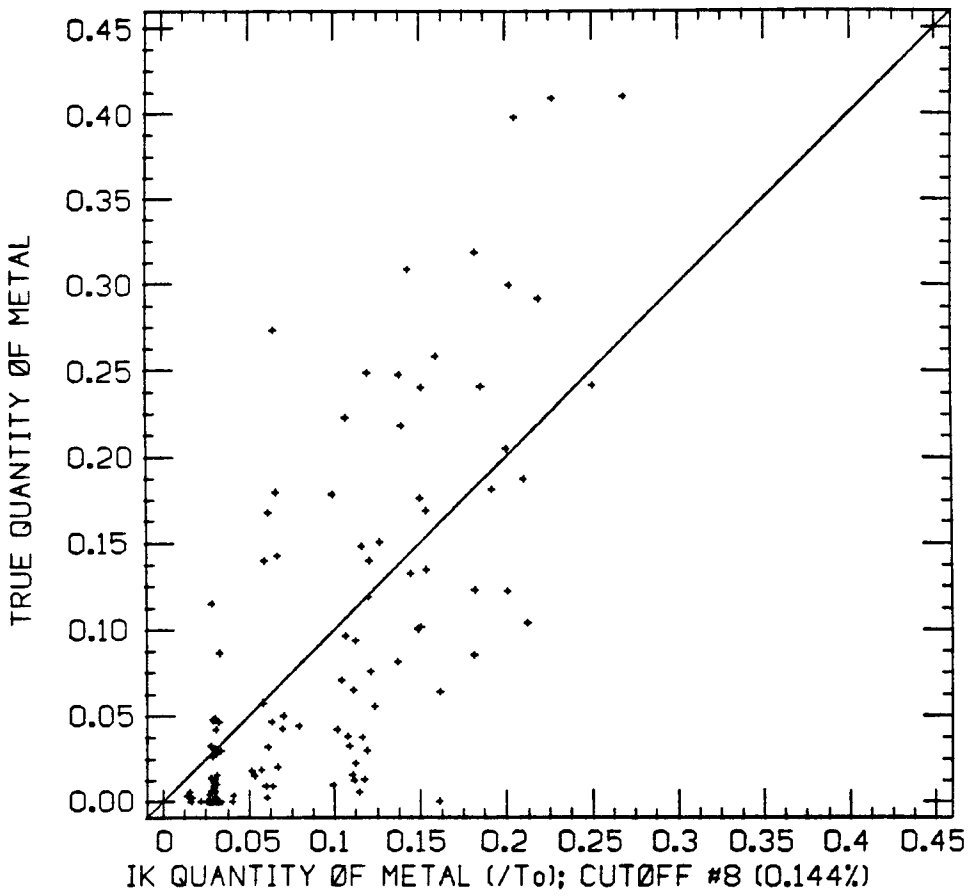

SUMMARY STATISTICS

	MEAN	VARIANCE
EST.	0.088	0.0040
TRUE	0.082	0.0101

RELATIVE BIAS = 0.0785

MEAN SQUARED ERROR = 0.0045

CORRELATION COEF. = 0.758

Figure 83: True vs. IK Estimated Quantity of Metal Recovery .144 oz/ton Cutoff, Campaign #1

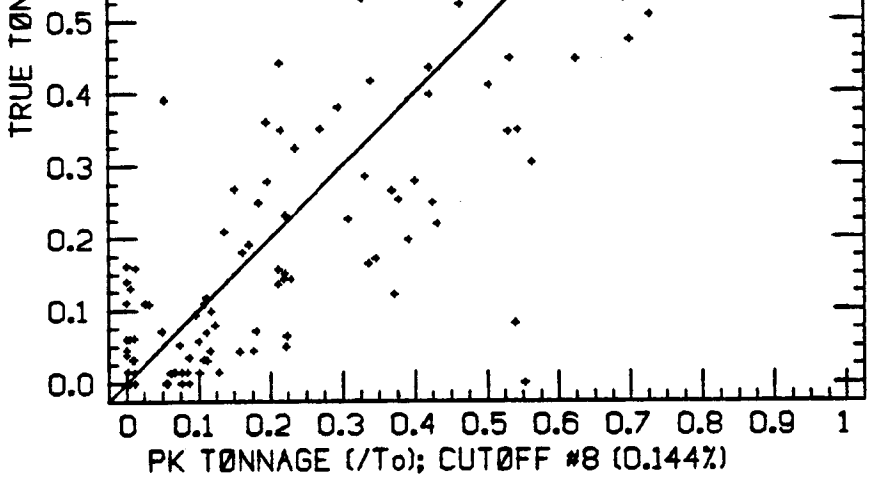

SUMMARY STATISTICS

	MEAN	VARIANCE
EST.	0.232	0.0563
TRUE	0.201	0.0454

RELATIVE BIAS = 0.1514

MEAN SQUARED ERROR = 0.0161

CORRELATION COEF. = 0.856

Figure 91: True vs. PK-OK Estimated Tonnage Recovery at the .144 oz/ton Cutoff, Campaign #2

RELATIVE BIAS = 0.0631

MEAN SQUARED ERROR = 0.0048

CORRELATION COEF. = 0.725

Figure 84: True vs. PK Estimated Quantity of Metal Recovery .144 oz/ton Cutoff, Campaign #1

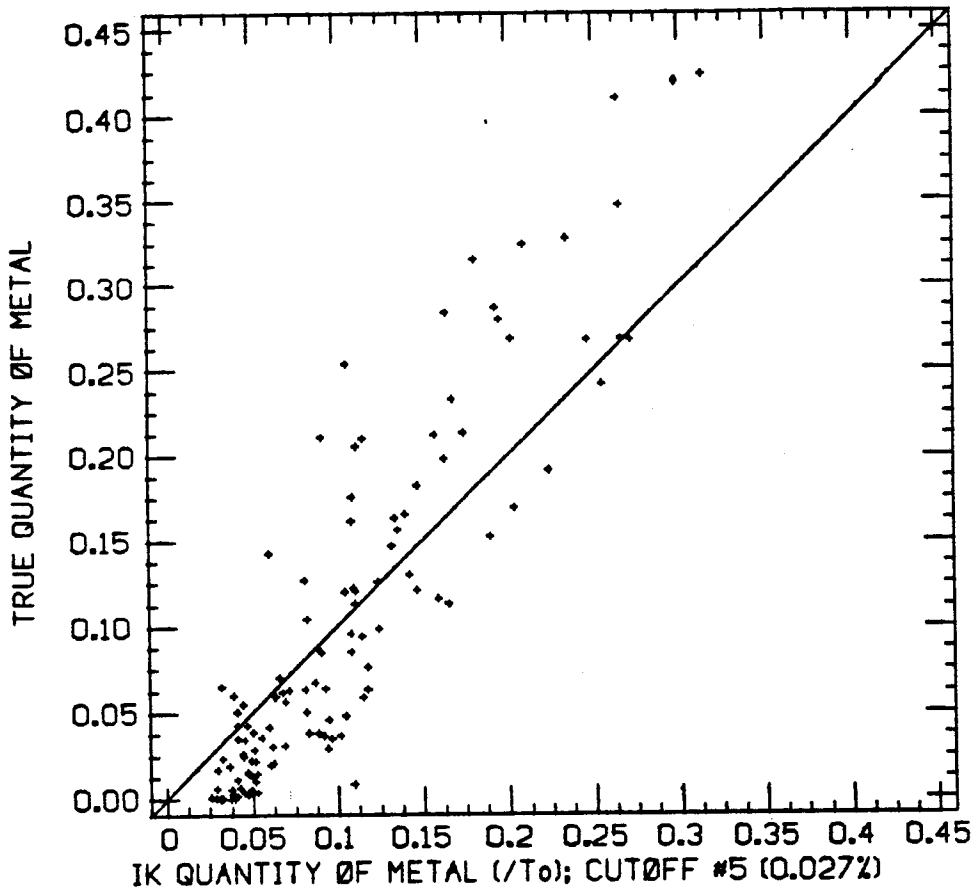

SUMMARY STATISTICS

	MEAN	VARIANCE
EST.	0.102	0.0046
TRUE	0.102	0.0108

RELATIVE BIAS = 0.0051

MEAN SQUARED ERROR = 0.0026

CORRELATION COEF. = 0.906

Figure 92: True vs. IK Quantity of Metal Estimates .027 oz/ton Cutoff, Campaign #2

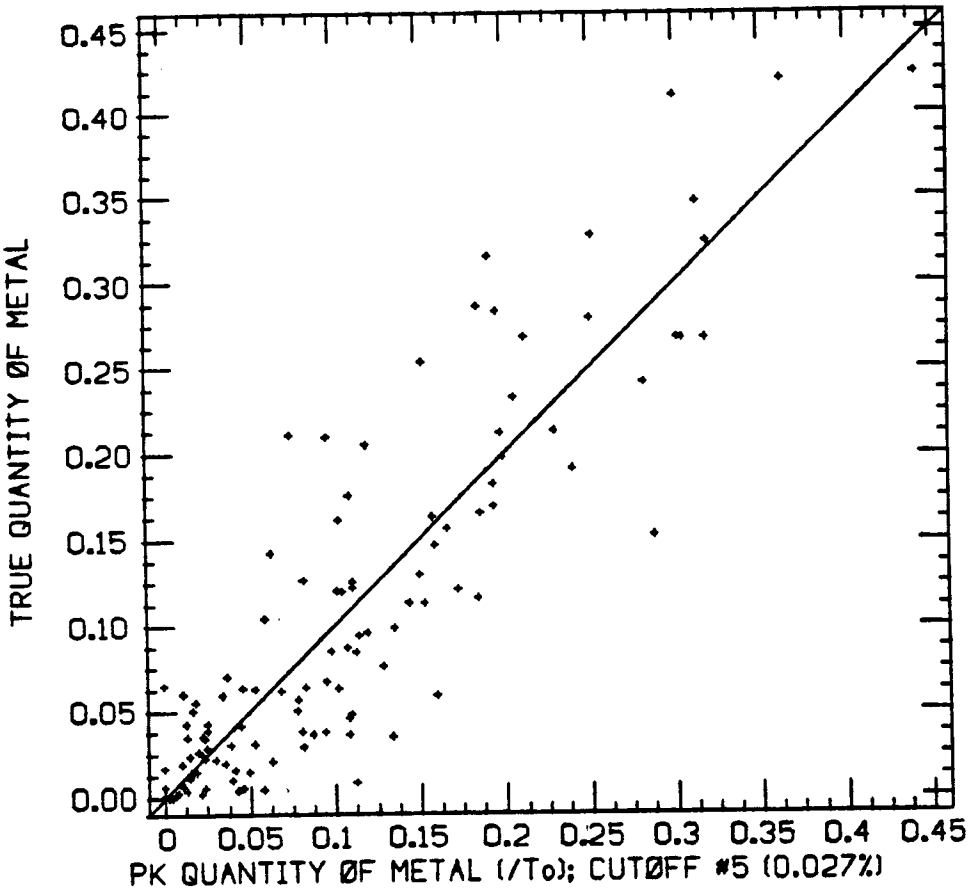

SUMMARY STATISTICS

	MEAN	VARIANCE
EST.	0.103	0.0090
TRUE	0.102	0.0108

RELATIVE BIAS = 0.0132

MEAN SQUARED ERROR = 0.0022

CORRELATION COEF. = 0.894

Figure 93: True vs. PK Quantity of Metal Estimates .027 oz/ton Cutoff, Campaign #2

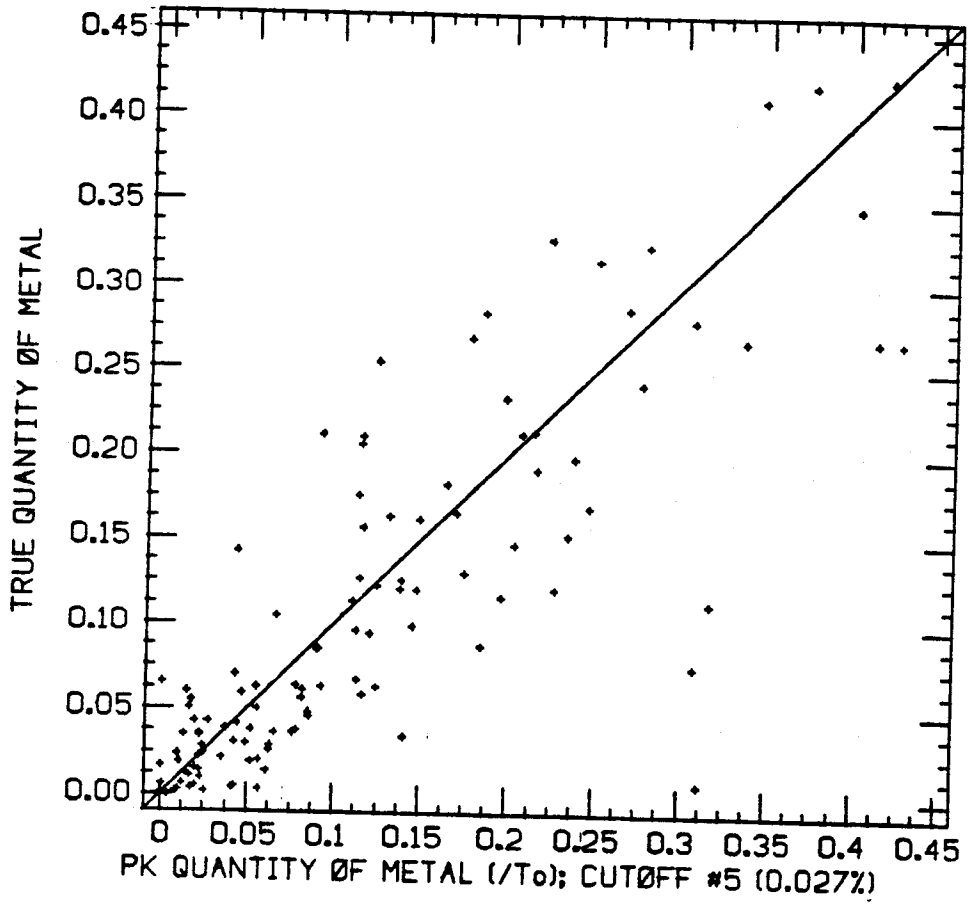

SUMMARY STATISTICS

	MEAN	VARIANCE
EST.	0.113	0.0117
TRUE	0.102	0.0108

RELATIVE BIAS = 0.1111

MEAN SQUARED ERROR = 0.0039

CORRELATION COEF. = 0.834

Figure 94: True vs. PK-OK Quantity of Metal Estimates .027 oz/ton Cutoff, Campaign #2

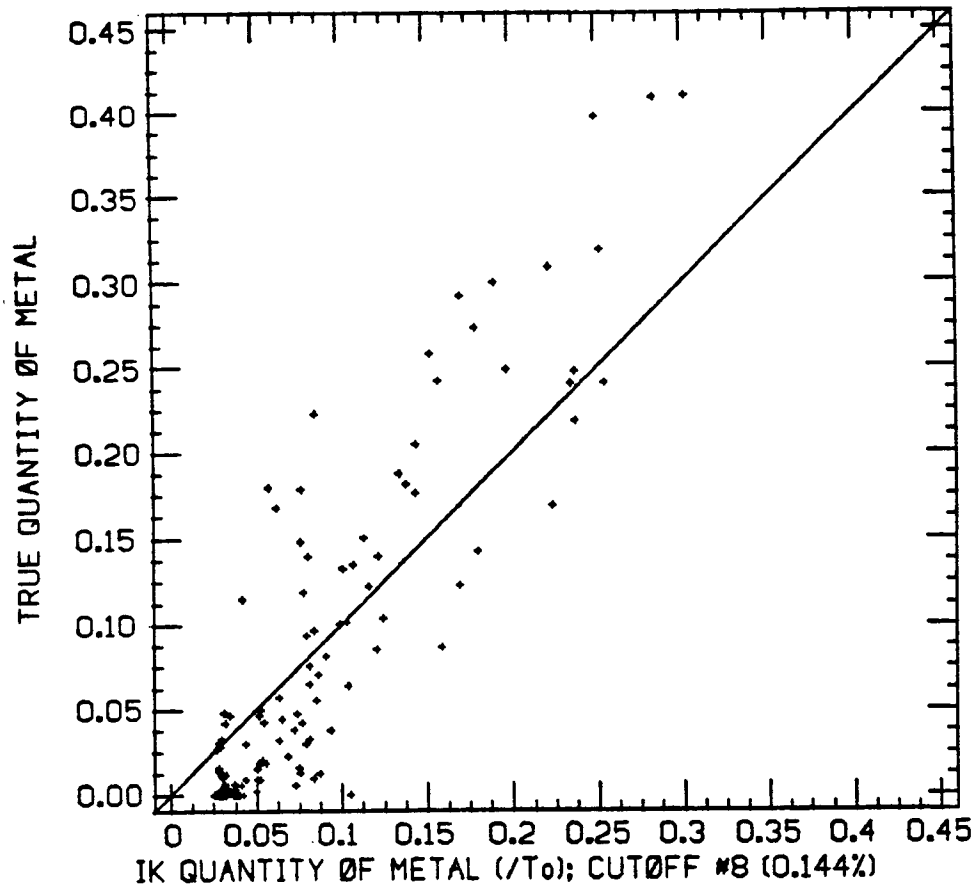

SUMMARY STATISTICS

	MEAN	VARIANCE
EST.	0.085	0.0043
TRUE	0.082	0.0101

RELATIVE BIAS = 0.0418

MEAN SQUARED ERROR = 0.0026

CORRELATION COEF. = 0.894

Figure 95: True vs. IK Quantity of Metal Estimates .144 oz/ton Cutoff, Campaign #2

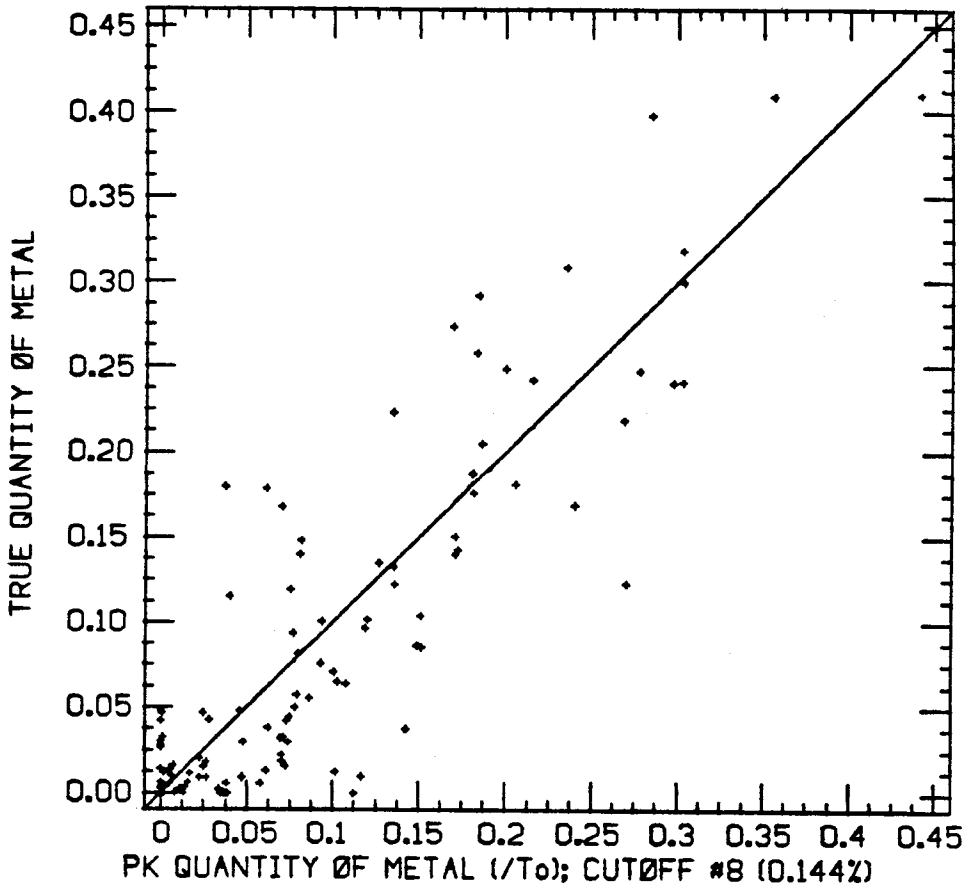

SUMMARY STATISTICS

	MEAN	VARIANCE
EST.	0.086	0.0088
TRUE	0.082	0.0101

RELATIVE BIAS = 0.0575

MEAN SQUARED ERROR = 0.0022

CORRELATION COEF. = 0.885

Figure 96: True vs. PK Quantity of Metal Estimates .144 oz/ton Cutoff, Campaign #2

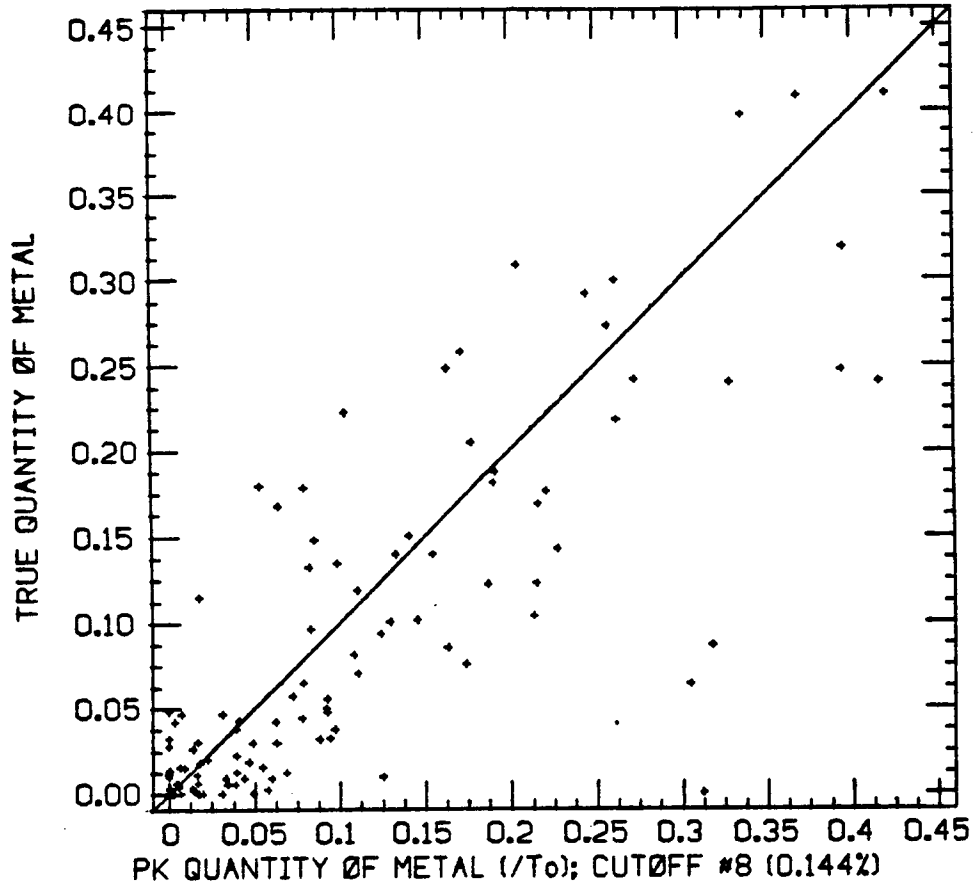

SUMMARY STATISTICS

	MEAN	VARIANCE
EST.	0.097	0.0118
TRUE	0.082	0.0101

RELATIVE BIAS = 0.1849

MEAN SQUARED ERROR = 0.0042

CORRELATION COEF. = 0.821

Figure 97: True vs. PK-OK Quantity of Metal Estimates .144 oz/ton Cutoff, Campaign #2

This indicates that the additional information provided in campaign #3 is of little value and that the additional in filling performed in campaign #3 is unwarranted for the purposes of estimating local recoverable reserves.

For the two chosen cutoffs all three estimators perform essentially the same so that it is difficult to choose a superior estimator. At the .144 oz/ton cutoff however the PK estimator is slightly better than either of the other two estimators.

In short, all three estimators perform very well given the data present in campaign #3. Hence campaign #3 is not a truly difficult or enlightening test of the strengths and weaknesses of the estimators as simply too much data is present.

4.5.3.7 Quantity of Metal Estimation Campaign #3

Again given the abundance of data available in campaign #3, all three estimators perform well and it is difficult to choose between them (figs. 104-109). The PK estimator does however have the best statistics and the PK scattergrams have the best overall appearance. The IK scattergram, again, has a slight conditional bias and shows slightly greater scatter than the PK estimator. The PK-OK estimator, on the other hand, shows a few more large errors than the PK estimator. For these reasons the PK estimator is the preferred choice, by a slim margin, for estimating recoverable reseves given the campaign #3 data configuration.

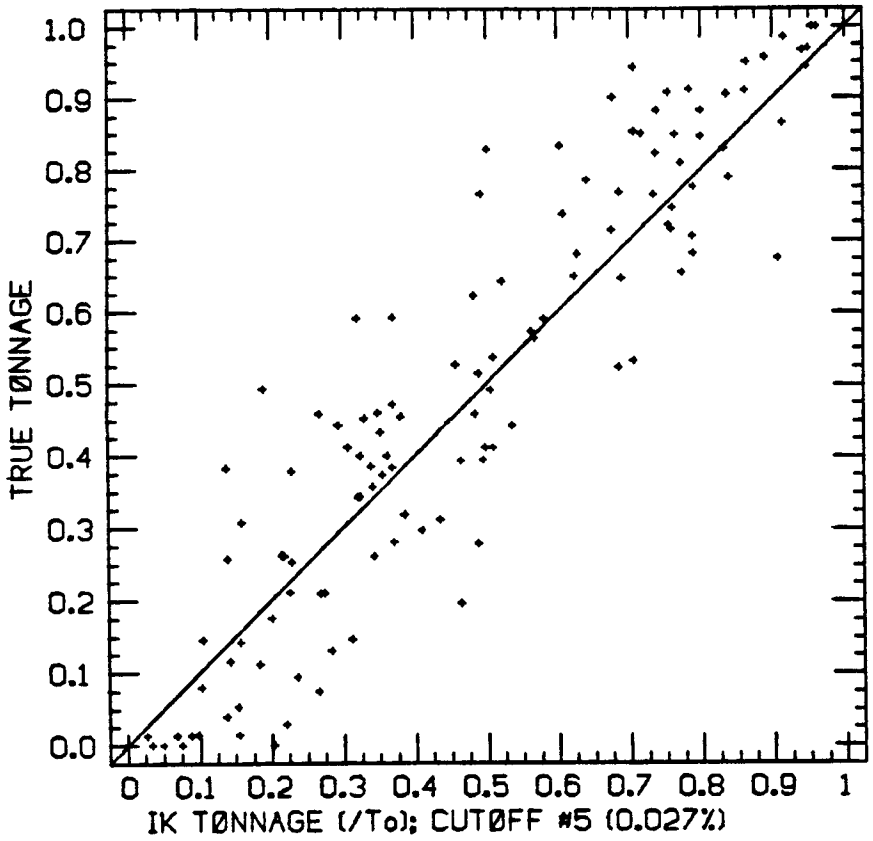

SUMMARY STATISTICS

	MEAN	VARIANCE
EST.	0.483	0.0686
TRUE	0.499	0.0890

RELATIVE BIAS =-0.0315

MEAN SQUARED ERROR = 0.0140

CORRELATION COEF. = 0.920

Figure 98: True vs. IK Estimated Tonnage Recovery .027 oz/ton Cutoff, Campaign #3

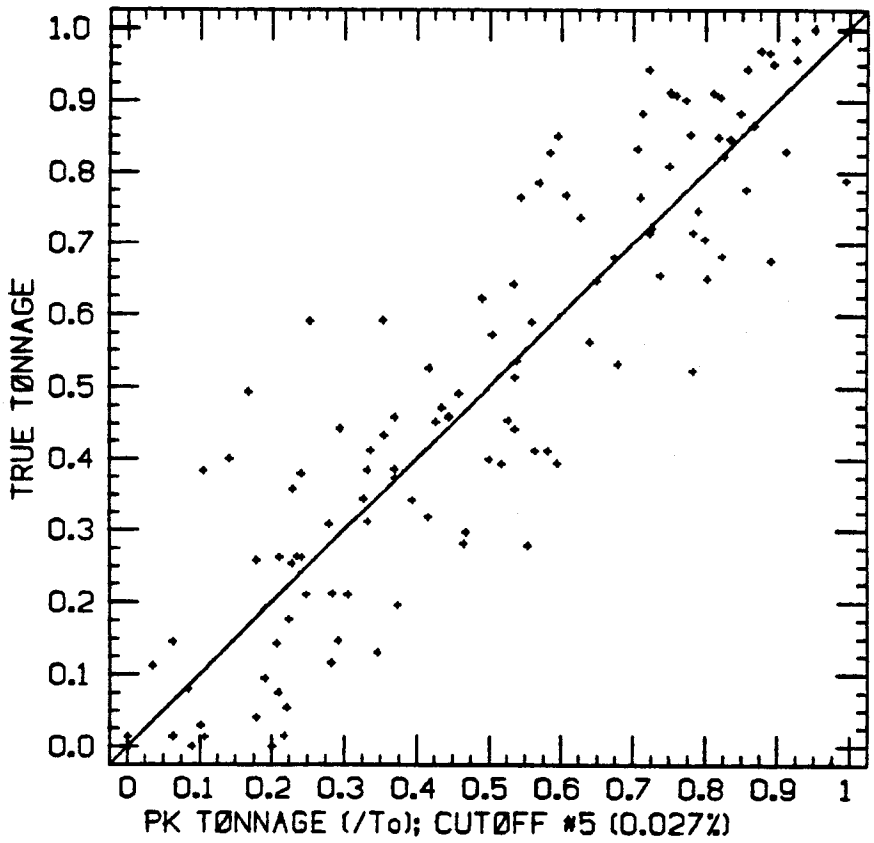

SUMMARY STATISTICS

	MEAN	VARIANCE
EST.	0.495	0.0736
TRUE	0.499	0.0890

RELATIVE BIAS =-0.0079

MEAN SQUARED ERROR = 0.0162

CORRELATION COEF. = 0.904

Figure 99: True vs. PK Estimated Tonnage Recovery .027 oz/ton Cutoff, Campaign #3

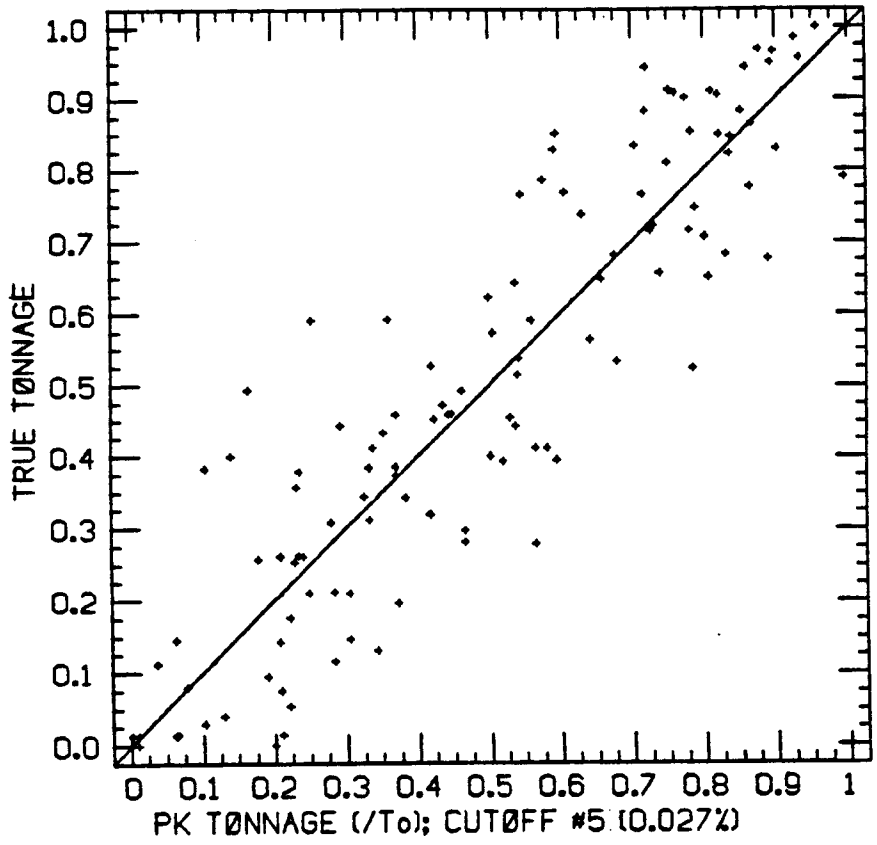

SUMMARY STATISTICS

	MEAN	VARIANCE
EST.	0.494	0.0755
TRUE	0.499	0.0890

RELATIVE BIAS =-0.0106

MEAN SQUARED ERROR = 0.0159

CORRELATION COEF. = 0.906

Figure 100: True vs. PK-OK Estimated Tonnage Recovery .027 oz/ton Cutoff, Campaign #3

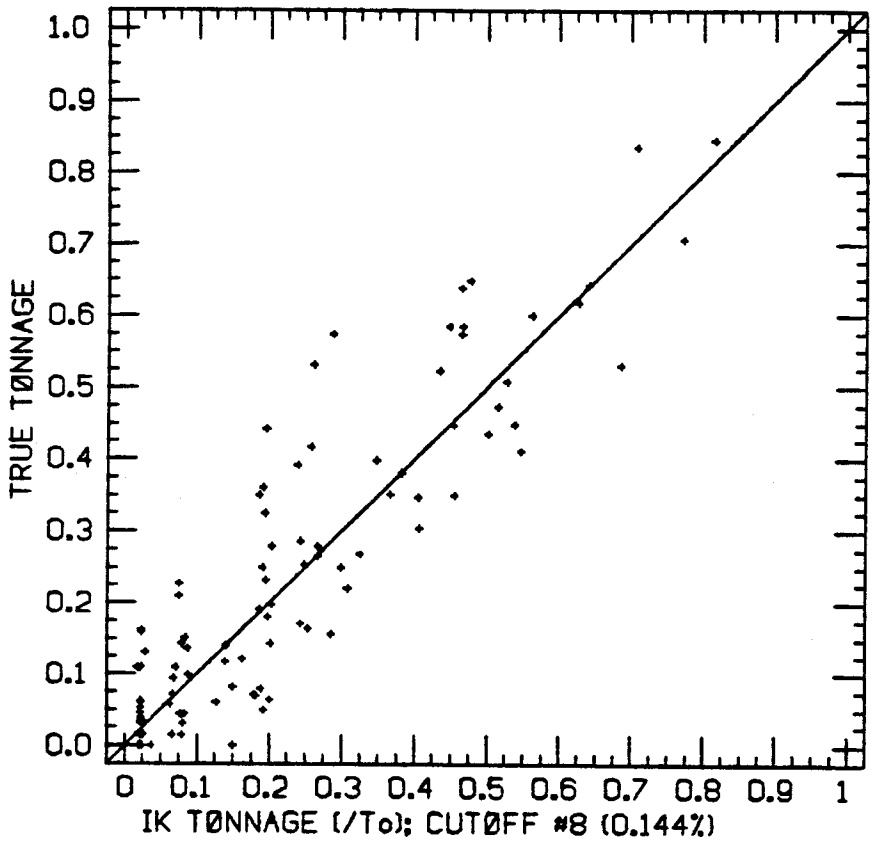

SUMMARY STATISTICS

	MEAN	VARIANCE
EST.	0.193	0.0386
TRUE	0.201	0.0454

RELATIVE BIAS =-0.0435

MEAN SQUARED ERROR = 0.0074

CORRELATION COEF. = 0.916

Figure 101: True vs. IK Estimated Tonnage Recovery .144 oz/ton Cutoff, Campaign #3

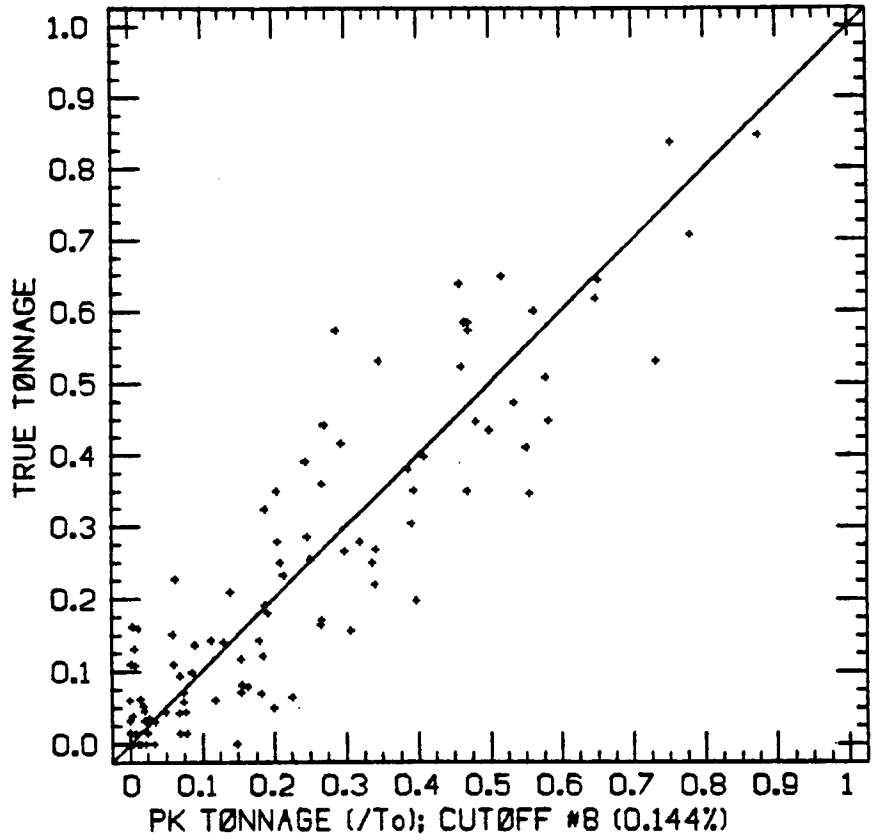

SUMMARY STATISTICS

	MEAN	VARIANCE
EST.	0.199	0.0457
TRUE	0.201	0.0454

RELATIVE BIAS =-0.0108

MEAN SQUARED ERROR = 0.0075

CORRELATION COEF. = 0.918

Figure 102: True vs. PK Estimated Tonnage Recovery .144 oz/ton Cutoff, Campaign #3

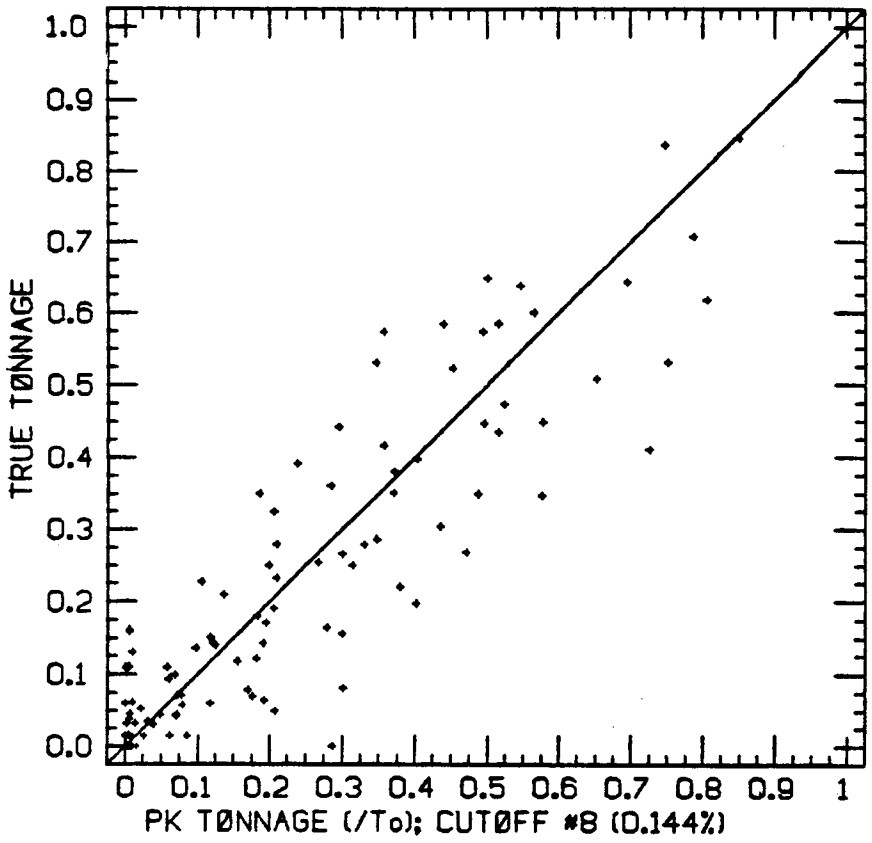

SUMMARY STATISTICS

	MEAN	VARIANCE
EST.	0.209	0.0511
TRUE	0.201	0.0454

RELATIVE BIAS = 0.0387

MEAN SQUARED ERROR = 0.0092

CORRELATION COEF. = 0.907

Figure 103: True vs. PK-OK Estimated Tonnage Recovery .144 oz/ton Cutoff, Campaign #3

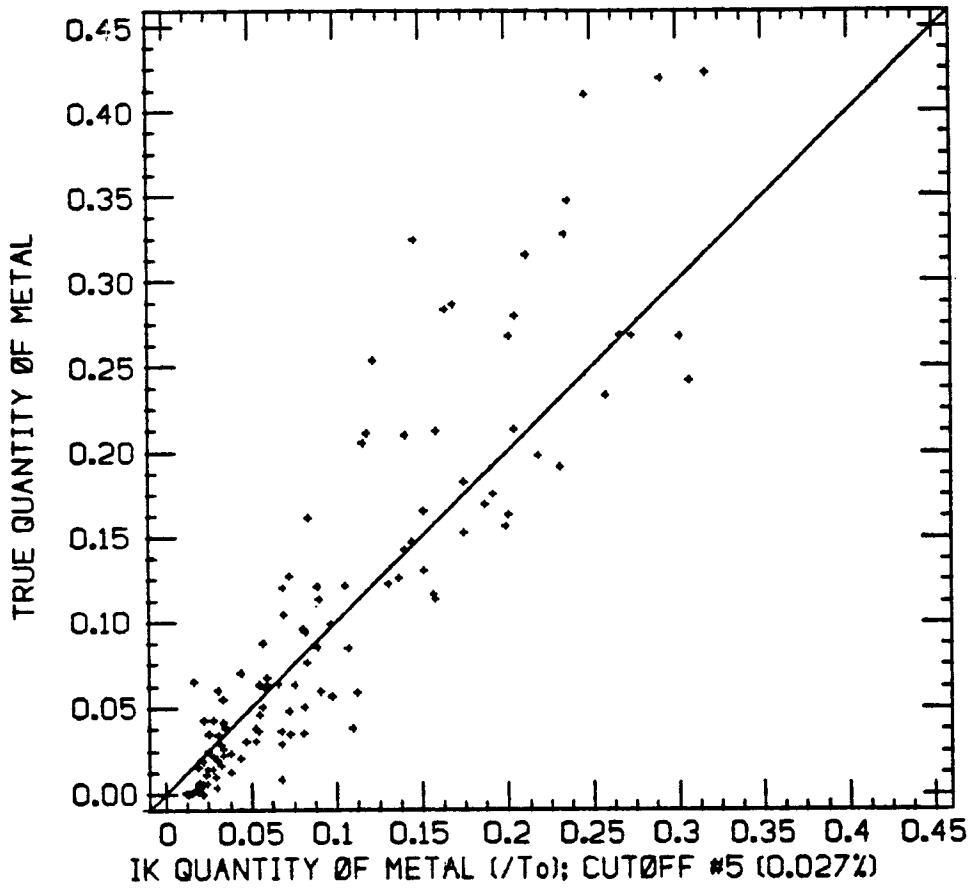

SUMMARY STATISTICS

	MEAN	VARIANCE
EST.	0.095	0.0062
TRUE	0.102	0.0108

RELATIVE BIAS =-0.0629

MEAN SQUARED ERROR = 0.0022

CORRELATION COEF. = 0.904

Figure 104: True vs. IK Estimated Quantity of Metal Recovery .027 oz/ton cutoff, Campaign #3

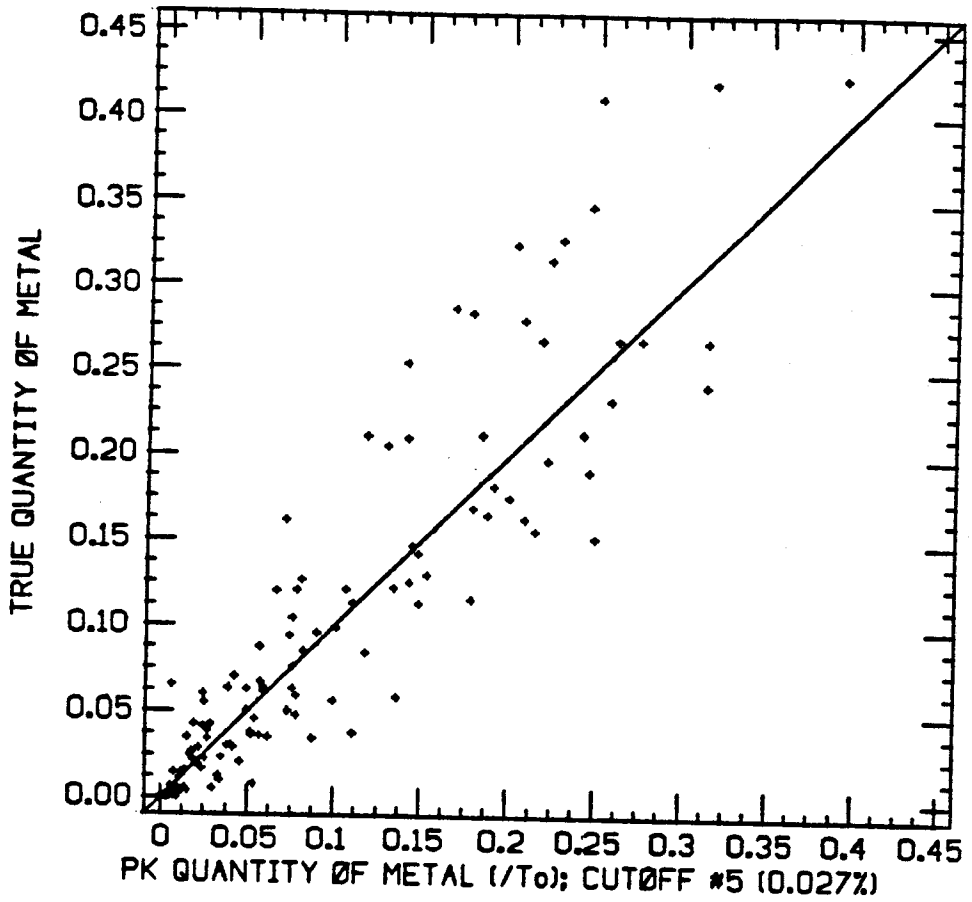

SUMMARY STATISTICS

	MEAN	VARIANCE
EST.	0.096	0.0080
TRUE	0.102	0.0108

RELATIVE BIAS =-0.0602

MEAN SQUARED ERROR = 0.0020

CORRELATION COEF. = 0.908

Figure 105: True vs. PK Estimated Quantity of Metal Recovery .027 oz/ton cutoff, Campaign #3

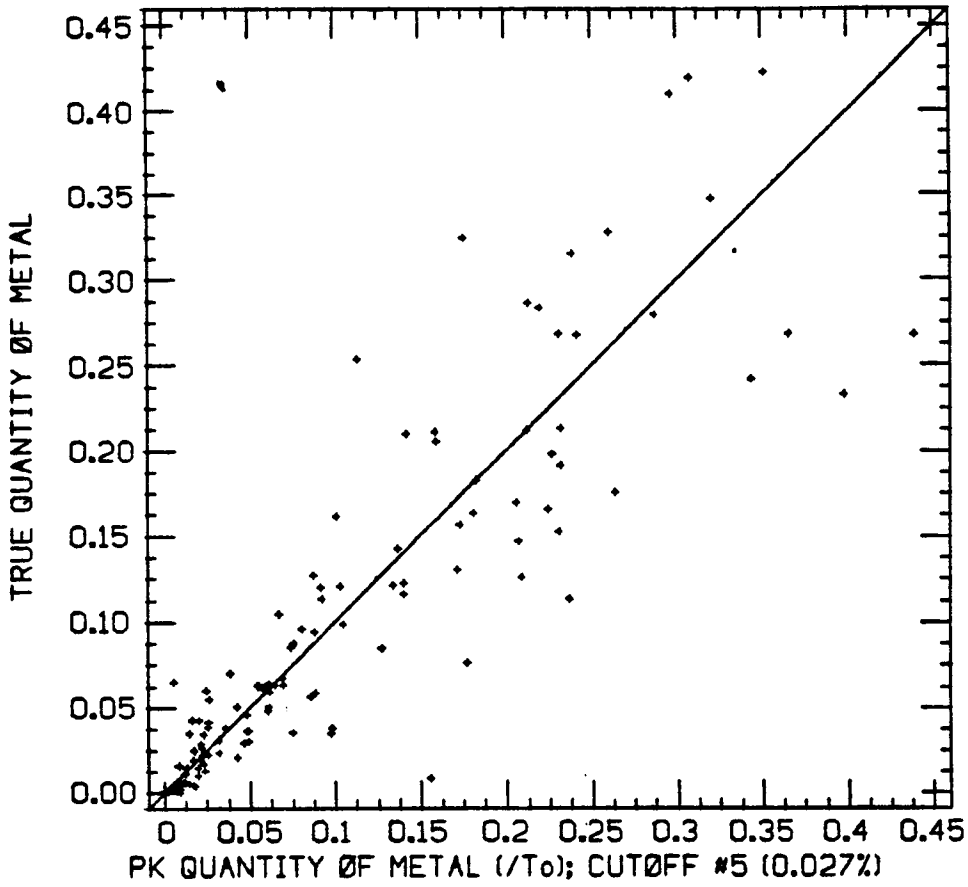

SUMMARY STATISTICS

	MEAN	VARIANCE
EST.	0.105	0.0106
TRUE	0.102	0.0108

RELATIVE BIAS = 0.0292

MEAN SQUARED ERROR = 0.0025

CORRELATION COEF. = 0.884

Figure 106: True vs. PK-OK Estimated Quantity of Metal Recovery .027 oz/ton cutoff, Campaign #3

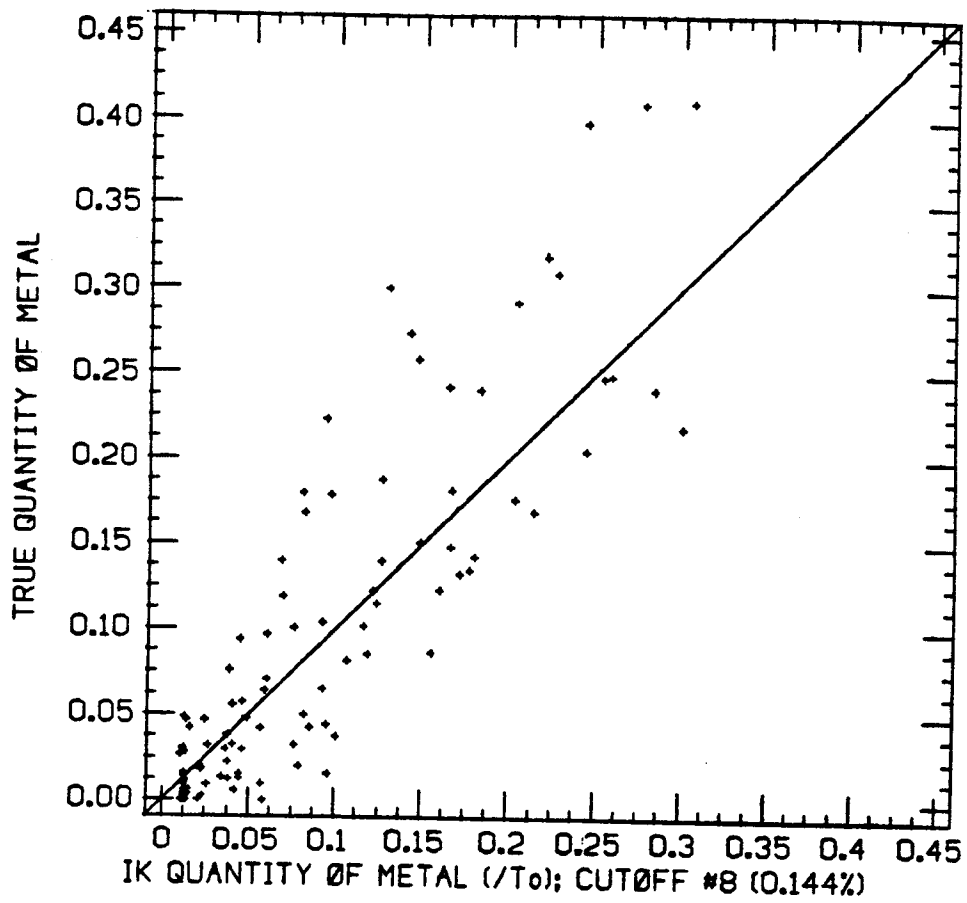

SUMMARY STATISTICS

	MEAN	VARIANCE
EST.	0.077	0.0061
TRUE	0.082	0.0101

RELATIVE BIAS =-0.0499

MEAN SQUARED ERROR = 0.0023

CORRELATION COEF. = 0.887

Figure 107: True vs. IK Estimated Quantity of Metal Recovery .144 oz/ton cutoff, Campaign #3

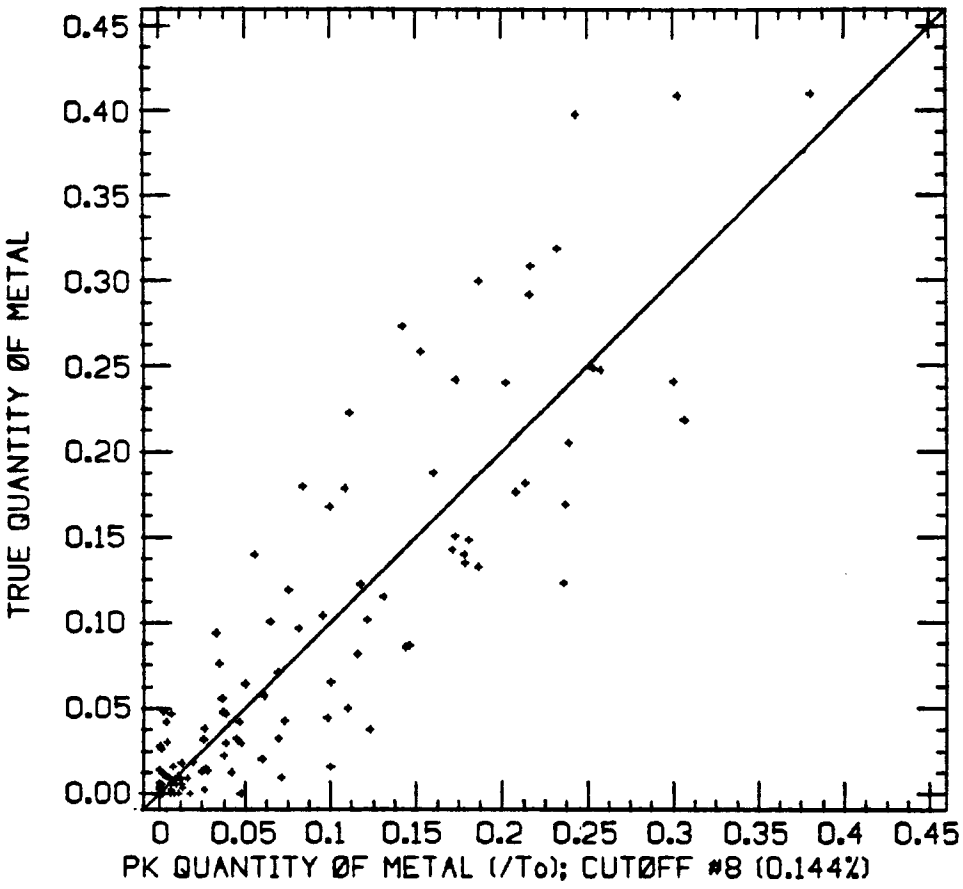

SUMMARY STATISTICS

	MEAN	VARIANCE
EST.	0.078	0.0079
TRUE	0.082	0.0101

RELATIVE BIAS =-0.0396

MEAN SQUARED ERROR = 0.0021

CORRELATION COEF. = 0.892

Figure 108: True vs. PK Estimated Quantity of Metal Recovery .144 oz/ton cutoff, Campaign #3

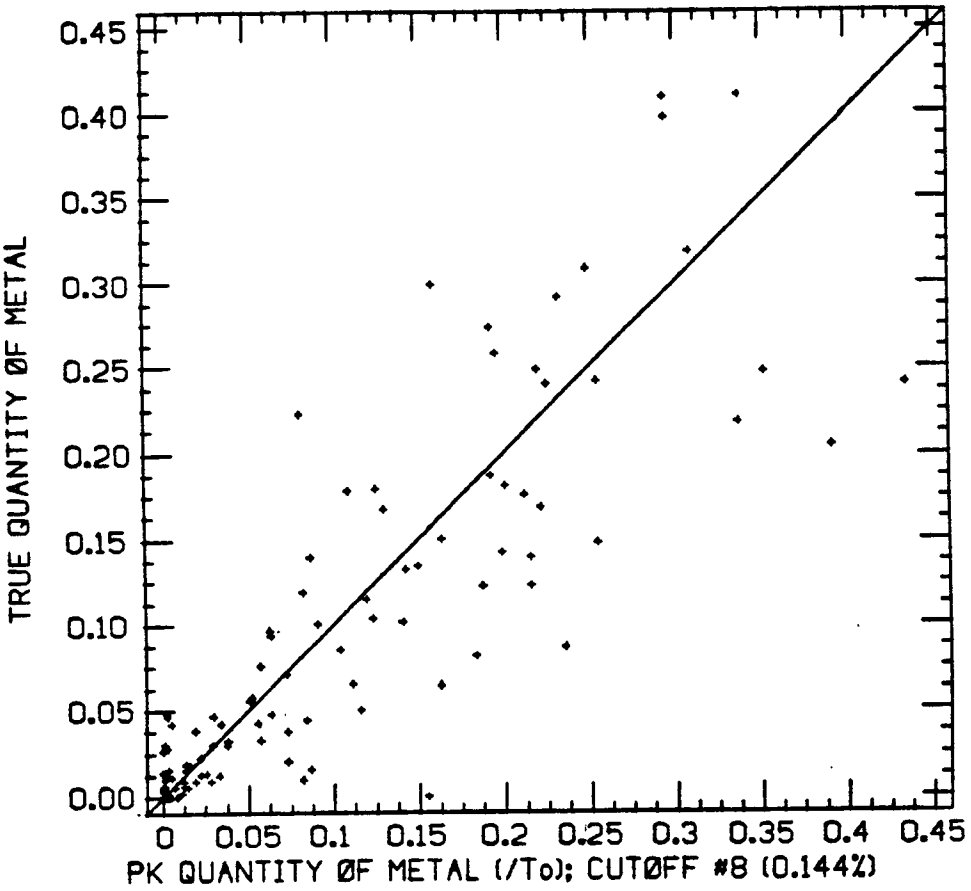

SUMMARY STATISTICS

	MEAN	VARIANCE
EST.	0.088	0.0107
TRUE	0.082	0.0101

RELATIVE BIAS = 0.0817

MEAN SQUARED ERROR = 0.0029

CORRELATION COEF. = 0.864

Figure 109: True vs. PK-OK Estimated Quantity of Metal Recovery .144 oz/ton Cutoff, Campaign #3

4.6 SUMMARY OF RESULTS

In the last two sections, a large amount of both global and local results have been presented. From these results it is possible to choose which estimators should be used in what situation and the quality of results which can be expected. In choosing between the three estimators more weight is given to the local results than the global results as these estimators were designed precisely for the purpose of estimating local recoveries.

The IK estimator exhibited the best overall nonbias properties. The other two estimators were not too far off, particularly for low cutoffs. Given the observed global bias of the IK estimator one can say with some certainty that both global tonnage and quantity of metal recovered can be confidently estimated within ±10% given the campaign #1 data configuration, ±8% given the campaign #2 configuration, and ±5% given the campaign #3 configuration.

As a local estimator, however IK lags behind the other techniques, especially PK. When the data are sparse, the nature of the indicator kriging estimator makes accurate estimation of local recoveries extremely difficult as shown by the results of campaign #1. As more data becomes available, the local characteristics of the IK estimator improve, however the estimator still shows conditional biases to varying degrees. As mentioned previously, conditional biases in a local estimator are not acceptable even if a cancellation effect is present which removes any global bias. In local estimation, the precise recovery within each panel must be determined and a conditional bias entails that a great number of panels may be poorly estimated.

The PK-OK estimator performs very well in campaigns #1 and #3. It does not perform well, however, in campaign #2. The problem encountered in campaign #2 is that the ordinary kriging estimates of mean panel grade, which is essential to the PK-OK estimator, were poor. Thus in any case where the ordinary kriging estimates are suspect the PK-OK estimator should not be used. In the case of campaign #2, the global mean of the kriged panels was 1.17 oz/ton while the mean of the 313 regularly spaced data was 1.07 oz/ton. From this discrepancy it is obvious that the ordinary kriging results for this campaign are poor so the PK-OK estimator should not be used.

The local results for campaign #1 show how useful the PK-OK estimator can be in difficult situations. The PK-OK estimator of tonnage and particularly quantity of metal recovered are clearly superior to those obtained by the other two techniques. Based on these results the PK-OK estimator is recommended whenever few data receive significant weight in the IK or PK kriging systems. As more data becomes available, however this method is not recommended for two reasons. First the PK-OK estimator contains no non-bias conditions on either the tonnage or quantity of metal recovered except for an implicit condition which forces the global mean panel grade to equal the kriged mean panel grade. Thus, as shown in the global results, the PK-OK estimator is not a good estimator of global recoveries. The second drawback of this method is as the number of available data increases, the PK or IK estimates of mean panel grade can be better estimates of panel mean than the OK estimates. Although OK provides the best linear estimate of panel mean, IK and PK are non linear estimators of panel mean, hence they can

provide superior estimates. In cases where the IK or PK estimators of panel mean are superior, there is no logical reason to condition the tonnage estimates to the inferior ordinary kriging estimates. Unfortunately, it is impossible to predict for which panel sizes, data configurations and spatial correlation combinations the OK panel mean estimates will be superior to the IK or PK panel mean estimates. Therefore the use of this technique should be restricted to instances where it is obvious that there is not enough data to accurately estimate recovered tonnage (i.e. situations similar to those encountered in campaign #1).

The PK estimator is the best estimator in most cases. In all of the examined data configurations it has proven to be a better overall estimator of tonnage and quantity of metal recovered than IK. When few data are present, the estimates of quantity of metal can show strong conditional biases. In such cases, as previously mentioned, the PK-OK estimator is preferred.

From this analysis the following recommendations are made

1. When few data receive significant weight in the IK kriging system use the PK-OK estimator.
2. In all other cases use the PK estimator.

Given the nature of most estimation problems, (i.e. few data available) the PK-OK estimator will be used in the majority of cases if these recommendations are followed.

4.7 APPENDIX - VARIATIONS OF THE PK ESTIMATOR

In developing the probability kriging estimator, three variations of the basic estimator were discussed. The difference between these estimators is only in the number and form of the non-bias constraints imposed on the estimators. The three variations and the required non-bias constraints are described in detail in section 2.6.1. Briefly, however, the three variations can be described as PK estimators which utilize 0, 1, or 2 non-bias constraints.

As mentioned in section 2.6.2, the number of non-bias constraints is positively correlated with the magnitude of the estimation variance. Hence the estimation variance of the three variations of the PK estimator is highest for the estimator with two non-bias conditions and lowest for the estimator with no non-bias conditions. In spite of this fact, the variation of the PK estimator with two non-bias conditions is utilized in all case studies. The reason for this apparent contradiction is that the two non-bias condition estimator is simply a better local estimator than either of the other two variations. To show this in one instance, a small case study is considered. All three variations are utilized to estimate the point support tonnage recovery at one cutoff utilizing the Campaign #1 set of data from the Bell Mine case study. The cutoff chosen is the median cutoff .027 oz/ton.

The local results at the .027 oz/ton cutoff (fig 110) show that as the number of non-bias conditions decreases the smoothing of the estimator increases. This smoothing is readily apparent for the estimator with no non-bias conditions as this estimator is also conditionally biased to a significant degree. The smoothing of the one

non-bias condition variation is much less, however it is apparent from the scattergrams that this estimator is smoother than the 2 non-bias condition variation. The variances of the estimators and the variance of the true values are summarized in table 14.

TABLE 14

Variances of the Three Variations of the PK Estimator

Estimator	Variance
PK0	.0235
PK1	.0572
PK2	.0716
TRUE	.0890

Thus on the basis of a smoothing criterion and overall appearence of the scattergrams (fig. 110) the PK estimator with two unbiased conditions is considered the best local estimator of recovered tonnage. This result points to the fact that the estimation variance is an incomplete measure of the overall quality of an estimator; therefore, in choosing a local estimator, consideration must be given to criteria other than the estimation variance.

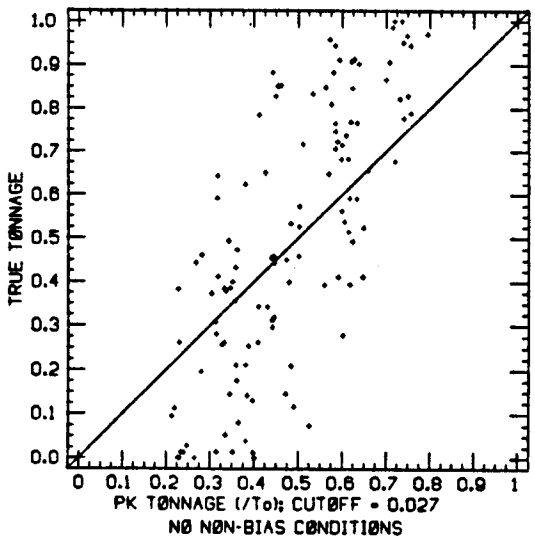

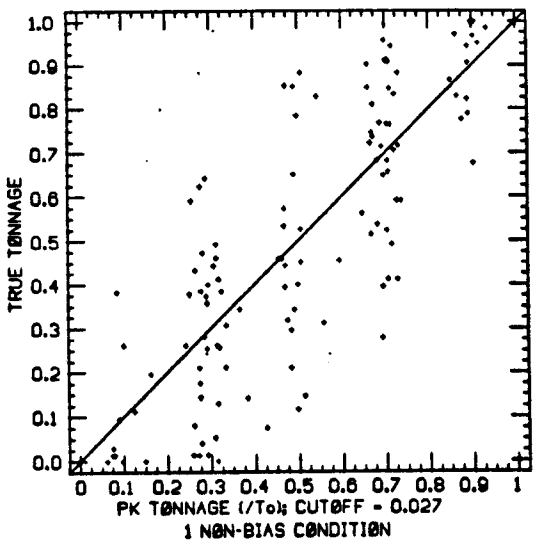

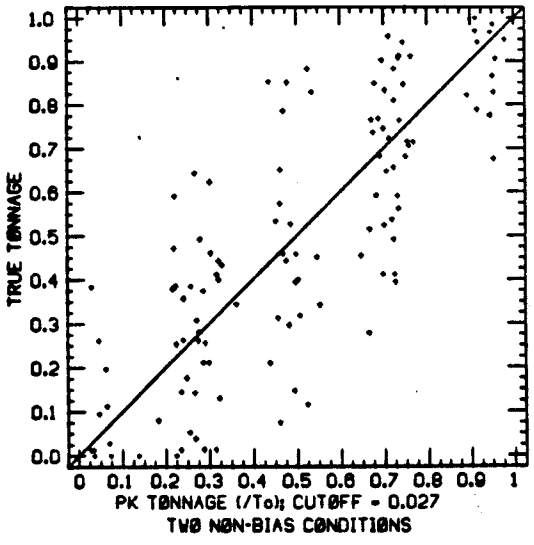

Figure 110: Local Results at the .027 oz/ton cutoff for three variations of the PK estimator

Chapter V

ESTIMATION OF BLOCK SUPPORT SPATIAL DISTRIBUTIONS

The previous chapter demonstrated that adequate to good results can be obtained using distribution free methods to estimate the distribution of point support selective mining units within a panel. Unfortunately, the impact of these results on the mining community is limited since the volume of a selective mining unit is typically much larger than a point (on the order of a few hundred tons for Carlin type gold deposits). To prove that spatial distribution estimators based on indicator data can be useful to the mining industry, the local spatial distribution of block support selective mining units within a panel must be estimated and, as a check on the accuracy of the method, compared with the local spatial distribution of true block support grades.

5.1 DEFINITION OF LOCAL BLOCK SUPPORT SPATIAL DISTRIBUTIONS

The local distribution of block support smus within a panel can be defined analogously to the local distribution of point support smus. Thus:

$$\phi_v(A,zc) = 1/(A) \cdot \int_A i_v(x,zc)\, dv \qquad (5.2)$$

$$\text{where: } i_v(x,zc) = \begin{cases} 1 \text{ if } z_v(x) \leq zc \\ 0 \text{ if } z_v(x) > zc \end{cases} \qquad (5.3)$$

$z_v(x)$ is the grade of an smu of size v centered on location x.

Notice that this definition of the block support spatial distribution is similar to the definition of point support spatial distributions; thus, it may appear that an estimator of $\phi_v(A,zc)$ can be derived in the same way that point support distribution estimators were developed. Unfortunately the block indicator data $i_v(x,zc)$ are not available as block support samples are not normally taken. Furthermore, it is not possible to develop a block support estimator from the available point support data (as is done, for example, when estimating mean block grade from point grade data) because density and distribution functions are non-additive variables. That is, while it is true (for large n) that

$$Z_v(x_0) = \sum_{i=1}^{n} Z(x_i)/n \tag{5.4}$$

where: $Z_v(x_0)$ is the average grade of a block v centered on point x_0
n is the number of points discretizing the block v
$z(x_i)$ is the point grade at point x_i located within v

it is not true that

$$\phi_v(v,zc) = \sum_{i=1}^{n} \phi(x_i,zc)/n \tag{5.5}$$

or, to simplify notation

$$f(z_v(x_0)) \neq \sum_{i=1}^{n} f(z(x_i))/n. \tag{5.6}$$

The local distribution of block support smus can, however, be derived in the following manner.

$$\text{Let} \quad Z_v(x_0) = \sum_{i=1}^{n} Z(x_i)/n \tag{5.7}$$

Make a one to one transformation

$$Z_v(x_0) = Y_1 = \frac{1}{n}\cdot\sum_{i=1}^{n} Z(x_i),\ Y_2 = Z(x_2),\ldots,Y_n = Z(x_n) \tag{5.8}$$

$$\text{Thus} \quad f(y_1,y_2,\ldots,y_n) = f(n\cdot y-\sum_{i=2}^{n} z(x_i),z(x_2),\ldots,z(x_n)) \tag{5.9}$$

$$\text{and } f(z_v(x_0)) = f(y_1) = \int_{-\infty}^{\infty}\ldots\int_{-\infty}^{\infty} f(y_1,y_2,\ldots,y_n)\, dy_2\ldots dy_n \tag{5.10}$$

$$= \int_{-\infty}^{\infty}\ldots\int_{-\infty}^{\infty} f(n\cdot y-\sum_{i=2}^{n} z(x_i),z(x_2),\ldots,z(x_n))\, dz(x_2)\ldots dz(x_n) \tag{5.11}$$

Thus determination of block support smu distributions requires knowledge of the n variate distribution of the point grades. This multivariate distribution cannot be inferred from the available data, so the only way to obtain block grade distributions utilizing the above formalism is to make some assumption concerning the multivariate distribution of the point grades[1]. Since a non-parametric solution is sought, no assumptions concerning the multivariate distribution of the data can or will be made here.

---

[1]See Verly (1984) for the solution to this problem under the assumption of multivariate normality.

The cost of remaining non-parametric in this case is that a theoretically consistent solution to this problem cannot be obtained. The non-parametric solutions which will be developed are based on reasonable assumptions[1] which are consistent with observations made on simulated deposits. Although the non-parametric solutions must utilize certain assumptions, this does not imply that parametric techniques are guaranteed to be superior to non-parametric techniques. Parametric techniques are only theoretically consistent given an underlying model, however the model hypothesis may be incorrect in which case theoretical consistency is of no practical importance. Thus in the case of block support recovery estimation, both parametric and non-parametric estimators make assumptions concerning the nature of the data which may not be verified for any given deposit. The choice of the set of assumptions which will be accepted is dependent on both the user and the problem at hand. However, an important piece of information which must be considered before choosing between parametric and non-parametric estimators is that non-parametric solutions are far easier to understand and apply and far less expensive to obtain than parametric solutions.

The following two sections discuss the type of assumptions which can be made and the type of non-parametric estimators which can be derived given these assumptions.

---

[1]Some of these assumptions concern the univariate distribution of the data, hence the solutions are not truly non-parametric. However, the term non-parametric estimator will be used to distinguish between the estimators which will be developed and completely parametric estimators which assume the data follow a particular distribution.

5.2 BLOCK RECOVERIES BASED ON PSEUDO BLOCK DATA

The most straightforward method of obtaining block support recoveries is to define block indicator data; since, if block indicator data were available, the procedure for obtaining block support recoveries would be in every way analogous to the procedure followed to obtain point recoveries from point support indicator data. Unfortunately bulk samples equal in volume and shape to the selective mining unit are extremely rare; therefore, actual block indicator data will never be available in sufficient quantity to be useful. It is possible, however to obtain estimated or pseudo block indicator data from the available point data.

At each sampled point in space a point support indicator random variable can be defined.

$$I(x,zc) = \begin{cases} 1 \text{ if } Z(x) \leq zc \\ 0 \text{ if } Z(x) > zc \end{cases} \qquad (5.12)$$

$$\text{with } E[I(x,zc)] = F(zc)$$

A block support indicator datum, for any given support v, can also be defined at the point x[1].

$$I_v(x,zc) = \begin{cases} 1 \text{ if } Z_v(x) \leq zc \\ 0 \text{ if } Z_v(x) > zc \end{cases} \qquad (5.13)$$

$$\text{with } E[(I_v(x,zc)] = F_v(zc)$$

In general

$$F_v(zc) \neq F(zc)$$

---

[1]The point x is taken as the center of gravity of the volume v.

however there always exists a cutoff zc′, such that

$$F_v(zc) = F(zc')$$

irregardless of the form of the distributions $F_v(zc)$ and $F(zc)$. Because of the equality between $F_v(zc)$ and $F(zc')$, zc′ will be referred to as an equivalent cutoff. Notice that if the exact form of $F_v(zc)$ is known the equivalent cutoffs would be known for all cutoffs of interest zc. Given an equivalent cutoff zc′ a globally unbiased estimator of block support recovered tonnage, at cutoff zc, could be obtained by performing point support indicator or probability kriging at cutoff zc′. The validity of this assertion is shown by the following.

Assume cutoffs zc′ and zc are known such that

$$F(zc') = F_v(zc)$$

$E[\Phi^*(A,zc')] = F(zc')$ for an unbiased estimator

hence $F_v(zc) = E[\Phi^*(A,zc')]$

so $\phi_{ik}^*(A,zc')$ or $\phi_{pk}^*(A,zc')$ are globally unbiased estimators of $\phi_v(A,zc)$

where $\phi_v(A,zc)$ is the local spatial distribution of blocks of size v within panel A.

Unfortunately the form of $F_v(zc)$ is unknown and as has been demonstrated cannot be determined without complete knowledge of the multivariate distribution of the data; thus, the equivalent cutoffs zc′ for any particular cutoff zc are unknown. Although the complete form of $F_v(zc)$ is not known, the mean and variance of the block support grades can be determined. The mean of the block grades is known, as it is

identical to the mean of the point data. The global variance of smus within the deposit can be inferred from the variogram model and Krige's relationship. Krige's relationship concerning the additivity of variances states

$$D^2(O/D) = D^2(v/D) + D^2(O/v)$$

That is, the variance of points within the deposit is the sum of the variance of smus within the deposit and the variance of points within an smu. Since the variance of points within the deposit can be estimated from the available data and the variance of points within an smu can be determined from the variogram model ($D^2(O/v)=\gamma(v,v)$) it is a simple matter to determine an estimate of $D^2(v/D)$.

Given the mean and variance only the shape of the distribution is required to completely define the global distribution of smu grades. Again there is no non-parametric method to theoretically obtain the shape of this distribution so a hypothesis must be invoked. Several permanence of shape hypotheses are available (JH, pg 468) which extrapolate the shape of the block support distribution from the shape of the point support distribution. A permanence of shape hypothesis which is well suited to the problem at hand is the affine correction[1]. The affine correction[2] assumes that:

---

[1]Other permanence of shape hypotheses could be used, however determining the equivalent cutoff would be more difficult. Since there is no theoretical justification for any permanence of shape hypothesis, the simple affine transform will be used as it has proven to provide reasonable results for minimal expenditure of time.

[2]For a discussion of the properties of the affine correction see section 5.4.

$$\frac{zc'-m}{\sigma} = \frac{zc-m_v}{\sigma_v} \tag{5.14}$$

where: zc' is the equivalent cutoff
zc is the cutoff of interest
σ is $\sqrt{D^2(0/D)}$
σ_v is $\sqrt{D^2(v/D)}$
m is the mean of the deposit

Thus the equivalent cutoff, zc', can easily be determined given any cutoff of interest zc.

$$zc' = \frac{\sigma}{\sigma_v} \cdot (zc-m) + m \tag{5.15}$$

Therefore, to determine block recoveries at cutoff zc, one simply performs point support indicator or probability kriging at cutoff zc'.

That is, at each data location a pseudo block indicator datum is defined

$$i_v'(x,zc) = \begin{cases} 1 \text{ if } z(x) \leq zc' \\ 0 \text{ if } z(x) > zc' \end{cases} \tag{5.16}$$

where $i_v'(x,zc)$ is the pseudo block indicator datum for cutoff zc and block v centered on location x.

Performing indicator or probability kriging utilizing these pseudo block indicator data will yield globally unbiased estimates of $\phi_v(A,zc)$.

This method, while globally unbiased, given a correct permanence of shape hypothesis and correct inputs, is rather simplistic as it assumes that the pseudo block indicator data will behave similarly

to the actual block indicator data $i_v(x,zc)$. In fact the spatial correlation of the actual block support indicator data is likely to be different from that of the pseudo block indicator data. Thus, an estimator based on these pseudo block indicator data is likely to be a poor local estimator.

To obtain pseudo block indicator data which more closely mimic the behavior of the actual block indicator data, the pseudo block indicator data can be defined on estimates of block grades at each sampled location. That is, pseudo block indicator data can be defined as

$$i_v'(x,zc) = \begin{cases} 1 \text{ if } z_v^*(x) \leq zc' \\ 0 \text{ if } z_v^*(x) > zc' \end{cases} \qquad (5.17)$$

where $i_v'(x,zc)$ is the pseudo block indicator datum
$z_v^*(x)$ is the estimate of a block support smu grade centered on sampled location x. Normally an ordinary kriging estimate is used as this provides the best estimate.
zc' is an equivalent cutoff.

The equivalent cutoff zc' is utilized since the variance of the estimated block grades is generally not equal to the variance of the true block grades. Hence a permanence of shape hypothesis must be utilized. Again the affine correction will be used; thus, it is assumed that

$$\frac{zc-m_v}{\sigma_v} = \frac{zc'-m_v^*}{\sigma_v^*}$$

where: zc is the cutoff of interest
zc' is the equivalent cutoff
m_v is the mean grade of the data
m_v^* is the mean grade of the estimated block grades

$\sigma_v = \sqrt{D^2(v/D)}$
σ_v^* is the standard deviation of the

estimated block grades $z_v^*(x)$.

Thus the equivalent cutoff can be defined as

$$zc' = \frac{\sigma_v^*}{\sigma_v} \cdot (zc - m_v) + m_v^* \qquad (5.18)$$

Given these equivalent cutoffs, zc', the block recoveries at each cutoff of interest are determined by performing indicator or probability kriging on the pseudo block indicator data $i_v'(x,zc)$.

The advantages of defining pseudo smu indicator data from kriged smu grades rather than point grades are:

1. The pseudo block indicator data defined from the kriged smu grades should better reproduce the spatial variation of true block grades than would pseudo block indicator data defined from point grades.

2. The correction of variance in going from kriged block grades to true block grades is generally less than when going from point grades to block grades. As the magnitude of the variance correction decreases so does the importance of the permanence of shape hypothesis.

5.3 OBTAINING BLOCK RECOVERIES FROM POINT RECOVERY ESTIMATES

In the practice of geostatistics it is common place to obtain the global distribution of block grades by applying some permanence of shape hypothesis to the global distribution of point grades. If such a correction were performed locally, the local block recoveries would easily be obtainable from local point recoveries.

The quantities which are usually required to perform a change of support from the distribution of points within a panel to the distribution of block support smus within a panel are the local variance of points within the panel, $s^2(0/P_i)$; the local variance of smus within the panel, $s^2(v/P_i)$; and the mean panel grade, m. Additionally the

shape of the distribution of smus must be inferred through a permanence of shape hypothesis.

The variance of points within a panel $s^2(0/P_i)$ is a realization of a random variable $S^2(0/P_i)$ which has expectation $D^2(0/P)$. Similarly $s^2(v/P_i)$ is a realization of the random variable $S^2(v/P_i)$ having expectation $D^2(v/P)$. Since these local variances are random variables, they could, in theory, be estimated utilizing a kriging type estimator based on a spatial correlation function of order four. Since the deposits on which this estimator will be used are erratic, it is often difficult to estimate a spatial correlation function of order 2. Therefore the difficulties which would be encountered in attempting to model a spatial correlation function of order 4 in any practical situation are nearly insurmountable. Thus, the local variances for each panel will not be estimated directly and an appropriate approximation must be sought.

One approximation is suggested by the formulation of this problem in the framework of the affine correction[1] permanence of shape hypothesis.

$$\frac{z_v-m}{\sigma_v} = \frac{z-m}{\sigma} \qquad (5.19)$$

where $\sigma_v^2 = s^2(v/P_i)$
$\sigma^2 = s^2(0/P_i)$
z_v is the cutoff of interest on blocks
z is a cutoff applied to the point distribution

Under this hypothesis of permanence of shape

$$z = \frac{\sigma}{\sigma_v}\cdot(z_v-m) + m. \qquad (5.20)$$

---

[1]See section 5.4 for a discussion of the affine correction.

The only unknown in this formulation is the ratio σ/σ_v. If this ratio is assumed constant[1] and equal to the expectations of the numerator and denominator, the affine correction and hence the local block support distributions would be completely defined.

5.4 THE AFFINE CORRECTION

In both methods which have been proposed to obtain block support recoveries a permanence of shape hypothesis is made. In particular the affine correction of variance is utilized. The assumption of the affine correction is that in correcting the variance of a variable Z to obtain a variable Y is

$$Y = \frac{\sigma_y}{\sigma_z} \cdot (Z - m_z) + m_y \qquad (5.21)$$

where: Z is the initial variable
Y is the corrected variable
σ_y is the standard deviation of Y
σ_z is the standard deviation of Z
m_z is the mean of Z
m_y is the mean of Y

Thus knowing the distribution of Z, the distribution of Y is easily obtained

$$F_y(y) = Pr(Y<y) = Pr(Z<z) = F_z(z)$$

where:

$$z = \frac{\sigma_z}{\sigma_y} \cdot (y - m_y) + m_z \qquad (5.22)$$

---

[1]The validity of this assumption is discussed in section 5.6.1.1.

An important feature of this particular permanence of shape hypothesis is that all the physical features (i.e. modes, secondary modes, and spikes) present in the histogram of Z will also be present in the histogram of Y. Thus the histograms of Z and Y will have similar shapes. This feature can be a drawback when obtaining a block histogram from a point histogram. Since block grades can be seen as an average of point grades and therefore influenced by the central limit theorem, it is unlikely that block grade distributions will exhibit large spikes as frequently observed in point grade distributions. Hence the distribution produced by the affine correction is generally not reliable for cutoffs near the spike. A second potentially troublesome feature of the affine correction is that when the ratio σ_y/σ_z is greater than 1 there is a chance that negative Y values will occur.

5.5 SMU GRADE DATA BASE

As at most other operating mines, true smu grade data is not available at the Bell Mine. Therefore true block grades must be determined through the averaging of point grades. As mentioned previously, there are an average of 67 blast holes or point assays per 100 foot panel. While this number of data is large enough to determine a true distribution of points within a 100 foot panel, it is much too small to determine a distribution of true block grades. To see this, consider attempting to define the distribution of 25 ft. smus within a 100 foot panel. Each of the sixteen 25 ft. smu grades would be defined by the average of approximately 4 point grades and the distribution of smus would be determined from these 16 smu estimates. There are several

difficulties with such a determination of the true smu distributions. First, the average of four irregularly spaced data does not yield an estimate of smu grade which can be assumed to be perfect. Second the distribution of 16 estimated 25 ft. smu grades within a panel is not a convincing estimate of the true distribution of smus within a panel. Third, the actual smu used at the Bell Mine ranges from 12 to 15 feet. The distribution of 25 ft smu grades within a panel cannot be taken as equal to the distribution of 12 to 15 foot smu grades. Therefore if the study is to address the actual problem met at the mine, 25 ft smu grades are not acceptable. To reproduce the actual situation at the Bell Mine, one could attempt to determine the grades of smus of smaller volume using the available data, however the true grade of each 12.5 foot smu cannot accurately be defined from the approximately 67 data per panel as there is an average of slightly greater than one datum per smu. Obviously the true smu grade cannot be determined from a single datum. Therefore to determine the true distributions of smu grades for smu sizes which are similar to those used in practice, more data must be obtained. Since actual blast hole data are available only on a 12 foot grid, more point data must be generated if the distribution of 12 to 15 ft smu grades within a panel is to be determined. This additional data will be generated through the technique of conditional simulation. Averaging of the simulated data located within an smu will be utilized to determine the smu grade. The simulated smu grades determined in this manner are not intended to be equal to the true smu grades, rather the simulated smu grades are assumed to closely mimic the local behavior of the true smu grades for the purposes of testing block recovery estimators.

5.5.1 Conditional Simulation

The additional point grade data which will be generated to define smu grades must be located on a sufficiently dense grid to allow the accurate determination of smu grades. For this study, the smu size which is chosen is 12.5 ft. by 12.5 ft. as this size is close to the actual size smu utilized at the Bell Mine and an even number of this size smu fit within a 100 ft by 100 ft. panel. It is felt that the average of nine point data will give an accurate determination of an smu grade; hence, the envisioned conditional simulation will consist of point data on a regular 4.167 ft. grid (see figure 111).

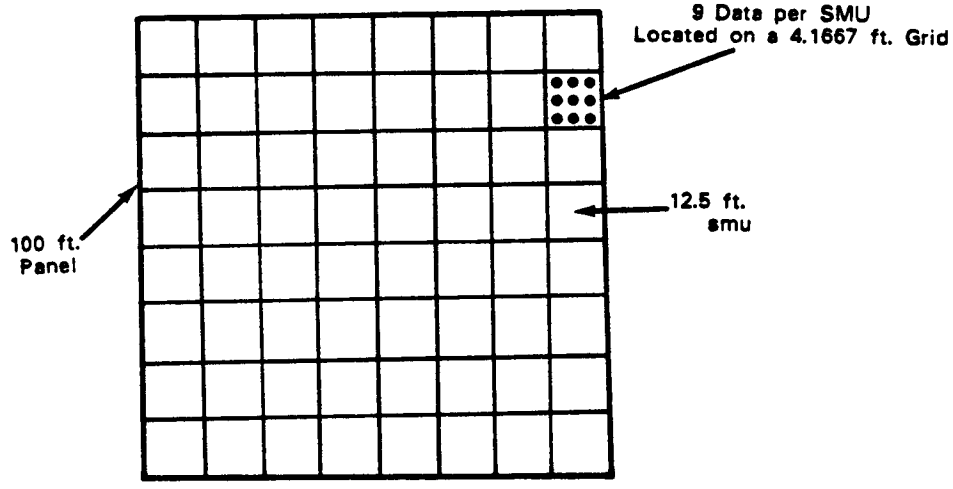

Figure 111: Representation of the Conditional Simulation

The technique of conditional simulation is well described by Journel and Huijbregts (1978) and Luster (1984) so the details of the technique will not be discussed here; rather, only the steps followed and the final results obtained will be given.

The steps of a conditional simulation are as follows:

1. Gaussian transformation of the data.
2. Variography on the transformed data.
3. Simulate gaussian values with a correlation structure equal to the modelled variogram.
4. Condition the simulation to the transformed data.
5. Back transform the simulated values.

Each step will be discussed individually.

5.5.1.1 Gaussian Transform of the Data

This conditional simulation will be performed bench by bench. That is a separate simulation is performed for each of the five benches. A three dimensional simulation of the deposit was not performed because all block recovery estimation as all point recovery estimation will be two dimensional. Examine, for example, the 7645 bench. This bench contains 1,694 blasthole assays. To begin the simulation procedure, these 1,694 data are transformed through a simple normal scores transform so that the data will follow a normal distribution with mean 0 and variance 1. This normal scores transform must be a one to one transform, hence before transformation any group of data with exactly equal values must be treated so that no two values are exactly equal. The treatment procedure, discussed in sec 3.3.1, adds a small amount to each of the data with equal values so that no two values are exactly equal.

Given this set of N(0,1) data, the next step is variography.

5.5.1.2 Variography

The variography performed on the transformed data is the standard variography of grade:

$$\gamma_y(h) = \frac{1}{2} \bullet E[(Y(x+h)-Y(x))^2] \qquad (5.23)$$

where Y(x) is the normal score transform of Z(x)
Y(x) → N(0,1)

This variogram can be modelled by any positive definite variogram model, however a circular variogram model is utilized as this covariance model is, as will be shown, convenient for the purpose of simulation. The variogram of Y(x) for the 7645 bench and its model are shown in figure 112.

5.5.1.3 Nonconditional Simulation of Values

Simulation of values with a given covariance or variogram model can be accomplished in a large number of ways (Luster, 1984). The simplest method, conceptually, is to move a geometric filter over a grid of random numbers. The filter is moved over the grid such that each of the random values is, in turn, located at its center of mass. As the filter is moved the point located at the center of mass is replaced by the average of all data found within the boundary of the filter.

Several common types of correlation structures can be obtained through this method using simple geometric shapes as filters. For instance, if a line of length L is passed over a column of random numbers, the resulting values will follow a linear transition variogram model.

$$\gamma(h) = \sigma^2 \bullet (h/L) \qquad \text{for } h \leq L$$

$$\gamma(h) = \sigma^2 \qquad \text{for } h > L$$

where σ^2 is a constant proportional to the variance of the data
L is the length of the filter

If a circular filter is moved over a two dimensional field of random numbers, the variogram of the resulting simulated values will follow a circular model.

$$\gamma(r) = [2C/(\pi a)^2][r\sqrt{a^2-r^2} + a^2\text{Arcsin}(r/a)] \text{ for } r \leq a$$
$$\gamma(r) = C \qquad \text{for } r > a$$

where: a is the diameter of the circular filter
C is the variance of the random data

Finally if a spherical filter is moved over a three dimensional field of random numbers, the variogram of the resulting values will follow a spherical model.

$$\gamma(h) = C\bullet((1.5\bullet(h/a)-.5\bullet(h/a)^3) \text{ for } h \leq a$$

$$\gamma(h) = C \qquad \text{for } h > a$$

where a is the diameter of the sphere

Since this method of reproducing a given variogram model is easily programmed, it was used on each of the five benches. That is, a circular filter of diameter equal to the required range was moved over each node of the grid of points to be simulated. For the 7645 bench, a circle of 120 ft. was moved over a grid of 21,875 points located on a regular 4.167 ft. grid. The resulting nonconditional simulation follows a normal distribution (due to the central limit theorem) which is standardized to mean 0 and variance 1.

The simulation of the nugget effect is accomplished by drawing a random normal number for each node on the grid. These uncorrelated

random numbers are also standardized to mean 0 and variance 1. The nugget effect structure is then combined with the structure having a 120 ft. range to yield the nonconditional simulated values.

$$Y_{nc}(x) = \sqrt{.18} \cdot Y_{nug}(x) + \sqrt{.70} \cdot Y_1(x) \qquad (5.24)$$

where the values .70 and .18 are the coefficients of the two structures Y_1 and Y_{nug} found in the model of the variogram of the transformed grades for the 7645 bench (see figure 112).

The variogram of these 21,875 nonconditionally simulated values is given is figure 112. The variogram of the simulated values is less than the input variogram model at all distances, however the discrepancy is not too large.

5.5.1.4 Conditioning of the Simulation

Conditioning of the simulation imparts the local characteristics of the data set, such as regions of high and low grades, to the simulation. The major property of a conditioned simulation is that at each data location

$$y_{sc}(x_\alpha) = y(x_\alpha) \qquad (5.25)$$

where $y(x)$ is the actual data value at point x
$y_{sc}(x)$ is the conditionally simulated value at point x

Conditioning is accomplished utilizing two sets of kriging estimators

$$y_{kd}^*(x_0) = \sum_{\alpha=1}^{n} \lambda_\alpha \cdot y(x_\alpha)$$

$$y_{ks}^*(x_0) = \sum_{\alpha=1}^{n} \lambda_\alpha \cdot y_s(x_\alpha) \qquad (5.26)$$

where $y(x_\alpha)$ is the datum at x_α
$y_s(x_\alpha)$ is the nonconditionally simulated value at the same location x_α

The conditionally simulated value is then defined as:

$$y_{cs}^*(x) = y_{kd}^*(x) + [y_s(x) - y_{ks}^*(x)] \qquad (5.27)$$

whenever a grid location x is exactly equal to a data location x_α

$$y_{kd}^*(x_\alpha) = y(x_\alpha)$$
$$y_{ks}^*(x_\alpha) = y_s(x_\alpha)$$

so

$$y_{cs}^*(x_\alpha) = y(x_\alpha)$$

Thus the conditional simulation passes through the data values.

In the case of the Bell Mine simulation, conditioning was performed only for those points on the non-conditionally simulated grid which were located within one of the 119 previously defined panels. Thus as portions of the nonconditionally simulated grid are not found within defined panels there are less conditionally simulated values than nonconditionally simulated values. The variogram of the conditionally simulated values is given in figure 112. Notice that the variogram of the conditional simulation is closer to the variogram model of the conditioning data than the variogram of the nonconditionally simulated values for short distances. Thus the conditioning to the data has improved the correspondence between the variogram of the transformed data and the variogram of the simulated values.

5.5.1.5 Back Transform

For the conditional simulation to be useful, it must have the same histogram as the original blast hole assays. Therefore, the normally distributed conditionally simulated values $y_{cs}(x)$ must be transformed to conditionally simulated values $z_{cs}(x)$; where $z_{cs}(x)$ is conditioned to the original data $z(x_\alpha)$.

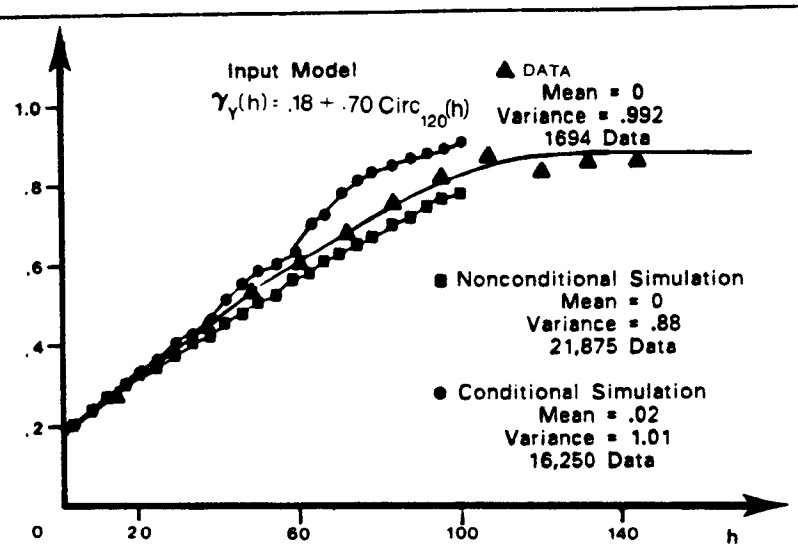

Figure 112: Variograms of the Conditional and Non-Conditional Simulated Values for the 7645 Bench

This back transformation is accomplished by a simple linear interpolation. Three sets of values are used to perform the interpolation; namely

1. z(x), the original untransformed data
2. y(x), the gaussian transform of z(x)
3. $y_{cs}(x)$, the conditionally simulated values

The three sets of data, z(x), y(x), and $y_{cs}(x)$, are sorted in ascending order. The z(x) and y(x) values are termed bounds. For each $y_{cs}(x_\alpha)$ value, the two y bounds which straddle $y_{cs}(x_\alpha)$ are found. The percentage distance between $y_{cs}(x_\alpha)$ and the lower bound is calculated i.e.

$$D = \frac{y_{cs}(x_\alpha) - y_{b1}}{y_{b2} - y_{b1}} \qquad (5.28)$$

where y_{b2} is the upper bound
y_{b1} is the lower bound

D is the percentage distance

The conditionally simulated z value, $z_{cs}(x_\alpha)$, is then defined as:

$$z_{cs}(x_\alpha) = z_{b1} + D*(z_{b2}-z_{b1})$$

where z_{b1} and z_{b2} are the bounds corresponding to y_{b1} and y_{b2}

5.5.1.6 Properties of the Simulation

Performing the back transform on all five benches, resulted in a conditional simulation containing a total of 75,000 point grade values. The histogram of these values and the histogram of the 7979 original conditioning data are shown in figure 113. As a further check of the accuracy of the simulation, the variograms of the simulation and the original data are given for each of the five benches which comprise the Bell Mine case study (figures 114 and 115).

To simulate smu grades for 12.5 ft smus, the 9 conditionally simulated values falling within each smu are averaged. The histogram of these 7,680 simulated 12.5 ft smu grades are given in figure 116.

Given these smu grades, the distribution of smus within a panel can be determined. These local distributions obtained from the simulation are assumed to be the true distributions of smus within each panel. Using the previously discussed methods, these local distributions will be estimated.

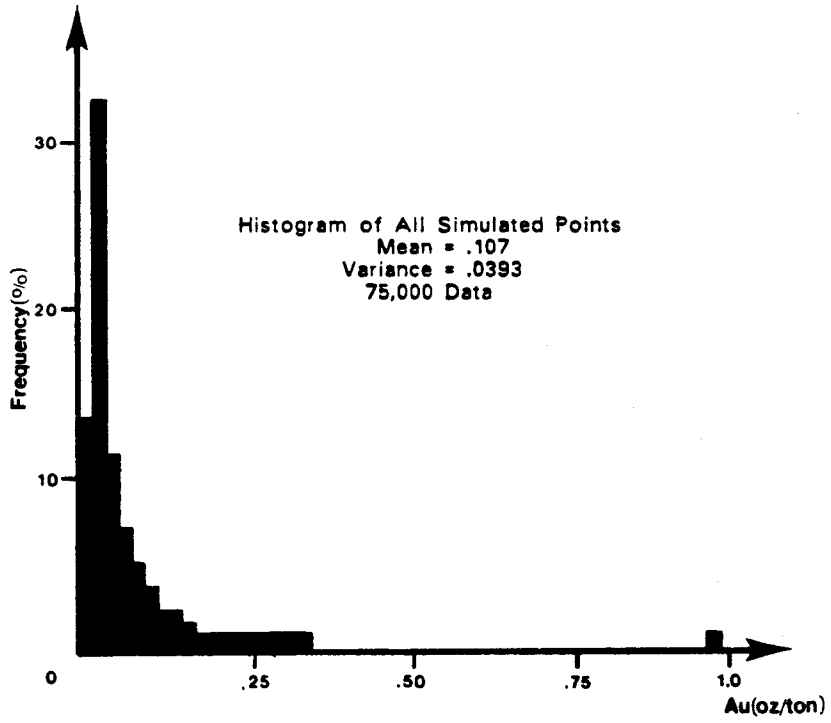

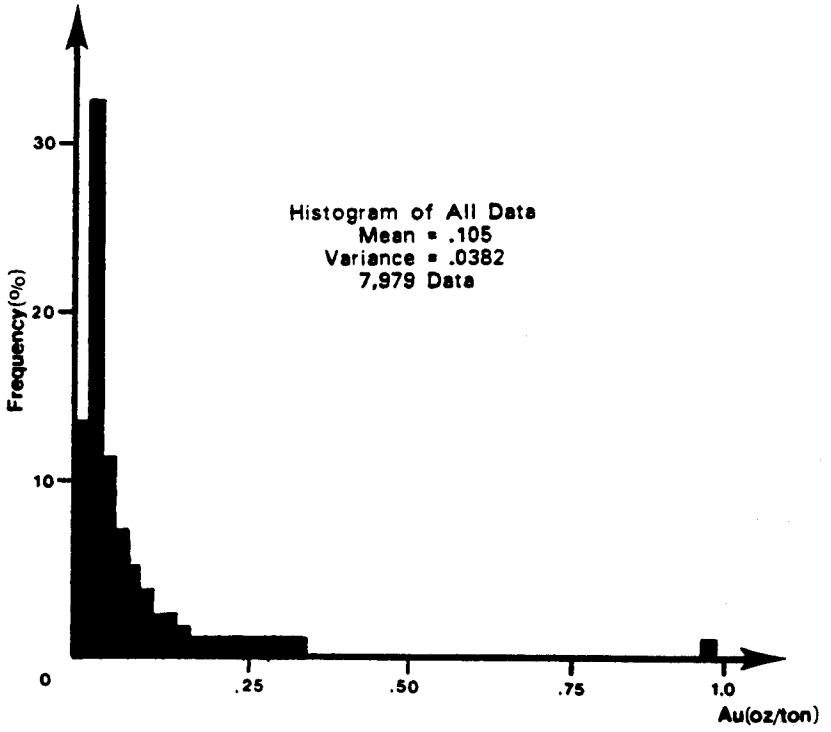

Figure 113: Histograms of the Simulated and Actual Values

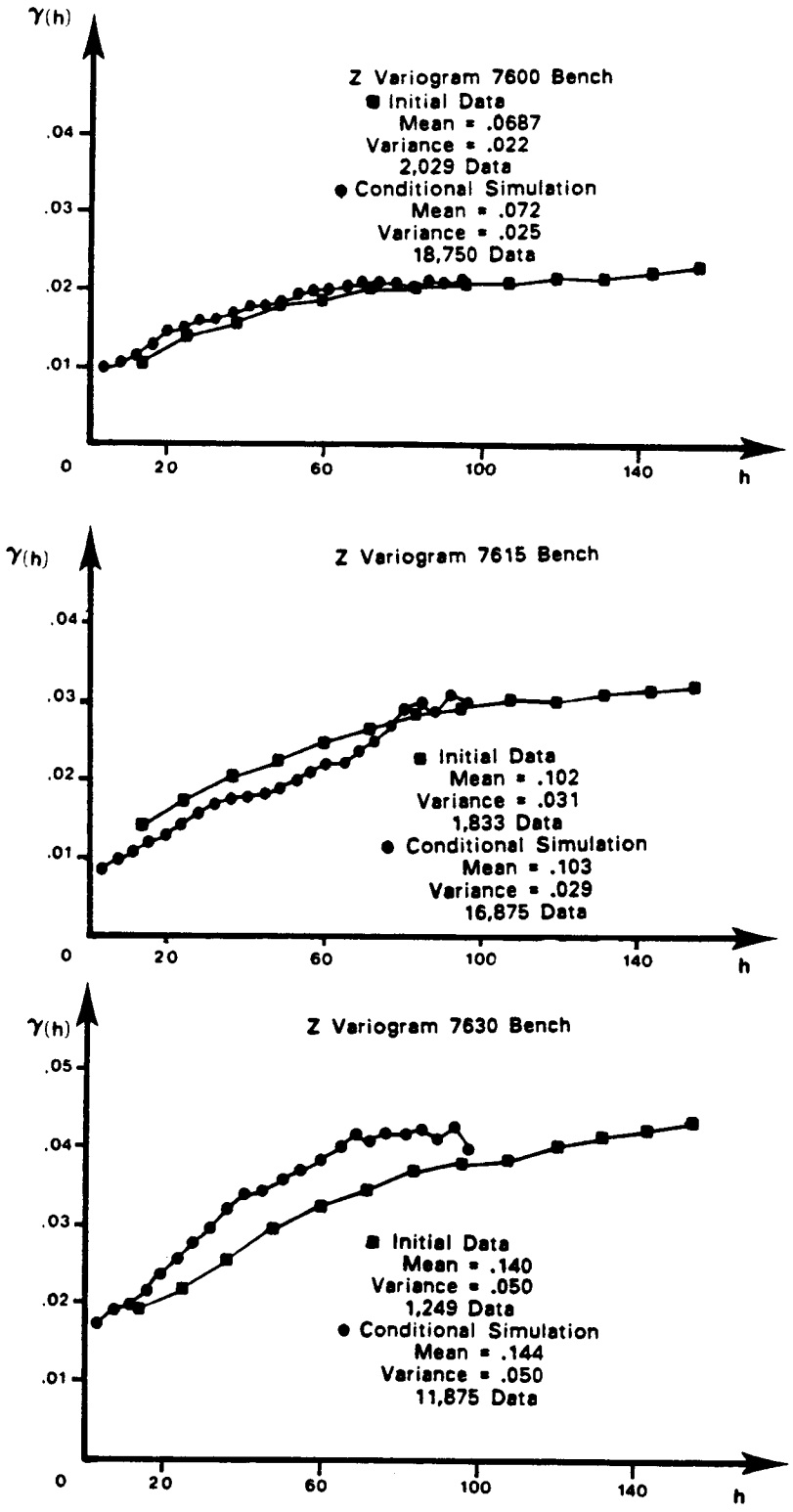

Figure 114: Variograms of the Simulation for the 7600, 7615, and 7630 Benches

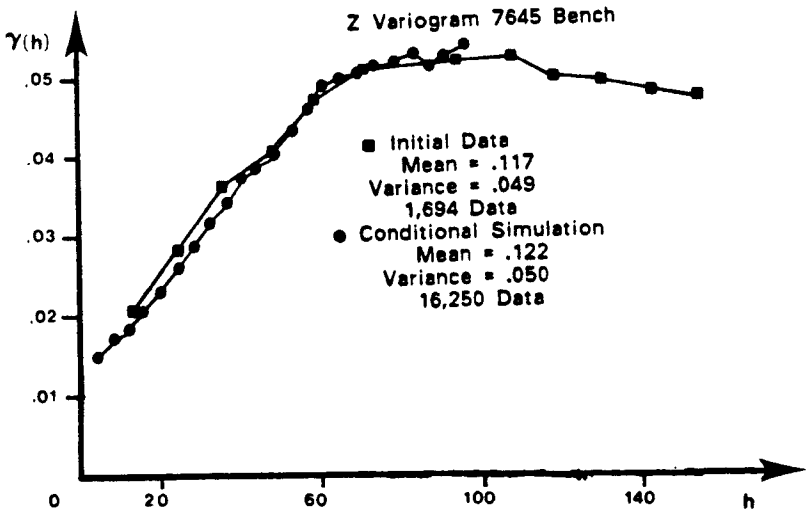

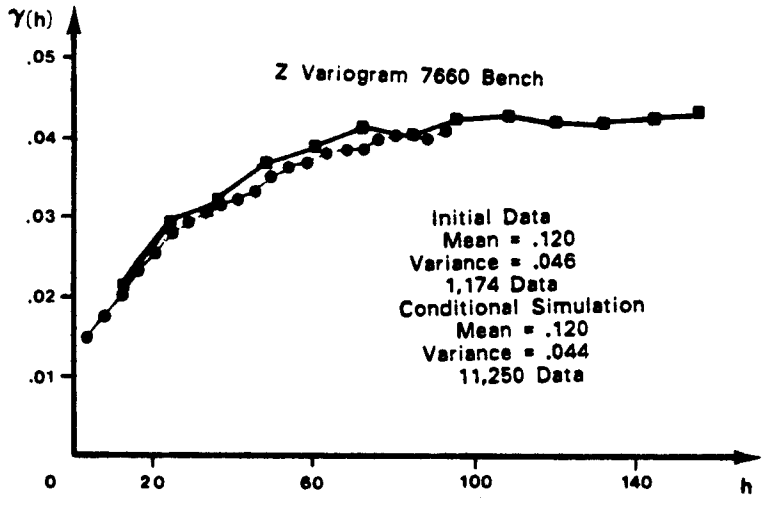

Figure 115: Variograms of the Simulation for the 7645 and 7660 Benches

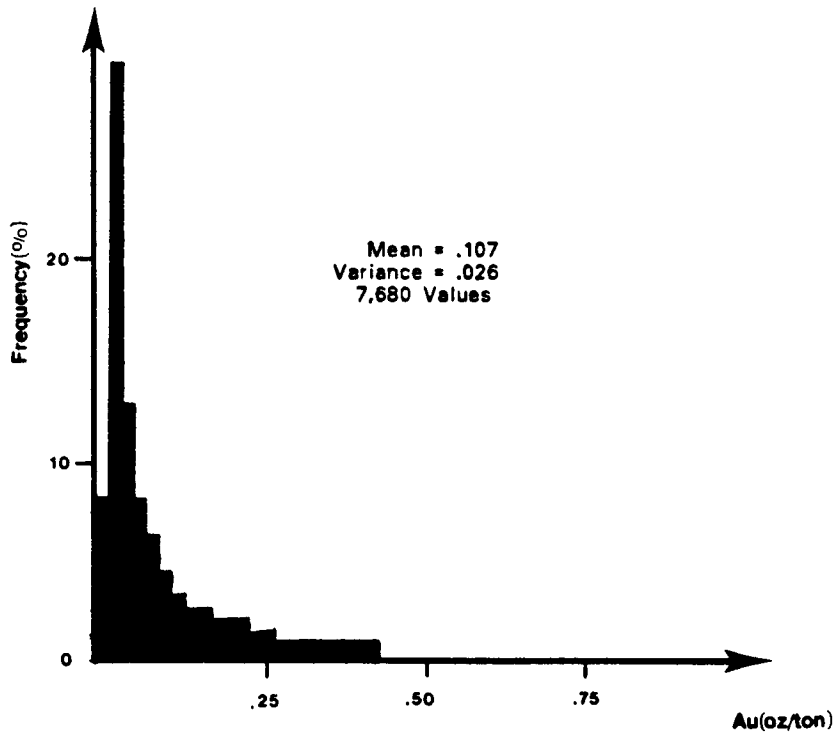

Figure 116: Histogram of the Simulated 12.5 ft SMU Grades

5.6 ESTIMATION OF BLOCK SUPPORT RECOVERIES AT THE BELL MINE

Block support smu recoveries will be estimated for the previously defined 119 panels of the Bell Mine. The estimated recoveries will be compared to the "true" recoveries obtained from the conditional simulation of the 119 panels. As in the point estimation case study, the estimators will be applied at 9 cutoffs. These cutoffs correspond to the deciles of the simulated true 12.5 ft smu grade distribution.

In the sections concerning point recoveries, various amounts of data were used to estimate the point recoveries. From these results, some

useful information concerning the amount of information required to obtain accurate estimates was obtained. As the techniques used to estimate block recoveries are similar to or based on the point estimation techniques, any conclusions drawn on the number of data required to accurately estimate point recoveries should also be valid for estimating block recoveries. Therefore only one set of data will be used to estimate block recoveries. The data set chosen is that of campaign #2 since it represents the midrange, in terms of data density, of the data configurations examined.

Ideally this study would consider several different smu sizes to obtain an idea of how the two block recovery estimation techniques perform over a range of different smu sizes. However since 100 ft. panels are considered and there are certain requirements for both the number of point grades within an smu and the number of smus within a panel, the number of feasible smu sizes is limited. For instance, if an smu of 25 ft x 25 ft were considered, there would be more than enough simulated values within an smu to accurately determine the smu grade however the distribution of smus within the panel would not be accurately determined from these smu grades as there are only sixteen such 25 ft smus within each 100 ft panel. The converse problem is encountered if very small smus are chosen, as the grades of such small smus would be poorly defined.

Given the available simulation the only satisfactory size smu is 12.5 ft x 12.5 ft. This size smu contains nine simulated data which are used to determine the mean grade of each smu and there are 64 such smus within each panel to define the distribution of smus within a 100 foot

panel. The average smu size actually used at the Bell Mine is very close to 12.5 ft in horizontal extent. Therefore a two dimensional estimation using the campaign #2 data set to estimate 12.5 ft. smu recoveries should be similar to the real life problem encountered at the Bell Mine; that is, estimation of smu recoveries for smus between 12 and 15 ft in horizontal extent using three dimensional data on a 100 foot grid.

5.6.1 Estimation of SMU Recoveries Utilizing Point Recoveries

Perhaps the simplest method of obtaining block smu recoveries is, as previously discussed, to correct each estimated distribution of points within a panel for the change in support to obtain the distribution of smus. As discussed, this support correction should be customized for each panel, however this is not possible so the values which would be used in a global change of support are applied locally.

5.6.1.1 Steps Required

An important step in determining block recoveries by this method is the determination of the point recoveries. The subject of point recoveries for the Bell Mine was discussed at length in chapter 4. Since point recovery estimation has already been performed on this deposit, no additional work is required for this step. The point recovery estimates which will be used are those obtained by the PK estimator utilizing the campaign #2 data.

Once the point recovery estimates are available, the parameters required to perform the change of support must be determined. Two

variances; namely, the dispersion variance of points within a 100 ft panel and the dispersion variance of 12.5 ft selective mining units within a 100 ft panel are required. Both of these variances are easily determined from the model of the variogram of grade.

$$D^2(0/100) = \bar{\gamma}(100,100)$$

$$D^2(12.5/100) = \bar{\gamma}(100,100) - \bar{\gamma}(12.5,12.5)$$

For the campaign #2 data set the model (see sec 4.4.1) for the variogram of grade is:

$$\gamma(h) = .006 + .019\ Sph_{65}(h) + .0155\ Sph_{175}(h)$$

hence the estimated dispersion variances are

$$D^{*2}(0/100) = .02794$$
$$D^{*2}(12.5/100) = .01904$$

These values can be compared with the true values obtained using all 75,000 simulated values

$$D^2(0/100) = .0294$$
$$D^2(12.5/100) = .01607$$

Notice that $\bar{\gamma}(12.5,12.5)$ determined from the campaign #2 variogram model, .0089, is much smaller than the true value, .013. This implies that the modelled nugget effect is lower than the true value. The effects of this inaccuracy in the modelling of the variogram will be examined by performing the local change of support twice. The first attempt will utilize the dispersion variances determined by the experimental variogram model while the second attempt will utilize the

true dispersion variances. In this way, some idea of the sensitivity of the method to incorrect variogram modelling will be obtained.

Once the global dispersion variances are determined, the next step is to perform the local change of support for each panel. This change of support, accomplished utilizing the affine transform shape hypothesis, can be seen as determining the cutoff which when applied to the local point distribution yields the local tonnage recovery for block support smus. According to the affine transform assumption

$$\frac{z_v - m}{\sigma_v} = \frac{z - m}{\sigma} \qquad (5.29)$$

or for any particular cutoff of interest z_v

$$z = \frac{\sigma}{\sigma_v} \cdot (z_v - m) + m$$

where z_v is the block recovery cutoff of interest
z is the cutoff which is applied to the point distribution to yield the block recovery

$\sigma_v = \sqrt{D^{*2}(12.5/100)} = .138$

$\sigma = \sqrt{D^{*2}(0/100)} = .167$

$\sigma/\sigma_v = 1.211$ compared to the true value of 1.35

m panel mean determined by ordinary kriging

Thus for any cutoff, z_v, for which block recoveries are required, a cutoff z can be determined. Applying the cutoff, z, to the local point distribution will yield an estimate of the local block support smu recovery at cutoff z_v.

In determining this cutoff z it is assumed that the ratio σ/σ_v is constant for all panels. Since the deposit has been conditionally simulated, the validity of this assumption can be examined. A histogram of the ratio of the two local standard deviations s(0/100) and

$s(12.5/100)$ is given in figure 117 (recall $E[s^2(0/100)]=D^2(0/100)$). Notice the symmetric shape of the distribution and the low coefficient of variation, .17. This low coefficient of variation indicates that this ratio is not highly variable for this deposit so that taking this ratio as constant is an acceptable assumption. Note however that it is not acceptable to assume that either of the two local variances, $s^2(0/100)$ and $s^2(12.5/100)$, is constant throughout the deposit as both of these variables are highly variable with coefficients of variation of approximately 1.5 (figure 118). Thus while it is not acceptable to assume that either of the dispersion variances are constant over the deposit it is reasonable to assume that the ratio of these two variances is constant.

Assuming a constant ratio of variances throughout the deposit, the cutoff z which will be applied to the estimated distribution of point grades can easily be determined for a cutoff of interest z_v. Since the point distribution is calculated for only a finite number of cutoffs zc_i, it is unlikely that the cutoff z for which the tonnage recovery must be obtained is exactly equal to any cutoff zc_i. Hence some type of interpolation must be performed to determine the tonnage recovered at cutoff z. For this deposit, a linear interpolation was used to determine the recovered tonnage of 12.5 ft. smu grades.

$$T_b = (z-zc_i)\bullet(T_i-T_{i+1})/(zc_{i+1}-zc_i) + T_i \qquad (5.30)$$

where: z is the cutoff given by the affine transform
zc_i and zc_{i+1} are cutoffs nearest to z for which tonnage estimates exist.
T_{i+1} and T_i are the point tonnage recoveries for cutoffs zc_{i+1} and zc_i
T_b is the block support tonnage recovered for cutoff z_v

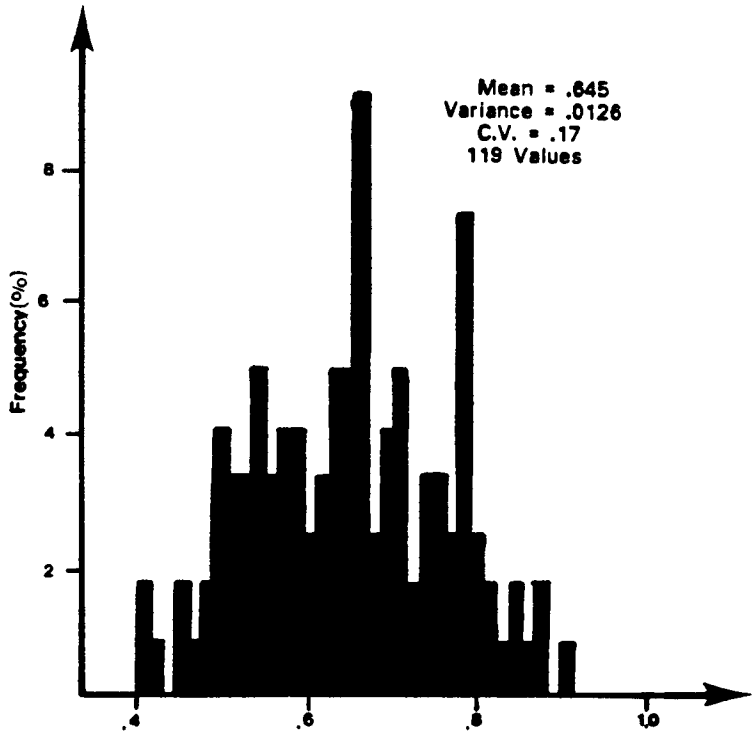

Figure 117: Ratio of the Local Standard Deviations s(0/100) and s(12.5/100)

Using the affine transform and the above relation, tonnage recoveries can be calculated fairly easily for any size smu once the point estimates are available. The only remaining step is the determination of the quantity of metal recovered.

The quantity of metal recovered or block support will be determined using the same approach as used in determining the quantity of metal for point support recoveries. Recall, (sec 2.8) that the quantity of metal can be determined from the estimated tonnages through the following relationship.

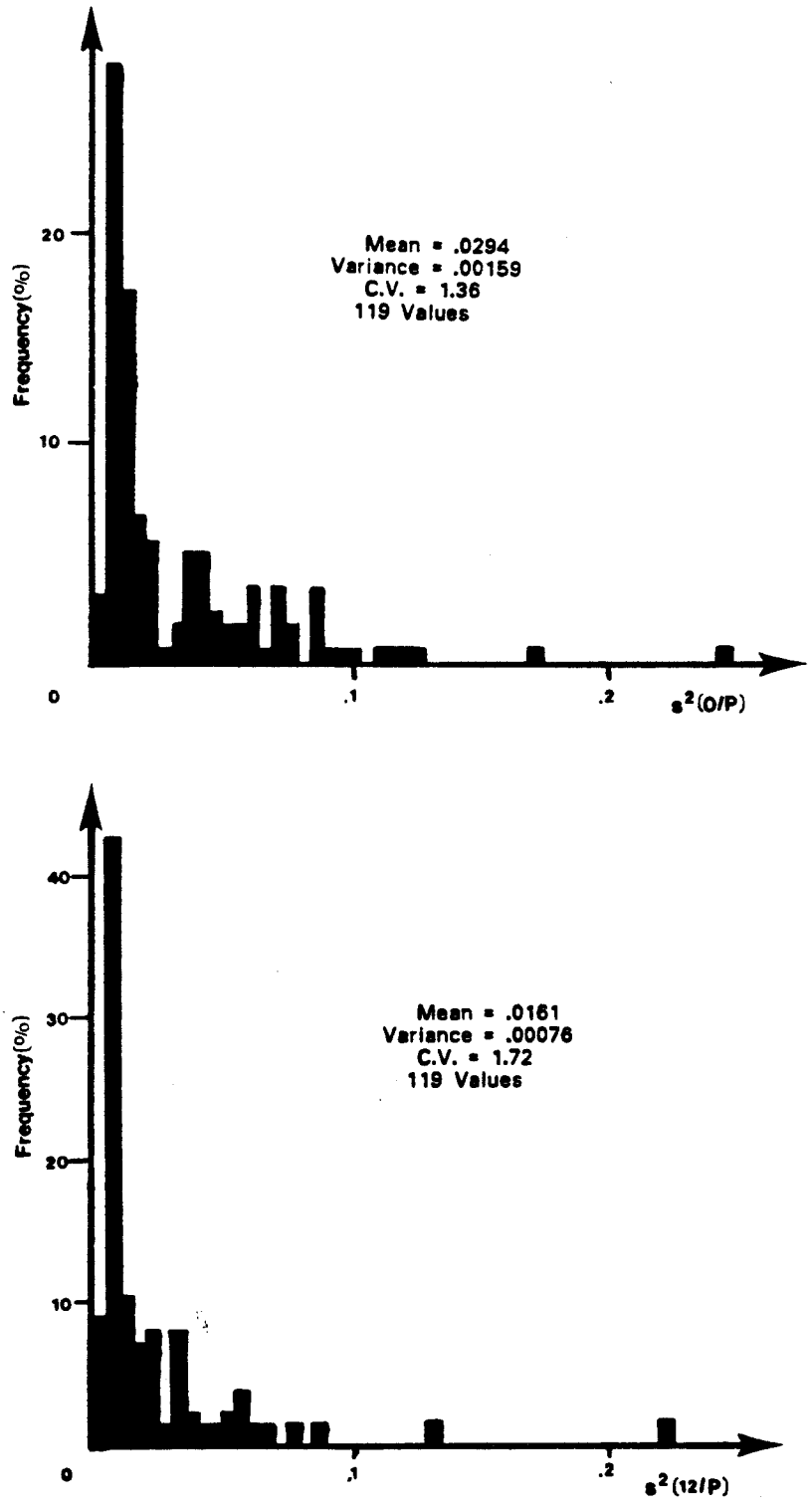

Figure 118: Histograms of Local Dispersion Variances

$$Q(z_i) = \sum_{k=i}^{nc} (T_k - T_{k+1}) \cdot c_k \qquad (5.31)$$

where c_k is some measure of central tendency for the material between cutoffs zc_k and zc_{k+1}
T_k is the tonnage recovered at cutoff k.

A similar relationship is available for block recoveries

$$Q_b(z_i) = \sum_{k=i}^{nc} (T_{bk} - T_{bk+1}) \cdot c_k \qquad (5.32)$$

The difficulty with evaluating this equation is that there are no block data, so the c_k values cannot be calculated directly from a mean of the available data. To correct this situation or in other words to obtain some block data from which a class mean can be obtained, the available point data will be transformed to create pseudo block data from which a class mean can be obtained. Again the affine transform is used.

$$z_b = \frac{\sigma_b}{\sigma} \cdot (z-m) + m$$

where $\sigma_b = \sqrt{\overline{D^2(12.5/D)}}$

$\sigma = \sqrt{\overline{D^2(0/D)}}$
m = mean grade of the deposit
z = point grade
z_b = pseudo block grade

Given these z_b grades, the average of the z_b grades between cutoffs of interest is found to determine the value c_k. With knowledge of these c_k values the block quantity of metal can be determined.

A summary of the steps required to determine recoverable reserves on block support utilizing the recoverable reserves on point support follows.

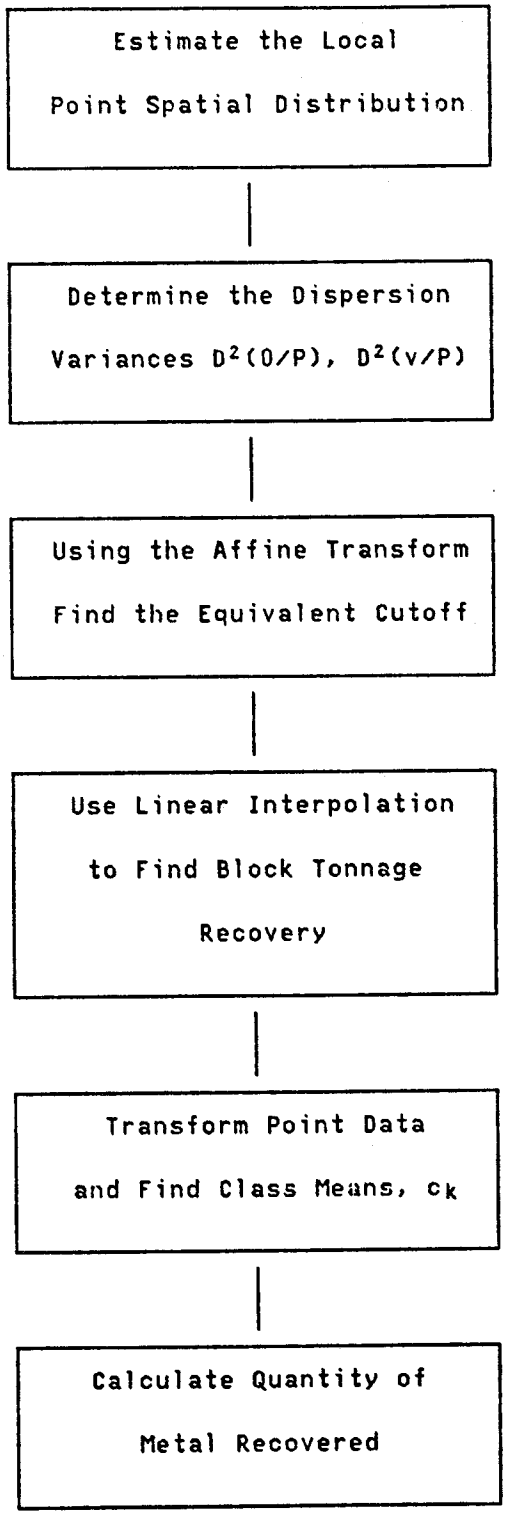

Steps Required to Obtain Estimated Block Recoveries From Estimated Point Recoveries

5.6.2 Estimating Block Recoveries Using Pseudo Block Indicator Data

The premise behind this approach to the problem is that if block indicator data were available the block recoveries could be obtained in a straightforward manner. Therefore the problem is to determine, using appropriate assumptions, block indicator data.

5.6.2.1 Obtaining Pseudo Block Indicator Data

The basic step of this approach is to obtain a kriged smu grade centered on each datum location. These kriged data, after correction for smoothing, will be transformed into pseudo block indicator data using the equivalent cutoff methodology. Given the pseudo block indicator data, recoveries are calculated as in the case of point support smus.

The first step in this approach is to perform ordinary kriging of an smu size block centered at each datum location. This kriging was performed on the 313 data locations of campaign #2 using the initial grade variogram model (sec 4.4.1) to yield 313 kriged 12.5 ft x 12.5 ft smu grades (fig 119). The mean of these values is .107 oz/ton and the variance is .0277 $(oz/ton)^2$.

The variance of these kriged smu grades is generally less than the true variance of 12.5 ft smu grades since kriging is generally a smooth estimator. Hence the kriged smu grades cannot be used to define smu support indicator data without correction for this smoothing. Fortunately an estimate of the true global variance of smu grades is available from Krige's variance relation (sec 5.2). For the campaign #2 data set of data the best estimate of $D^2(12.5/D)$ is

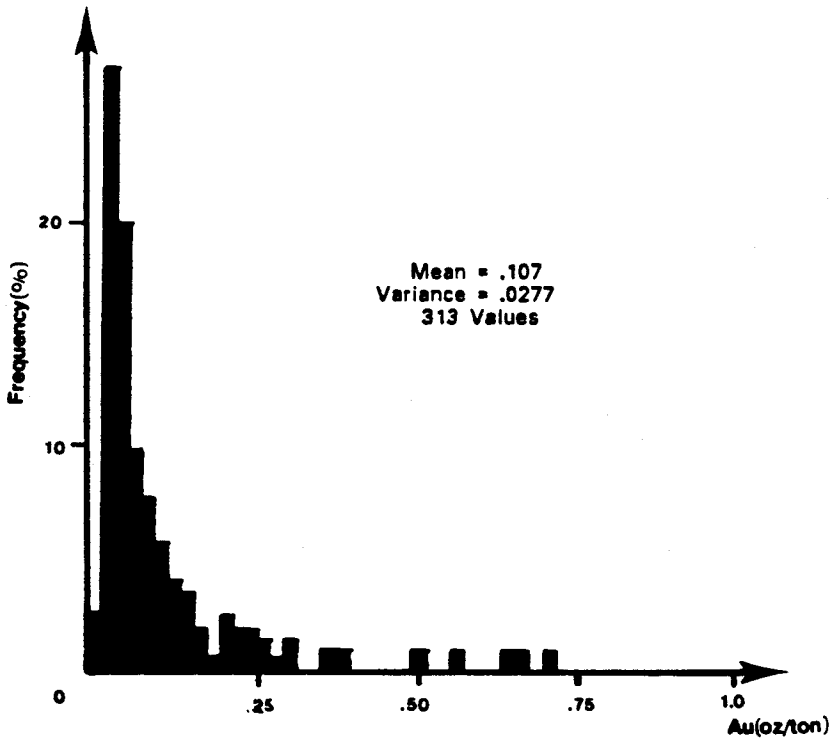

Figure 119: Histogram of Estimated 12.5 ft. SMU Grades Centered on Initial Point Data Locations

$$D^2(12.5/D) = D^2(0/D) - \bar{\gamma}(12.5,12.5)$$
$$= .0416 - .0089$$
$$= .0327$$

This compares with the actual variance of 12.5 ft smu grades within the deposit, .026. With this estimate of the variance of smus within the deposit, equivalent cutoffs based on the affine transform permanence of shape hypothesis can be defined.

$$zc' = \frac{\sqrt{D_k{}^2 * (v/D)}}{\sqrt{D^2(v/D)}} \cdot (zc-m) + m \qquad (5.33)$$

where zc' is the equivalent cutoff

zc is the cutoff of interest
m is the deposit mean = .107
$D_k^{*2}(v/D)$ is the variance of kriged smu values =.0277
$D^2(v/D)$ is the variance of smu grades =.0327
obtained from Krige's relationship.

Using this relationship yields the equivalent cutoffs shown in table 15.

TABLE 15

Equivalent Cutoffs Used to Define Pseudo Block Indicator Data

Cutoff of Interest (oz/ton)	Equivalent Cutoffs (oz/ton)
.004	.012
.008	.016
.015	.022
.025	.032
.041	.046
.066	.069
.105	.105
.174	.169
.311	.295

Pseudo block indicator data are determined for each data location by applying the equivalent cutoffs to the kriged grades. Indicator and cross variograms are then calculated on the pseudo block indicator data. These variograms show longer ranges than the point indicator variogram models which indicates that the block indicator data are more highly correlated than the point indicator data. The block indicator and cross variograms are not shown, however, as, besides the longer range, the block indicator variograms are similar to the point indicator variograms.

Given these indicator and cross variograms, probability kriging is performed on the 100 ft panels utilizing the pseudo indicator data for each equivalent cutoff to yield the tonnage recovery estimates. The estimates obtained are then attributed to the cutoffs of interest.

Quantity of metal estimation is accomplished in the same manner as presented in section 5.5.1.1. The class mean values, c_k, are obtained from an average of the corrected kriged smu data falling between cutoffs of interest z_k and z_{k+1}. These values are then utilized to determine the recovered quantity of metal.

A summary of the steps involved in determining block recoveries by this method follows.

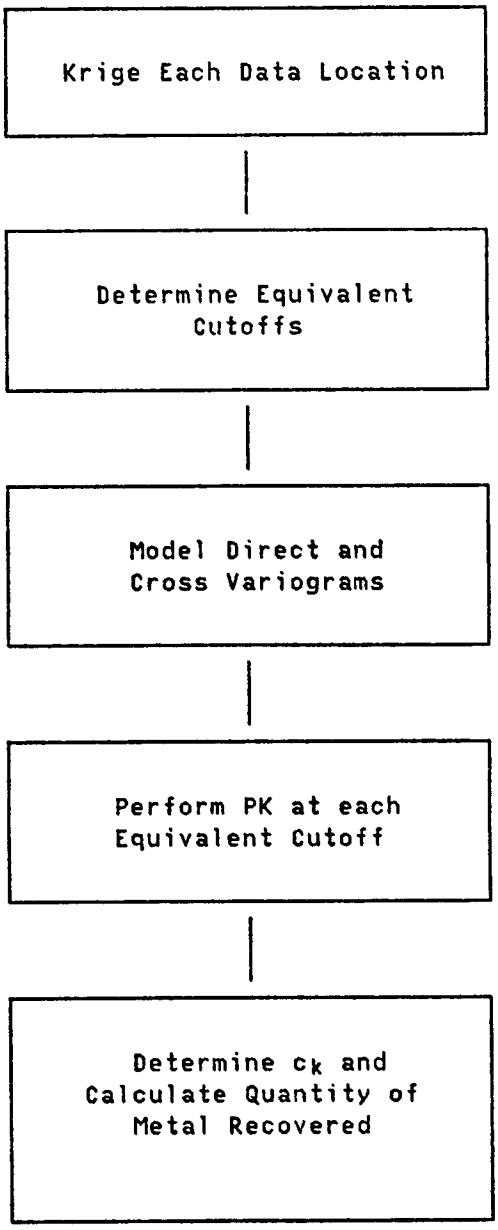

Steps Required to Determine Block Recoveries from Pseudo Block Indicator Data

5.7 RESULTS

Estimation of the tonnage and quantity of metal recovered, based on a selective mining unit size of 12.5 x 12.5 ft, was performed using both the pseudo block indicator data method and the correction of support of

local point recovery estimates method. As a check of the accuracy of these two methods the results are compared with the true recoveries of 12.5 ft smus obtained from the conditional simulation of the Bell Mine.

As in the point case both the global and local accuracy of each method will be examined. Both tonnage and quantity of metal recovery were estimated for each of the 9 cutoffs of interest. The global results are presented in tabular form and consist of an examination of the global recovery, global bias and mean square error of the estimators. As with the point results, the local results will be presented in the form of scattergrams of true versus estimated recovery for selected cutoffs. These results will give an indication of the overall accuracy of each of the proposed methods and will provide a basis for determining which, if either, of these methods should be adopted for future use.

5.7.1 Global Results

As previously discussed, the global reserves refer to total recoverable reserves over all of the 119 panels.

Three separate estimates of tonnage and quantity of metal are examined. Two of these estimates are, however the same method utilizing different inputs. The three estimators and are:

1. The pseudo block indicator data method (sec 5.2, 5.6.2).
2. Correction of the point recovery estimates using variances determined from the experimental variogram model (sec 5.3, 5.6.1).
3. Correction of the point recovery estimates using the true variances (sec 5.3, 5.6.1).

5.7.1.1 Global Tonnage Recovery Factor

The global tonnage recovery factor is defined in much the same way as the global tonnage recovery factor defined in section 4.5. The only difference is that in this case the global recovery factor is the fraction of the entire deposit recovered on 12.5 ft smus rather than point support smus. The estimated tonnage recovery factor for each of the estimators is defined as the estimated number of smus above a given cutoff divided by the total number of smus. The true tonnage recovery factor is defined as the number of smus whose actual grade is above a given cutoff divided by the total number of smus.

The results given by the three estimators are presented in table 16. Notice that the two estimators based on the point estimates yield essentially identical results. Both of these estimators give slightly better estimates of the global tonnage recovered than the method based on pseudo block indicator data. Notice however that all three estimators produce results which are very close to the true values at the majority of cutoffs. The one exception is at the lowest cutoff, .004 oz/ton, where true recovery is underestimated. This result is to be expected as the affine correction permanence of shape hypothesis preserves the spike of data observed in the point distribution at .003 oz/ton in the block distribution. Since block distributions rarely have spikes of this magnitude, the poor results obtained at this low cutoff are expected. Luckily the actual economic cutoff grades are much larger than .004 oz/ton so the poor results at this low cutoff are of no practical importance. If however accurate results are required at this cutoff a different permanence of shape hypothesis must be used. Aside

from the results at the lowest cutoff, all three estimators perform well when estimating global tonnage recovered at the Bell Mine.

5.7.1.2 Global Tonnage Relative Bias

The global tonnage relative bias contains the same information as the global tonnage recovery however the information is presented in a form which is easier to interpret. The global relative bias gives the global bias of the estimator as a percentage of the true recovery. Global relative bias for a given cutoff is defined as:

(Estimated Recovery - True Recovery)/(True Recovery)

If an estimator is perfect, the estimated recovery would exactly equal the true recovery and the global bias would be zero. Therefore in examining the relative bias of the estimators (table 16), those estimators which have close to zero relative bias are considered superior (under this criterion) to estimators with large relative biases.

As shown in table 16, the two estimators based on the point estimates have very little global relative bias at all but the highest cutoff. For all other cutoffs the relative bias is less than 5% and for most cutoffs the relative bias is well below 5%. The interesting feature of these results is that the relative biases observed when estimating point recoveries (see table 17) are larger than the values observed in this case of estimating block support smu recoveries. This result is unexpected since no knowledge of the smu block grades is available locally or globally. The global block smu recovery estimates are strongly a function of the support hypothesis (in this case the affine

transform) used to perform the local change of support. Because of the change of support hypothesis it is expected that the block smu global recovery estimates would be less accurate than the point recovery estimates. It must be assumed that, for this deposit, the local affine correction used in the estimators based on the point estimates was adequate. It cannot be assumed, however that global, block smu, results which are as accurate as those observed here will be obtained for all deposits.

Another interesting feature of the results based on the point estimates is that the estimator utilizing variances inferred from the experimental variogram performs slightly better than the estimator utilizing the true variances. The difference between these estimators is small but it does suggest that the affine transform is not strictly correct for this deposit as if it were the results given by the estimator utilizing the true variances would be superior to the estimator utilizing the experimental variances. Hence even though the affine transform does not hold for this deposit and even when the variances used are not equal to the true variances the global tonnage estimates obtained by an estimator based on point estimates are very good.

The global relative bias of the estimator based on the pseudo block indicator data is larger than that obtained by the other two estimators. The relative bias of this estimator is less than 10% for all cutoffs but it is almost always greater than 5%. The magnitude of this bias is similar to that observed in the point case. Again these results indicate that the affine correction change of support hypothesis is not

strictly correct for this deposit, however it is certainly an acceptable approximation.

5.7.1.3 Tonnage Mean Square Error

The tonnage mean square error gives an indication of the local accuracy of the estimator averaged over the entire deposit. This quantity is defined as :

$$MSE(zc_i) = \sum_{j=1}^{NP} (T_j(zc_i) - TT_j(zc_i))^2/NP \qquad (5.34)$$

where: zc_i is a cutoff grade
T_j is the estimated recovery for panel j
TT_j is the true recovery for panel j
NP is the number of panels (119 in this case)

At all cutoffs both of the estimators based on the local point recovery estimates have identical mean square error values (see table 16). The estimator based on pseudo block indicator data however has higher mean square error at all cutoffs. This indicates that this estimator has lesser local accuracy over the deposit than either of the other estimators.

5.7.1.4 Quantity of Metal Global Recovery Factor

The quantity of metal recovery factor is a unitless value. When this value is multiplied by the total tonnage of the deposit, the ounces of potentially recoverable gold, assuming selection of 12.5 ft smu grades, is determined.

The quantity of metal recovery factor is determined through the following relationship:

TABLE 16

Global Tonnage Recovery Results

Tonnage Recovery

Cutoff	Method* A	B	C	True
.004	.855	.871	.873	.902
.008	.793	.807	.805	.807
.015	.744	.698	.691	.699
.025	.631	.595	.589	.599
.041	.527	.498	.487	.497
.066	.432	.383	.376	.397
.105	.304	.305	.295	.299
.174	.221	.202	.194	.201
.311	.112	.121	.120	.101

Tonnage Relative Bias

Cutoff	Method* A	B	C
.004	-.051	-.034	-.032
.008	-.018	.001	-.003
.015	.064	-.001	-.011
.025	.053	-.007	-.018
.041	.060	.001	-.021
.066	.086	-.036	-.054
.105	.015	.019	-.013
.174	.103	.005	-.032
.311	.104	.190	.181

Tonnage Mean Squared Error

Cutoff	Methods* A	B	C
.004	.037	.025	.025
.008	.049	.029	.029
.015	.053	.032	.031
.025	.038	.030	.030
.041	.043	.028	.028
.066	.040	.026	.026
.105	.022	.022	.021
.174	.016	.012	.012
.311	.008	.008	.008

*Methods A - Recoveries utilizing pseudo block indicator data
B - Recoveries utilizing point estimates (Actual Variance)
C - Recoveries utilizing point estimates (True Variances)

TABLE 17

Comparison of Relative Biases for Point and Block Tonnage Recovery Estimators

Percentile of Distribution	Relative Bias of Tonnage Estimates	
	Point Estimator	Block Estimator
20	.080	.001
30	.040	-.001
40	.035	-.007
50	.061	.001
60	.002	-.036
70	.095	.019
80	.092	.005
90	.210	.190

The point estimates are the PK estimates for campaign #2.
The block estimates are the recoveries obtained from the PK point estimates utilizing the actual variances.
The percentiles refer to the distribution of point grades or the distribution of block grades depending on the estimator under consideration.

$$QF_v(zc) = \sum_{j=1}^{NP} Q_{vj}(zc)/NP \qquad (5.35)$$

where: zc is the cutoff of interest
NP is the number of panels (119 in this case)
Q_{vj} is the estimated quantity of metal recovered in panel j at cutoff zc
QF_v is the quantity of metal recovery factor

The quantity of metal recovery factors for the three estimators are compared with the true quantity of metal recovery factor obtained by replacing the estimated quantity of metal by the true quantity of metal recovered in the above equation.

All three of the estimators considered are nearly unbiased at low cutoffs (table 18). However at high cutoffs there is some discrepancy

between the estimated and true recoveries. This discrepancy is less for the method utilizing the pseudo block indicator data than for either of the methods based on the point support estimates. This is in contrast to the global tonnage recovery results for which the results of the estimators based on the point estimates were superior. Notice that both estimators based on the point estimates again give nearly identical results, so at least for global recoveries of both tonnage and quantity of metal the difference between the experimental and true variances has not adversely affected the results.

5.7.1.5 Quantity of Metal Relative Bias

As discussed previously, the relative bias is used to express the discrepancy between true and estimated recovery as a relative error. The quantity of metal relative bias is defined as the estimated global recovered quantity of metal less the true global recovered quantity of metal divided by the true global quantity of metal recovered. The quantity of metal relative bias for the three estimators considered is shown in table 18. The estimator based on pseudo block indicator data has, at all cutoffs, less than 10% relative bias. In addition, for cutoffs other than the largest cutoff the bias is far less than 10%, as it is less than 1% for the majority of cutoffs. The estimators based on the point estimates are slightly less accurate although the bias is less than 5% for cutoffs less than the seventieth percentile. For larger cutoffs the bias is above 10% and it is above 30% at the highest cutoff.

There appears to be some systematic bias in the quantity of metal estimates obtained by the estimators based on the point estimates, as

the magnitude of the bias increases as the cutoff increases. The most likely cause of such a systematic bias is that the class mean value chosen for the material above the largest cutoff is too large and/or as is definitely true in this case there is an overestimation (see see table 16) of the tonnage above the highest cutoff (recall that the global quantity of metal recovered above the highest cutoff is simply the global tonnage recovery multiplied by the class mean). This overestimation of quantity of metal recovered above the highest cutoff is carried along to all of the other cutoffs due to the nature of the algorithm used (see sec 4.4.4.2). Some correction of this bias does occur at lower cutoffs, however as about 50% of the ounces of gold are found above the highest cutoff it is difficult to completely compensate for the large bias which is introduced by the material above the largest cutoff. Thus this bias is found to some degree at all cutoffs.

From this examination of the global bias properties of these estimators it appears that if an estimator based on the point estimate is utilized one can confidently estimate the global tonnage recovered easily within 5% at all but the largest cutoffs and the global quantity of metal recovered within 10% again at all but the largest cutoffs. This type of global accuracy should be more than sufficient for most practical applications.

5.7.1.6 Quantity of Metal Mean Squared Error

The quantity of metal mean squared error can be seen as a measure of the local accuracy of an estimator. It is defined as

$$MSE = \sum_{j=1}^{NP} (QT_j(zc) - Q_j(zc))^2/NP \qquad (5.36)$$

where: $QT_j(zc)$ is the true quantity of metal above

cutoff zc for panel j.
$Q_j(zc)$ is the estimated quantity of metal above cutoff zc for panel j.
NP is the number of panels (119 in this case).

The quantity of metal mean squared errors for the various estimators are given in table 18. Notice that all three estimators give nearly identical results. Thus, although the estimators based on the point recovery estimates have larger global quantity of metal biases than the estimator based on pseudo block indicator data, the overall local properties of both types of estimators as measured by the mean squared error are nearly equal.

TABLE 18

Global Quantity of Metal Recovery Results

Quantity of Metal Recovery Factor
Method*

Cutoff	A	B	C	True
.004	.107	.109	.109	.108
.008	.106	.109	.109	.107
.015	.106	.108	.108	.106
.025	.103	.107	.106	.104
.041	.100	.104	.104	.101
.066	.095	.100	.099	.096
.105	.086	.094	.094	.087
.174	.077	.084	.083	.074
.311	.056	.068	.068	.051

Quantity of Metal Relative Bias
Method*

Cutoff	A	B	C
.004	-.009	.015	.010
.008	-.009	.018	.012
.015	-.004	.021	.015
.025	-.009	.026	.020
.041	-.011	.035	.028
.066	-.005	.043	.037
.105	-.020	.082	.073
.174	.036	.132	.120
.311	.097	.348	.332

Quantity of Metal Mean Squared Error
Method*

Cutoff	A	B	C
.004	.0024	.0023	.0022
.008	.0024	.0023	.0023
.015	.0024	.0023	.0023
.025	.0024	.0023	.0023
.041	.0025	.0024	.0024
.066	.0026	.0024	.0024
.105	.0024	.0025	.0025
.174	.0024	.0025	.0025
.311	.0023	.0028	.0027

*Methods: A - Recoveries based of pseudo block indicator data
B - Recoveries based on point estimates (Actual Variance)
C - Recoveries based on point estimates (True Variances)

5.7.2 Local Recoveries

Although the global properties of these estimators, particularly the bias properties, are important these estimators are designed as local estimators of recoverable reserves. Hence it is necessary to examine the error made at each panel. As in discussing the local performance of the point recovery estimators, scattergrams between true and estimated recovery will be utilized so that the true and estimated local recoveries for all 119 panels can be examined simultaneously. As in the case of the point recovery estimates, the scattergrams for only two cutoffs will be examined in detail. The two cutoffs which are chosen for examination span an interesting portion of the range of cutoffs as most economic cutoffs will fall between these two chosen cutoffs. The chosen cutoffs, .041 oz/ton and .174 oz/ton, are the median and 80th percentiles of the distribution of simulated smu grades.

5.7.2.1 Tonnage Recovery at the .041 oz/ton Cutoff

The scattergrams of tonnage recovered at the median, .041 oz/ton, cutoff show that the estimators based on the point recovery estimates are superior to the estimator based on pseudo block indicator data (figs. 120-122). The scattergram for the estimator based on block indicator data shows a number of large errors, in particular these errors are most common when the true tonnage recovered is near 50%. The cause of this poor estimation for these particular panels is unknown, however the effects of the poor estimation are easily seen as it results in a conditional bias. The conditional bias is such that panels with

estimated low recoveries are, on average, underestimated (that is when the panel is removed more tonnage will be recovered than predicted) and panels with high estimated recoveries are on average underestimated. This type of conditional bias is certainly undesirable in an estimator.

The estimators based on the point recovery estimates do not show any type of conditional bias. The cloud of points is well centered about the line corresponding to true equals estimated recovery and there are few very large errors. The small number of large errors results in small mean square errors for both of these estimators. Additionally these two estimators have very small relative biases and relatively high correlation between true and estimated recovery as measured by the correlation coefficient. The similarity between the estimator utilizing the actual experimental variances and the estimator utilizing the true variances is great. In the scattergrams for both of these estimators, the same groups of points can be observed in nearly the same locations. This similarity between the results of these two estimators implies that some errors can be made in variogram modelling without adversely affecting the block recovery results. This is a strong feature of this method as it is often difficult to accurately model the variogram of grade and therefore it is difficult to accurately determine the variances required to make a change of support.

5.7.2.2 Tonnage Recovery at the .174 oz/ton Cutoff

The .174 oz/ton cutoff represents the 80th percentile of the 12.5 ft. smu grade distribution. It is, therefore a high quantile of the distribution and estimation of recoveries for this cutoff should be an

interesting and difficult test of the methods. The scattergrams for this cutoff (figs 123-125) show that all three estimators perform well at this cutoff. The conditional bias presented by the estimator based on pseudo block indicator data at the .041 oz/ton cutoff has been removed at this higher cutoff. The only difficulty this estimator has at this cutoff is in estimating the global recovery as it overestimates by 10%. Otherwise this estimator performs as well as either of the estimators based on estimated point recoveries.

The two estimators based on the point recovery estimates are again very similar. Both estimators have small global biases, small scatter about the true equals estimate line, and high correlation between true and estimated recovery. In short, the estimator based on point recoveries has shown that it can be used to accurately estimate the tonnage recovered when selection is based on block support. Interestingly the quality of the local block smu recovery estimate is as good as the quality of the local point smu recovery estimate (fig 90). Thus the assumptions which have been made to accomplish the change of support from point smus to block smus has not diminished the accuracy of the tonnage estimates.

5.7.2.3 Quantity of Metal Recovery at the .041 oz/ton Cutoff

The quantity of metal estimates at the .041 oz/ton cutoff (figs 126-128) are similar for all three estimators. None of the estimators shows a conditional bias or a great number of large errors. All three estimators do show, however small global biases and high correlations between true and estimated quantity of metal recovered. In summary all

three estimators provide good local estimates of quantity of metal recovered at this cutoff.

5.7.2.4 Quantity of Metal Recovery at the .174 oz/ton Cutoff

Again at the .174 oz/ton cutoff, the estimated quantity of metal recovered determined by all three estimators are accurate representations of the true quantity of metal recovered. In fact, all three scattergrams are very similar (figs 129-131). The only apparent difference between the estimators is that the estimators based on the point recovery estimates have larger global bias.

5.7.3 Local Recovery at the .008 oz/ton Cutoff

As seen in the discussion of the global results, the proposed block recovery estimation techniques do not accurately estimate the global tonnage recovery at the lowest cutoffs. As mentioned the poor global results at this cutoff can be attributed to the affine transform permanence of shape hypothesis which was utilized. As discussed, this permanence of shape hypothesis is not realistic at low cutoffs so poor results are expected for these cutoffs. Not surprisingly, therefore, the local results at the .008 oz/ton cutoff are also poor (see fig 132). The results at this cutoff emphasize the necessity of utilizing a change of support hypothesis which is adequate for the problem at hand. In most cases recoveries are required at cutoffs which are near or larger than the median grade and as has been demonstrated by the local results at the .041 and .174 oz/ton cutoffs, the affine transform hypothesis is adequate for these uses. If, however, recoveries at extremely low

cutoffs are required, a different change of support hypothesis, preferably one based on some assumption of normality of the data, should be used since the affine transform is not adequate in such cases.

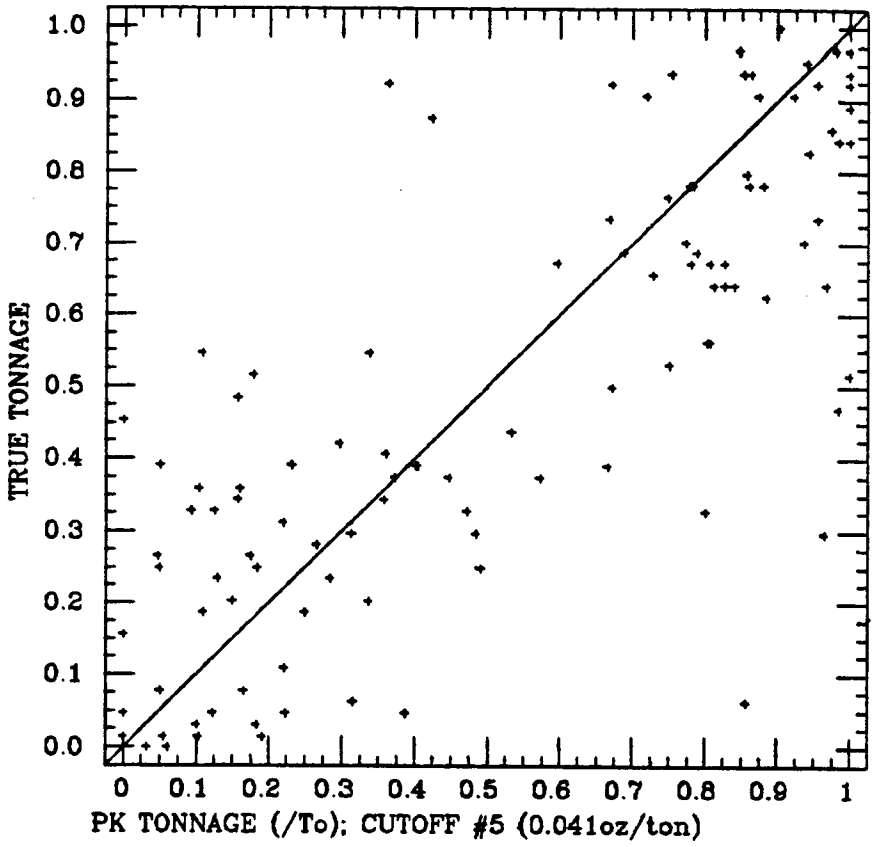

SUMMARY STATISTICS

	MEAN	VARIANCE
EST.	0.527	0.1288
TRUE	0.497	0.1056

RELATIVE BIAS = 0.0597

MEAN SQUARED ERROR = 0.0425

CORRELATION COEF. = 0.826

Figure 120: Block Support Tonnage Recovery at the .041 oz/ton Cutoff (Estimates based on pseudo block indicator data)

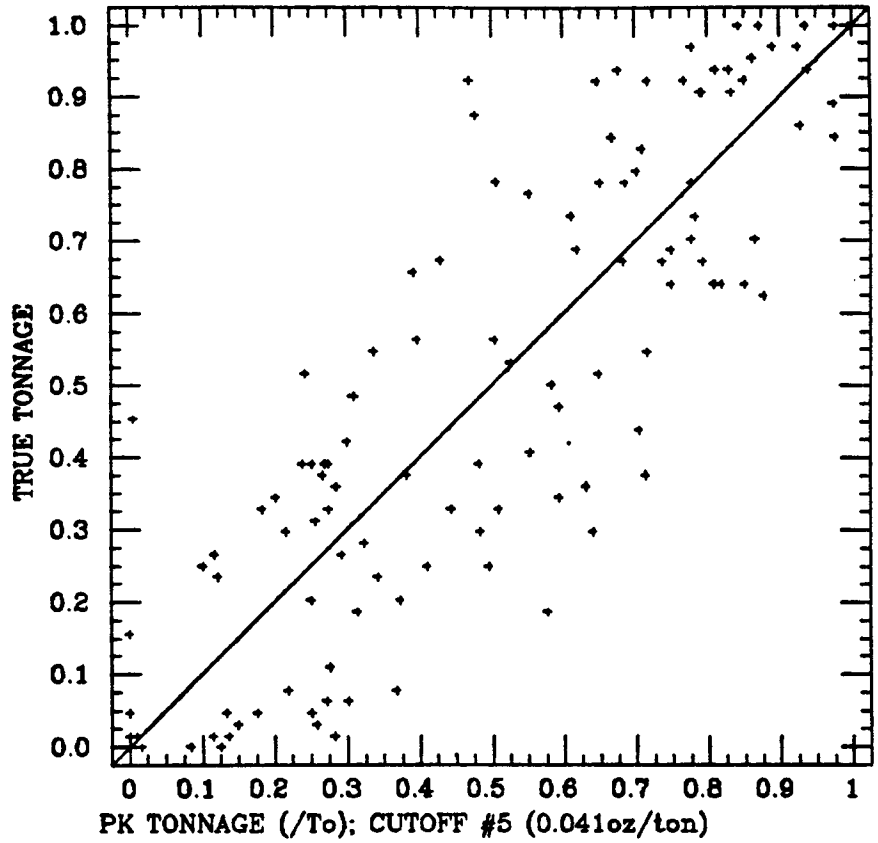

SUMMARY STATISTICS

	MEAN	VARIANCE
EST.	0.498	0.0844
TRUE	0.497	0.1056

RELATIVE BIAS = 0.0010

MEAN SQUARED ERROR = 0.0283

CORRELATION COEF. = 0.856

Figure 121: Block Support Tonnage Recovery at the .041 oz/ton Cutoff (Estimates based on point estimates using actual variances)

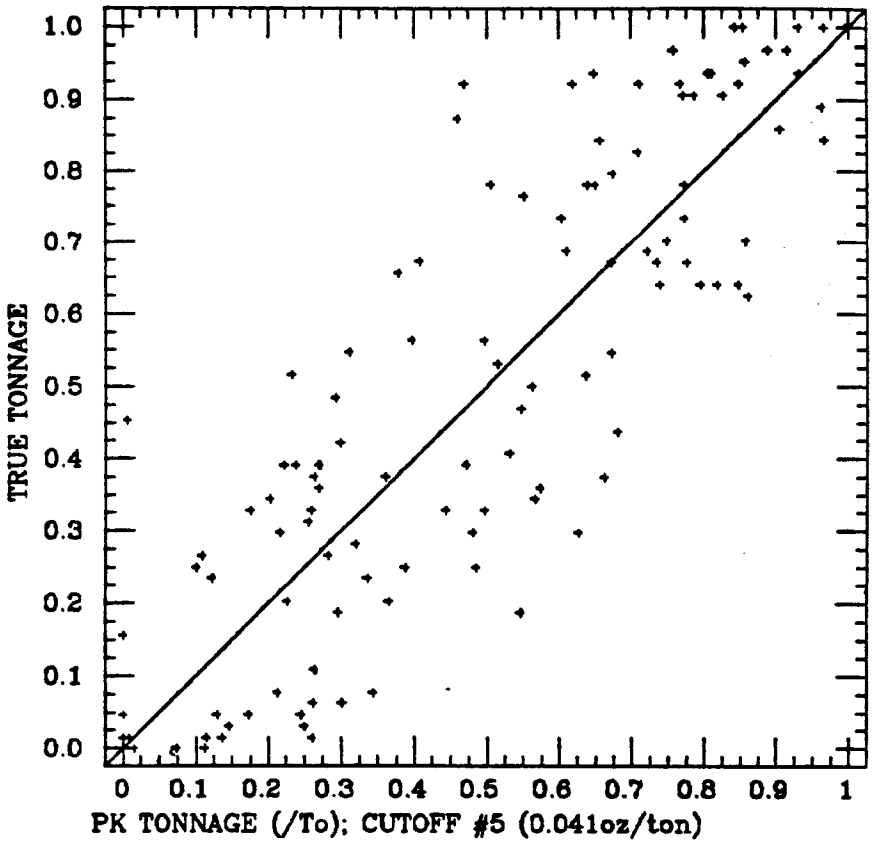

SUMMARY STATISTICS

	MEAN	VARIANCE
EST.	0.487	0.0829
TRUE	0.497	0.1056

RELATIVE BIAS =-0.0213

MEAN SQUARED ERROR = 0.0275

CORRELATION COEF. = 0.861

Figure 122: Block Support Tonnage Recovery at the .041 oz/ton Cutoff (Estimates based on point estimates using true variances)

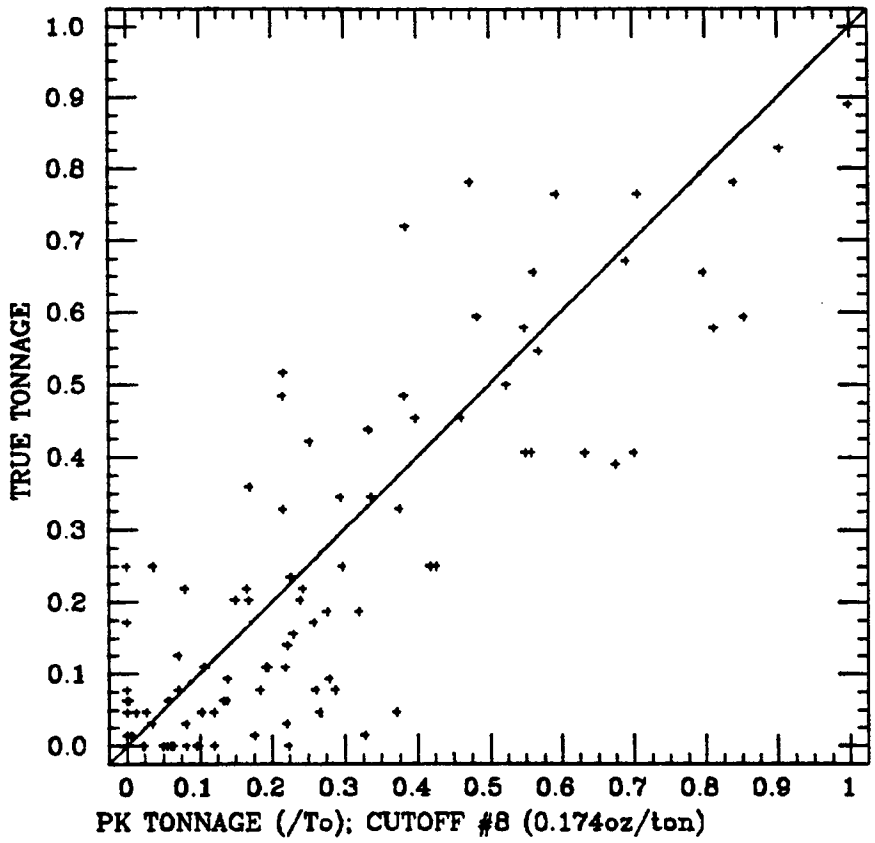

SUMMARY STATISTICS

	MEAN	VARIANCE
EST.	0.221	0.0593
TRUE	0.201	0.0564

RELATIVE BIAS = 0.1032

MEAN SQUARED ERROR = 0.0156

CORRELATION COEF. = 0.869

Figure 123: Block Support Tonnage Recovery at the .174 oz/ton Cutoff (Estimates based on pseudo block indicator data)

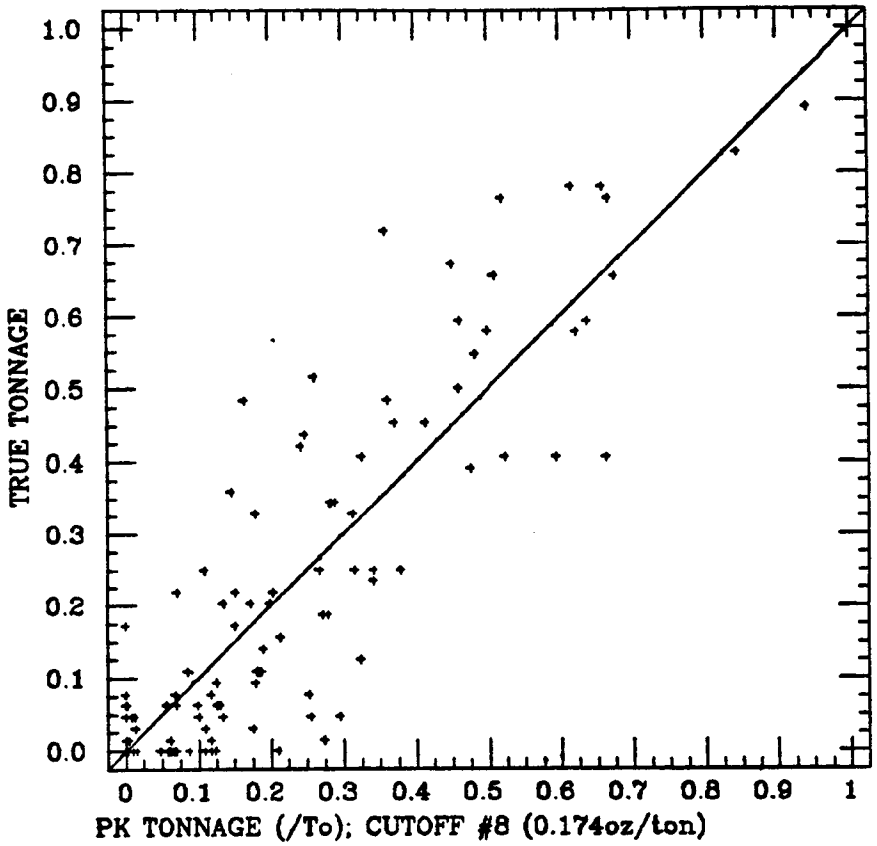

SUMMARY STATISTICS

	MEAN	VARIANCE
EST.	0.202	0.0436
TRUE	0.201	0.0564

RELATIVE BIAS = 0.0047

MEAN SQUARED ERROR = 0.0121

CORRELATION COEF. = 0.887

Figure 124: Block Support Tonnage Recovery at the .174 oz/ton Cutoff (Estimates based on point estimates using estimated variances)

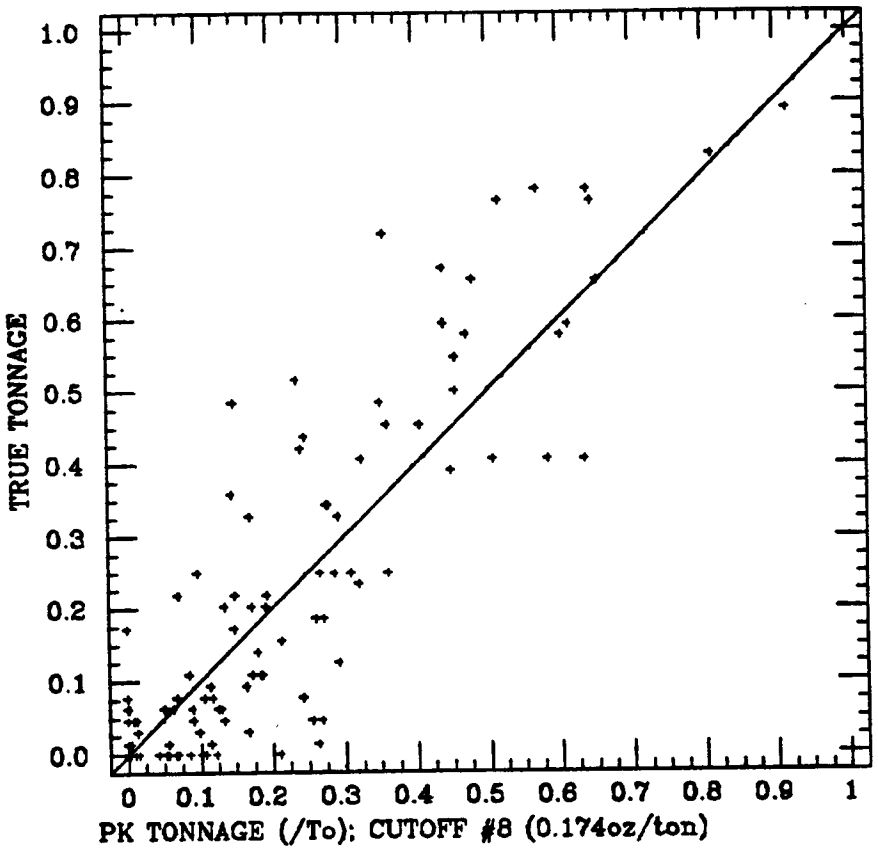

SUMMARY STATISTICS

	MEAN	VARIANCE
EST.	0.194	0.0407
TRUE	0.201	0.0564

RELATIVE BIAS =-0.0319

MEAN SQUARED ERROR = 0.0120

CORRELATION COEF. = 0.888

Figure 125: Block Support Tonnage Recovery at the .174 oz/ton Cutoff (Estimates based on point estimates using true variances)

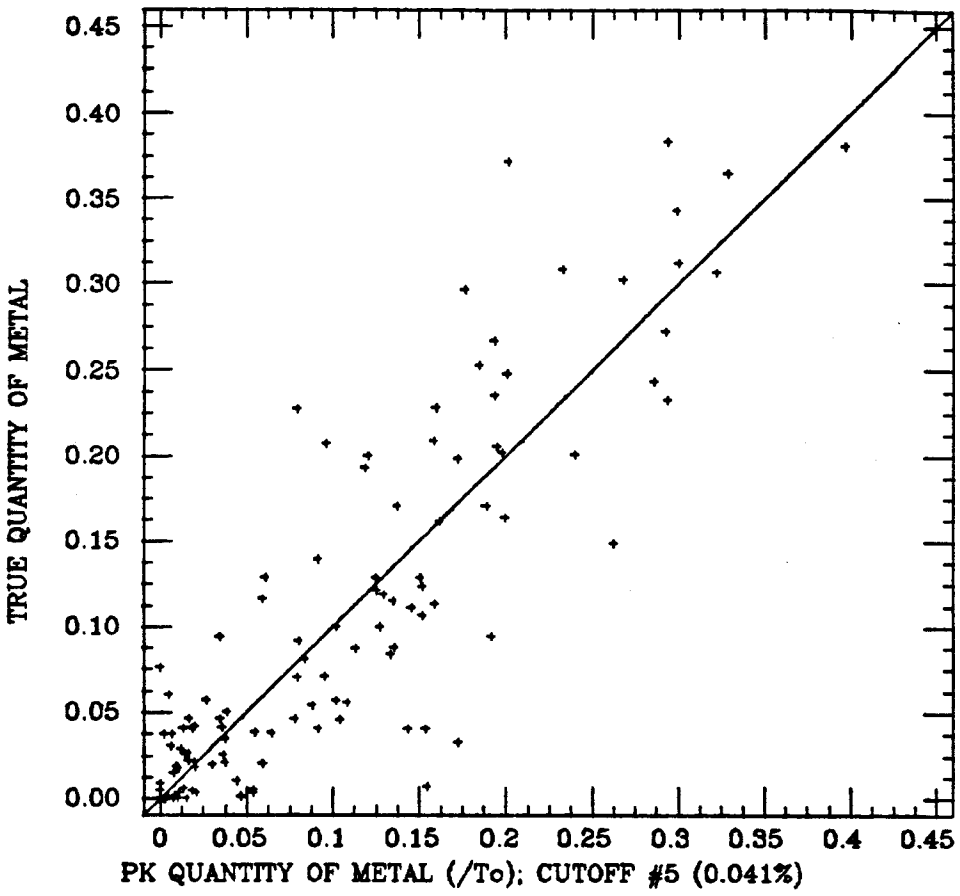

SUMMARY STATISTICS

	MEAN	VARIANCE
EST.	0.100	0.0087
TRUE	0.101	0.0107

RELATIVE BIAS =-0.0114

MEAN SQUARED ERROR = 0.0025

CORRELATION COEF. = 0.876

Figure 126: Block Support Quantity of Metal Recovery at the .041 oz/ton Cutoff (Estimates based on pseudo block indicator data)

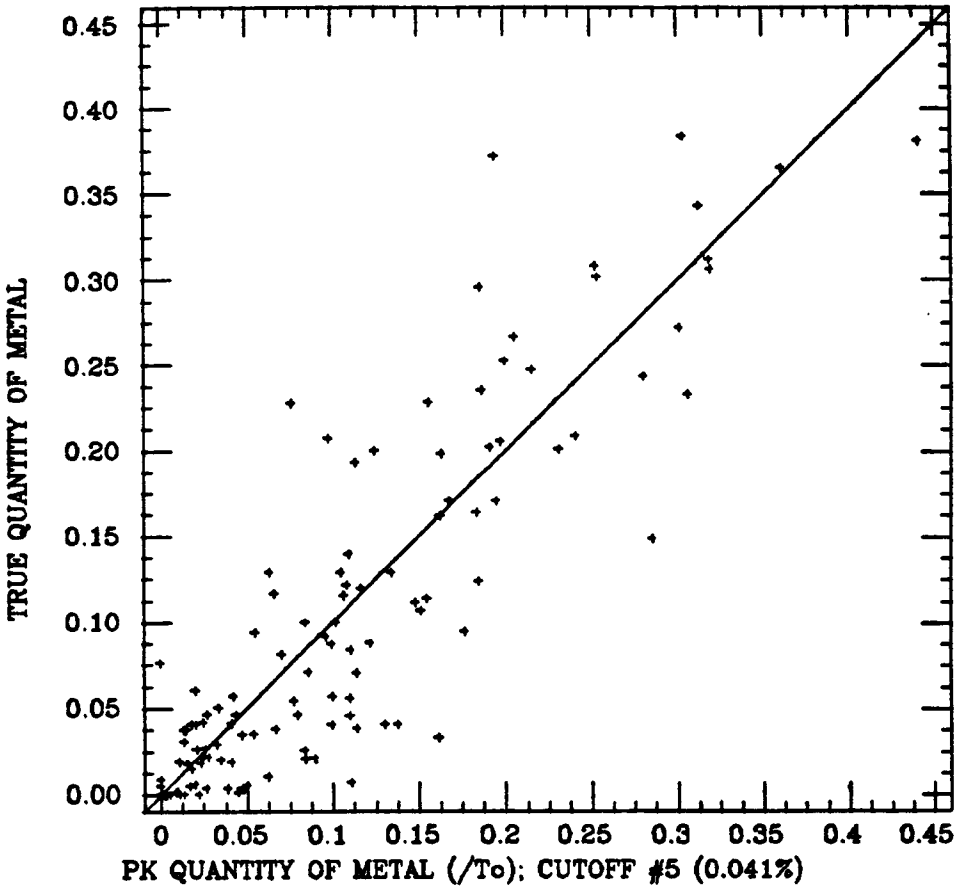

SUMMARY STATISTICS

	MEAN	VARIANCE
EST.	0.104	0.0089
TRUE	0.101	0.0107

RELATIVE BIAS = 0.0350

MEAN SQUARED ERROR = 0.0024

CORRELATION COEF. = 0.883

Figure 127: Block Support Quantity of Metal Recovery at the .041 oz/ton Cutoff (Estimates based on point estimates using estimated variances)

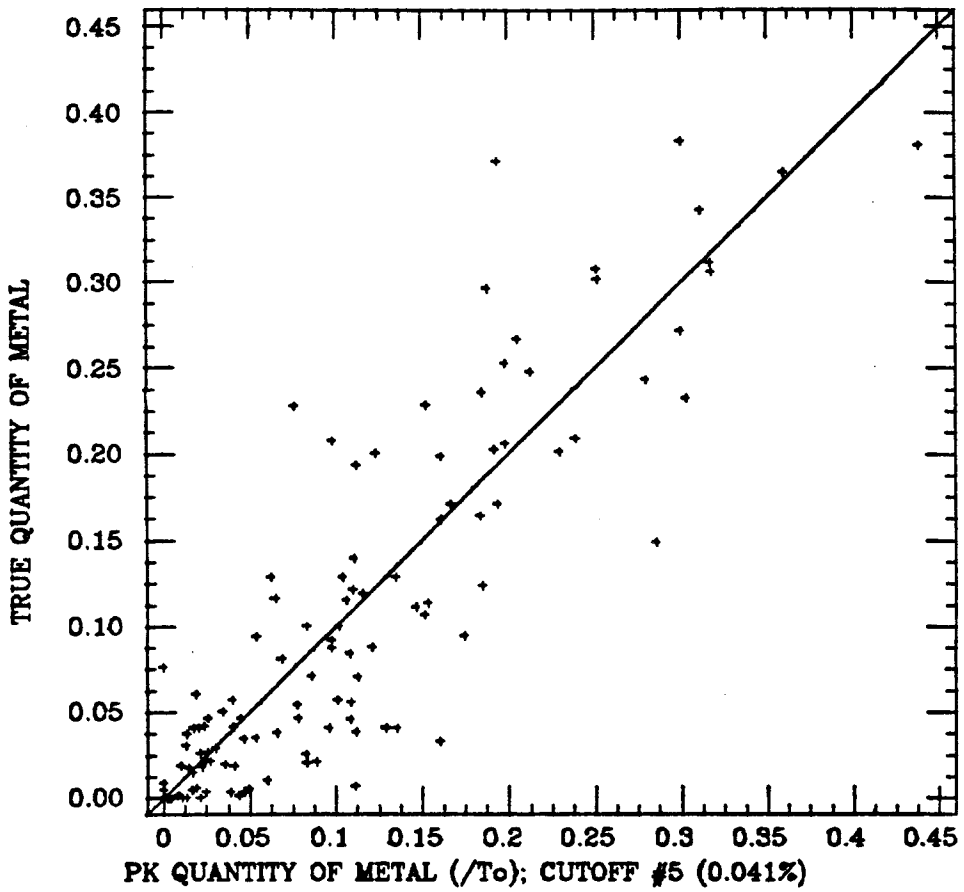

SUMMARY STATISTICS

	MEAN	VARIANCE
EST.	0.104	0.0088
TRUE	0.101	0.0107

RELATIVE BIAS = 0.0278

MEAN SQUARED ERROR = 0.0024

CORRELATION COEF. = 0.884

Figure 128: Block Support Quantity of Metal Recovery at the .041 oz/ton Cutoff (Estimates based on point estimates using true variances)

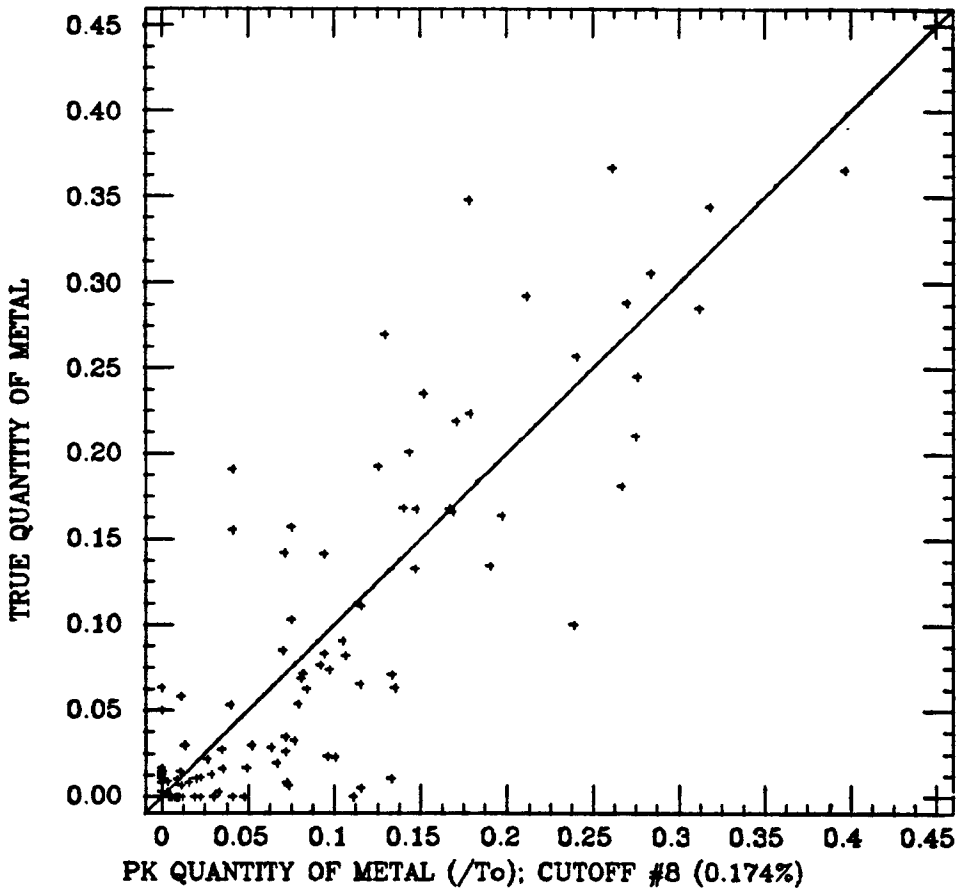

SUMMARY STATISTICS

	MEAN	VARIANCE
EST.	0.077	0.0077
TRUE	0.074	0.0096

RELATIVE BIAS = 0.0357

MEAN SQUARED ERROR = 0.0024

CORRELATION COEF. = 0.869

Figure 129: Block Support Quantity of Metal Recovery at the .174 oz/ton Cutoff (Estimates based on pseudo block indicator data)

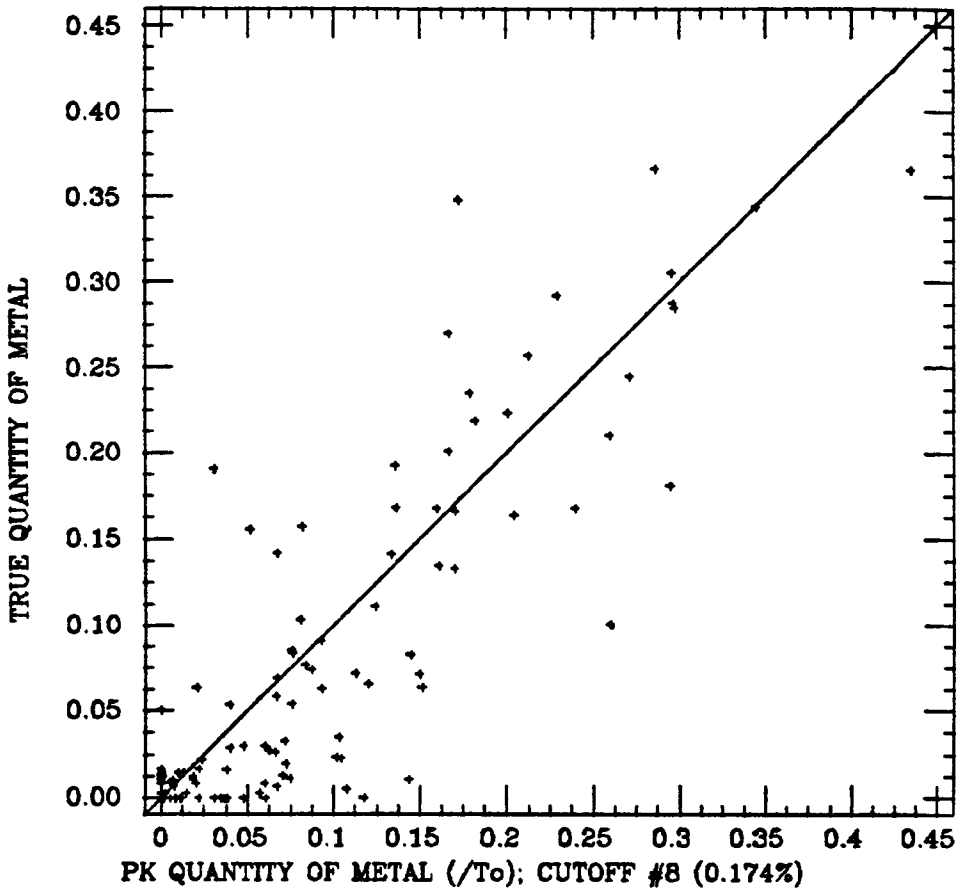

SUMMARY STATISTICS

	MEAN	VARIANCE
EST.	0.084	0.0084
TRUE	0.074	0.0096

RELATIVE BIAS = 0.1322

MEAN SQUARED ERROR = 0.0025

CORRELATION COEF. = 0.868

Figure 130: Block Support Quantity of Metal Recovery at the .174 oz/ton Cutoff (Estimates based on point recoveries using estimated variances)

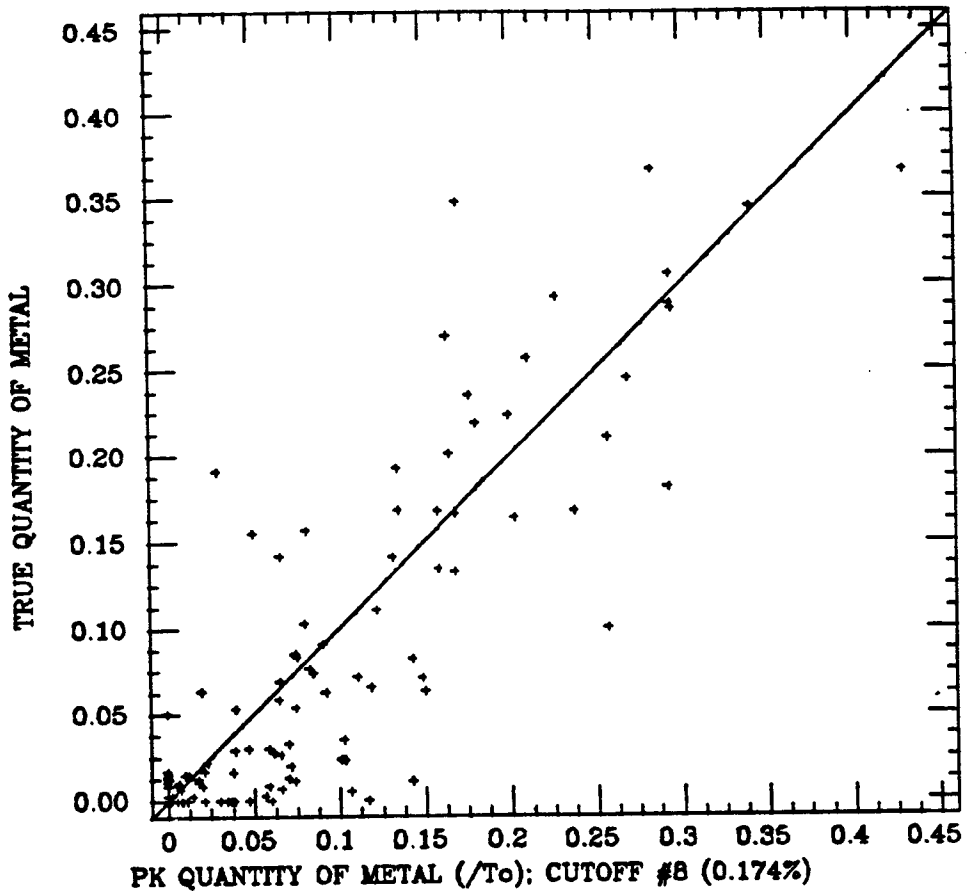

SUMMARY STATISTICS

	MEAN	VARIANCE
EST.	0.083	0.0083
TRUE	0.074	0.0096

RELATIVE BIAS = 0.1199

MEAN SQUARED ERROR = 0.0025

CORRELATION COEF. = 0.868

Figure 131: Block Support Quantity of Metal Recovery at the .174 oz/ton Cutoff (Estimates based on point recoveries using true variances)

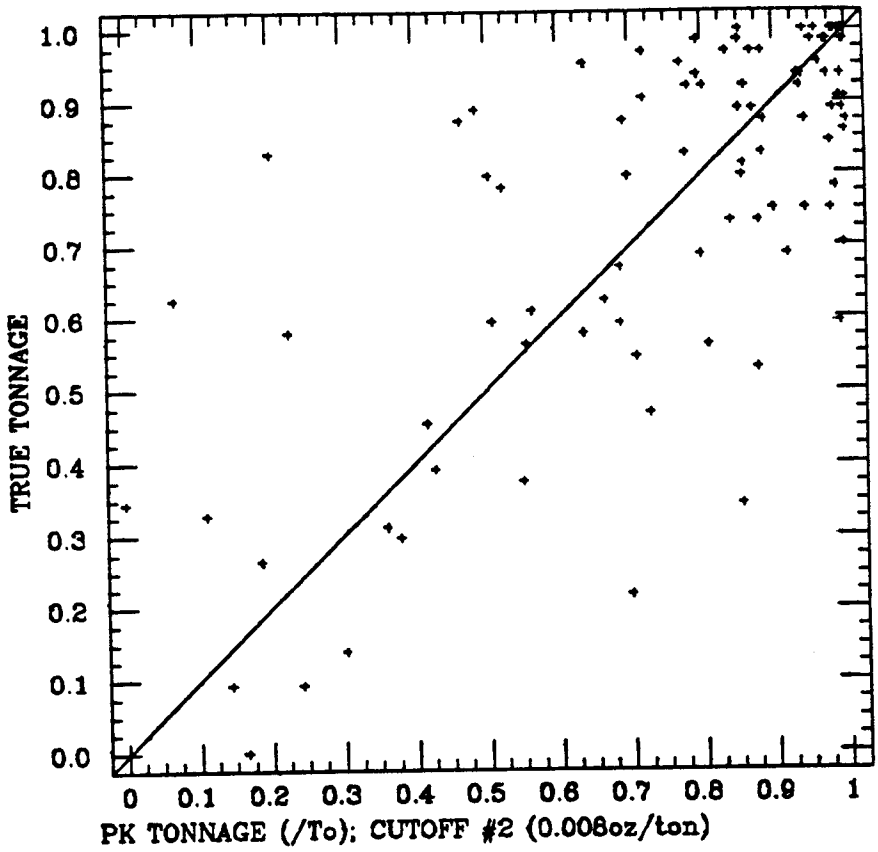

SUMMARY STATISTICS

	MEAN	VARIANCE
EST.	0.805	0.0647
TRUE	0.807	0.0599

RELATIVE BIAS =-0.0026

MEAN SQUARED ERROR = 0.0288

CORRELATION COEF. = 0.769

Figure 132: Block Support Tonnage Recovery at the .008 oz/ton Cutoff

5.7.4 Error Maps

The scattergrams provided in the previous section present the true versus estimated results for each panel in an easily examined form. Any global or conditional biases are easily seen and the general quality of the estimator can be examined. Scattergrams do, however, have a weakness in that the location of each panel is ignored. Thus, although a scattergram may show that an estimator is both conditionally and globally unbiassed, it cannot show how this unbiasedness is achieved. As an example, consider two estimators utilized at a producing mine which present equivalent scattergrams. Estimator A over-estimates monthly recoveries for each month in a six month period. This estimator is unbiased over a period of a year, however, as it under-estimates monthly recoveries in each of the next six months by an equivalent amount. Estimator B, on the other hand, is unbiased for each month over the same twelve month period. Although both estimators are unbiased over the course of a year, estimator B is certainly the preferred estimator. Thus, in examining the local accuracy of an estimator it is important to check the spatial location of the errors.

To examine the spatial location of the errors, tonnage errors made by the PK estimator based on the initial point estimates at the .174 oz/ton cutoff for each panel are plotted in a series of figures (fig 133-137). The error plotted is estimated tonnage less true tonnage, so positive errors correspond to overestimation. A single quantity of metal error map (fig 138) is also presented for the same estimator and cutoff. The quantity of metal error maps show much the same features as the tonnage error maps so only this single map is presented.

The error maps show that the absolute tonnage errors can be as large as 15%, however the great majority of panels have errors less than ±10%. Given the limited number of panels on each of the benches, it is difficult to see if the errors show any trend. However, it can be said that these maps do not show any obvious trends so it is expected that if this deposit were recovered there would not be any long periods of overestimation followed by equally long periods of underestimation.

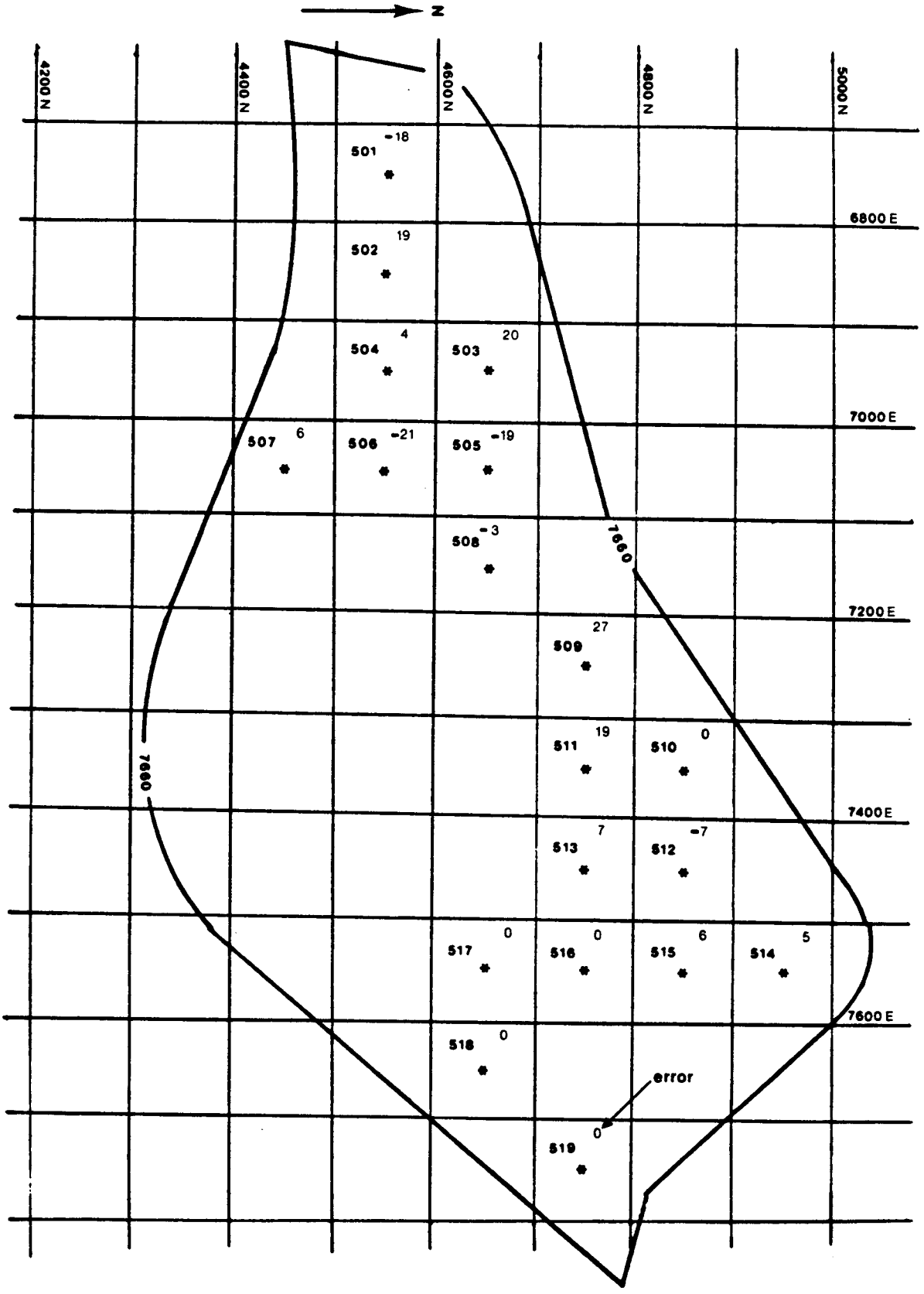

Figure 133: Tonnage Errors for the 7660 Bench

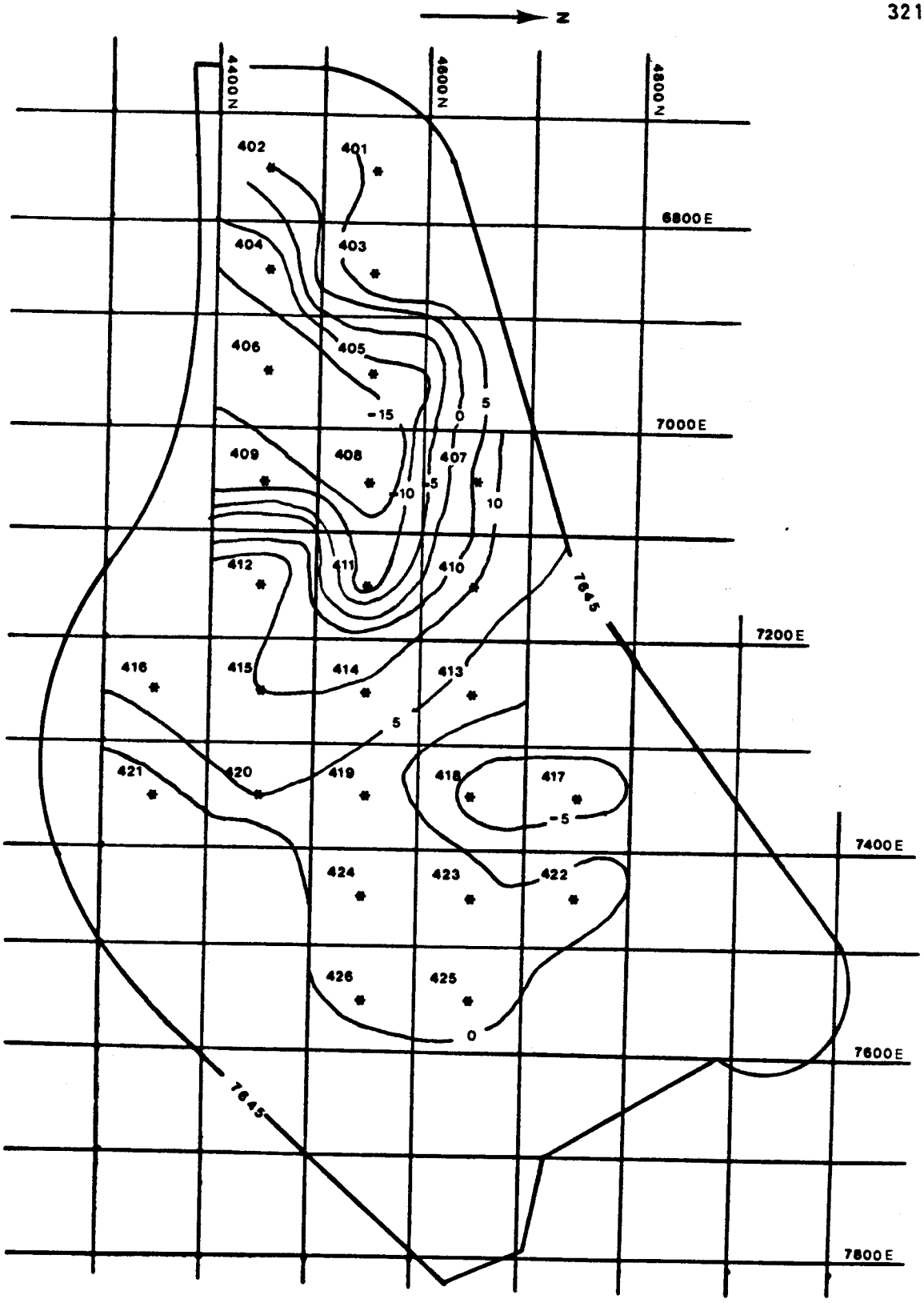

Figure 134: Tonnage Errors for the 7645 Bench

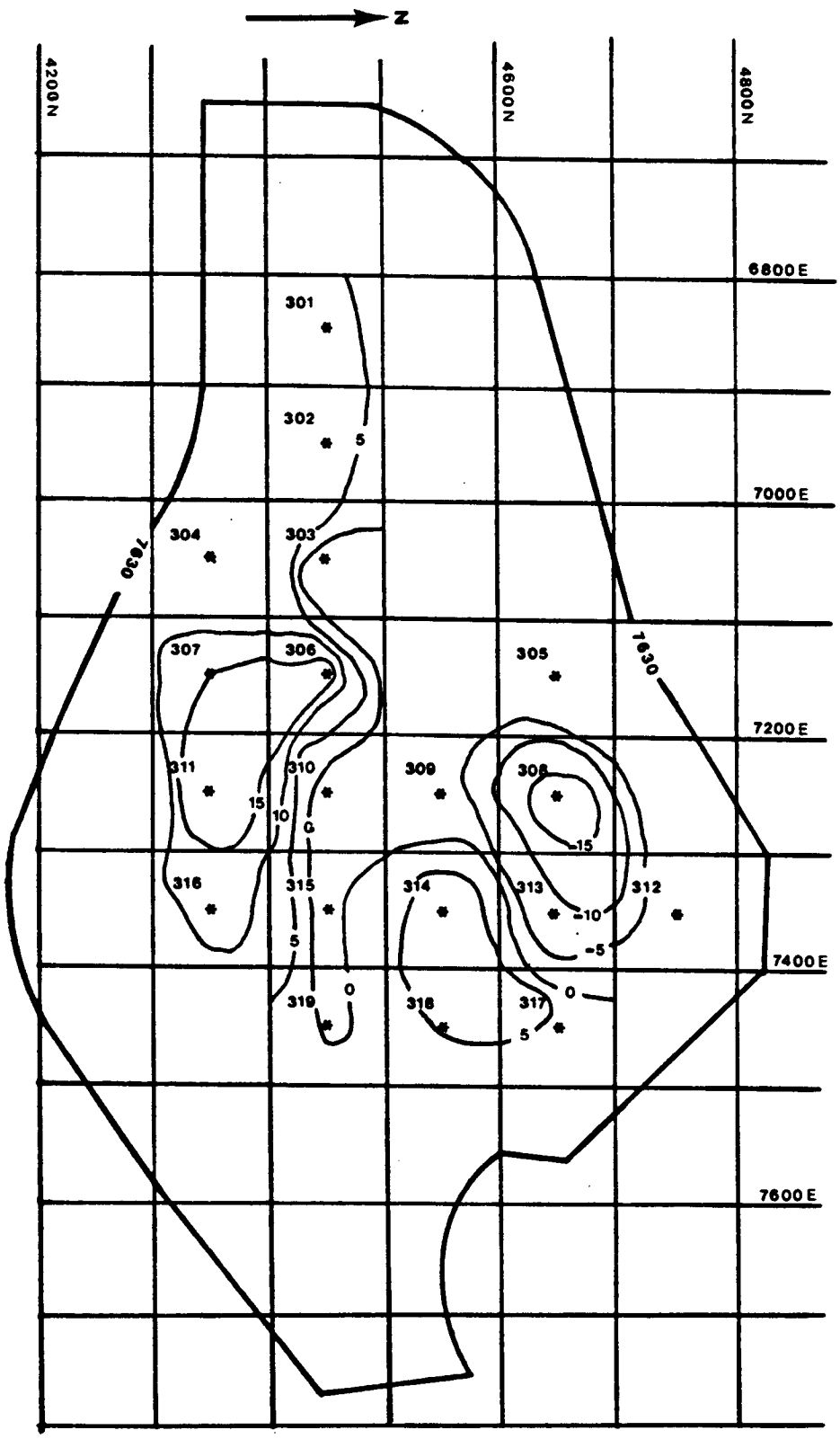

Figure 135: Tonnage Errors for the 7630 Bench

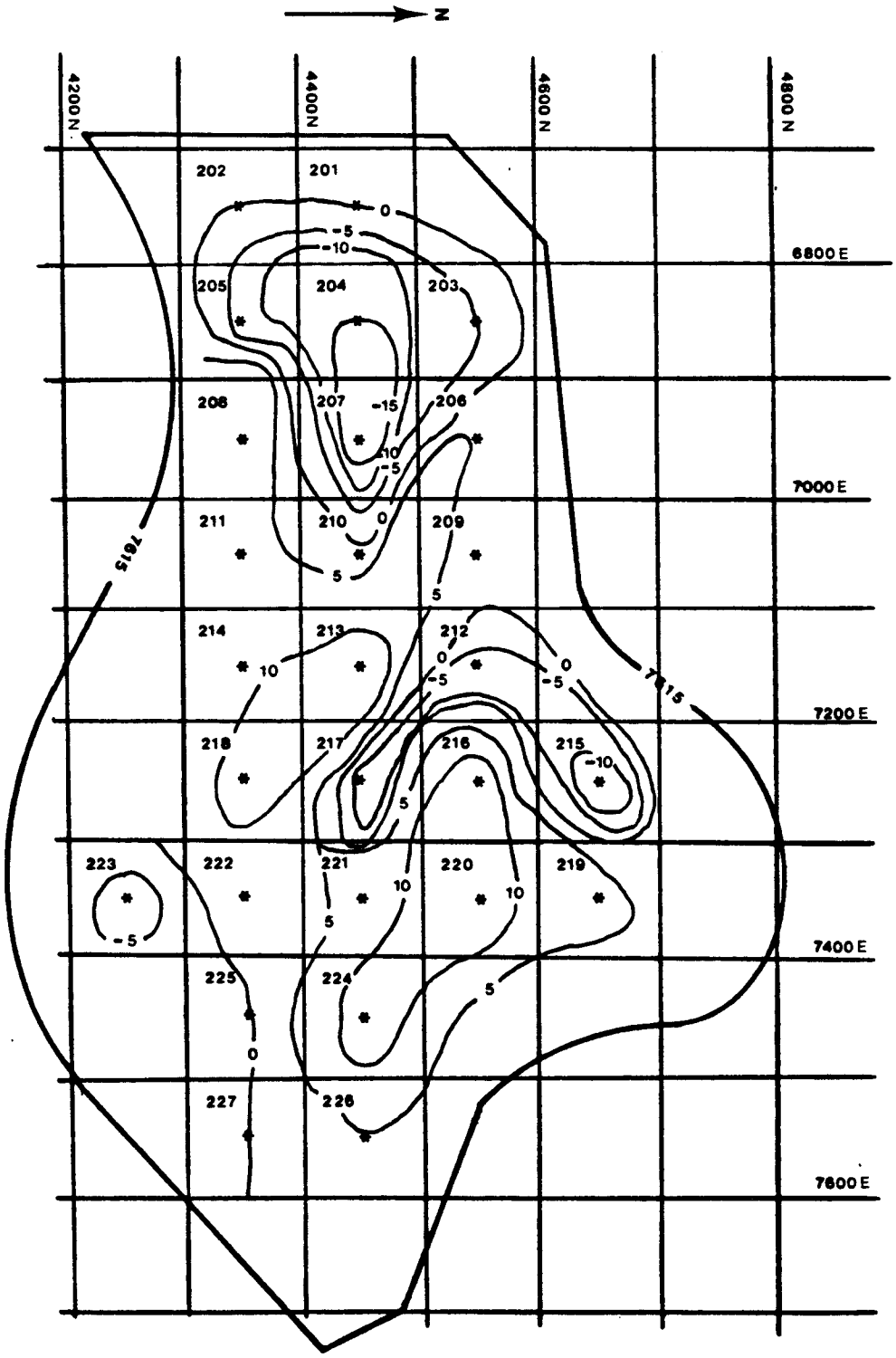

Figure 136: Tonnage Errors for the 7615 Bench

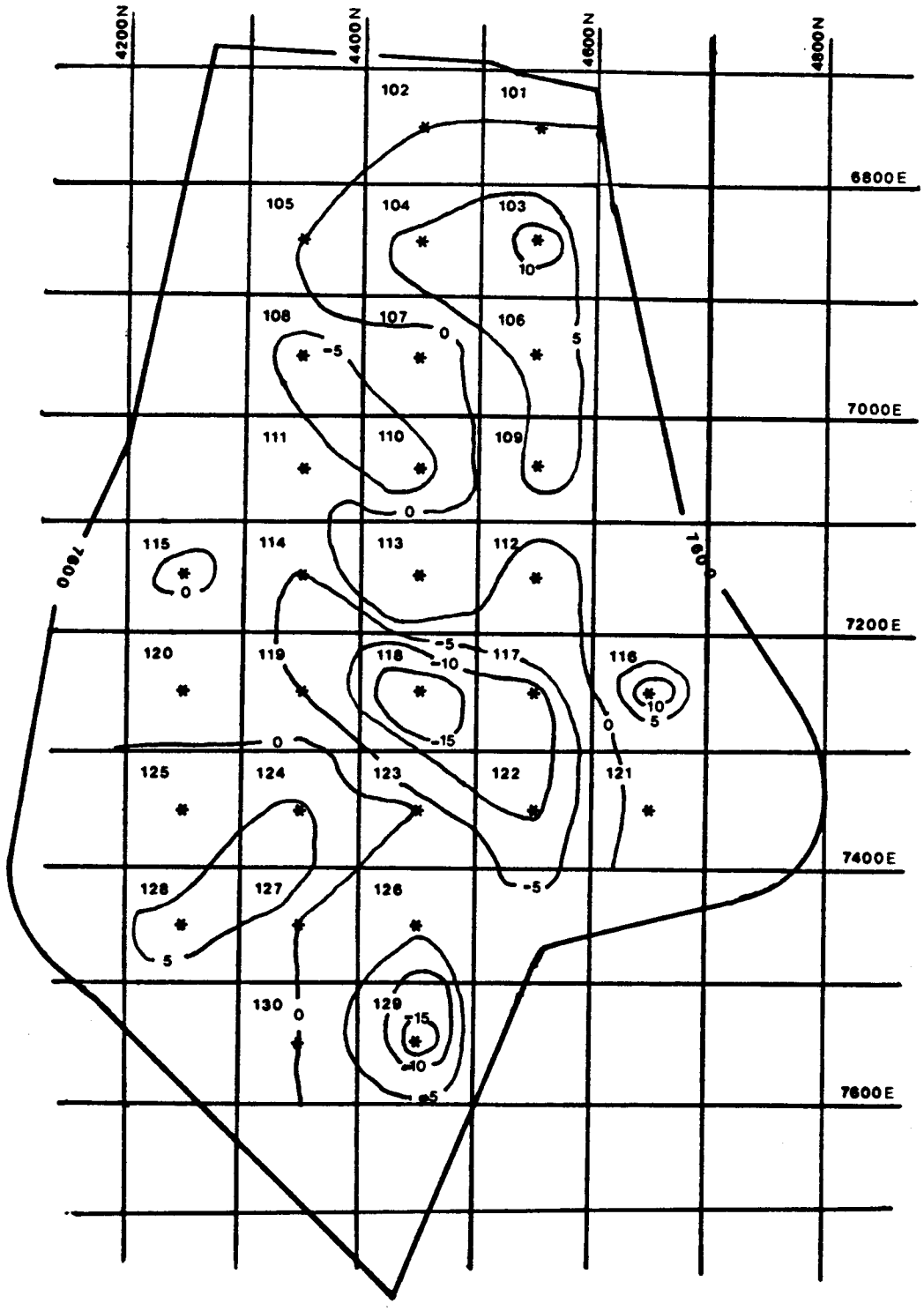

Figure 137: Tonnage Errors for the 7600 Bench

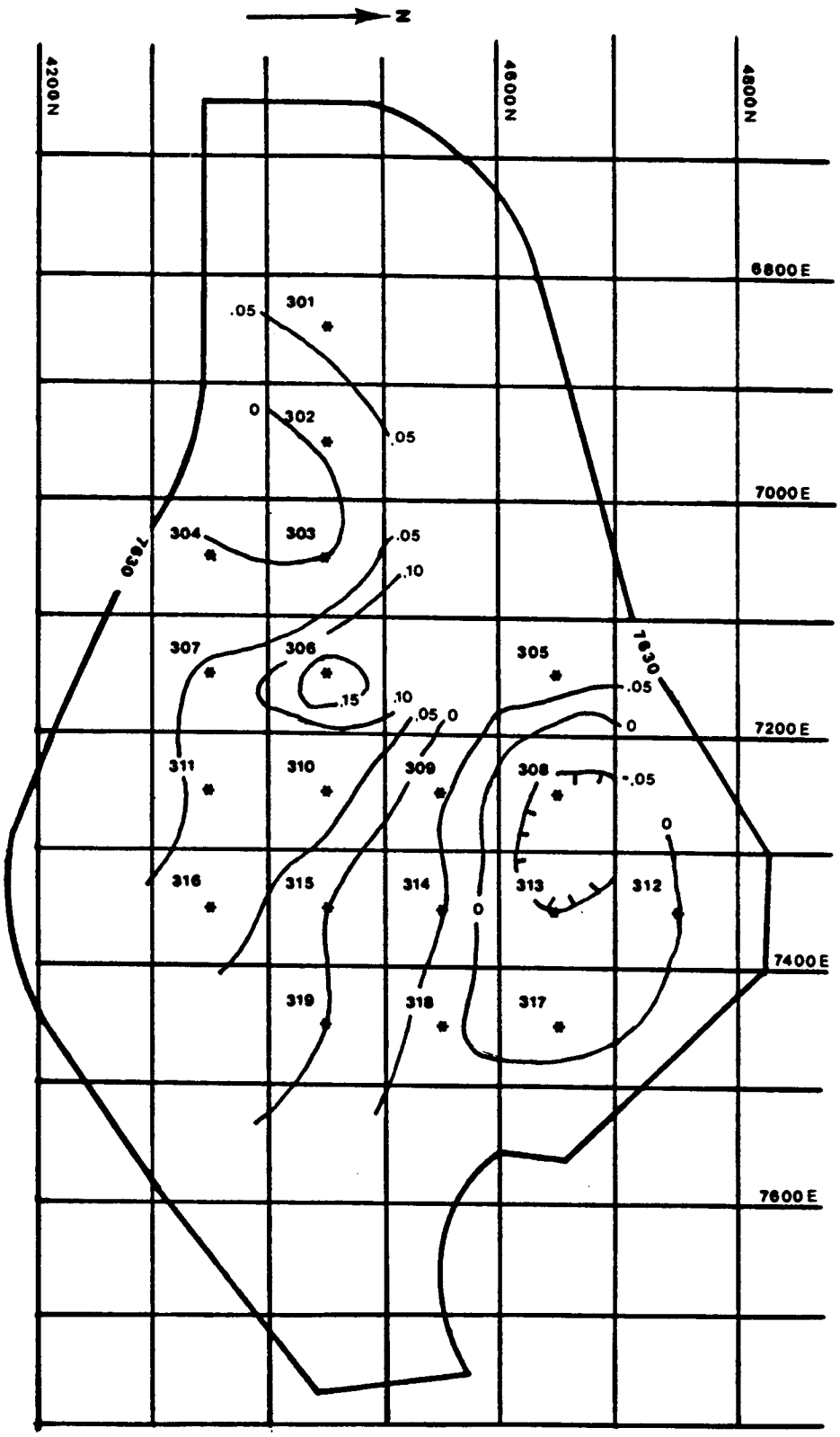

Figure 138: Quantity of Metal Errors for the 7630 Bench

5.8 SUMMARY OF RESULTS

This chapter dealt with the intrinsically difficult problem of estimating the distribution of block support smus within a panel. The proposed solutions to this problem are simple derivatives of the basic indicator and probability kriging estimators of point spatial distributions. Thus the solutions to this difficult problem remain easy to comprehend and apply.

Two varieties of solutions were proposed. The first determines the distribution of block support smus directly from the distribution of point support smus. The second determines block support data which are used to determine the local distribution of block support smus just as point support data are used to estimate the distribution of point support smus. Globally both of these estimators perform well. Surprisingly, in fact, these estimators perform as well as or better than estimators of point support recoveries at equivalent quantiles. Locally, however, the method based on the estimated local point distributions outperformed the estimator based on block data. Furthermore, the method based on estimated point recoveries is robust with respect to deviations of the inputs from the actual values. This was demonstrated by the near equivalence of the local results for estimators based on the true and actual variances used to correct the point distribution. On the basis of these results the estimator based on point recoveries is the preferred estimator. However it must be noted that the hypotheses which form the basis of this estimator were verified to a large degree for this case study. There is no guarantee that the results observed here will also be observed in other case studies.

Chapter VI

SUMMARY AND CONCLUSION

The primary focus of this work has been the development and application of non-parametric estimators of spatial distributions. The two primary estimators which were introduced are termed the indicator and probability kriging estimators. These estimators are optimal in the sense that the estimates obtained minimize the estimation variance. These estimators are therefore very similar in form to the ordinary kriging (minimum estimation variance) estimator of mean grade.

These two estimators were applied to a simulated deposit to examine the capabilities of each of the estimators. The results of this case study indicated that the PK estimator is a better estimator of point support spatial distributions than the IK estimator.

To further examine the capabilities of these two estimators, the local recoverable reserves assuming point support selective mining units were estimated for the Bell Mine. In examining the expression of recovered quantity of metal, it was observed that a spatial distribution estimator utilizing the panel mean could be developed. Such an estimator requires the solution of a quadratic program to preserve the order relations.

The difficult problem of estimating the local recoveries for non-point support smus was also considered. As strictly non-parametric estimators of non-point support recoveries can not be derived,

hypotheses are made which allow the development of two estimators. The first estimator is based on the correction of the estimated point support recoveries for a change of support. The second estimator is based on the determination of block support data. In order to obtain a block support data base to compare to the estimates, a conditional simulation of the Bell Mine was performed.

6.1 FINDINGS OF INTEREST

1. The order relation problems which occasionally occur when applying indicator or probability kriging are small and easily rectified.

2. The indicator kriging estimator is smoother than the probability kriging estimator, hence the local PK estimates are superior. This is especially true when estimating recovered quantity of metal.

3. The estimators introduced require an assumption of bivariate stationarity. The estimators are, however, robust with regard to deviations from bivariate stationarity.

4. When few data are available, a PK or IK type estimator which utilizes the mean panel grade can be superior to either the PK or IK estimators.

5. The quality of the estimates increases with the number of data; however, there is a definite point of diminishing increase in quality.

6. The global recovery of block support tonnage and quantity of metal can be estimated within ±5%.

7. The local block support tonnage and quantity of metal can be estimated nearly as well as the corresponding point support quantities.

6.2 FURTHER WORK

Further work on non-parametric estimators of spatial distributions can be conducted in the following areas.

1. Development of estimators which are based on optimality criteria other than minimum estimation variance.
2. Development of a direct estimator of quantity of metal which obeys all order relations.
3. Examine other models of coregionalization (besides the linear model) which yield positive definite covariance matrices.
4. Determine for which cases the linear ordinary kriging estimates of mean grade are superior to the non-linear estimates given by IK or PK.
5. Examine other permanence of shape hypotheses for determining the distribution of block grades from the distribution of point grades.
6. Derive other estimators of block smu recoveries

6.3 CONCLUSION

The results presented here show that high quality estimators of spatial distributions can be determined which are easy to apply and comprehend. The results, although promising, may not be accepted by the community of mining engineers, however, as the estimators of block smu recoveries were compared to true results obtained from a simulated deposit. To remove any doubt concerning the capabilities of these estimators a comprehensive study utilizing actual production information should be performed.

Chapter VII

APPENDIX - COMPUTER PROGRAMS

This appendix contains the major subroutines necessary to perform a probability or indicator kriging study. The use of each subroutine is demonstrated by a simple case study so that the inputs and the form of the results given can be examined.

7.1 VARIOGRAPHY

The subroutine for determining the indicator and cross variograms necessary to perform probability kriging (subroutine GAMV3) is demonstrated on the campaign #1 data from the Bell mine case study located on the 7600 bench. Only one cross and one direct variogram are calculated in two directions in this demonstration; however, it is possible to use this routine to calculate as many cross or direct variograms as required. It is recommended that this subroutine be used in conjunction with a routine which will plot the experimental variogram values on a plotter or graphics terminal as this will allow for much faster modelling of the variograms. Such a plotting routine is not included here since such routines are very machine and device dependent.

The results given by the GAMV3 routine for the 44 campaign #1 data located on the 7600 bench are:

SEMI - VARIOGRAM

DIRECT VARIOGRAM
VARIOGRAM BETWEEN VARIABLE 1 AND VARIABLE 1

MEAN = 0.29545E 00 VARIANCE = 0.20816E 00 # OF DATA = 44/ 44
TEST = -1.000

	AZIMUTH = 0.0			AZIMUTH = 45.0		
	PLUNGE = 90.0			PLUNGE = 90.0		
	AZIM. TOL.= 15.0			AZIM. TOL.= 15.0		
	PLUN. TOL.= 0.1			PLUN. TOL.= 0.1		
	LAG = 100.0			LAG = 70.7		
	LAG TOL. = 50.0			LAG TOL. = 35.0		
LAG	NP DIST	1/2 VARIO	AV/LAG	NP DIST	1/2 VARIO	AV/LAG
1	0 0.00	0.0000E 00	0.000	0 0.00	0.0000E 00	0.000
2	18 99.93	0.1389E 00	0.306	0 0.00	0.0000E 00	0.000
3	18 198.88	0.1389E 00	0.250	16 141.51	0.1250E 00	0.250
4	10 298.99	0.1000E 00	0.200	0 0.00	0.0000E 00	0.000
5	11 407.39	0.1364E 00	0.136	14 284.03	0.1786E 00	0.250

SEMI - VARIOGRAM

CROSS VARIOGRAM
VARIOGRAM BETWEEN VARIABLE 1 AND VARIABLE 2

MEAN = 0.34032E-01 VARIANCE = 0.34805E-02 # OF DATA = 44/ 44
TEST = -1.000

	AZIMUTH = 0.0			AZIMUTH = 45.0		
	PLUNGE = 90.0			PLUNGE = 90.0		
	AZIM. TOL.= 15.0			AZIM. TOL.= 15.0		
	PLUN. TOL.= 0.1			PLUN. TOL.= 0.1		
	LAG = 100.0			LAG = 70.7		
	LAG TOL. = 50.0			LAG TOL. = 35.0		
LAG	NP DIST	1/2 VARIO	AV/LAG	NP DIST	1/2 VARIO	AV/LAG
1	0 0.00	0.0000E 00	0.000	0 0.00	0.0000E 00	0.000
2	18 99.93	-0.5167E-01	0.490	0 0.00	0.0000E 00	0.000
3	18 198.88	-0.5023E-01	0.474	16 141.51	-0.4793E-01	0.462
4	10 298.99	-0.6217E-01	0.475	0 0.00	0.0000E 00	0.000
5	11 407.39	-0.7984E-01	0.506	14 284.03	-0.5385E-01	0.506

The input data used are: (Note that these values are non-linear transforms of the actual gold grades):

TRANSFORMED DATA FROM THE 7600 BENCH

NORTHING	EASTING	GRADE	NORTHING	EASTING	GRADE
424310.0	387591.0	0.0259	424504.0	387104.0	0.3575
424396.0	387605.0	0.0363	424208.0	387494.0	0.4041
424703.0	387406.0	0.0777	424599.0	386903.0	0.4093
424307.0	387401.0	0.0829	424404.0	387095.0	0.4249
424305.0	387301.0	0.0933	424495.0	386904.0	0.4508
424299.0	386791.0	0.1140	424305.0	387096.0	0.4560
424403.0	387501.0	0.1192	424503.0	387400.0	0.5026
424302.0	387502.0	0.1295	424498.0	387005.0	0.5130
424404.0	386802.0	0.1347	424393.0	387204.0	0.5389
424594.0	386808.0	0.1451	424403.0	387402.0	0.5596
424396.0	386694.0	0.1606	424600.0	386999.0	0.5803
424297.0	386697.0	0.1865	424200.0	387300.0	0.5959
424494.0	387594.0	0.1917	424606.0	387397.0	0.6062
424602.0	387095.0	0.2021	424504.0	386806.0	0.6839
424302.0	386998.0	0.2124	424400.0	387291.0	0.6891
424701.0	387203.0	0.2228	424495.0	387300.0	0.7098
424500.0	387498.0	0.2435	424400.0	386995.0	0.7202
424203.0	387194.0	0.2487	424300.0	387193.0	0.7565
424504.0	386708.0	0.2746	424601.0	387306.0	0.8135
424298.0	386903.0	0.2953	424603.0	387197.0	0.8808
424202.0	387402.0	0.3057	424700.0	387299.0	0.9016
424399.0	386895.0	0.3420	424504.0	387204.0	0.9585

The following is the actual variogram subroutine with a simple driver program.

```
$WATFIV TIME=1000
$ASSIGN 8 TO FILE DATA1 INPUT
$ASSIGN 9 TO FILE RES OUTPUT
      DIMENSION AZM(3),PLG(3),ATOL(3),PTOL(3),TEST(2),X(65),Y(65),
     1Z(65),VR(130),IV(2),JV(2),NP(800),GAM(800),DG(800),UG(800),
     2ND(2),UD(2),VD(19),XLAG(5),DTOL(5),CUT(1),VV(65)
C
C          DEFINE INPUT PARAMETERS
C
      CUT(1) = .2
      IOUT=9
      NV=1
      NT=44
      NVA=2
      IS=1
      LMAX=5
      NDI=2
C
C          DEFINE THE DIRECTIONS ALONG WHICH THE VARIOGRAM WILL
C          BE CALCULATED
C
      DO 2 I=1,2
      AZM(I)=(I-1)*45.
      PLG(I)=90.
      PTOL(I)=.05
      ATOL(I)=15.
   2  CONTINUE
      DO 3 I=1,2
      TEST(I)=-1.
 3    CONTINUE
C
C         DEFINE THE LAG LENGTH AND TOLERANCE FOR EACH DIRECTION
C
      XLAG(1)=100.
      XLAG(2)=70.7
      DTOL(1)=50.
      DTOL(2)=35.
C
C         READ IN THE DATA
C
      READ(8,1000)(X(I),Y(I),Z(I),VV(I),I=1,NT)
 1000 FORMAT(3F10.1,10X,F10.4)
C
C         LOAD DATA VALUE ARRAY VR.  THE FIRST NT VALUES ARE INDICATORS
C         THE SECOND NT DATA ARE UNIFORM DATA
C
       DO 70 I=1,2
       DO 75 J=1,NT
       K=(I-1)*NT + J
       VR(K)=VV(J)
       IF (I.EQ.2) GO TO 75
       VR(K)=1.
       IF(VV(J).GT.CUT(I)) VR(K)=0.
 75    CONTINUE
 70    CONTINUE
C
C         DEFINE THE TYPE OF VARIOGRAMS WHICH WILL BE CALCULATED
C         IN THIS CASE 1 DIRECT AND 1 CROSS VARIOGRAM
C
        IV(1)=1
        IV(2)=1
        JV(1)=1
        JV(2)=2
       CALL GAMV3(IOUT,LMAX,XLAG,DTOL,NDI,AZM,PLG,ATOL,PTOL,TEST,NT,IV,
      1JV,NVA,1,X,Y,Z,VR,ND,UD,VD,NP,DG,GAM,UG,IS)
       STOP


       SUBROUTINE GAMV3 (IOUT,LMAX,XLAG,DTOL,NDI,AZM,PLG,ATOL,PTOL,
      *TEST,NT,IV,JV,NVA,NV,X,Y,Z,VR,ND,UD,VD,NP,DG,GAM,UG,IS)
```

```
C
C
C       THIS ROUTINE CALCULATES THE DIRECT VARIOGRAM FOR VARIABLES
C       WHICH ARE IRREGULARLY OR REGULARLY SAMPLED IN ONE, TWO, OR
C       THREE DIMENSIONS.  IN ADDITION THE CROSS VARIOGRAM BETWEEN
C       ANY TWO VARIABLES CAN BE CALCULATED.
C
C       OUTPUT INCLUDES THE OVERALL MEAN, VARIANCE, AND NUMBER OF DATA
C       FOR EACH VARIABLE, AS WELL AS THE VALUE OF THE EXPERIMENTAL
C       VARIOGRAM IN ANY DIRECTION OR FOR ANY LAG SIZE CHOSEN BY THE
C       USER.
C
C
C  PARAMETERS
C  **********
C       INPUT:
C
C            IOUT              PRINTER UNIT NUMBER
C            LMAX              MAXIMUM NUMBER OF LAGS
C            XLAG(NDI)         LENGTH OF THE UNIT LAG
C            DTOL(NDI)         LAG DISTANCE TOLERANCE
C                              IF DTOL.LE.0.,THEN DTOL=XLAG/2.
C            NDI               NUMBER OF DIRECTIONS FOR WHICH THE
C                              VARIOGRAM WILL BE CALCULATED
C            AZM(NDI)          ANGLE DEFINING THE HORIZONTAL DIRECTION
C                              0 DENOTES WEST-EAST, 90 DENOTES NORTH-SOUTH
C            PLG(NDI)          PLUNGE ANGLE (ANGLE WITH THE VERTICAL)
C                              0=VERTICAL, 90=HORIZONTAL
C            2*ATOL(NDI)       TOLERANCE ANGLE FOR THE AZIMUTH
C                              IF ATOL(NDI).LE.0.0,THEN
C                              ATOL(NDI)=45.0 DEGREES
C            2*PTOL(NDI)       TOLERANCE ANGLE FOR THE PLUNGE
C                              IF PTOL(ID).LE.0 THEN PTOL(ID)=45. DEGREES
C            TEST(NV)          INDICATOR VALUE FOR MISSING DATA
C                              IF THE GRADE VALUE IS < TEST, THEN
C                              THIS DATA VALUE IS CONSIDERED
C                              MISSING AND IS IGNORED
C            NT                NUMBER OF DATA POINTS PER VARIABLE
C                              INCLUDING MISSING DATA VALUES
C            IV(NVA),JV(NVA)   VARIABLE INDICATOR ARRAYS. IF IV=JV=1
C                              A DIRECT VARIOGRAM FOR VARIABLE 1 IS
C                              COMPUTED.  IF IV=1 AND JV=2
C                              A CROSS VARIOGRAM BETWEEN VARIABLES 1
C                              AND 2 IS COMPUTED.
C                              EXAMPLE:
C                              CALCULATE DIRECT AND CROSS VARIOGRAMS
C                              FOR THREE VARIABLES.
C                                     ELEMENTS OF ARRAYS
C                                     ******************
C
C                                       JV        IV
C                                       **        **
C                                        1         1
C                                        2         2
C                                        3         3
C                                        1         2
C                                        1         3
C                                        2         3
C
C            NVA               TOTAL NUMBER OF VARIOGRAM MODELS
C                              NVA=6 IN THE PREVIOUS EXAMPLE
C            NV                NUMBER OF DIRECT VARIOGRAMS
C                              NV=3 IN THE PREVIOUS EXAMPLE
C            X(NT)             COORDINATES OF DATA POINTS
C            Y(NT)
C            Z(NT)
C            VR(NT*NV)         DATA VALUE ARRAY. VALUES ARE STORED
C                              COLUMNWISE. THAT IS, THE FIRST NT VALUES
C                              IN VR ARE FOR VARIABLE 1 FOLLOWED BY THE
C                              NT VALUES FOR VARIABLE 2 AND SO ON.
C
C       OUTPUT:
```

```
C
C            ND(NV)              NUMBER OF DATA PER VARIABLE
C            UD(NV)              AVERAGE OF DATA PER VARIABLE
C            VD(NV)              VARIANCE OF DATA PER VARIABLE
C            NP(LMAX*NDI*NV)     NUMBER OF PAIRS USED
C            DG(LMAX*NDI*NV)     MEAN DISTANCE OF DATA PAIRS
C            GAM(LMAX*NDI*NV)    SEMI-VARIOGRAM VALUES
C            UG(LMAX*NDI*NV)     AVERAGE OF DATA USED TO CALCULATE
C                                THE SEMI-VARIOGRAM
C                                UG CAN BE USED TO INDICATE THE PRESENCE
C                                OF A PROPORTIONAL EFFECT.
C
C      WORKING ARRAYS:
C
C       CX,CY,CZ,SZ,CT,CS        SINE AND COSINE OF DIRECTION AND
C                                TOLERANCE ANGLES
C
C  OPTIONS
C  *******
C              IS.EQ.1           PRINT RESULTS (1 PAGE/VARIABLE)
C                                 MAXIMUM: 4 DIRECTIONS/PAGE/VARIABLE
C
C
      DIMENSION AZM(1),PLG(1),ATOL(1),PTOL(1),TEST(1),X(1),Y(1),Z(1)
     1,VR(1),XLAG(1),DTOL(1),IV(1),JV(1)
      DIMENSION ND(1),UD(1),VD(1),NP(1),DG(1),GAM(1),UG(1)
      DIMENSION CX(15),CY(15),CZ(15),SZ(15),CT(15),CS(15)
      CHARACTER AD(6),AC(6)
C
      DATA IA/' '/
      DATA AD /'D','I','R','E','C','T'/
      DATA AC /'C','R','O','S','S',' '/
C
C       TOLERENCES ARE DEFINED FOR EACH DIRECTION
C
      PI=3.14159265
      DO 1 KD=1,NDI
      IF(DTOL(KD).LE.0) DTOL(KD)=XLAG(KD)/2.
      IF(ATOL(KD).LE.0.OR.ATOL(KD).GT.90) ATOL(KD)=45.
      IF(PTOL(KD).LE.0.OR.PTOL(KD).GT.90) PTOL(KD)=45.
      A=PI*AZM(KD)/180.
      B=PI*PLG(KD)/180.
      T=PI*ATOL(KD)/180.
      S=PI*PTOL(KD)/180.
      CX(KD)=COS(A)
      CY(KD)=SIN(A)
      CZ(KD)=COS(B)
      CT(KD)=COS(T)
      SZ(KD)=SIN(B)
      CS(KD)=COS(S)
      IF(CT(KD).LE..001) CT(KD)=0.
      IF(CS(KD).LE..001) CS(KD)=0.
 1    CONTINUE
C
C        INITIALIZATION OF ARRAYS USED IN DETERMINING THE VARIOGRAM
C        VALUES
C
      LMM=NVA*LMAX*NDI
      DO 40 IL=1,LMM
      NP(IL)=0
      DG(IL)=0.0
      GAM(IL)=0.0
40    UG(IL)=0.0
C
C       INITIALIZATION OF VARIABLE STATISTICS ARRAYS
C
      DO 50 KV=1,NVA
      UD(KV)=0.
      VD(KV)=0.
      ND(KV)=0.
      IV1=IV(KV)
      JV1=JV(KV)
```

```
      IF(IV1.NE.JV1) GO TO 51
      IT=NT*IV1
      VRIT=VR(IT)
      IF(VRIT.LE.TEST(KV)) GO TO 50
      ND(KV)=1
      UD(KV)=VRIT
      VD(KV)=VRIT*VRIT
      GO TO 50
 51   VRI=VR(IV1*NT)
      VRJ=VR(JV1*NT)
      IF(VRI.LE.TEST(IV1).OR.VRJ.LE.TEST(JV1)) GO TO 50
      ND(KV)=ND(KV)+1
      VVV=VRI*VRJ
      UD(KV)=UD(KV)+VVV
      VD(KV)=VD(KV)+VVV*VVV
 50   CONTINUE
C
C       BEGIN CALCULATION OF VARIOGRAM
C
      NT1=NT-1
      DO 300 I=1,NT1
C
C       CHOOSE A SEED POINT AND UPDATE THE STATISTICS ON EACH VARIABLE
C
C
         DO 210 KV=1,NVA
         IV1=IV(KV)
         JV1=JV(KV)
         IF(IV1.NE.JV1) GO TO 211
         IP=I+NT*(IV1-1)
         VRIP=VR(IP)
         IF(VRIP.LE.TEST(KV)) GO TO 210
         ND(KV)=ND(KV)+1
         UD(KV)=UD(KV)+VRIP
         VD(KV)=VD(KV)+VRIP*VRIP
         GO TO 210
 211     IVV=(IV1-1)*NT + I
         JVV=(JV1-1)*NT + I
         VRI=VR(IVV)
         VRJ=VR(JVV)
         IF(VRI.LT.TEST(IV1).OR.VRJ.LT.TEST(JV1)) GO TO 210
         ND(KV)=ND(KV)+1
         VVV=VRI*VRJ
         UD(KV)=UD(KV)+VVV
         VD(KV)=VD(KV)+VVV*VVV
210      CONTINUE
              I1=I+1
              DO 200 J=I1,NT
C
C       CHOOSE A NEW ENDPOINT FOR THE SEED POINT
C
              ISGN=1
              DX=X(J)-X(I)
              IF(DX.LT.0) ISGN=-1
              DY=Y(J)-Y(I)
              IF(DX.EQ.0.AND.DY.LT.0) ISGN=-1
              DZ=Z(J)-Z(I)
              H=SQRT(DX*DX+DY*DY+DZ*DZ)
C
C       LOOP THROUGH ALL DIRECTIONS AND DETERMINE IF THE CURRENT
C       PAIR SHOULD BE USED IN THE VARIOGRAM CALCULATION
C
                DO 120 ID=1,NDI
                IF(H.LT.0.001*DTOL(ID)) GO TO 199
                L=INT(H/XLAG(ID)+0.5)+1
                IF(L.GT.LMAX.OR.ABS(H-(L-1)*XLAG(ID)).GT.DTOL(ID))
     1          GO TO 120
                XY=SQRT(DX*DX+DY*DY)
                IF(XY.EQ.0) GO TO 122
                CD=(DX*CX(ID)+DY*CY(ID))/XY
                IF(ABS(CD).LT.CT(ID)) GO TO 120
 122            CE=(ISGN*XY*SZ(ID)+DZ*CZ(ID))/H
```

```
                ICE=CE*1000+.1
                ICS=CS(ID)*1000+.1
                IF(IABS(ICE).LT.ICS) GO TO 120
C
C       CALCULATION OF SEMI-VARIOGRAM VALUE
C
                IL0=L+LMAX*(ID-1)
                   DO 110 KV=1,NVA
                   IP=I+NT*(IV(KV)-1)
                   IP1=J+NT*(IV(KV)-1)
                   JP=I+NT*(JV(KV)-1)
                   JP1=J+NT*(JV(KV)-1)
                   IL=IL0+NDI*LMAX*(KV-1)
                   IF(VR(IP).LE.TEST(KV).OR.VR(IP1).LE.TEST(KV))
     1             GO TO 110
                   NP(IL)=NP(IL)+1
                   DG(IL)=DG(IL)+H
                   GAM(IL)=GAM(IL)+0.5*(VR(IP)-VR(IP1))*(VR(JP)-VR(JP1
     1             ))
                   UG(IL)=UG(IL)+(VR(IP)+VR(JP1))
110                CONTINUE
120             CONTINUE
               GO TO 200
C
C       DUPLICATED DATA MESSAGE
C
199             WRITE(IOUT,2000)I,X(I),Y(I),J,X(J),Y(J)
C
200             CONTINUE
300   CONTINUE
C
C       RESULTS ARE COMPUTED
C
      DO 400 KV=1,NVA
      IF (ND(KV).EQ.0) GO TO 400
C
C         OVERALL STATISTICS ARE CALCULATED FOR EACH VARIABLE
C
      VD(KV)=(VD(KV)-UD(KV)*UD(KV)/ND(KV))/ND(KV)
      UD(KV)=UD(KV)/ND(KV)
C
C         VARIOGRAM VALUES ARE CALCULATED FOR EACH LAG, DIRECTION AND
C         VARIABLE
C
      IL0=NDI*LMAX*(KV-1)+1
      IL1=IL0+LMAX*NDI-1
           DO 310 IL=IL0,IL1
           NPP=MAX0(1,NP(IL))
           DG(IL)=DG(IL)/NPP
           GAM(IL)=GAM(IL)/NPP
           UG(IL)=UG(IL)/NPP/2.
310        CONTINUE
400   CONTINUE
C
C         PRINT RESULTS?
C
      IF(IS.EQ.0) GO TO 3000
C
C         DETERMINE THE NUMBER OF OUTPUT PAGES REQUIRED FOR EACH VARIABLE
C
      IMP=(NDI-1)/4+1
      IDM=FLOAT(NDI)/FLOAT(IMP)+0.9999
C
C         PRINT RESULTS
C
      DO 600 KV=1,NVA
      DO 500 IM=1,IMP
      IF(JV(KV).EQ.IV(KV)) WRITE(IOUT,2001) IM,(AD(JH),JH=1,6),IV(KV),
     1JV(KV)
      IF(IV(KV).NE.JV(KV)) WRITE(IOUT,2001) IM,(AC(JH),JH=1,6),IV(KV),
     1JV(KV)
      WRITE(IOUT,2002) UD(KV),VD(KV),ND(KV),NT,TEST(KV)
      ID1=1+IDM*(IM-1)
```

```
      ID2=MIN0(NDI,IDM*IM)
      WRITE(IOUT,2003) (IA,AZM(ID),ID=ID1,ID2)
      WRITE(IOUT,2004) ( IA,PLG(ID),ID=ID1,ID2)
      WRITE(IOUT,2005) (IA,ATOL(ID),ID=ID1,ID2)
      WRITE(IOUT,2006) (IA,PTOL(ID),ID=ID1,ID2)
      WRITE(IOUT,2007)(IA,XLAG(ID),ID=ID1,ID2)
      WRITE(IOUT,2008)(IA,DTOL(ID),ID=ID1,ID2)
      WRITE(IOUT,2009) (IA,ID=ID1,ID2)
      IL0=NDI*LMAX*(KV-1)+LMAX*(ID1-1)
      ILM=IL0+LMAX*(ID2-ID1)
C
C       PRINT EXPERIMENTAL VARIOGRAM VALUES
C
          DO 410 L=1,LMAX
          IL1=L+IL0
          IL2=L+ILM
          WRITE(IOUT,2010)L,(NP(IL),DG(IL),GAM(IL),UG(IL),
     *     IL=IL1,IL2,LMAX)
410       CONTINUE
500   CONTINUE
600   CONTINUE
      WRITE(IOUT,2011)
C
C       FORMAT STATEMENTS
C
2000  FORMAT(1H1,'DUPLICATED DATA***GAM-V3***  DATA',I4,
     *' X= ',F9.4,' Y= ',F9.4
     *,'  DATA  ',I4,' X= ',F9.4,' Y= ',F9.4)
2001  FORMAT(1H1,45X,' SEMI - VARIOGRAM          ',30X,'***PAGE:',I2,
     *///,26X,6A1,' VARIOGRAM',/,
     120X,'VARIOGRAM BETWEEN VARIABLE',I5,' AND VARIABLE',I5)
2002  FORMAT(//,6X,'MEAN =',E12.5,3X,'VARIANCE =',E12.5,3X,'# OF DATA ='
     1,I4,'/',I4,4X,'TEST =',F8.3,/)
2003  FORMAT(1H ,4X,'|',4(A1,5X,'AZIMUTH   =',F6.1,8X,'|'))
2004  FORMAT(1H ,4X,'|',4(A1,5X,' PLUNGE   =',F6.1,8X,'|'))
2005  FORMAT(1H ,4X,'|',4(A1,5X,'AZIM. TOL.=',F6.1,8X,'|'))
2006  FORMAT(1H ,4X,'|',4(A1,5X,'PLUN. TOL.=',F6.1,8X,'|'))
2007  FORMAT(1H ,4X,'|',4(A1,7X,'LAG     =',F6.1,8X,'|'))
2008  FORMAT(1H ,4X,'|',4(A1,6X,'LAG TOL. =',F6.1,8X,'|'))
2009  FORMAT(1H ,'LAG |',
     *4(A1,' NP',3X,'DIST',3X,'1/2 VARIO',2X,'AV/LAG|'))
2010  FORMAT(1H ,I3,1X,'|',4(I4,F7.2,2X,E11.4,F7.3,'|'))
2011  FORMAT('1')
3000  RETURN
      END
```

7.2 PROBABILITY AND INDICATOR KRIGING ROUTINES

The probability and indicator kriging programs are demonstrated on a simple case study which utilizes four data from the campaign #1 data set of the Bell Mine case study to estimate the tonnage and quantity of metal recovered for one panel. The inputs to the PK routine (PK3D) and the IK routine (IK3D) are similar so once the workings of one routine are understood it is a simple matter to understand the other. Each of these routines calls three other subroutines: COVA which calculates covariances between pairs of points; KSOL which solves linear systems of equations; and ORDER which resolves order relation problems.

The results of probability kriging for one panel are given below. This comprehensive output was obtained by specifying the debug option in the call of PK3D.

```
          **** PROBABILITY KRIGING FOR  2 CUTOFFS ***


VARIOGRAM PARAMETERS USED
     NOTE: THE FIRST  2 MODELS ARE INDICATOR VARIOGRAMS
           THE SECOND  2 MODELS ARE CROSS VARIOGRAMS
           THE LAST VARIOGRAM MODEL IS FOR THE U VARIOGRAM


 FOR MODEL #  1 THERE ARE 1 NESTED STRUCTURES
              NUGGET= 0.0350
                       STRUCTURE # 1 IS A TYPE 1 MODEL
                            C  =    0.1290
                            RANGE= 140.00
                            X ANIS. FACTOR 1.0000
                            Y ANIS. FACTOR 1.0000
                            Z ANIS. FACTOR 1.0000

 FOR MODEL #  2 THERE ARE 1 NESTED STRUCTURES
              NUGGET= 0.0450
                       STRUCTURE # 1 IS A TYPE 1 MODEL
                            C  =    0.0450
                            RANGE= 130.00
                            X ANIS. FACTOR 1.0000
                            Y ANIS. FACTOR 1.0000
                            Z ANIS. FACTOR 1.0000

 FOR MODEL #  3 THERE ARE 1 NESTED STRUCTURES
              NUGGET=-0.0045
                       STRUCTURE # 1 IS A TYPE 1 MODEL
                            C  =   -0.0776
                            RANGE= 180.00
                            X ANIS. FACTOR 1.0000
                            Y ANIS. FACTOR 1.0000
                            Z ANIS. FACTOR 1.0000

 FOR MODEL #  4 THERE ARE 1 NESTED STRUCTURES
              NUGGET=-0.0045
                       STRUCTURE # 1 IS A TYPE 1 MODEL
                            C  =   -0.0293
                            RANGE= 150.00
                            X ANIS. FACTOR 1.0000
                            Y ANIS. FACTOR 1.0000
                            Z ANIS. FACTOR 1.0000
```

```
 FOR MODEL #  5 THERE ARE 1 NESTED STRUCTURES
                NUGGET= 0.0400
                        STRUCTURE # 1 IS A TYPE 1 MODEL
                             C =    0.0490
                             RANGE= 420.00
                             X ANIS. FACTOR 1.0000
                             Y ANIS. FACTOR 1.0000
                             Z ANIS. FACTOR 1.0000

                NOTE
                A TYPE 0 MODEL IS EXPONENTIAL
                A TYPE 1 MODEL IS SPHERICAL
                A TYPE 2 MODEL IS LINEAR


 PANEL TO BE KRIGED:

 CENTER OF PANEL:    X = 387350.    Y = 424650.    Z =  7600.
 BLOCK DIMENSIONS:      X-DIR.:  100.00 Y-DIR.:  100.00 Z-DIR.:    1.00
 DISCRETIZATION POINTS: X-DIR.:       6 Y-DIR.:       6 Z-DIR.:       1


 NUMBER OF SAMPLES GIVEN:     4

       X-COORD.      Y-COORD.      Z-COORD.      GRADE    LOCATION #
      387406.       424703.        7600.        0.078         1
      387397.       424606.        7600.        0.606         2
      387306.       424601.        7600.        0.813         3
      387299.       424700.        7600.        0.902         4


 CUTOFF GRADES USED
   0.8000  0.9000


       INDICATOR DATA
LOCATION #    1    2    3    4
 CUTOFF  1
              1    1    0    0
 CUTOFF  2
              1    1    1    0


                *** COVARIANCE MATRICES FOR ALL CUTOFFS ***

                     COVARIANCES FOR CUTOFF = 0.8000
   RHS                       LEFT HAND SIDE
 0.033 0.164
 0.043 0.016 0.164
 0.042 0.000 0.021 0.164
 0.037 0.010 0.000 0.015 0.164
-0.029-0.082-0.021-0.005-0.017 0.089
-0.035-0.021-0.082-0.024-0.006 0.032 0.089
-0.035-0.005-0.024-0.082-0.020 0.025 0.033 0.089
-0.032-0.017-0.006-0.020-0.082 0.031 0.026 0.032 0.089
 1.000 1.000 1.000 1.000 1.000 0.000 0.000 0.000 0.000 0.000
 0.000 0.000 0.000 0.000 0.000 1.000 1.000 1.000 1.000 0.000 0.000

                     COVARIANCES FOR CUTOFF = 0.9000
   RHS                       LEFT HAND SIDE
 0.010 0.090
 0.014 0.004 0.090
 0.013 0.000 0.005 0.090
 0.012 0.002 0.000 0.003 0.090
-0.008-0.034-0.005-0.000-0.003 0.089
```

```
-0.011-0.005-0.034-0.006-0.000 0.032 0.089
-0.011-0.000-0.006-0.034-0.004 0.025 0.033 0.089
-0.009-0.003-0.000-0.004-0.034 0.031 0.026 0.032 0.089
 1.000 1.000 1.000 1.000 1.000 0.000 0.000 0.000 0.000 0.000
 0.000 0.000 0.000 0.000 0.000 1.000 1.000 1.000 1.000 0.000 0.000

WEIGHTS FOR ALL CUTOFFS
CUTOFF                      WEIGHTS
0.8000 0.223 0.269 0.257 0.250 0.011-0.003-0.005-0.003-0.010-0.001
0.9000 0.234 0.261 0.256 0.249 0.009-0.006-0.003-0.001-0.012 0.001
```

MESSAGE FROM SUBROUTINE ORDER

INPUT TONNAGES	OUTPUT TONNAGES
0.5151	0.5151
0.2553	0.2553

RECOVERIES FOR PANEL 121

X = 387350.0 Y = 424650.0 Z = 7600.0

CUTOFF	TONNAGE	METAL	GRADE
0.80	0.515	0.217	0.421
0.90	0.255	0.164	0.641

Similarly the results of applying indicator kriging to the same panel are:

```
                ***** INDICATOR KRIGING FOR  2 CUTOFFS ****


        VARIOGRAM PARAMETERS USED


        FOR CUTOFF #  1 THERE ARE 1 NESTED STRUCTURES
                        NUGGET= 0.0350
                                STRUCTURE # 1 IS A TYPE 1 MODEL
                                     C  =    0.1290
                                     RANGE= 140.00
                                     X ANIS. FACTOR 1.0000
                                     Y ANIS. FACTOR 1.0000
                                     Z ANIS. FACTOR 1.0000

        FOR CUTOFF #  2 THERE ARE 1 NESTED STRUCTURES
                        NUGGET= 0.0450
                                STRUCTURE # 1 IS A TYPE 1 MODEL
                                     C  =    0.0450
                                     RANGE= 130.00
                                     X ANIS. FACTOR 1.0000
                                     Y ANIS. FACTOR 1.0000
                                     Z ANIS. FACTOR 1.0000

                        NOTE
                        A TYPE 0 MODEL IS EXPONENTIAL
                        A TYPE 1 MODEL IS SPHERICAL
                        A TYPE 2 MODEL IS LINEAR


        PANEL TO BE KRIGED:

        CENTER OF PANEL:    X =  387350.0    Y =  424650.0    Z =  7600.0
        BLOCK DIMENSIONS:      X-DIR.:  100.00 Y-DIR.:  100.00 Z-DIR.:   1.00
        DISCRETIZATION POINTS: X-DIR.:       6 Y-DIR.:       6 Z-DIR.:      1


        NUMBER OF SAMPLES GIVEN:     4

              X-COORD.      Y-COORD.      Z-COORD.      GRADE   LOCATION #
             387406.0      424703.0       7600.00       0.078        1
             387397.0      424606.0       7600.00       0.606        2
             387306.0      424601.0       7600.00       0.813        3
             387299.0      424700.0       7600.00       0.902        4


        CUTOFF GRADES USED
          0.8000  0.9000


        INDICATOR DATA
LOCATION #
                1    2    3    4
 CUTOFF  1
                1    1    0    0
 CUTOFF  2
                1    1    1    0


                *** COVARIANCE MATRICES FOR ALL CUTOFFS ***
```

COVARIANCES FOR CUTOFF = 0.8000

RHS	LEFT HAND SIDE			
0.0329	0.1640			
0.0435	0.0161	0.1640		
0.0422	0.0000	0.0208	0.1640	
0.0375	0.0099	0.0002	0.0148	0.1640

COVARIANCES FOR CUTOFF = 0.9000

RHS	LEFT HAND SIDE			
0.0099	0.0900			
0.0136	0.0039	0.0900		
0.0131	0.0000	0.0054	0.0900	
0.0115	0.0020	0.0000	0.0035	0.0900

WEIGHTS FOR ALL CUTOFFS

CUTOFF	WEIGHTS			
0.8000	0.1666	0.2217	0.2111	0.1992
0.9000	0.1017	0.1386	0.1330	0.1205

MESSAGE FROM SUBROUTINE ORDER

INPUT TONNAGES	OUTPUT TONNAGES
0.4505	0.4505
0.1711	0.1711

RECOVERIES FOR PANEL 121

X = 387350.0 Y = 424650.0 Z = 7600.0

CUTOFF	TONNAGE	METAL	GRADE
0.80	0.451	0.167	0.371
0.90	0.171	0.110	0.641

The routines PK3D, COVA, KSOL, and ORDER as well as the driver program used to obtain the previous results are:

```
$WATFIV   TIME=1000
$ASSIGN 8 TO FILE UDAT INPUT
$ASSIGN 9 TO FILE RES OUTPUT
$ASSIGN 10 TO FILE LOC INPUT
C
C
      DIMENSION X(400),Y(400),Z(400),VR(4400),TN(10),TNV(10),Q(10)
       DIMENSION GRA(400),IV2(200),TRUE(200),EST(200),VAR(200)
      DIMENSION ISP(400),XX(400),YY(400),ZZ(400),VR1(500),CUT(2)
     1,IPPP(130)
      DIMENSION AVE(2),XL(120),YL(120),ZL(120),TT(10),CUT1(1)
      DOUBLE PRECISION NAM(10)
      COMMON INP,IOUT,TEST,NV,NAM
      COMMON /STRUC/ NST(5),C0(5),AA(1,5),C(1,5),IT(1,5),AX(1,5)
     1,AY(1,5),AZ(1,5),COSAL,SINAL
      DATA CUT/.80,.90/
      DATA IT/5*1/
      DATA C0/.035,.045,-.0045,-.0045,.04/
      DATA AA/140.,130.,180.,150.,420./
      DATA C/.129,.045,-.0776,-.0293,.049/
      DATA AVE/.205,.641/
      DATA NST/5*1/
      DATA AX/5*1./
      DATA AY/5*1./
      DATA AZ/5*1./
      NV=5
      TEST=-9.99
      INP=8
      IOUT=9
C
C       ENTER KRIGING PARAMETERS
C
      COSAL=1.
      SINAL=0.
      DBX=100.
      DBY=100.
      DBZ=1
      NX=6
      NY=6
      NZ=1
      NKMAX=9
      RADIUS=110*110
      IS=1
      NC=2
C
C      READ IN DATA
C
C
       NP=30
       READ(INP,853)(Y(I),X(I),Z(I),GRA(I),I=1,44)
 853   FORMAT(1X,3F10.1,10X,F10.4)
C
C        READ IN PANEL LOCATIONS
C
       READ(10,953) (IPPP(I),XL(I),YL(I),ZL(I),I=1,NP)
 953   FORMAT(I3,F7.0,F7.0,F5.0)
      DO 8 I=1,NP
C
C          SINCE KRIGING WILL BE PERFORMED ON ONLY ONE PANEL THE
C          FOLLOWING TEST IS INCLUDED
C
      IF(IPPP(I).NE.121) GO TO 8
      XOB=XL(I)
      YOB=YL(I)
      ZOB=ZL(I)
      WRITE(6,199) XOB,YOB,ZOB
 199  FORMAT('  NOW WORKING ON PANEL',3F10.1)
C
```

```
C        FIND DATA IN KRIGING NEIGHBORHOOD
C
      K=0
      DO 15 J=1,44
      IF(Z(J).NE.ZOB) GO TO 15
      R2=(X(J)-XOB)**2+(Y(J)-YOB)**2
      IF(R2.GT.RADIUS) GO TO 15
      K=K+1
      XX(K)=X(J)
      YY(K)=Y(J)
      ZZ(K)=Z(J)
      VR(K)=GRA(J)
 15   CONTINUE
C
C          CALL PK3D TO KRIGE THIS PANEL
C
      CALL PK3D(XX,YY,ZZ,VR,K,XOB,YOB,ZOB,DBX,DBY,DBZ,NX,NY,NZ,NC,CUT,
     1AVE,TN,Q,TE,TM,1,2,1,0)
C
C           PRINT OUT RESULTS FOR THIS PANEL
C
      WRITE(IOUT,2000) IPPP(I),XL(I),YL(I),ZL(I)
      DO 40 LL=1,NC
      XM=0
      IF(TN(LL).EQ.0) GO TO 41
      XM=Q(LL)/TN(LL)
 41   WRITE(IOUT,2001) CUT(LL),TN(LL),Q(LL),XM
 40   CONTINUE
2000  FORMAT(//,20X,'RECOVERIES FOR PANEL',I4,//,13X,'X =',F9.1,'  Y =',
     1F9.1,'  Z =',F7.1,//,17X,'CUTOFF',3X,'TONNAGE',3X,'METAL',2X,
     2'GRADE')
2001  FORMAT(18X,F4.2,5X,F5.3,4X,F5.3,2X,F5.3)
8     CONTINUE
      STOP
      END
      SUBROUTINE PK3D(X,Y,Z,VR,ND,XB,YB,ZB,DBX,DBY,DBZ,NBX,NBY,NBZ,NC,
     1CUT,AVE,TN,Q,TE,TM,IDBUG,INC,IOR,IMED)
C
C
C                          ***** PK3D *****
C
C        THIS ROUTINE PERFORMS PROBABILITY KRIGING TO ESTIMATE THE
C        LOCAL SPATIAL DISTRIBUTION WITHIN A PANEL OR AT A POINT.
C
C     IMPORTANT!
C
C     THIS ROUTINE PERFORMS PROBABILITY KRIGING ON ONLY A SINGLE PANEL.
C     THE DATA ARRAYS MUST CONTAIN ONLY THE DATA WHICH WILL BE USED
C     TO ESTIMATE THE PANEL.  ALL SEARCHING FOR DATA IN THE NEIGHBORHOOD
C     OF THE PANEL MUST BE DONE PRIOR TO CALLING THE SUBROUTINE AND
C     THE SUBROUTINE MUST BE CALLED ONCE FOR EACH PANEL WHICH WILL
C     BE ESTIMATED.
C
C     THE DATA AND CUTOFF VALUES SUPPLIED TO THIS ROUTINE MUST BE THE
C     UNIFORM TRANSFORM U(X) OF THE GRADE RATHER THAN THE GRADE VALUE
C     ITSELF. THE TRANSFORMATION FROM THE GRADE U(X) TO THE INDICATOR
C     DATA IS DONE WITHIN THE SUBROUTINE.
C
C     THIS ROUTINE RETURNS THE TONNAGE AND QUANTITY OF METAL ESTIMATES
C     FOR EACH OF THE CUTOFFS OF INTEREST AS WELL AS THE ESTIMATED
C     MEAN AND MEDIAN OF THE PANEL.
C
C     WHERE  APPLICABLE, LOAD ALL ARRAYS IN ASCENDING CUTOFF ORDER.
C     THAT IS, THE FIRST ENTRY IN THE ARRAY APPLIES TO THE LOWEST CUTOFF
C     THE SECOND ENTRY APPLIES TO THE SECOND LOWEST CUTOFF AND SO ON.
C
C     THE TONNAGE ESTIMATES RETURNED BY THIS ROUTINE MAY HAVE
C     ORDER RELATION PROBLEMS.  USE SUBROUTINE ORDER IN CONJUNCTION
C     WITH THIS PROGRAM TO FIX ANY ORDER RELATION PROBLEMS
C
C*************************************************************************
C
```

```
C                       PARAMETERS TO SUPPLY
C
C     COMMON
C            INP        INPUT UNIT
C            IOUT       OUTPUT UNIT
C            DUM        NOT USED
C            NV         NUMBER OF VARIOGRAM MODELS (# OF CUTOFFS*2+1)
C            NAM(NV)    NAME OF EACH VARIABLE (A8) (NOT USED)
C
C     VARIOGRAM STRUCTURAL PARAMETERS:
C
C     COMMON /STRUC/     NST,C0,A,C,IT,AX,AY,AZ,COSAL,SINAL
C                        (SEE SUBROUTINE COVA)
C                        THE TOTAL NUMBER OF VARIOGRAMS REQUIRED IS
C                        (# OF CUTOFFS)*2 + 1
C                        LOAD INDICATOR VARIOGRAM MODELS FIRST FOLLOWED
C                        BY CROSS INDICATOR VARIOGRAM MODELS.  THE U(X)
C                        VARIOGRAM MODEL IS LAST.
C                        N.B. DIMENSIONS OF COMMON ARRAYS IN CALLING PGM.
C                        AND SUBROUTINES MUST MATCH UP
C
C     INPUT
C     *****
C
C          X  Y Z (ND)   COORDINATES OF DATA LOCATIONS
C          VR (ND)       UNIFORM TRANSFORM OF THE DATA THAT WILL BE
C                        USED TO ESTIMATE THE PANEL
C          ND            NUMBER OF DATA PASSED IN ARRAY VR
C          XB YB ZB      COORDINATES OF THE CENTER OF THE PANEL BEING
C                        ESTIMATED
C          DBX DBY DBZ   BLOCK DIMENSIONS IN THE X Y AND Z DIRECTIONS
C          NBX NBY NBZ   NUMBER OF DISCRETIZATION POINTS / BLOCK ALONG
C                        X,Y AND Z (MAX. OF 64 POINTS/BLOCK ASSUMED)
C          NC            NUMBER OF CUTOFFS FOR WHICH ESTIMATES ARE
C                        OBTAINED
C          CUT(NC)       CUTOFF VALUES FOR WHICH TONNAGES WILL BE
C                        ESTIMATED.  CUT(1) IS THE LOWEST CUTOFF VALUE
C                        AND CUT(NC) IS THE HIGHEST. (CUT IS EXPRESSED
C                        IN TERMS OF THE UNIFORM TRANSFORM OF GRADE)
C          AVE(NC)       USED TO CALCULATE THE QUANTITY OF METAL
C                        RECOVERED.  AVE IS SOME MEASURE OF CENTRAL
C                        TENDENCY OF THE MATERIAL BETWEEN CUTOFFS
C                        I-1 AND I.  FOR INSTANCE AVE(NC-1) COULD BE
C                        THE AVERAGE OF ALL DATA WITH VALUES BETWEEN
C                        CUTOFFS NC-1 AND NC.
C    OUTPUT
C    ******
C
C          TN(NC)        ESTIMATED TONNAGE RECOVERED AT EACH OF THE NC
C                        CUTOFFS.
C          Q(NC)         ESTIMATED QUANTITY OF METAL RECOVERED.
C                        IF SUBROUTINE ORDER IS NOT CALLED, THE VALUES
C                        RETURNED IN Q(NC),TE, MAY BE MEANINGLESS
C
C          TE            ESTIMATED MEAN GRADE
C          TM            ESTIMATED MEDIAN GRADE
C                        IF THE ESTIMATED MEDIAN GRADE IS LARGER
C                        THAN THE LARGEST CUTOFF THE MEDIAN GRADE IS
C                        UNDEFINED AND A VALUE OF -9. IS RETURNED IN TM
C
C    OPTIONS
C    *******
C
C          IDBUG         IF IDBUG=1 THE FOLLOWING INFORMATION WILL BE
C                        PRINTED.
C                             DATA LOCATIONS AND GRADES
C                             THE CORRESPONDING INDICATOR VALUES
C                             ALL COVARIANCE MATRICES
C                             ALL WEIGHTS
C          INC           INC IS THE # OF NON BIAS CONDITIONS UTILIZED
C                        SET INC=2 FOR STANDARD PK
C          IOR           IF IOR=1 SUBROUTINE ORDER IS CALL TO REMOVE
```

```
C                       ANY ORDER RELATION PROBLEMS
C          IMED         IF IMED=1 MEDIAN PK IS PERFORMED. THAT IS, THE
C                       INDICATOR AND CROSS VARIOGRAM MODELS AR
C                       IDENTICAL FOR ALL CUTOFFS SO ORDER RELATIONS
C                       ARE ENSURED.  HENCE IF IMED=1 SET IOR=0
C                       ALSO IF IMED=1 ONLY ONE INDICATOR AND CROSS
C                       VARIOGRAM MODEL NEED BE SUPPLIED REGARDLESS OF
C                       THE NUMBER OF CUTOFFS OF INTEREST NC.
C
C
C
C      SUBROUTINES
C          COVA         COVARIANCE CALCULATION
C          KSOL         SOLUTION OF KRIGING SYSTEMS
C          ORDER        REMOVES ORDER RELATION PROBLEMS
C
C
C**************************************************************************
C
C        INTERNAL VARIABLES
C
C
C        NEQ             NUMBER OF EQUATIONS (NEQ=ND*2+INC)
C        A R RR IER      KRIGING MATRIX VARIABLES (SEE KSOL)
C
C        XS(NC*NEQ)      SOLUTION ARRAY
C        CB,CB1,COV(NC)  AVERAGE COVARIANCES
C        DNX DNY DNZ     SPACING BETWEEN DISCRETIZATION POINTS ALONG X,Y,Z
C        XDB,YDB,ZDB(NBX*NBY*NBZ) COORDINATES OF DISCRETIZATION POINTS
C                                 RELATIVE TO CENTER OF BLOCK
C        IVR(NC*ND)      INDICATOR DATA
C
C
      DIMENSION X(1),Y(1),Z(1),VR(1),TN(1),TNV(1),Q(1),CUT(1),
     1AVE(1)
      DIMENSION R(275),RR(275),XS(275),A(3575),CB(21),CB1(21),
     1          COV(21),XDB(64),YDB(64),ZDB(64),
     2          IVR(130),CBB(21)
C
      DOUBLE PRECISION NAM(10)
      COMMON INP,IOUT,TEST,NV,NAM
      COMMON/STRUC/NST(5),C0(5),AA(1,5),C(1,5),IT(1,5),AX(1,5),
     1AY(1,5),AZ(1,5),COSAL,SINAL
      NC1=NC-1
      NCC=NC
      IF(IMED.EQ.1) NC=1
C
C*****PRINT VARIOGRAM AND PANEL LOCATION INFORMATION
C
         IF (IDBUG.NE.1) GO TO 2
      WRITE(IOUT,1000) NCC
      IF(IMED.EQ.1) WRITE(IOUT,1001)
      WRITE(IOUT,1002) NC,NC
      DO 1 IV=1,NV
      WRITE(IOUT,1003) IV,NST(IV),C0(IV)
      NS=NST(IV)
      WRITE(IOUT,1004)(IK,IT(IK,IV),C(IK,IV),AA(IK,IV),AX(IK,IV),
     1AY(IK,IV),AZ(IK,IV),IK=1,NS)
 1    CONTINUE
      WRITE(IOUT,1005)
      WRITE(IOUT,1006) XB,YB,ZB,DBX,DBY,DBZ,NBX,NBY,NBZ
C
C       PRINT DATA VALUES
C
      WRITE(IOUT,1007) ND
      WRITE(IOUT,1008) (X(LL),Y(LL),Z(LL),VR(LL),LL,LL=1,ND)
 2    CONTINUE
C
C      DEFINE INDICATOR DATA
C
      L=0
      DO 3 J=1,NCC
```

```
      DO 3 K=1,ND
      L=L+1
      IVR(L)=0
      IF(VR(K).LT.CUT(J)) IVR(L)=1
 3    CONTINUE
C
C      PRINT OUT INDICATOR DATA AND CUTOFF GRADES IF NECESSARY
C
      IF (IDBUG.NE.1) GO TO 4
      WRITE(IOUT,1009)(CUT(IU),IU=1,NCC)
      WRITE(IOUT,1010) (IU,IU=1,ND)
      DO 5 I=1,NCC
      L1=(I-1)*ND + 1
      L2=I*ND
      WRITE(IOUT,1011) I,(IVR(L),L=L1,L2)
 5    CONTINUE
 4    CONTINUE
C
C*****DISCRETIZATION POINTS
C
      NDB=NBX*NBY*NBZ
      N=0
C
      DNX=DBX/FLOAT(NBX)
      DNY=DBY/FLOAT(NBY)
      DNZ=DBZ/FLOAT(NBZ)
C
      X0=0.5*(DNX-DBX)
      Y0=0.5*(DNY-DBY)
      Z0=0.5*(DNZ-DBZ)
C
      DO 10 K=1,NBZ
      ZN=Z0+(K-1)*DNZ
      DO 10 J=1,NBX
      XN=X0+(J-1)*DNX
      DO 10 I=1,NBY
      N=N+1
      ZDB(N)=ZN
      XDB(N)=XN
      YDB(N)=Y0+(I-1)*DNY
10    CONTINUE
C
C***** BEGIN KRIGING
C
            NEQ=ND*2+INC
            NN=(NEQ+1)*NEQ/2
C
C*****      SET UP KRIGING MATRICES
C
            IN=0
            DO 80 J=1,ND
            N1=(J+ND-1)*(J+ND)/2
            DO 75 I=1,J
            IN=IN+1
            N2=(I+ND-1)*(I+ND)/2
            IN1=N1+I
            IN2=N2+J
            IN3=IN1+ND
C
C*****      COVARIANCE BETWEEN SAMPLES
C
            CALL COVA(X(I),Y(I),Z(I),X(J),Y(J),Z(J),COV)
            DO 70 IV=1,NC
            K1=IN+NN*(IV-1)
            K2=IN1+NN*(IV-1)
            K3=IN2+NN*(IV-1)
            K4=IN3+NN*(IV-1)
            IV2=IV+NC
            IV3=NV
C
C           LOAD LEFT HAND SIDE MATRIX
C
```

```
            A(K1)=COV(IV)
            A(K2)=COV(IV2)
            A(K3)=COV(IV2)
            A(K4)=COV(IV3)
70          CONTINUE
75          CONTINUE
C
C*****      COVARIANCE BETWEEN SAMPLES AND BLOCK
C
            DO 76 IV=1,NV
            CB(IV)=0.
76          CONTINUE
C
            XX=X(J)-XB
            YY=Y(J)-YB
            ZZ=Z(J)-ZB
            DO 77 J1=1,NDB
            CALL COVA(XX,YY,ZZ,XDB(J1),YDB(J1),ZDB(J1),COV)
            DO 77 IV=1,NC
            CB(IV)=CB(IV) + COV(IV)
            IV2=NC+IV
            CB(IV2)=CB(IV2)+COV(IV2)
77          CONTINUE
C
C          LOAD RIGHT HAND SIDE MATRIX
C
            DO 80 IV=1,NC
            CB(IV)=CB(IV)/FLOAT(NDB)
            IV2=IV+NC
            K=J + NEQ*(IV-1)
            CB(IV2)=CB(IV2)/FLOAT(NDB)
            R(K)=CB(IV)
            RR(K)=R(K)
            KK=K+ND
            R(KK)=CB(IV2)
            RR(KK)=R(KK)
80          CONTINUE
C
C               LOAD ROWS IN LHS MATRIX CORRESPONDING TO NON BIAS
C               CONDITIONS
C
            IF(INC.EQ.0) GO TO 801
            NUC=ND*INC*2 + INC +INC-1
            IT2=NUC-INC
            IT1=IT2-ND
            IN=IN3
            DO 79 L=1,NUC
            IN=IN+1
            DO 79 IV=1,NC
            K=IN+(IV-1)*NN
            A(K)=0
            IF(L.LE.ND) A(K)=1.
            IF(L.GT.IT1.AND.L.LE.IT2) A(K)=1.
 79         CONTINUE
             DO 81 IV=1,NC
             KB=NEQ*IV
             RR(KB)=1.
             R(KB)=1.
             IF(INC.EQ.1) GO TO 81
             R(KB-1)=1
             RR(KB-1)=1
             R(KB)=0
             RR(KB)=0
 81          CONTINUE
801          CONTINUE
C
C
C
C       PRINT OUT MATRICES IF REQUIRED
C
      IF (IDBUG.NE.1) GO TO 83
            L1=0
```

```
            IEN=0
            WRITE(IOUT,1012)
            DO 89 IV=1,NC
            WRITE(IOUT,1013) CUT(IV)
C
            DO 82 JG=1,NEQ
            L1=L1+1
            IST=IEN+1
            IEN=IST+JG-1
            WRITE(IOUT,1014) R(L1),(A(KX),KX=IST,IEN)
 82         CONTINUE
 89         CONTINUE
 83     CONTINUE
C
C*****      SOLVE THE SYSTEM
C
            CALL KSOL(NC,NEQ,1,1,1,A,R,XS,IER)
            IF(IER .NE. 0) WRITE(IOUT,1015) XB,YB,ZB
C
C       PRINT OUT WEIGHTS IF REQUIRED
C
            IF (IDBUG.NE.1) GO TO 90
            WRITE(IOUT,1016)
            DO 85 J=1,NC
            L1=NEQ*(J-1)+1
            L2=NEQ*J
            WRITE(IOUT,1017)CUT(J),(XS(L),L=L1,L2)
  85        CONTINUE
  90        CONTINUE
C
C*****    SOLUTION
C
         DO 100 IV=1,NCC
         WTS=0
         TNN=0.
         DO 95 I=1,ND
         IK=I+NEQ*(IV-1)
         IF(IMED.EQ.1) IK=I
         IKK=ND+IK
         IKD=I+ND*(IV-1)
         WTS=WTS+XS(IK)
         IF(INC.EQ.2)TNN=TNN + XS(IK)*IVR(IKD)+VR(I)*XS(IKK)
         IF(INC.EQ.1)TNN=TNN+XS(IK)*IVR(IKD)+(VR(I)
     1   (CUT(IV)-.5))*XS(IKK)
         IF(INC.EQ.0) TNN=TNN+XS(IK)*IVR(IKD)+(.5-VR(I))*XS(IKK)
 95      CONTINUE
         IF(INC.EQ.0) TNN=WTS*CUT(IV)+TNN
         TN(IV) = 1 - TNN
 100  CONTINUE
      IF(IOR.EQ.1) CALL ORDER(TN,NCC,IDBUG)
C
C     FIND QUANTITY OF METAL, MEAN AND MEDIAN ESTIMATES
C
      IF(NCC.EQ.1) GO TO 134
      Q(NCC)=TN(NCC)*AVE(NCC)
      TE=Q(NCC)
      TYM=TN(NCC)
      IF(TYM.LT..5) GO TO 120
      TM = -9.
 120  DO 130 LJ=2,NCC
      LLJ=NCC-LJ+1
      TE=(AVE(LLJ))*(TN(LLJ)-TN(LLJ+1))+TE
      Q(LLJ)=TE
      IF(TN(LJ).LT..5.AND.TN(LJ-1).GE..5) GO TO 140
      GO TO 130
 140  DIF=(TN(LJ)-.5)/(TN(LJ)-TN(LJ-1))
      TM=CUT(LJ)-DIF*(CUT(LJ)-CUT(LJ-1))
 130  CONTINUE
 134  CONTINUE
C
C          FORMAT STATEMENTS
C
```

```
C
 1000 FORMAT('1',44X,'**** PROBABILITY KRIGING FOR ',I2,' CUTOFFS *** ')
 1001 FORMAT(/,55X,'MEDIAN PK OPTION')
 1002 FORMAT(////,10X,'VARIOGRAM PARAMETERS USED',/,15X,
     1'NOTE: THE FIRST',I3,' MODELS ARE INDICATOR VARIOGRAMS',/,
     215X,'      THE SECOND',I3,' MODELS ARE CROSS VARIOGRAMS',/,
     315X,'      THE LAST VARIOGRAM MODEL IS FOR THE U VARIOGRAM'//)
 1003 FORMAT(/,10X,' FOR MODEL #',I3,' THERE ARE',I2,
     1' NESTED STRUCTURES',/,26X,'NUGGET=',F7.4)
 1004 FORMAT(35X,'STRUCTURE #',I2,' IS A TYPE',I2,' MODEL',/,40X,
     1'C  =   ',F7.4,/,40X,'RANGE=',F7.2,/,40X,'X ANIS. FACTOR',F7.4,
     2/,40X,'Y ANIS. FACTOR',F7.4,/,40X,'Z ANIS. FACTOR',F7.4)
 1005 FORMAT(/,26X,'NOTE',/,26X,'A TYPE 0 MODEL IS EXPONENTIAL',/,
     126X,'A TYPE 1 MODEL IS SPHERICAL',/,26X,
     2'A TYPE 2 MODEL IS LINEAR')
 1006 FORMAT(///10X,'PANEL TO BE KRIGED:'//
     3          10X,'CENTER OF PANEL:    X = ',F7.0, '    Y = ',
     4   F7.0,4X,'Z =',F7.0,/ 10X,
     5'BLOCK DIMENSIONS:      X-DIR.: ',F7.2,' Y-DIR.: ',F7.2,' Z-DIR.:'
     6  ,F7.2,/ 10X,'DISCRETIZATION POINTS: X-DIR.: ',I7,
     7              ' Y-DIR.: ',I7,' Z-DIR.:',I7,//)
 1007 FORMAT(//10X,'NUMBER OF SAMPLES GIVEN: ',I5,///
     1 17X,'X-COORD.',5X,'Y-COORD.',5X,'Z-COORD.',6X,'GRADE',3X
     2,'LOCATION #')
 1008 FORMAT(10X,5X,F8.0,5X,F8.0,5X,F8.0,5X,F8.3,3X,I6)
 1009 FORMAT(//,10X,'CUTOFF GRADES USED',/,10X,14F8.4)
 1010 FORMAT(///,10X,'INDICATOR DATA',/,2X,'LOCATION #',25I5,//)
 1011 FORMAT(3X,'CUTOFF',I3,/,12X,25I5)
 1012 FORMAT(///,20X,'*** COVARIANCE MATRICES FOR ALL CUTOFFS ***')
 1013 FORMAT(/,25X,'COVARIANCES FOR CUTOFF =',F7.4,/,5X,'RHS',24X,
     1'LEFT HAND SIDE')
 1014 FORMAT(2X,21F6.3)
 1015 FORMAT(1X,'****************** FOR BLOCK: XB = ',F8.1,'YB = ',
     1F8.1,' ZB=',F8.3)
 1016 FORMAT(/,'  WEIGHTS FOR ALL CUTOFFS',/,2X,'CUTOFF',20X,'WEIGHTS')
 1017 FORMAT(1X,F7.4,20F6.3)
      RETURN
      END
C
C
C
C
      SUBROUTINE KSOL(NRIGHT,NEQ,KSDIM,KADIM,NSB,A,R,S,ISING)
C
C               SOLUTION OF A SYSTEM OF LINEAR EQUATIONS
C               ----------------------------------------
C
C               -UPPER TRIANGULAR LEFT HAND SIDE MATRIX
C               -PIVOTS ARE ON THE DIAGONAL
C               -DOES NOT SEARCH FOR MAX. ELEMENT FOR PIVOT
C               -SEVERAL RIGHT HAND SIDE MATRICES
C               -FOR OK AND SK ONLY!!
C                NOT TO BE USED IF DOING UK
C
C  ***INPUT***
C
C             NRIGHT*NSB      -NUMBER OF COLUMNS IN RIGHT HAND SIDE
C                              MATRIX
C                              FOR CHAIN, NRIGHT=1
C                              FOR OKB2D, NRIGHT=NUMBER OF VARIABLES
C                              FOR CHAIN, NSB=NUMBER OF SUBBLOCKS
C                                         PER SUPERBLOCK
C                              FOR OKB2D, NSB=1
C
C             NEQ              -NUMBER OF EQUATIONS
C                              SAME FOR CHAIN AND OKB2D
C                              FOR SK, NEQ=MAXIMUM NUMBER OF DATA
C                                          RETAINED IN A SEARCH (MAXNA)
C                              FOR OK, NEQ=MAXNA+1
C
C             DIMENSIONS CALCULATED BY SUBR. SETUP IN CHAIN
C
```

```
C               KSDIM           -DIMENSION OF RIGHT HAND SIDE MATRIX:
C                                (MAXNA+1)*NRIGHT*NSB
C
C               KADIM           -DIMENSION OF UPPER TRIANGULAR LEFT HAND
C                                SIDE MATRIX:  (MAXNA+1)*(MAXNA+2)/2
C
C
C:::::INPUT ARRAYS TO DIMENSION IN CALLING PROGRAM
C
C               A(KADIM)        -UPPER TRIANGULAR LEFT HAND SIDE MATRIX
C                                (STORED COLUMNWISE)
C               R(KSDIM)        -RIGHT HAND SIDE MATRIX
C                                (STORED COLUMNWISE)
C                                FOR CHAIN, ONE COLUMN PER SUBBLOCK
C                                FOR OKBCD, ONE COLUMN PER VARIABLE
C
C  ***OUTPUT***
C
C:::::OUTPUT ARRAY TO DIMENSION IN CALLING PROGRAM
C
C               S(KSDIM)        -SOLUTION ARRAY, SAME DIMENSION AS  R  ABOVE.
C
C               ISING           -SINGULARITY INDICATOR
C                   =  0        -NO SINGULARITY PROBLEM
C                   = -1        -NEQ .LE. 1
C                   =  K        -A NULL PIVOT APPEARED AT THE KTH ITERATION
C
C
C?????DIMENSIONING MACHINE-DEPENDENT
      DIMENSION A(1),R(1),S(1)
C
C*****NUMBER OF EQUATIONS .LE. 1?
      IF(NEQ .LE. 1) GO TO 150
C
C*****INITIALIZATIONS
C
      TOL=0.0
      ISING=0
      NN=NEQ*(NEQ+1)/2
      NM=NSB*NEQ
      M1=NEQ-1
      KK=0
C
C*****START TRIANGULATION
        DO 70 K=1,M1
        KK=KK+K
        AK=A(KK)
        IF(AK-TOL)20,10,20
 10     ISING=K
        RETURN
C
 20     KM1=K-1
          DO 60 IV=1,NRIGHT
          NM1=NM*(IV-1)
          II=KK+NN*(IV-1)
          PIV=1./A(II)
          LP=0
            DO 50 I=K,M1
            LL=II
            II=II+I
            AP=A(II)*PIV
            LP=LP+1
            IJ=II-KM1
              DO 30 J=I,M1
              IJ=IJ+J
              LL=LL+J
              A(IJ)=A(IJ)-AP*A(LL)
 30           CONTINUE
C
              DO 40 LLB=K,NM,NEQ
              IN=LLB+LP+NM1
              LL1=LLB+NM1
```

```
            R(IN)=R(IN)-AP*R(LL1)
 40         CONTINUE
 50       CONTINUE
 60     CONTINUE
 70   CONTINUE
C
      IJM=IJ-NN*(NRIGHT-1)
      IF(A(IJM)-TOL)90,80,90
 80   ISING=NEQ
      RETURN
C
C*****END OF TRIANGULATION
C
C*****START SOLVING BACK
C
 90     DO 140 IV=1,NRIGHT
        NM1=NM*(IV-1)
        IJ=IJM+NN*(IV-1)
        PIV=1./A(IJ)
          DO 100 LLB=NEQ,NM,NEQ
          LL1=LLB+NM1
          S(LL1)=R(LL1)*PIV
 100      CONTINUE
C
        I=NEQ
        KK=IJ
          DO 130 II=1,M1
          KK=KK-I
          PIV=1./A(KK)
          I=I-1
            DO 120 LLB=I,NM,NEQ
            LL1=LLB+NM1
C
            IN=LL1
            AP=R(IN)
            IJ=KK
              DO 110 J=I,M1
              IJ=IJ+J
              IN=IN+1
              AP=AP-A(IJ)*S(IN)
 110          CONTINUE
            S(LL1)=AP*PIV
 120        CONTINUE
 130  CONTINUE
 140  CONTINUE
      RETURN
C
C
 150  ISING=-1
      RETURN
      END
      SUBROUTINE COVA(X1,Y1,Z1,X2,Y2,Z2,COV)
C
C       COVARIANCE FUNCTION BETWEEN TWO POINTS.  NV VARIABLES
C
C  PARAMETERS
C         X1,Y1,Z1          REAL COORDINATES OF THE FIRST POINT
C         X2,Y2,Z2          REAL COORDINATES OF THE SECOND POINT
C         COV(NV)           COVARIANCE VALUE/VARIABLE
C
C    COMMON /STRUC/
C         NST(NV)           # OF NESTED STRUCTURES (.LE. 3)/VARIABLE
C         C0(NV)            NUGGET EFFECT
C         A(NST,NV)         RANGES OF THE NESTED STRUCTURES
C                           (1/3 OF PRACTICAL RANGE IF EXPONENTIAL STRUC)
C                           (DUMMY RANGE IF VARIOGRAM IS LINEAR)
C         C(NST,NV)         MULTIPLICATIVE FACTORS OF THE NESTED
C                           STRUCTURES.
C                           (SILL-C0) FOR EXPONENTIAL AND SPHERICAL STRUC.
C                           (DUMMY SILL - C0) FOR LINEAR STRUCTURE
C         IT(NST,NV)=0      NESTED STRUCTURE IS EXPONENTIAL, PARAMETER A
C                           I.E. PRACTICAL RANGE IS 3A
```

```
C                   =1    NESTED STRUCTURE IS SPHERICAL, RANGE A
C                   =2    LINEAR VARIOGRAM, DUMMY RANGE A
C                          NOTE:  DUMMY RANGE A IS THE MAXIMUM DISTANCE
C                                 FOR WHICH VARIOGRAM IS USED;
C                                 DUMMY SILL (I.E. C0+C) IS SEMI-VARIO-
C                                 GRAM VALUE AT THE DUMMY RANGE DISTANCE
C               WARNING!!  IF A LINEAR VARIOGRAM IS USED, THEN THERE
C                          MAY BE NO OTHER NESTED STRUCTURES!!!
C
C         AX,AY,AZ(NST,NV)  AFFINITY CORRECTION PARAMETERS/STRUCTURE/
C                           VARIABLE (GEOMETRIC ANISOTROPY)
C         COSAL,SINAL       DIRECTION COSINE AND SINE DEFINING THE
C                           ANGLE OF ROTATION OF THE COORDINATE
C                           SYSTEM.  IDENTICAL FOR ALL STRUCTURES AND
C                           ALL VARIABLES.  IF NO ROTATION IS NEEDED
C                           (I.E. ROTATION ANGLE IS ZERO), THEN
C                           COSAL=1.  AND  SINAL=0.
C
C
      DIMENSION COV(1)
      DOUBLE PRECISION NAM(5)
      COMMON INP,IOUT,TESTK,NV,NAM
      COMMON/STRUC/NST(5),C0(5),A(1,5),C(1,5),IT(1,5),AX(1,5),
     1AY(1,5),AZ(1,5),COSAL,SINAL
      DO 100 IV=1,NV
  100 COV(IV)=0.
C          ROTATE AXES
      DX=(X2-X1)*COSAL+(Y2-Y1)*SINAL
      DY=(X1-X2)*SINAL+(Y2-Y1)*COSAL
      DZ=Z2-Z1
      H=DX*DX+DY*DY+DZ*DZ
      DO 30 IV=1,NV
      IF (IT(1,IV) .EQ. 2) GO TO 15
      IF(H.GT.0.001)GO TO 10
      NS=NST(IV)
      COV(IV)=C0(IV)
      DO 1 IS=1,NS
    1 COV(IV)=COV(IV)+C(IS,IV)
      GO TO 30
10    NS=NST(IV)
      DO 12 IS=1,NS
      DX1=DX*AX(IS,IV)
      DY1=DY*AY(IS,IV)
      DZ1=DZ*AZ(IS,IV)
      H=SQRT(DX1*DX1+DY1*DY1+DZ1*DZ1)/A(IS,IV)
      IF(IT(IS,IV).EQ.0)GO TO 13
      IF(H.GE.1.)GO TO 12
      COV(IV)=COV(IV)+C(IS,IV)*(1.-H*(1.5-0.5*H*H))
      GO TO 12
   13 COV(IV)=COV(IV)+C(IS,IV)*EXP(-H)
   12 CONTINUE
      GO TO 30
C
   15 SILL=C0(IV) + C(1,IV)
      IF(H .GT. 0.001)GO TO 20
      COV(IV)=SILL
      GO TO 30
C
   20 H=SQRT(H)
      IF(H .GT. A(1,IV)) GO TO 25
      COV(IV)=C(1,IV)*(1 - H/A(1,IV))
      GO TO 30
C
   25 COV(IV)=0.0
30    CONTINUE
      RETURN
      END
      SUBROUTINE ORDER(T,NC,IDBUG)
C
C        SUBROUTINE ORDER RESOLVES ANY ORDER RELATION PROBLEMS
C        BY TAKING THE AVERAGE OF ALL POINTS IN THE REGION OF
C        THE PROBLEM.  THE SOLUTION GIVEN BY THIS ROUTINE IS NEARLY
```

```
C        IDENTICAL TO THAT GIVEN BY QUADRATIC PROGRAMMING.
C
C        INPUT
C        *****
C
C        T(NC)      IK OR PK RECOVERED TONNAGE ESTIMATES
C        NC         NUMBER OF CUTOFFS
C        IDBUG      IF IDBUG=1 THE INPUT AND OUTPUT TONNAGES ARE PRINTED
C
C        OUTPUT
C        ******
C
C        T(NC)     TONNAGE ESTIMATES WHICH OBEY THE ORDER RELATIONS
C
C        COMMON     INP,IOUT,GARB,NV,NAM
C                   IOUT=OUTPUT FILE
C                   ALL OTHER ELEMENTS ARE NOT USED
C
C
      DIMENSION T(1),TT(20),TO(20)
      COMMON INP,IOUT,GARB,NV,NAM
C
C         INITIALIZE ARRAYS
C
      DO 5 I=1,NC
      TO(I)=T(I)
      IF(T(I).LT.0) T(I)=0.
      IF(T(I).GT.1) T(I)=1.
      T(I)=1-T(I)
   5  CONTINUE
      TT(1)=T(1)
      IF (T(1).LT.0) TT(1)=0
      IF(T(1).GT.1) TT(1)=1.
C
C         INITIALIZE OR RE-INITIALIZE COUNTERS
C
  23  IS=0
      J=1
      LE=0
           DO 10 I=2,NC
           IF(T(I).LE.0) TT(I)=0
           IF(T(I).GT.1) TT(I)=1.
           IF(LE+1.GT.I) GO TO 10
C
C             ORDER RELATION PROBLEMS?
C
           IF(T(I).LT.TT(I-1)) GO TO 11
           TT(I)=T(I)
           GO TO 10
C
C             FIX ORDER RELATION PROBLEMS
C
  11       AV=TT(I-1)
            IS=1
  12       K=I+J
           AV=AV+T(K-1)
           J=J+1
           AVE=AV/J
            IF(AVE.GT.1) AVE=1.
           IF(K.GT.NC) GO TO 18
           IF(AVE.GT.T(K)) GO TO 12
  18       CONTINUE
           LS=I-1
           LE=LS+J-1
           J=1
                DO 16 L=LS,LE
                TT(L)=AVE
                T(L)=AVE
  16            CONTINUE
  10       CONTINUE
      IF(IS.EQ.0) GO TO 24
      DO 25 IJ=1,NC
```

```
      T(IJ)=TT(IJ)
 25   CONTINUE
C
C           RETURN TO THE START AND CHECK FOR OTHER ORDER RELATION
C           PROBLEMS
C
      GO TO 23
 24   DO 30 I=1,NC
      T(I)=1-TT(I)
 30   CONTINUE
      IF(IDBUG.NE.1) GO TO 20
      WRITE(IOUT,1000)
      WRITE(IOUT,1001)(TO(I),T(I),I=1,NC)
 20   CONTINUE
C
C         OUTPUT FORMAT
C
 1000 FORMAT(//,16X,'MESSAGE FROM SUBROUTINE ORDER',//,20X,'INPUT',
     111X,'OUTPUT',/,19X,'TONNAGES',8X,'TONNAGES')
 1001 FORMAT( 19X,F7.4,9X,F7.4)
      RETURN
      END
$DATA
```

The routine IK3D as well as the driver routine used to obtain the previous IK results are;

```
$WATFIV   TIME=1000
$ASSIGN 8 TO FILE UDAT INPUT
$ASSIGN 9 TO FILE RES OUTPUT
$ASSIGN 10 TO FILE LOC INPUT
C
C
      DIMENSION X(400),Y(400),Z(400),VR(4400),TN(10),Q(10)
       DIMENSION GRA(400),IV2(200),TRUE(200),EST(200),VAR(200)
      DIMENSION ISP(400),XX(400),YY(400),ZZ(400),VR1(500),CUT(2)
     1,IPPP(130),CDF(2)
      DIMENSION AVE(2),XL(120),YL(120),ZL(120),TT(10),CUT1(1)
      DOUBLE PRECISION NAM(10)
      COMMON INP,IOUT,TEST,NV,NAM
      COMMON /STRUC/ NST(2),C0(2),AA(1,2),C(1,2),IT(1,2),AX(1,2)
     1,AY(1,2),AZ(1,2),COSAL,SINAL
      DATA CUT/.80,.90/
      DATA CDF/.80,.90/
      DATA IT/2*1/
      DATA C0/.035,.045/
      DATA AA/140.,130./
      DATA C/.129,.045/
      DATA AVE/.205,.641/
      DATA NST/2*1/
      DATA AX/2*1./
      DATA AY/2*1./
      DATA AZ/2*1./
      NV=2
      TEST=-9.99
      INP=8
      IOUT=9
C
C       ENTER KRIGING PARAMETERS
C
      COSAL=1.
      SINAL=0.
      DBX=100.
      DBY=100.
      DBZ=1
      NX=6
      NY=6
      NZ=1
      NKMAX=9
      RADIUS=110*110
      IS=1
      NC=2
C
C      READ IN DATA
C
C
       NP=30
       READ(INP,853)(Y(I),X(I),Z(I),GRA(I),I=1,44)
 853   FORMAT(1X,3F10.1,10X,F10.4)
C
C        READ IN PANEL LOCATIONS
C
       READ(10,953) (IPPP(I),XL(I),YL(I),ZL(I),I=1,NP)
 953   FORMAT(I3,F7.0,F7.0,F5.0)
      DO 8 I=1,NP
C
C         SINCE KRIGING WILL BE PERFORMED ON ONLY ONE PANEL THE
C         FOLLOWING TEST IS INCLUDED
C
      IF(IPPP(I).NE.121) GO TO 8
      XOB=XL(I)
      YOB=YL(I)
      ZOB=ZL(I)
      WRITE(6,199) XOB,YOB,ZOB
 199  FORMAT('  NOW WORKING ON PANEL',3F10.1)
C
C        FIND DATA IN KRIGING NEIGHBORHOOD
```

```
C
      K=0
      DO 15 J=1,44
      IF(Z(J).NE.ZOB) GO TO 15
      R2=(X(J)-XOB)**2+(Y(J)-YOB)**2
      IF(R2.GT.RADIUS) GO TO 15
      K=K+1
      XX(K)=X(J)
      YY(K)=Y(J)
      ZZ(K)=Z(J)
      VR(K)=GRA(J)
 15   CONTINUE
C
C          CALL PK3D TO KRIGE THIS PANEL
C
      CALL IK3D(XX,YY,ZZ,VR,K,XOB,YOB,ZOB,DBX,DBY,DBZ,NX,NY,NZ,NC,CUT,
     1CDF,AVE,TN,Q,TE,TM,1,0,1)
C
C           PRINT OUT RESULTS FOR THIS PANEL
C
      WRITE(IOUT,2000) IPPP(I),XL(I),YL(I),ZL(I)
      DO 40 LL=1,2
      XM=0
      IF(TN(LL).EQ.0) GO TO 41
      XM=Q(LL)/TN(LL)
 41   WRITE(IOUT,2001) CUT(LL),TN(LL),Q(LL),XM
 40   CONTINUE
2000  FORMAT(//,20X,'RECOVERIES FOR PANEL',I4,//,13X,'X =',F9.1,'  Y =',
     1F9.1,'  Z =',F7.1,//,17X,'CUTOFF',3X,'TONNAGE',3X,'METAL',2X,
     2'GRADE')
2001  FORMAT(18X,F4.2,5X,F5.3,4X,F5.3,2X,F5.3)
8     CONTINUE
      STOP
      END
      SUBROUTINE IK3D(X,Y,Z,VR,ND,XB,YB,ZB,DBX,DBY,DBZ,NBX,NBY,NBZ,
     1NC,CUT,CDF,AVE,TN,Q,TE,TM,IDBUG,IMED,IOR)
C
C
C                          ***** IK3D *****
C
C     INDICATOR KRIGING OF A THREE-DIMENSIONAL PANEL OR POINT
C
C     IMPORTANT!
C
C     THIS ROUTINE PERFORMS INDICATOR KRIGING ON ONLY A SINGLE PANEL.
C     THE DATA ARRAYS MUST CONTAIN ONLY THE DATA WHICH WILL BE USED
C     TO ESTIMATE THE PANEL.  ALL SEARCHING FOR DATA IN THE NEIGHBORHOOD
C     OF THE PANEL MUST BE DONE PRIOR TO CALLING THE SUBROUTINE AND
C     THE SUBROUTINE MUST BE CALLED ONCE FOR EACH PANEL WHICH WILL
C     BE ESTIMATED.
C
C     THIS ALGORITHM USES SIMPLE KRIGING SO THE LOCAL MEAN MUST BE
C     PROVIDED.
C
C     THE TRANSFORMATION FROM THE GRADE Z(X) TO THE INDICATOR DATA
C     IS DONE WITHIN THE SUBROUTINE.  THE USER MUST SUPPLY THE GRADE
C     AT EACH LOCATION ALONG WITH THE CUTOFFS OF INTEREST TO THE
C     SUBROUTINE.
C
C     THIS ROUTINE RETURNS THE TONNAGE AND QUANTITY OF METAL ESTIMATES
C     FOR EACH OF THE CUTOFFS OF INTEREST AS WELL AS THE ESTIMATED
C     MEAN AND MEDIAN.
C
C*****************************************************************************
C
C                         PARAMETERS TO SUPPLY
C
C     COMMON
C            INP         INPUT UNIT
C            IOUT        OUTPUT UNIT
C            DUM         NOT USED
C            NV          NUMBER OF VARIOGRAM MODELS
```

```
360
C                       NV EQUALS THE NUMBER OF CUTOFFS OF INTEREST
C                       UNLESS MEDIAN IK IS PERFORMED IN THIS CASE NV=1
C            NAM(NV)    NAME OF EACH VARIABLE (NOT USED)
C
C     VARIOGRAM STRUCTURAL PARAMETERS:
C
C     COMMON /STRUC/     NST,C0,A,C,IT,AX,AY,AZ,COSAL,SINAL
C                        (SEE SUBROUTINE COVA)
C                        N.B. DIMENSIONS OF COMMON ARRAYS IN CALLING PGM.
C                        AND SUBROUTINES MUST MATCH UP
C
C     INPUT
C     *****
C
C          X Y Z(ND)      COORDINATES OF SAMPLES
C          VR (ND)        GRADES OF THE DATA USED TO ESTIMATE THE
C                         PANEL
C          ND            NUMBER OF DATA LOCATIONS
C          XB YB ZB       COORDINATES OF THE CENTER OF THE PANEL BEING
C                         ESTIMATED
C          DBX DBY DBZ    PANEL DIMENSIONS IN THE X Y AND Z DIRECTIONS
C          NBX NBY NBZ    NUMBER OF DISCRETIZATION POINTS IN THE
C                         X,Y AND Z DIRECTIONS (MAX. OF 64 POINTS)
C          CUT(NC)        CUTOFF VALUES FOR WHICH TONNAGES WILL BE
C                         ESTIMATED.  CUT(1) IS THE LOWEST CUTOFF VALUE
C                         AND CUT(NC) IS THE HIGHEST.
C          CDF(NC)        LOCAL CDF VALUE OBTAINED FROM THE LOCAL
C                         DECLUSTERIZED HISTOGRAM.
C          AVE(NC)        USED TO CALCULATE THE QUANTITY OF METAL
C                         RECOVERED.  AVE IS SOME MEASURE OF CENTRAL
C                         TENDENCY FOR THE MATERIAL BETWEEN CUTOFFS
C                         I AND I+1.  FOR INSTANCE AVE(NC-1) COULD BE
C                         THE AVERAGE OF ALL DATA WITH VALUES BETWEEN
C                         CUTOFFS NC-1 AND NC.
C
C
C    OUTPUT
C    ******
C
C          TN(NC)         ESTIMATED TONNAGE RECOVERED AT EACH OF THE NC
C                         CUTOFFS.
C          Q(NC)          ESTIMATED QUANTITY OF METAL RECOVERED.
C          TE             ESTIMATED MEAN GRADE
C          TM             ESTIMATED MEDIAN GRADE OF THE PANEL
C
C   OPTIONS
C   *******
C
C          IDBUG          IF IDBUG=1 THE FOLLOWING INFORMATION WILL BE
C                         PRINTED.
C                              DATA LOCATIONS AND GRADES
C                              THE CORRESPONDING INDICATOR VALUES
C                              ALL COVARIANCE MATRICES
C                              ALL WEIGHTS
C          IMED           IF IM=1 ONLY MEDIAN INDICATOR KRIGING WILL BE
C                         PERFORMED.
C                         IF IM=1 SET NV=1 AND INPUT ONLY THE MEDIAN
C                         INDICATOR VARIOGRAM MODEL IN THE STRUC COMMON
C          IOR            IF IOR=1 SUBROUTINE ORDER IS CALLED TO
C                         RESOLVE ANY ORDER RELATION PROBLEMS. IF IMED=1
C                         SET IOR=0.
C
C
C
C
C      SUBROUTINES
C          COVA          COVARIANCE CALCULATION
C          KSOL          SOLUTION OF KRIGING SYSTEM
C          ORDER         RESOLVES ORDER RELATION PROBLEMS
C
C
C*******************************************************************************
```

```
C
C       INTERNAL VARIABLES
C
C
C       A R RR IER      KRIGING MATRIX VARIABLES (SEE KSOL)
C
C       XS(NC*ND)       SOLUTION ARRAY
C       CB,CB1,COV(NC)  AVERAGE COVARIANCES
C       DNX DNY DNZ     SPACING BETWEEN DISCRETIZATION POINTS ALONG X,Y,Z
C       XDB,YDB,ZDB(NBX*NBY*NBZ)  COORDINATES OF DISCRETIZATION POINTS
C                                 RELATIVE TO CENTER OF BLOCK
C       IVR(NC*ND)      INDICATOR DATA
C
C
      DIMENSION X(1),Y(1),Z(1),VR(1),TN(1),TNV(1),Q(1),CDF(1),CUT(1),
     1AVE(1)
      DIMENSION R(275),RR(275),XS(275),A(3575),CB(11),CB1(11),
     1          COV(11),XDB(64),YDB(64),ZDB(64),
     2          IVR(100),CBB(11)
C
      DOUBLE PRECISION NAM(10)
      COMMON INP,IOUT,TEST,NV,NAM
      COMMON/STRUC/NST(2),C0(2),AA(1,2),C(1,2),IT(1,2),AX(1,2),AY(1,2),
     1AZ(1,2),COSAL,SINAL
      NC1=NC-1
      NCC=NC
      IF(IMED.EQ.1) NC=1
C
C*****PRINT VARIOGRAM AND PANEL LOCATION INFORMATION
C
         IF (IDBUG.NE.1) GO TO 2
      WRITE(IOUT,1000) NCC
      IF(IMED.EQ.1) WRITE(IOUT,1001)
      WRITE(IOUT,1002)
      DO 1 IV=1,NV
      WRITE(IOUT,1003) IV,NST(IV),C0(IV)
      NS=NST(IV)
      WRITE(IOUT,1004)(IK,IT(IK,IV),C(IK,IV),AA(IK,IV),AX(IK,IV),
     1AY(IK,IV),AZ(IK,IV),IK=1,NS)
 1     CONTINUE
      WRITE(IOUT,1005)
      WRITE(IOUT,1006) XB,YB,ZB,DBX,DBY,DBZ,NBX,NBY,NBZ
C
C       PRINT DATA VALUES
C
      WRITE(IOUT,1007) ND
      WRITE(IOUT,1008) (X(LL),Y(LL),Z(LL),VR(LL),LL,LL=1,ND)
 2     CONTINUE
C
C      DEFINE INDICATOR DATA
C
      L=0
      DO 3 J=1,NCC
      DO 3 K=1,ND
      L=L+1
      IVR(L)=0
      IF(VR(K).LT.CUT(J)) IVR(L)=1
 3    CONTINUE
C
C      PRINT OUT INDICATOR DATA AND CUTOFF GRADES IF NECESSARY
C
      IF (IDBUG.NE.1) GO TO 4
      WRITE(IOUT,1009)(CUT(IU),IU=1,NCC)
      WRITE(IOUT,1010) (IU,IU=1,ND)
      DO 5 I=1,NCC
      L1=(I-1)*ND + 1
      L2=I*ND
      WRITE(IOUT,1011) I,(IVR(L),L=L1,L2)
 5    CONTINUE
 4    CONTINUE
C
C*****DISCRETIZATION POINTS
```

```
C
      NDB=NBX*NBY*NBZ
      N=0
C
      DNX=DBX/FLOAT(NBX)
      DNY=DBY/FLOAT(NBY)
      DNZ=DBZ/FLOAT(NBZ)
C
      X0=0.5*(DNX-DBX)
      Y0=0.5*(DNY-DBY)
      Z0=0.5*(DNZ-DBZ)
C
      DO 10 K=1,NBZ
      ZN=Z0+(K-1)*DNZ
      DO 10 J=1,NBX
      XN=X0+(J-1)*DNX
      DO 10 I=1,NBY
      N=N+1
      ZDB(N)=ZN
      XDB(N)=XN
      YDB(N)=Y0+(I-1)*DNY
10    CONTINUE
C
C***** BEGIN KRIGING
C
            NEQ=ND
            NN=(NEQ+1)*NEQ/2
C
C*****      SET UP KRIGING MATRICES
C
            IN=0
            DO 80 J=1,ND
            DO 75 I=1,J
            IN=IN+1
C*****      COVARIANCE BETWEEN SAMPLES
C
            CALL COVA(X(I),Y(I),Z(I),X(J),Y(J),Z(J),COV)
            DO 70 IV=1,NC
            K=IN+NN*(IV-1)
            A(K)=COV(IV)
70          CONTINUE
75          CONTINUE
C
C*****      COVARIANCE BETWEEN SAMPLES AND BLOCK
            DO 76 IV=1,NC
            CB(IV)=0.
76          CONTINUE
C
            XX=X(J)-XB
            YY=Y(J)-YB
            ZZ=Z(J)-ZB
            DO 77 J1=1,NDB
            CALL COVA(XX,YY,ZZ,XDB(J1),YDB(J1),ZDB(J1),COV)
            DO 77 IV=1,NC
            CB(IV)=CB(IV) + COV(IV)
77          CONTINUE
C
            DO 80 IV=1,NC
            CB(IV)=CB(IV)/FLOAT(NDB)
            K=J + NEQ*(IV-1)
            R(K)=CB(IV)
            RR(K)=R(K)
80          CONTINUE
C
C
C
C       PRINT OUT MATRICES IF REQUIRED
C
      IF (IDBUG.NE.1) GO TO 83
            L1=0
            IEN=0
            WRITE(IOUT,1012)
```

```
            DO 81 IV=1,NC
            WRITE(IOUT,1013) CUT(IV)
C
            DO 82 JG=1,ND
            L1=L1+1
            IST=IEN+1
            IEN=IST+JG-1
            WRITE(IOUT,1014) R(L1),(A(KX),KX=IST,IEN)
 82         CONTINUE
 81         CONTINUE
 83     CONTINUE
C
C*****      SOLVE THE SYSTEM
C
            CALL KSOL(NC,NEQ,1,1,1,A,R,XS,IER)
            IF(IER .NE. 0) WRITE(IOUT,1015) XB,YB,ZB
C
C      PRINT OUT WEIGHTS IF REQUIRED
C
            IF (IDBUG.NE.1) GO TO 90
            WRITE(IOUT,1016)
            DO 85 J=1,NC
            L1=ND*(J-1)+1
            L2=ND*J
            WRITE(IOUT,1017)CUT(J),(XS(L),L=L1,L2)
  85        CONTINUE
  90        CONTINUE
C
C*****    SOLUTION
C
          DO 100 IV=1,NCC
          TNN=0.
          DO 95 I=1,ND
          IK=I+ND*(IV-1)
          IKK=IK
          IF (IMED.EQ.1) IK=I
          TNN=TNN + XS(IK)*(IVR(IKK)-CDF(IV))
 95       CONTINUE
          TN(IV) = 1 - TNN - CDF(IV)
 100  CONTINUE
      IF(IOR.EQ.1) CALL ORDER(TN,NCC,IDBUG)
C
C     FIND QUANTITY OF METAL, MEAN AND MEDIAN ESTIMATES
C
      IF (NCC.EQ.1) GO TO 134
      Q(NCC)=TN(NCC)*AVE(NCC)
      TE=Q(NCC)
      TYM=TN(NCC)
      IF(TYM.LT..5) GO TO 120
      TM=-9.
 120  DO 130 LJ=2,NCC
      LLJ=NCC-LJ+1
      TE=(AVE(LLJ))*(TN(LLJ)-TN(LLJ+1))+TE
      Q(LLJ)=TE
      IF(TN(LJ).LT..5.AND.TN(LJ-1).GE..5) GO TO 140
      GO TO 130
 140  DIF=(TN(LJ)-.5)/(TN(LJ)-TN(LJ-1))
      TM=CUT(LJ)-DIF*(CUT(LJ)-CUT(LJ-1))
 130  CONTINUE
 134  CONTINUE
C
C        OUTPUT FORMATS
C
 1000 FORMAT('1',44X,'***** INDICATOR KRIGING FOR ',I2,' CUTOFFS **** ')
 1001 FORMAT(/,55X,'MEDIAN IK OPTION')
 1002 FORMAT(////,10X,'VARIOGRAM PARAMETERS USED',//)
 1003 FORMAT(/,10X,'FOR CUTOFF #',I3,' THERE ARE',I2,
     1' NESTED STRUCTURES',/,26X,'NUGGET=',F7.4)
 1004 FORMAT(35X,'STRUCTURE #',I2,' IS A TYPE',I2,' MODEL',/,40X,
     1'C  =   ',F7.4,/,40X,'RANGE=',F7.2,/,40X,'X ANIS. FACTOR',F7.4,
     2/,40X,'Y ANIS. FACTOR',F7.4,/,40X,'Z ANIS. FACTOR',F7.4)
 1005 FORMAT(/,26X,'NOTE',/,26X,'A TYPE 0 MODEL IS EXPONENTIAL',/,
```

```
     126X,'A TYPE 1 MODEL IS SPHERICAL',/,26X,
     2'A TYPE 2 MODEL IS LINEAR')
 1006 FORMAT(///10X,'PANEL TO BE KRIGED:'//
     3          10X,'CENTER OF PANEL:    X = ',F9.1, '    Y = ',
     4   F9.1,4X,'Z =',F8.1,/ 10X,
     5'BLOCK DIMENSIONS:      X-DIR.: ',F7.2,' Y-DIR.: ',F7.2,' Z-DIR.:'
     6  ,F7.2,/ 10X,'DISCRETIZATION POINTS: X-DIR.: ',I7,
     7              ' Y-DIR.: ',I7,' Z-DIR.:',I7,//)
 1007 FORMAT(//10X,'NUMBER OF SAMPLES GIVEN: ',I5,///
     1 17X,'X-COORD.',5X,'Y-COORD.',5X,'Z-COORD.',6X,'GRADE',3X
     2,'LOCATION #')
 1008 FORMAT(10X,5X,F9.1,5X,F9.1,5X,F8.2,4X,F8.3,3X,I6)
 1009 FORMAT(//,10X,'CUTOFF GRADES USED',/,10X,14F8.4)
 1010 FORMAT(///,10X,'INDICATOR DATA',/,2X,'LOCATION #',/,12X,25I5,//)
 1011 FORMAT(3X,'CUTOFF',I3,/,12X,25I5)
 1012 FORMAT(///,20X,'*** COVARIANCE MATRICES FOR ALL CUTOFFS ***')
 1013 FORMAT(/,25X,'COVARIANCES FOR CUTOFF =',F7.4,/,9X,'RHS',20X,
     1'LEFT HAND SIDE')
 1014 FORMAT(2X,12F10.4)
 1015 FORMAT(1X,'****************** FOR BLOCK: XB = ',F8.1,'YB = ',
     1F8.1,' ZB=',F8.3)
 1016 FORMAT(/,'  WEIGHTS FOR ALL CUTOFFS',/,2X,'CUTOFF',20X,'WEIGHTS')
 1017 FORMAT(1X,F7.4,12F10.4)
      RETURN
      END
```

REFERENCES CITED

Anderson, T.W., 1972, An Introduction to Multivariate Statistical Analysis, Wiley and Sons, New York, 374 pp.

Birak, D.J., 1979, Petrography of Jerritt Canyon Rock Types, unpublished Freeport Exploration Company Report

Birak, D.J. and Hawkins, R.B. 1984, The Geology of the Enfield Bell Mine and the Jerritt Canyon District, Elko County, Nevada, To be published as a bulletin of the United States Geological Survey

Boyle, R.W., 1979, The Geochemistry of Gold and its Deposits, Geological Survey of Canada, Bulletin 280, 579 pp.

Hillier, F. and Lieberman, G., 1980, Introduction to Operations Research Holden-Day Inc., San Francisco, Ca. 829 pp.

Jackson, M. and Marechal, A., 1979, Recoverable Reserves Estimated by Disjunctive Kriging: A Case Study, in, Proceedings of the 16th APCOM Symposium, Tucson, Arizona, AIME, New York, pp 240-249

Journel, A.G. and Huijbregts, C., 1978, Mining Geostatistics, Academic Press, London, 600 pp.

Journel, A.G., 1980, The Lognormal Approach to Predicting Local Distributions of Selective Mining Unit Grades, Journal of the International Association for Mathematical Geology, Vol. 12, pp. 285-304

Journel, A.G., 1982, The Indicator Approach to the Estimation of Spatial Distributions, in, Proceedings of the 17th APCOM Symposium, Golden, Colorado, AIME, New York, pp. 793-806

Journel, A.G., 1983, Non Parametric Estimation of Spatial Distributions, Journal of the International Association for Mathematical Geology, Vol. 15, No 3, pp. 445-468

Lemmer, I.C., 1984a, Estimating Local Recoverable Reserves Via Indicator Kriging, in, Verly, et al. eds., Geostatistics for Natural Resource Characterization, D. Reidel, Dordrect, Netherlands, pp 349-364

Lemmer, I.C., 1984b, The Mononodal Cutoff, Ph.D. Dissertation, Stanford University, Stanford, California

Luster, G.R., 1984, Raw Materials for Portland Cement: Applications of Conditional Simulation of Coregionalization Ph.D. Dissertation, Stanford University, Stanford, Ca.

Marechal, A., 1976, Selecting Mineable Blocks: Experimental Results Observed on a Simulated Orebody, in, Guarascio, M. ed., Advanced Geostatistics in the Mining Industry, D. Reidel, Dordrecht (Netherlands), pp 137-161

Matheron, G., 1974, Les Fonctions de Transfert des Petits Panneaux, Note Geostatistique No. 127, Fontainebleau Series No. N-395

Matheron, G., 1976a, A Simple Substitute for Conditional Expectation: Disjunctive Kriging, in, Guarascio, M. ed., Advanced Geostatistics in the Mining Industry, D. Reidel, Dordrecht (Netherlands), pp 221-236

Matheron, G., 1976b, Forecasting Block Grade Distributions: the Transfer Functions, in, Guarascio, M. ed., Advanced Geostatistics in the Mining Industry, D. Reidel, Dordrecht (Netherlands), pp 237-251

Merrian, C.W., and Anderson, C.A., 1942, Reconnaisance Survey of the Roberts Mountains, Nevada, Geological Society of America Bulletin, Vol. 53, pp. 1675-1728

Parker, H.M., 1975, The Geostatistical Evaluation of Ore Reserves Using Conditional Probability Distributions - A Case Study for the Area 5 Prospect, Warren Maine, Ph.D. Dissertation, Stanford University, Stanford, Ca.

Parker, H.M., and Switzer, P., 1975, Use of Conditional Probability Distributions in Ore Reserve Estimation: A Case Study. in, Proceedings of the 13th APCOM Symposium, Clausthal, West Germany, Verlag Gluckauf, GMBH, Essen

Parker, H.M., Journel, A.G., and Dixon, 1979, Conditional Lognormal Probability Distributions for the Estimation of Open-Pit Ore Reserves in Stratabound Uranium Deposits: A Case Study, in, Proceedings of the 16th APCOM Symposium, Tucson, Arizona, AIME, New York, pp. 133-148

Radtke, A.S., and Scheiner, C., 1970, Studies of Hydrothermal Gold Deposition: Carlin Gold Deposit, Nevada. The Role of Carbonaceous Material in Gold Deposition, Economic Geology, Vol 65, pp 87-102

Rendu, J.M., 1979, Normal and Lognormal Estimation, Journal of the International Association of Mathematical Geology, Vol 11, No. 4, pp. 407-422

Roberts, R.J., Radtke, A.S., Coats, R.R., Silberman, M.L., and McKee,E.H., 1971, Gold-bearing Deposits in North-central Nevada and Southwestern Idaho, Economic Geology, Vol 66, pp 14-23

Stieljes, J., 1918, Recherches Sur les Fractions Continues, Oeuvres, Groningen

Sullivan, J., 1984, Conditional Recovery Estimation Through Probability Kriging - Theory and Practice, in, Verly et al. eds., Geostatistics for Natural Resource Characterization, D. Reidel, Dordrecht, Netherlands, pp 365-384

Switzer, P., 1977, Estimation of Distribution Functions from Correlated Data, Bull. Inter. Stat. Inst., Vol. 47, No. 2, pp 123-137

Verly, G., 1983, The Multigaussian Approach and its Applications to the Estimation of Local Recoveries, Journal of the International Association for Mathematical Geology, Vol. 15, No. 2, pp 259-286

Verly, G., 1984, Estimation of Spatial Point and Block Distributions: The Multigaussian Model, Ph.D. Dissertation, Stanford University, Stanford, Ca.

Verly, G. and Sullivan, J., 1984, Multigaussian and Probability Krigings - Application to the Jerritt Canyon Deposit, Presented at the SME-AIME Annual Meeting, Los Angeles, California, February, 1984, Preprint #84-52

Wells, J.D., 1971, Association of Gold and Arsenic with Pyrite, Cortez and Carlin Mines, Nevada, Economic Geology, Vol 66, 1270-1271

Young, D., 1982, Development and Application of the Disjunctive Kriging Model: Discrete Gaussian Model, in, Proceedings of the 17th APCOM Symposium, Golden, Colorado, AIME, New York, pp 544-561